Synthesis and Evaluation of Novel Bio-Based Solvents and Solubilizers

Dissertation

zur Erlangung des Doktorgrades der Naturwissenschaften (Dr. rer. nat.)
der Fakultät für Chemie und Pharmazie
der Universität Regensburg

vorgelegt von
Katharina Häckl
aus Altötting

Regensburg 2019

Promotionsgesuch eingereicht am: Donnerstag, 23. Mai 2019.

Die Arbeit wurde angeleitet von: Prof. Dr. Werner Kunz.

Preface

The present thesis is based on the work carried out between April 2016 and May 2019 in the Institute of Physical and Theoretical Chemistry of the University of Regensburg under the supervision of Prof. Dr. Werner Kunz. Some further experiments were accomplished at the University of Lille and the University of Perth guided by Prof. Dr. Véronique Nardello-Rataj and Prof. Dr. Rob Atkin, respectively.

Submitted:	23rd May 2019
Colloquium:	18th July 2019
1st Referee:	Prof. Dr. Werner Kunz
2nd Referee:	Prof. Dr. Véronique Nardello-Rataj
3rd Referee:	Prof. Dr. Hubert Motschmann
Chair:	Prof. em. Dr. Jörg Daub

Acknowledgement

The realization of this thesis was only possible with the contribution and support of several people to whom I would like to express my honest gratitude.

First of all, I would like to thank Prof. Dr. Werner Kunz for providing this interesting topic, for offering the possibility and trust to work in his group, for his supervision and advice, for supporting all my research stays abroad and enabling the participation in several conferences and workshops.
Moreover, I would like to thank Prof. Dr. Véronique Nardello-Rataj und Prof. Dr. Hubert Motschmann for taking the roles as second and third referee of this thesis.
Furthermore, I would like to acknowledge Prof. Dr. Rainer Müller, Prof. Dr. Richard Buchner and Prof. Dr. Hubert Motschmann for providing access to their laboratories and equipment as well as for offering profound knowledge and practical advice. Thanks to Dr. Didier Touraud for his innovative ideas, valuable input and scientific discussions.
I am grateful to Prof. Dr. Véronique Nardello-Rataj for giving me the chance to work in her laboratories at the University of Lille for several weeks as well as to her group for offering such a warm welcome to France. In addition, I am indebted to Prof. Dr. Rob Atkin for allowing me to work in his group at the University of Western Australia for several months, for his scientific support and expertise in the laboratory. Thanks to all group members for contributing to a pleasant time in Australia. I also want to acknowledge the International PhD Program at the University of Regensburg (*iP*UR) for their financial support of the latter research stay.

I am thankful to Barbara Goricnik and Nadja Hinterreiter from the Institute of Analytical Chemistry, Chemo- and Biosensors for performing cytotoxicity measurements. Thanks to Johannes Mehringer who kindly provided his egg white solutions for some experiments of this work.
I am likewise grateful to Franz, Verena, Johanna, Thomas, Katarzyna, Jordan and Jonas for their practical support in the laboratory.
I would like to thank Rosi, Sonja and Bianca for their organizational support, their great patience and their permanent approachability with any matters as well as Hellmuth, Franzi, Theresa and Georg for their availability and help in regard to all practical matters.

Of course, I would like to thank all my collegues for the relaxed and friendly atmosphere, for scientific support, for conversations, discussions and the entertaining evening events. Special thanks go to Alex, Claudi and Damian for the homelike, familiar atmosphere and many many cups of coffees. It was a pleasure to share one office with you.
Thanks to Alex, Claudi and especially Matthias for reading this manuscript and giving helpful comments and advice for its improvement.

I finally want to mention those persons who are most important to me: my Papa Georg and my sisters Lisa and Marlene. Thank you for encouraging and supporting me throughout my whole life in any respect. Thanks to Matthias for his mental and practical support and for always offering a muesli bar, when it is needed.

Abstract

The field of green chemistry rapidly gained interest in recent years due to the increasing visibility of present environmental problems. In particular, the replacement of conventional organic solvents is considered urgently important in view of the fact that they are often volatile compounds, obtained from petroleum resource and highly abundant in chemical processes and industry. The idea of this thesis was to develop new approaches towards the development of green, alternative solvents and solubilization concepts. Several substance classes accessed by means of different strategies were studied to reach this aim. Firstly, the naturally originating *L*-carnitine was found to be a valuable starting material for the development of ionic liquids, cationic hydrotropes and surfactants. Starting from the zwitterionic natural molecule, cationic carnitine ester species were synthesized and the greenness of the employed reaction pathways was evaluated. The properties of the resulting pure substances and aqueous solutions were determined next to their applicability in terms of solubilization. In a second approach, the rather new solvent class of deep eutectic solvents was studied by extending the so far investigated range of members of this class. Mixtures consisting of betaine or carnitine in combination with carboxylic acids were found to exhibit a certain ionic liquid character. Furthermore, the suitability of biologically relevant substances, such as antioxidants was assessed for the formation of functional deep eutectic solvents. Natural hormones, in particular sodium salts of dehydroepiandrosterone sulphate, indole-3-acetic acid and indole-3-butyric acid were found to feature hydrotropic character. This allowed for the consideration of hormones being relevant for mechanisms in the organism beyond their primary function as hormones. The presented work has shown that numerous approaches relying on the utilization of well-known natural substances or modified derivatives thereof hold promise for their use as solvents or solubilizers in green chemistry.

Zusammenfassung

Das wachsende Bewusstsein für bestehende Umweltprobleme hat dazu geführt, dass in den letzten Jahren die Sparte ‚grüne Chemie' an Bedeutung gewonnen hat. Insbesondere der Ersatz organischer Lösemittel durch nachhaltigere Alternativen wird dabei als wichtig erachtet. Grund dafür sind ihre vermehrte Freisetzung in die Umwelt durch Verdampfen, ihre Herkunft aus fossilen Rohstoffen und ihre Allgegenwärtigkeit in chemischen Prozessen und der Industrie. Ziel dieser Doktorarbeit war es, nachhaltige Lösemittel und dahingehende Konzepte zu entwickeln. In diesem Zuge wurden mehrere Substanzklassen anhand unterschiedlicher Methoden und Herangehensweisen untersucht. Natürlich vorkommendes *L*-Carnitin hat sich als geeignetes Ausgangsmaterial für die Herstellung ionischer Flüssigkeiten, kationischer Hydrotrope und Tenside erwiesen. Dazu wurde aus dem natürlichen Carnitin-Zwitterion auf zwei unterschiedlichen Wegen ein Carnitin-Ester synthetisiert und die Nachhaltigkeit der jeweiligen Reaktion geprüft. Die erhaltenen Carnitin-Ester und ihre wässrigen Lösungen wurden charakterisiert und ihre Anwendbarkeit getestet. Der zweite Teil dieser Arbeit handelt von den sogenannten ‚tiefen Eutektika', einer relativ neuen Lösemittel-Klasse, die hierdurch um einige bisher unbekannte Lösemittel erweitert werden konnte. Es wurde festgestellt, dass tiefe Eutektika, die Betain und Carnitin enthalten, zu einem gewissen Grad auch den Charakter ionischer Flüssigkeiten aufweisen. Nachweislich sind auch biologisch relevante Substanzen, zum Beispiel Antioxidanzien, im Stande, tief-eutektische Lösemittel zu bilden. Schließlich konnte gezeigt werden, dass natürliche Hormone, in diesem Fall die Natriumsalze von Dehydroepiandrosteron, Indol-3-Essigsäure und Indol-3-Buttersäure, Hydrotrop-Charakter besitzen. Diese Erkenntnis lässt darauf schließen, dass Hormone neben ihrer bekannten Wirkweise als Hormon noch andere Funktionen im Organismus übernehmen. Im Allgemeinen konnte durch diese Arbeit demonstriert werden, dass natürliche Substanzen und deren Derivative vielversprechende Ausgangsmaterialien zur Entwicklung nachhaltiger, alternativer Lösemittel und Lösevermittler darstellen.

Abbreviations

AChCl	Acetylcholine chloride
ACS	American Chemical Society
AFM	Atomic Force Microscopy
Ag_2O	Silver(I)oxide
Amb15	Amberlyst 15
ATP	Adenosine triphosphate
BASIL	Basic Acidic Scavenging utilizing Ionic Liquids
Bet	Betaine
BetHCl	Betaine hydrochloride
BMU	Federal Ministry of the Environment, Nature, Conservation and Nuclear Safety
CA	Caffeic acid
CAC	Critical aggregation concentration
CAPE	Caffeic acid phenethyl ester
Car	Carnitine
CarHCl	Carnitine hydrochloride
ChCl	Choline chloride
$CHCl_3$	Chloroform
CiA	Citric acid
CMC	Critical micellar concentration
$[C_nBet]X$	Betaine alkyl ester
$[C_nCar]X$	Carnitine alkyl ester
$[C_4C_1Im]Br$	1-Butyl-3-methylimidazolium bromide
CO	Carbon monoxide
CO_2	Carbon dioxide
COSMO-RS	Conductor like Screening Model for Real Solvents
CTAB	Cetyltrimethylammonium bromide
C_nTAB	Alkyltrimethylammonium bromide
DES	Deep eutectic solvent
D-Fru	*D*-fructose
DDT	Dichlordiphenyltrichlorethan
DHEA	Dehydroepiandrosterone
DHEAS, NaDHEAS	Sodium dehydroepiandrosterone sulfate
DLS	Dynamic light scattering
DNA	Deoxyribonucleic acid
DPnP	Di(propylene glycol) propyl ether
DPPC	Dipalmitoylphosphatidylcholine
DSC	Differential scanning calorimetry
DR13	Disperse red 13
ECHA	European Chemicals Agency
EC_{50}	Half maximal effective concentration
EG	Ethylene glycol

e.g.	*exempli gratia*
EPA	Environmental Protection Agency
eq.	Mole equivalent
et al.	*et alii*
EtOH	Ethanol
EU	European Union
FA	Formic acid
FeA	Ferulic acid
GA	Gallic acid
Gly	Glycerol
GlyA	Glycolic acid
GVL	γ-Valerolactone
HaCaT	Human keratinocytes
HBA	Hydrogen bond acceptor
HBD	Hydrogen bond donor
H-bond	Hydrogen bond
HOPG	Highly oriented pyrolytic graphite
HPLC	High performance liquid chromatography
H_2	Hydrogen
H_2O	Water
H_2SO_4	Sulfuric acid
^1H	Proton
IA	Itaconic acid
IAA	Indole-3-acetic acid
IBA	Indole-3-butyric acid
i.e.	*id est*
IL	Ionic liquid
LA	Levulinic acid
LaA	Lactic acid
LCA	Life cycle analysis
MA	Malonic acid
MalA	Malic acid
MaleA	Maleic acid
ManA	Mandelic acid
MeCN	Acetonitrile
$MeSO_3H$	Methylsulfonic acid
MeTHF	2-Methyl-tetrahydrofurane
MHC	Minimum hydrotropic concentration
NADES	Natural deep eutectic solvent
NaIAA	Sodium indole-3-acetate
NaIBA	Sodium indole-3-butyrate
NaSal	Sodium salicylate
n.d.	not determined
NMR	Nuclear magnetic resonance
OA	Oxalic acid
OCP	Open-circuit potential

OECD	Organization for Economic Cooperation and Development
O_2	Oxygen
PET	Polyethyleneterepthalate
PGE	Propylene glycol ether
PnP	Propylene glycol propyl ether
PSD	Power spectral density
PTFE	Polytetrafluoroethylene
QA	Quinic acid
REACH	Registration, Evaluation, Authorisation and Restriction of Chemicals
rt	Room temperature
SA	Succinic acid
SalA	Salicylic acid
SAXS	Small-angle X-ry scattering
SDS	Sodium dodecyl sulfate
ShiA	Shikimic acid
SILP	Supported ionic liquid phase
SLS	Static light scattering
SoA	Sorbic acid
SVHC	Substances of very high concern
SXS	Sodium xylene sulphonate
TA	Tartaric acid
TGA	Thermal gravimetric analysis
THF	Tetrahydrofurane
TLC	Thin layer chromatography
T_{deg}	Degradation temperature
T_g	Glass temperature
T_m	Melting temperature
UN	United Nations
US	United States
UV/Vis	Ultraviolet-visible
wt%	Weight percent

Symbols

Γ_i	Molar surface excess concentration [mol/m^2]
A	General interfacial area [m^2]
A_i	Mean area per molecule [m^2]
n_i	Molar amount [mol]
N_A	Avogadro constant [1/mol]
m	Numerical factor
R	Gas constant [J/(mol*K)]
T	Temperature [K]
σ	Surface tension [N/m]
c_i	Concentration [mol/m^3]
π	Surface pressure [N/m]
N_S	Packing parameter
V_h	Volume of hydrophobic tail [m^3]
L_h	Length of hydrophobic tail [m]
a_0	Cross-sectional area of head group [m^2]
κ	Specific conductivity [S/m]
$^{2/3}J$	Coupling constant [Hz]
δ	Chemical shift [ppm]
f	Solubility factor
a	Specific coefficient determined from linear fits

Table of Contents

Preface I

Acknowledgement III

Abstract V

Zusammenfassung VI

Abbreviations VII

Symbols X

Table of Contents XI

Introduction 3

References 6

1 Basic Framework 9

1.1 Green Chemistry 9

1.1.1 Definition 9

1.1.2 History 9

1.1.3 Current Situation and Challenges 13

1.2 Importance of Nature for Green Chemistry 16

1.2.1 Natural, renewable resources 16

1.2.2 Concepts and Techniques Adopted from Nature 18

1.3 Green Solvents 20

1.3.1 No-solvent Systems 20

1.3.2 Water as Solvent 21

1.3.3 Classical Green Solvents 21

1.3.4 Reactions in Subcritical, Supercritical and Switchable Solvents 24

1.3.5 Ionic Liquids (ILs) 25

1.3.6 Deep Eutectic Solvents (DESs) 30

1.4 Amphiphiles 36

1.4.1 Classical Surfactants 37

1.4.2 Hydrotropes 38

1.4.3 Physico-chemical Properties 40

1.4.4 Green Surfactants and Hydrotropes 48

1.5 References 49

2 *L*-Carnitine-Based Ionic Liquids, Hydrotropes and Surfactants 59

2.1 Introduction 59

2.2 *L*-carnitine-based Ionic Liquids 62

2.2.1 Synthesis 62

2.2.2 Characterization of *L*-Carnitine-Based Ionic Liquids 67

2.2.3 Critical Discussion of *L*-Carnitine-Based Ionic Liquids 70

2.3 [C_nCar]Br – Ionic Liquids, Hydrotropes and Surfactants 73

2.3.1 Synthesis 73

2.3.2 Characterization 74

2.3.3 Application for the Solubilization of Vanillin 82

2.4 [C_nCar]$MeSO_3$-Surfactants 83

2.4.1 Synthesis 84

2.4.2 Characterization 85

2.5 Conclusion 90

2.6 Experimental Part 92

2.6.1 Synthesis 93

2.6.2 Nuclear Magnetic Resonance Spectroscopy 94

2.6.3 Determination of Water Solubility 97

2.6.4 Karl-Fischer Coulometry 97

2.6.5 Thermal Analysis 97

2.6.6 Surface Tension Measurements 97

2.6.7 Dynamic Light Scattering 98

2.6.8 Solubility 98

2.6.9 Penetration Scan and Polar Microscopy 99

2.6.10 Cytotoxicity 99

2.7 References 100

3 Deep Eutectic Solvents 107

3.1 Introduction 107

3.2 Betaine- and Carnitine-Based Deep Eutectic Solvents 109

3.2.1 Binary Mixtures of Zwitterionic Betaine and Carnitine 110

3.2.2 Ternary Mixtures of Carnitine, Carnitine Hydrochloride and a Carboxylic Acid.. 112

3.2.3 Deep Eutectic Solvents Based on Betaine and Carnitine Alkyl Esters 117

3.2.4 Betaine- and Carnitine-Based Deep Eutectic Solvents for the Solubilization of Melanin 119

3.3 Deep Eutectic Solvents Containing Biologically Relevant HBDs 122

3.3.1 Binary Deep Eutectic Solvents Containing Biologically Relevant Hydrogen Bond Donors 123

3.3.2 Ternary Mixtures Containing Gallic Acid 124

3.3.3 Application of Deep Eutectic Solvents as Ephemeral Reaction Solvents 126

3.4 Atomic Force Microscopy Study of the Behaviour of Surfactants at a Deep Eutectic Solvent-Graphite Interface 131

3.4.1 General Considerations.. 131

3.4.2 Interfacial Behaviour of Deep Eutectic Solvents at a Graphite Surface 133

3.4.3 Surfactant Aggregation at a Deep Eutectic Solvent-Graphite Interface 135

3.4.4 Influence of Electric Surface Potential on the Aggregation Behaviour of Surfactants at a Deep Eutectic Solvent-Graphite Interface 140

3.4.5 Summary of the Results Obtained from the Atomic Force Microscopy Study of the Deep Eutectic Solvent-Graphite Interface.. 142

3.5 Conclusion 142

3.6 Experimental.. 145

3.6.1 Chemicals 145

3.6.2 Synthesis of Betaine- and Carnitine-Based Alkyl Esters 145

3.6.3 Preparation of Deep Eutectic Solvents.. 146

3.6.4 Differential Scanning Calorimetry.. 146

3.6.5 Karl-Fischer Coulometry 147

3.6.6 Atomic Force Microscopy 147

3.6.7 Procedure for the Solubilization of Melanin.. 147

3.6.8 Solubilization of *n*-Alkyl Alcohols 148

3.6.9 Synthesis of Gallic Acid Alkyl Ester... 148

3.6.10 High Performance Liquid Chromatography (HPLC)... 148

3.7 References 149

4 **Amphiphilic Hormones: Physical-Chemical Characterization** 155

4.1 Introduction 155

4.2 Hormones 157

4.2.1 General Function of Hormones 157

4.2.2 Dehydroepiandrosterone and its Sulphate 158

4.2.3 Auxins 159

4.3 Interfacial and Self-Aggregation Behaviour of Hormones in Aqueous Solution 160

4.3.1 Surface Tension 160

4.3.2 Conductivity 162

4.3.3 Dynamic Light Scattering 163

4.4 Evaluation of the Hydrotropic Efficiency of Hormones 165

4.4.1 Solubilization of Disperse Red 13 165

4.4.2 Influence of Hormone Sodium Salts on Water/Propylene Glycol Ether Mixtures 166

4.4.3 Influence of Sodium Dehydroepiandrosterone Sulphate on an Aqueous Egg White Solution 171

4.5 Interaction with a Dipalmitoylphosphatidylcholine Monolayer 173

4.5.1 General Considerations 173

4.5.2 Surface Pressure-Area Isotherms 174

4.6 Conclusion 178

4.7 Experimental Part 179

4.7.1 Chemicals 179

4.7.2 Surface Tension Measurements 180

4.7.3 Conductivity Measurements 180

4.7.4 Dynamic Light Scattering 180

4.7.5 Solubility 180

4.7.6 Determination of the Lowest Solution Temperatures of Water/Propylene Glycole Ether Mixtures 181

4.7.7 Langmuir Film Balance 181

4.8 References 182

5 Concluding Remarks 187

References 191

6 Appendix 195

6.1 Chemical Structures of Deep Eutectic Solvent Components 195

6.1.1 Hydrogen Bond Acceptors Based on Quaternary Ammonium Compounds 195

6.1.2 Hydrogen Bond Donors 196

6.2 Collection of Mixtures Considered for the Formation of Deep Eutectic Solvents 197

6.2.1 Binary Mixtures Containing Betaine or Carnitine Zwitterions 197

6.2.2 Binary Mixtures Containing Betaine or Carnitine Hydrochloride 198

6.2.3 Binary Mixtures Containing Betaine or Carnitine Alkyl Esters 199

6.2.4 Binary Mixtures Containing Biologically Relevant Hydrogen Bond Donors 200

6.2.5 Ternary Mixtures Containing Gallic Acid 200

6.3 Nuclear Magnetic Resonance Spectra of Reference Substances According to Section 3.2.2 201

6.3.1 Nuclear Magnetic Resonance Spectrum of Maleic Acid 201

6.4 Complementary Force Curves Recorded by Atomic Force Microscopy 202

6.4.1 Force Curves of the Pure (ChCl-EG)-Deep Eutectic Solvent 202

6.4.2 Force Curves of SDS-Deep Eutectic Solvent Solutions 202

6.4.3 Force Curves of SDS-Deep Eutectic Solvent Solutions with Applied Electric Surface Potential 203

List of Figures 205

List of Tables 211

Scientific Contributions 213

Poster Presentations 213

Publications 213

Declaration 215

Introduction

Introduction

'Sustainability' plays an increasingly important role in various sectors of modern life. According to Fig. 1.1.1-1, it is defined by the interplay of three main aspects, in particular society, economy and environment. The compatibility of these aspects became more and more challenging over the last century due to considerable developments related to industrialization and the ever-accelerating technological evolution: the growth of population, increasing demand and consumption of consumer goods, endeavouring to comply with financial interests and strong influence of politics, just to mention a few. As a consequence, the responsibility towards nature and the environment has often been neglected in this period. The realization of substantial shortcomings regarding ecological aspects led to growing interest in environmental protection and the present progress in sustainability. Despite considerable efforts towards sustainability in recent years, the great challenge of finding a balance between social desires, economic feasibility and environmental responsibility remains.

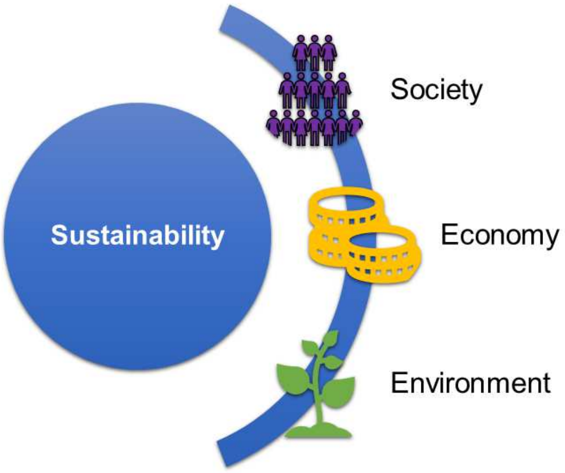

Fig. 1.1.1-1: Concept of sustainability taking into account social, economic and environmental aspects.

Chemical research plays a major role in the assessment of sustainable products, processes and technologies. Since the 1990s, the so-called '12 Principles of Green Chemistry' published by Anastas and Warner[1] (see section 1.1.2) have been used as a guideline for the development of sustainable chemical products and reactions. Besides respecting these general principles individually, green chemistry doubtlessly requires global and interdisciplinary collaboration and efforts in order to efficiently and successfully design sustainable alternatives with improved environmental compatibility.

In general, chemical processes both in research and industry often require high amounts of chemical solvents. Therein, they are assumed to account for an average of 80 % of the total volume of the employed chemicals.[2] This was equivalent to a solvent amount of approximately 20 million metric tonnes in 2015.[3] The importance of different industry sectors is illustrated in Fig. 1.1.1-2 including paint and pharmaceutical industry as those sectors with the highest solvent consumption. Due to this abundance of chemical solvents, it is an urgent requirement for green chemistry research to replace currently used organic solvents, which are often critical in view of their hazard potential and environmental impact. At the same time, the choice of the solvent is pivotal for the rate of the reaction and the solubility of the solute. Consequently, only both an adequate performance and an environmental compatibility qualifies a solvent to be suitable for a certain application and to replace the traditional method.

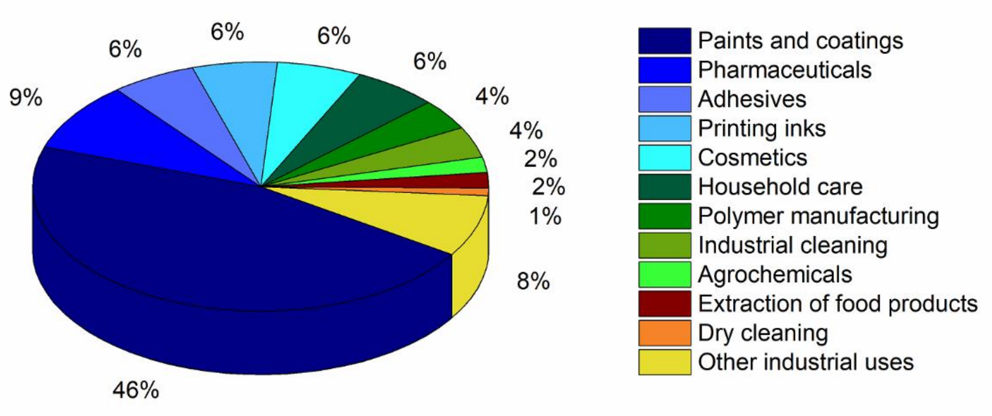

Fig. 1.1.1-2: Solvent consumption by industry sectors according to Ref. [3].

The research conducted within the scope of this thesis intended to design novel chemical solvents and solubilization concepts according to the principles of green chemistry. Furthermore, their potential to replace currently used solvents in certain applications was evaluated. In this respect, ionic liquids, hydrotropes, surfactants and deep eutectic solvents were in the focus of this work.

Three individual studies united by their intention to investigate and develop novel solvents and solubilization concepts are presented, thereby employing three strategies based on different considerations:

(1) Studying the applicability of an available, interesting, renewable molecule as green solvent or solubilizer after chemical modification (chapter 2).
(2) Extending the research area of a relatively new type of green solvents (chapter 3).
(3) Having in hand biologically relevant molecules whose primary function in biology is already known and examining their potential as natural solubilizers on the basis of their structural features as amphiphiles (chapter 4).

Serving as the theoretical framework of this thesis, chapter 1 is intended to provide fundamental basic information. Firstly, it reports on the definition and the historical background of green chemistry alongside a discussion of its current relevance. Secondly, related scientific aspects of the relevant substance classes, *i.e.,* ionic liquids, deep eutectic solvents, hydrotropes and surfactants, are given.

L-Carnitine as a source for the development of novel green solvents and solubilizers is described in chapter 2. It is a natural substance occurring in a wide range of organisms. Due to its appearence especially in meat, its name can be traced back to originate from the Latin term 'carnis' for meat.[4] The chemical modification of *L*-carnitine allows for the assessment of a cationic species with variable counter-ion. The suitability of several reaction routes in terms of their greenness is studied. In particular, two types of reactions for each reaction step, *i.e.,* the esterification and the anion exchange, are examined and compared in view of their potential as green reactions. The thermal properties of the synthesized *L*-carnitine alkyl ester substances are determined. They are shown to be ionic liquids at certain alkyl chain lengths. In addition, the interfacial and aggregation behaviour in aqueous solution is investigated, whereby the influence of the counter-ion is discussed. Concluding from these experiments, the studied *L*-carnitine alkyl ester compounds are identified either as hydrotropes or surfactants depending on the chain length. Their recognition as alternative cationic hydrotropes and surfactants is rationalized by comparing them to traditionally used substances and studying their cytotoxicity as well as their applicability for the solubilization of a model biomolecule.

Deep eutectic solvents as such first appeared at the beginning of the 21st century and are a rather new class of solvents.[5] Similar to ionic liquids, they exhibit several advantageous solvent properties, such as non-volatility, non-flammability and high conductivity. As additional benefit over ionic liquids, they are quick and simple to prepare. An investigation of this solvent class is presented in chapter 3. Therein, the focus is on two different types of deep eutectic solvents: (1) Betaine- and carnitine-based deep eutectic solvents and (2) deep eutectic solvents containing at least one biologically relevant component. For the former, their capability of solubilizing melanin is examined, while the latter are utilized as reaction media for several esterification reactions. Deep eutectic solvents have been reported to be suitable as solvents for electrochemical applications. In this context, the deep eutectic solvent-graphite interface is studied, in particular the behaviour of ionic surfactants at the interface when applying an electric surface potential. Finally, a summary about promises and limitations of deep eutectic solvents in practical applications is given.

The fourth chapter comprises the study of two types of hormone sodium salts: (1) dehydroepiandrosterone sulphate, which is a human hormone of steroid type and (2) auxins (3-indole-carboxylic acids), which are plant growth factors. In their function as hormones, they are powerful molecules that affect and regulate biological processes, when present in very low concentrations. Their molecular structures reveal amphiphilic character. Their interfacial and aggregation behaviour in aqueous solution is investigated in order to determine whether they feature hydrotrope or surfactant properties and potential activity as natural solubilizers. Besides, so far 'hidden' secondary functions of the studied hormones in biology appearing as a result of their hydrotropic character are discussed. Exemplarily, the recently reported role of dehydroepiandrosterone sulphate in the underlying mechanism of Alzheimer's disease is evaluated from a physico-chemical point of view.

References

[1] P. T. Anastas, J. C. Warner, *Green chemistry. Theory and practice,* 1. ed., Oxford Univ. Press, Oxford, **2000**.

[2] D. A. Alonso, A. Baeza, R. Chinchilla, G. Guillena, I. M. Pastor, D. J. Ramón, *Eur. J. Org. Chem.* **2016**, 612–632.

[3] J. H. Clark, T. J. Farmer, A. J. Hunt, J. Sherwood, *Int. J. Mol. Sci.* **2015**, *16*, 17101–17159.

[4] G. Fraenkel, *Biol Bull.* **1953**, *104*, 359–371.

[5] A. P. Abbott, G. Capper, D. L. Davies, H. L. Munro, R. K. Rasheed, V. Tambyrajah, *Chem. Commun.* **2001**, 2010–2011.

Chapter 1
Basic Framework

Green Chemistry
Amphiphiles
Green Solvents

1 Basic Framework

The present chapter intends to give the theoretical framework for this thesis. It contains a description of the fundamental concept of 'green chemistry' and its relevance for the future of our planet. The central role of nature in the field of green chemistry is pointed out, where it either serves as renewable resource or as conceptual model for technology and development. Currently available types of 'green solvents' are specified with particular focus on ionic liquids and deep eutectic solvents and their applications. Finally, amphiphiles, including the substance classes of surfactants and hydrotropes, are discussed with particular emphasis on the properties of their aqueous solutions.

1.1 Green Chemistry

1.1.1 Definition

The terms 'green chemistry' and 'green solvent' frequently lead to associations with the colour green. In the sense of physics, it is the colour appearing in the visible spectrum at wavelengths from approximately 500 to 570 nm. In nature, chlorophyll is the largest origin of the colour green. It can be found in the plant world as a motor for photosynthesis and animals use this colour as camouflage. Humans have had different associations and meanings of this colour. In the post-classical and modern Europe this colour was adopted by merchants and bankers as a feature for their prosperity. Nowadays, it is known to be the colour of safety and admission and assocciated with hope, youth, life, health and nature.[1]

But what do we really mean, when we are talking about green chemistry?

'Green chemistry is the utilisation of a set of principles that reduces or eliminates the use or generation of hazardous substances in the design, manufacture and application of chemical products'. [2]

This quotation originates from the widely-cited handbook of green chemistry by Paul T. Anastas and John C. Warner in 1998 with the title 'Green Chemistry: Theory and Practice'.[2] The term green chemistry alongside several others, such as clean chemistry, sustainable chemistry, environmental chemistry or benign chemistry, which essentially have the same meaning, has been used before. However, the book of Anastas and Warner was the first comprehensive work concentrating on the whole philosophy of the issue.

1.1.2 History

The idea of green chemistry dates back to the 1960s, and the most important milestones related to this issue are depicted in Fig. 1.1.2-1. Basic information regarding the historical aspects of green chemistry were collected from a series of articles.[3] Specific sources are indicated where required.

In 1962, Rachel Carson published a book entitled 'Silent Spring', where she primarily issued the negative influence of pesticides to the environment and criticized industry and politics for ignoring obvious impacts.[4] With this, political and public discussions as well as environmental awareness were awakened. Thereupon, the United States (US) Environmental Protection Agency (EPA) was founded in 1970, which is the national agency for the protection of human health and environment. Banning dichlorodiphenyltrichloroethane (DDT) and other pesticides was among its first actions, for example. In 1972, the United Nations' (UN) Environment Program was started. During the 1980s, discussions about green chemistry advanced to an international level, e.g. in the Organization for Economic Cooperation and Development (OECD) and a shift from pollution clear-up to pollution prevention was promoted. However, the groundbreaking decade for green chemistry must have been the 1990s with considerable contribution by the US EPA and the establishment of the Pollution Prevention Act 1990. Annual award programs for scientific development in green chemistry were launched, congresses on the topic were organized, the American Chemical Society (ACS) Green Chemistry Institute was founded and green chemistry university education started. Finally, in 1998, the above mentioned 'Green Chemistry – Theory and Practice' by Anastas and Warner was published and the idea of green chemistry received a precise definition by stating the **'12 Principles of Green Chemistry'** (see Tab. 1.1.2-1). They deliver a guideline on how to perform green chemistry.[2]

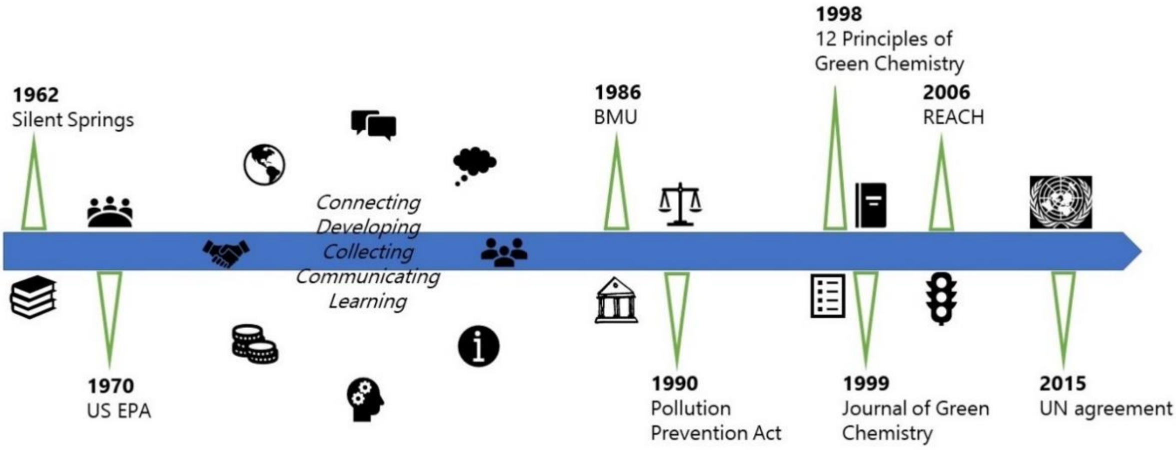
1962
Silent Springs
1970
US EPA
Connecting
Developing
Collecting
Communicating
Learning
1986
BMU
1990
Pollution
Prevention Act
1998
12 Principles of
Green Chemistry
1999
Journal of Green
Chemistry
2006
REACH
2015
UN agreement

Fig. 1.1.2-1: Time scale of the development of green chemistry.

Tab. 1.1.2-1: The 12 Principles of Green Chemistry.[2]

🗑	**1. Waste Prevention** Prioritize the prevention of waste, rather than cleaning up and treating waster after it has been created. Plan ahead to minimize waste at every step.	♻	**7. Use of Renewable Feedstocks** Use chemicals which are made from (renewable (i.e. plant-based) resources, rather than other equivalent resources originating from petrochemical resources.
⚛	**2. Atom Economy** Reduce waste at the molecular level by maximizing the number of atoms from all reagents that are incorporated into the final product. Use atom economy to evaluate reaction efficiency.	⬡	**8. Reduce Derivatives** Minimize the use of temporary derivatives such as protecting groups. Avoid derivatives to reduce reaction steps, resources required and waste created.
⚠	**3. Less Hazardous Chemical Synthesis** Design chemical reactions and synthetic routes to be as safe as possible. Consider the hazards of all substances handled during the reaction, including waste.	⏱	**9. Catalysis** Use catalytic instead of stochiometric reagents in reactions. Choose catalysts to help increase selectivity, minimize waste and reduce reaction times and energy demands.
☠	**4. Designing Safer Chemicals** Minimize toxicity directly by molecular design. Predict and evaluate aspects such as physical properties, toxicity and environmental fate throughout the design process.	✂	**10. Design for Degradation** Design chemicals that degrade and can be discarded easily. Ensure that both chemicals and their degradation products are not toxic, bio-accumulative or environmentally persistent.
⚗	**5. Safer Solvents and Auxiliaries** Choose the safest solvent available for any given step. Minimize the total amount of solvents and auxiliary substances used, as these make up a large percentage of the total waste created.	🏭	**11. Real-Time Pollution Prevention** Monitor chemical reactions in real-time as they occur to prevent the formation and release of any potentially hazardous and polluting substances.
💡	**6. Design for Energy Efficiency** Choose the least energy-intensive chemical route. Avoid heating and cooling, as well as pressurized and vacuum conditions (i.e. ambient temperature and pressure are optimal).	☄	**12. Safer Chemistry for Accident Prevention** Choose and develop chemical procedures that are safer and inherently minimize the risk of accidents. Know the possible risks and assess them beforehand.

While these evolutions manly took place in the USA, a similar development could be observed in Germany and throughout Europe. In the 1970s, the German government launched an environmental program, a waste disposal law and the federal control of pollution act. The Federal Ministry of the Environment, Nature, Conservation and Nuclear Safety (BMU) was founded in 1986 as a reaction to the nuclear reactor accident in Chernobyl.[5] The European Community's Chemistry Council – now European Chemical Society (EuChemS) – came up with several influential paper contributions in the 1990s, while only later their division for green and sustainable chemistry was affiliated. In 1998, James Clark from the University of York initiated the foundation of the Green Chemical Network within the Royal Chemical Society (RSC) in the United Kingdom (UK). Only one year later, their first edition of the scientific journal 'Green Chemistry' was published. It has grown to a reputable journal with a current impact factor of 8.586 (2017).

What followed was a decade of worldwide emphasis on green chemistry education realized in terms of numerous congresses, conferences, symposia and trainings. Research in the field of green chemistry increased drastically. The scientific publication database Scifinder® was used as an instrument for illustrating the temporal progress of green chemistry in terms of the number of the publications in this field. The compiled number includes books, journal articles, commentaries, reports and reviews containing the search term 'Green Chemistry' in their title, abstract or keywords. According to the results depicted in Fig. 1.1.2-2, a significant rise in the number of publications related to green chemistry started in the year 2000. While there was a constant increase until 2014, it seems like the curve was forming a peak and starts to decrease. This observation leads to the question: Is green chemistry just a hype? Is the interest in green chemistry after passing the hype maximum now decreasing? Hopefully not. This situation can be explained by the increased education in the field and awareness of the need for green chemistry: while the amount of publications regarding comments and discussions about the definition of green chemistry might decrease, research should by now automatically be based on the Principles of Green Chemistry and this is not explicitly mentioned in abstract or key words anymore.

Besides research and education, numerous new projects, initiatives, networks and collaborations dedicated to green chemistry were initiated in the course of the 2000s. In 2007, the Registration, Evaluation, Authorization and Restriction of Chemicals (REACH) regulatory was introduced, which is a central database that captures hazard, toxicity and risk information for chemicals. The registration includes the evaluation of a chemical by the producer and its registration at the European Chemical Agency (ECHA). A substance evaluation is performed by ECHA with emphasis on risky and highly concerning chemicals. While in general the use of a chemical in the European Union (EU) does not have to be authorized, REACH requires an authorization for substances of very high concern (SVHC). In the case of a substance of the latter class, the applicant has to prove that the risk can be controlled and that the socio-economic benefit outweighs the risk. In this context, the ECHA is entitled to prohibit or restrict the use of a SVCH.[6]

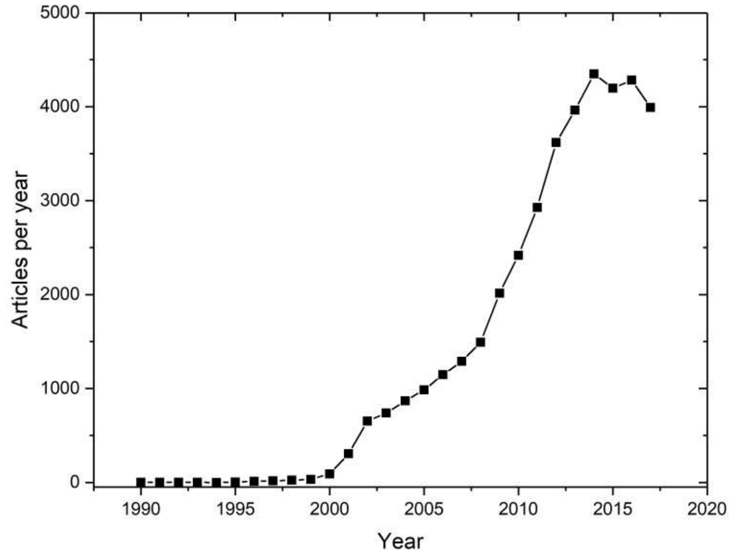

Fig. 1.1.2-2: Number of articles containing the concept 'Green Chemistry' published between 1990 and 2018.

In 2015, 193 member states of the UN agreed to act in league by announcing a global mission aiming for a sustainable future for our planet known as the Parisian Climate Agreement.[7] Numerous other foundations, agreements, regulations etc. have been established around the world combining people from industry, academia and politics. The following paragraph aims to work out that sustainability and green chemistry is not only related to the institutions mentioned above. In terms of aiming for a green planet, everyone is confronted with challenges in order to reach common goals.

1.1.3 Current Situation and Challenges

Despite of the ongoing progress described above, the world is facing severe environmental problems. A point is reached, where joint action is required, as the world is confronted with global warming and a scarcity of fossil resources. Our earth has been suffering for decades from the emission of greenhouse gases, fine particulates from combustion engines, microplastics from the immense consumption of plastic goods and an extreme overexploitation, *e.g.* regarding petroleum and crops. The rise in population and the average living standard cause ever increasing demands.

The huge challenge of our generation is to change the present trend and treat the planet well. Unfortunately, this purpose is complicated and frequently suffers from severe setbacks. A recent example is the decision of the US president to withdraw from the Parisian Climate Agreement. A further problem is that the mentioned problems are certainly global. However, environmental awareness, education and the capacity of legal regulation and action are not equal and vary extremely depending on a nation’s financial, economic, social and educational situation. Developing countries frequently have to fight other problems, like poverty and hunger. Often, their economy and social demands grow fast, so that environmental requirements cannot be satisfied. A good example is India, which is on its transition from a developing to a developed country. It experienced a fast growth of population (1.36 Bn., Feb. 2019)[8] and a strong economic boom (42.9 % growth of gross domestic product, 2012-2017).[9] However, this enormous economic growth was accompanied by serious environmental problems, such as deforestation, pollution, threats to biodiversity and a massive increase in energy consumption. Fortunately, the Indian government started to invest in clean technologies, such as renewable energy, where especially solar energy is promoted.[10] Although environmental laws exist, India is still facing major problems, such as air pollution from vehicle and industrial emissions, water pollution from raw sewages and inadequate sanitation, municipal solid waste and the utilization of inappropriate agricultural practices. This is caused by the absence of appropriate facilities and a lack of education. Sustainable industry is not always realizable, as a large number of small and medium sized enterprises do not have resources or the technical skills to adopt regulations and the government's enforcement is lax.

Although green chemistry is certainly not able to address all the above mentioned issues, its importance has never been higher. The production of chemical products is constantly growing, whereas still about 95 % thereof are derived from petroleum resource.[11] The transfer of green chemistry from academia to industry and real life will be existentially important in the years ahead. This includes the utilization of natural resources instead of petroleum resources, developing applicable strategies for energy storage and carbon dioxide (CO_2) capture, replacing organic solvents by greener alternatives, the production of green products for the end-consumer and thereby reducing waste and emissions. All in all, this is a complex and protracted endeavour. Besides process development and engineering, evaluation plays a key role: once alternative materials and technologies have been designed, it is at least as important to evaluate, whether their entire environmental impact is really reduced compared to existing techniques. In fact, the compatibility of ecological aspects with economic feasibility is most relevant. For evaluating these conditions, it is necessary to consider all stages and steps of a process. The so-called Life-Cycle Assessment (LCA) is a supporting tool to evaluate and quantify both benefits and deficiencies of a product or process regarding their environmental, economic and social aspects.[12] There are four main steps in the course of a LCA:[13]

1) Definition of goal and scope.
2) Life-cycle inventory analysis (includes input, such as material and energy, and output, such as product, waste and emission).
3) Life-cycle impact analysis (includes environmental impact of product and all process steps).
4) Life-cycle interpretation (includes identification of issues, evaluation and conclusion).

Several metrics are essential for a LCA in green chemistry and technology (see Fig. 1.1.3-1). The necessity of LCA in green chemistry and technology can be showcased by an example from cosmetics. Secchi *et al.* performed a comparative LCA for an already existing face crème. A synthetic, fossil-based oil component was replaced by an analogue derived from by-products of the olive oil industry.[14] It revealed a less favourable environmental performance of the considered product when employing the eco-based ingredient. This was due to treatments and arrangements required to make the new ingredient suitable for this particular chemical formulation. In this case, the dominating factor was the impact of the chosen materials and the way they were processed, whereas in other cases contributions like water and energy consumption can play the major role. Therefore, LCA is inevitable to evaluate, whether modifications in terms of designing greener products and processes really reduce environmental impact in all stages.

Once the advantageous performance of a product or process is proved by LCA, there are still numerous strong factors influencing its launch and market success: supply chain requirements, cost and efficiency, politics, market trends and the consumer. The good news is that a mentality change can be observed in the consumers' behaviour. The market demand of eco-products increases, as the consumers' sense and awareness for the protection of our planet is growing. Thus, it is a vital necessity to find a compromise between keeping our comfortable life standard and caring for our planet.

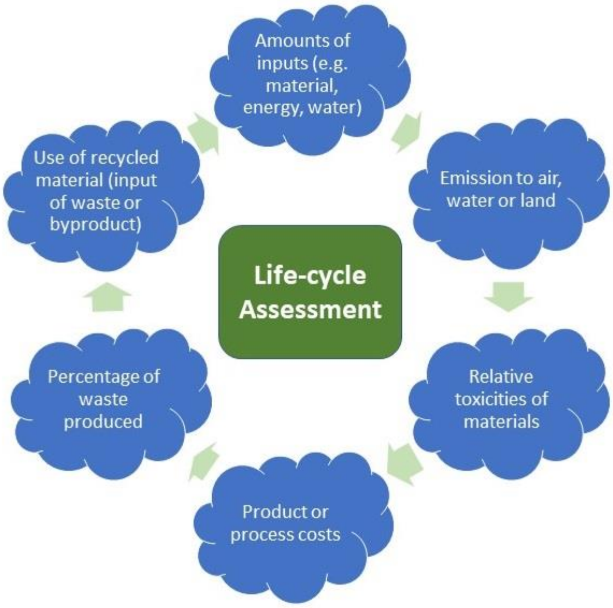
Amounts of inputs (e.g. material, energy, water)
Emission to air, water or land
Relative toxicities of materials
Product or process costs
Percentage of waste produced
Use of recycled material (input of waste or byproduct)
Life-cycle Assessment

Fig. 1.1.3-1: Metrics for Life Cycle Analysis.[12]

Facing all these challenges, the scientific researcher is assigned with the task to develop green chemistry that meets the requirements of economy with the aim of being applicable and affordable on large scale in industry and to meet the demands of the customers. Therefore, it is most important to collaborate with industry and concentrate on application-based research. In parallel, it is deemed a smart strategy to study concepts and techniques that are known to work already. The best place to find these concepts and techniques is nature. It is essential to study natural and biological materials and mechanisms, as in numerous cases, they hold a high potential for green chemistry as the key for tackling the existing environmental challenges.

1.2 Importance of Nature for Green Chemistry

Ever since, humans have been studying nature. Earliest records go back to ancient times and to the works of Thales (625-546 BC) and Aristoteles (384-322 BC). Nature has always been a closed circuit following the principle of reciprocity. As described in the former section, nature is forced to cope with negative impacts caused by mankind and it increasingly struggles with maintaining its natural balance. In order to keep our earth in equilibrium, green chemistry plays a key role and studying nature is an essential part of it: on the one hand to recognize the caused damages, on the other hand to find sustainable materials and concepts to avoid negative impacts.

1.2.1 Natural, renewable resources

Mostly, the term ‘renewable resources’ is associated with energy supply and the demand for replacing fossil-based fuels. In Europe, huge efforts are being made to replace them by renewable energy from sun, water, wind and biomass. Many people might not be aware that there is another issue with fossil resources: most of our everyday products are based on petrochemicals gained from fossil resources and approximately 10 % of fossil material is used for the production of chemical products.[15] Therefore, it is a major challenge to develop alternative ways to produce chemicals and materials.

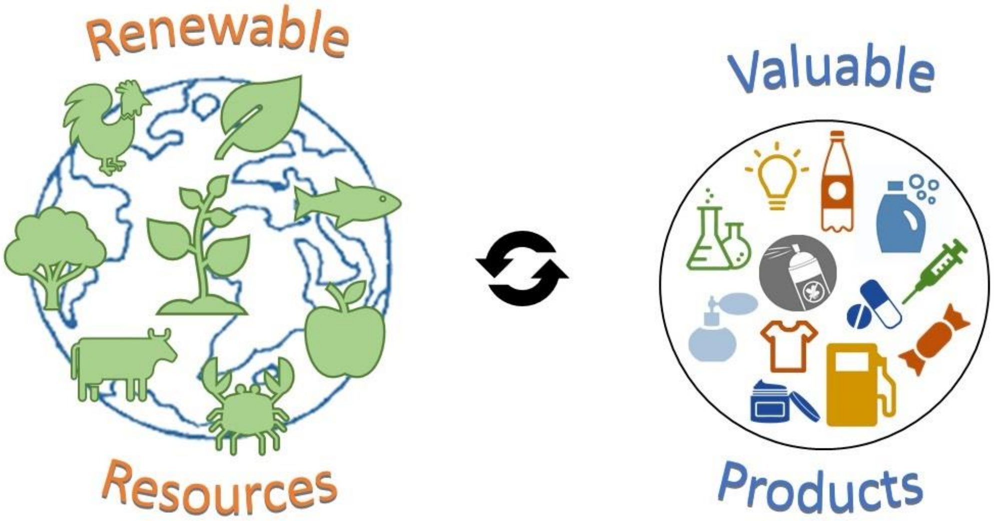

Fig. 1.2.1-1: Variety of valuable products obtained from nature in terms of biorefinery.

The furthest advanced technique is the utilization of biomass as a source for bio-based chemicals and materials. Biomass includes agricultural crops, wood, plants, algae, animal residues, sewage, municipal waste and industrial residues. The concept of processing biomass to obtain fuels, energy, chemical building blocks and materials from biological

]

feedstock and its implementation into the existing infrastructure is referred to as biorefinery.[16] It comprises the breakdown of initially complex biological structures to simpler building blocks, so-called platform molecules, which in turn are used for the build-up of a range of products of industrial and public interest (see Fig. 1.2.1-1). The biomass material contains mainly carbohydrates (including sugars, starch, cellulose, hemicellulose), oils, proteins, lignin and other secondary metabolites. According to Fig. 1.2.1-2, there are several ways for obtaining a variety of products:[17] (1) the extraction of secondary metabolites or biopolymers for direct use, (2) the total breakdown of the biomolecules by heat or fermentation to obtain syn-/biogas and (3) the chemical or biotechnological modification of the key components of carbohydrates, oils, proteins and lignins to platform molecules for the formation of new products.

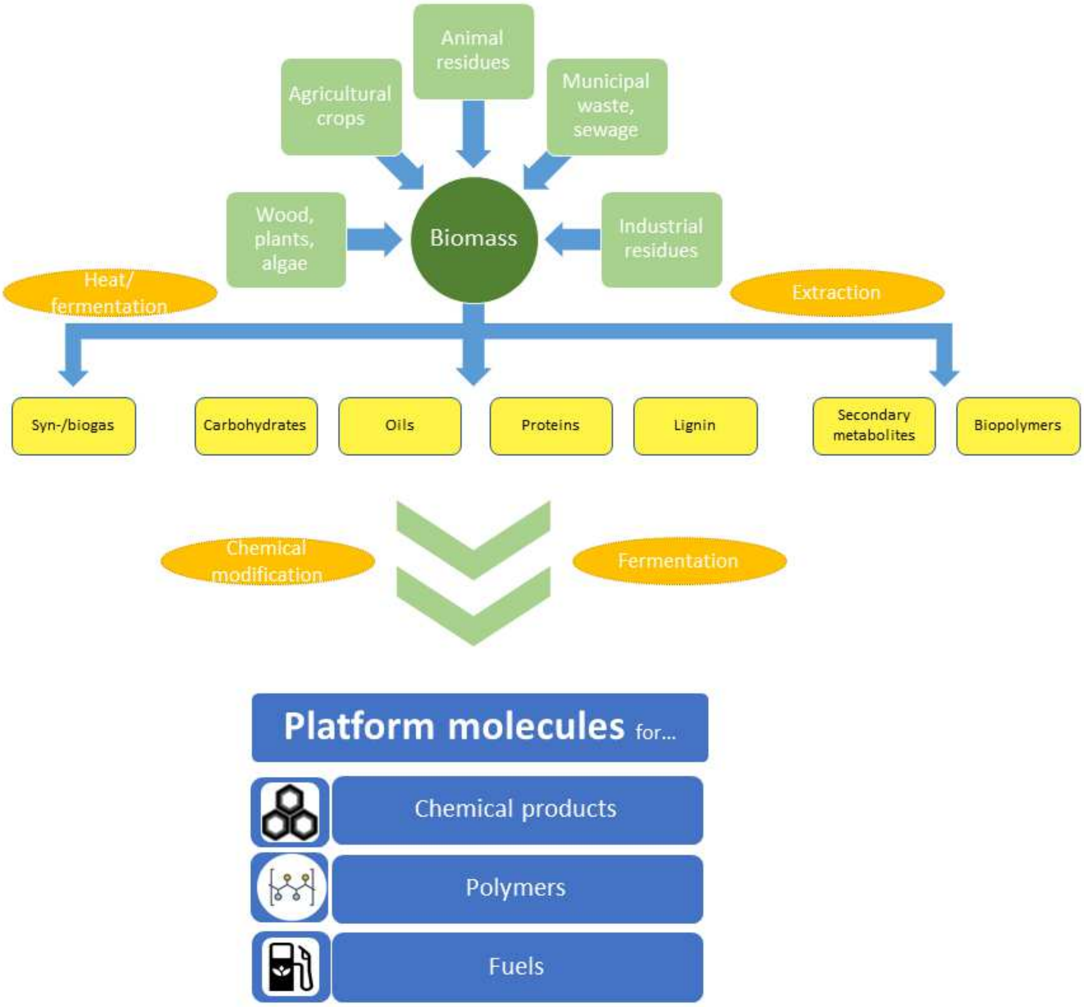
Animal residues
Agricultural crops
Municipal waste, sewage
Wood, plants, algae
Biomass
Industrial residues
Heat/ fermentation
Extraction
Syn-/biogas
Carbohydrates
Oils
Proteins
Lignin
Secondary metabolites
Biopolymers
Chemical modification
Fermentation
Platform molecules for...
Chemical products
Polymers
Fuels

Fig. 1.2.1-2: Scheme of the biorefinery of biomass.

1.2.2 Concepts and Techniques Adopted from Nature

Biological organisms and nature are consisting of numerous natural cycles, equilibria and rhythms: photosynthesis, metabolic pathways, cellular respiration, blood sugar level, acid-base balance, cell osmosis, nitrogen cycle, carbon cycle, just to name a few of them. In the course of evolution, nature has developed an overwhelming diversity of such advanced, perfectly synergetic concepts, structures and materials. Recently, our planet seems to be increasingly unbalanced as a result of negative impact of humankind, in particular industrialization and growing population. This becomes increasingly apparent in terms of climate change. To counteract this negative trend, humans are now responsible for developing new approaches to safe nature and environment. It is considered highly valuable to extensively study nature and imitate smart materials and concepts that can be implemented in the light of green chemistry and technology. In fact, the concept of biomimetics or biomimicry describes this approach well. An uncountable number of biomimetic concepts has successfully been introduced to chemistry, technology and human life. Catalysis is one famous and thriving example. This principle has been used in industry since the beginning of the 20th century and gave rise to huge economic benefits by accelerating reactions and reducing by-products. The natural analogue thereof is nature’s utilization of enzymes – natural catalysts that control all biological mechanisms and reactions in the organism. Catalysis is a highly important instrument in green chemistry, as it can minimize energy consumption and waste production. Two natural catalysis-related examples shall be discussed briefly: biotechnology and photocatalysis.

1.2.2.1 Biotechnology

Although biotechnology is not classified as biomimicry in the common sense, it is undoubtedly based on the utilization of natural mechanisms and enzymatically catalyzed processes. According to Zaid *et al.*, it can be defined as:

‘any technological application that uses biological systems, living organisms, or derivatives thereof, to make or modify products or processes for specific use’.[18]

It describes an interdisciplinary field with multiple applications. The production of alcoholic beverages by fermentation of sugars is probably one of the oldest and best-established examples. While biotechnology is not necessarily green in the sense defined above, its combination with green chemistry is often called ‘white biotechnology’. It can have beneficial effects in terms of reduction of greenhouse gases, water and energy consumption, lower production costs, improved selectivity and application of safer and more sustainable materials.[19]

Biopolymers, *i.e.* bio-synthetically produced polymers, can be produced by living organisms and the application of biotechnology. They regularly exhibit several advantages over conventional polymers. Their environmental footprint is less concerning, as they are biodegradable and cause less pollutants during synthesis. Sometimes, waste or byproducts from other processes can be used as starting materials for their production. If non-toxic and compatible with the biological homeostasis, they can be used for food or medical applications, *e.g.* as control medium for slow drug release or medical implants.[19] A good example for this substance group is Xanthan. It is frequently used in food industry as thickener and/or stabilizer and commercially produced in a process relying on bacteria.

The massive importance associated with the area of biotechnology was substantiated by the Nobel Prize for chemistry in 2018. It has been awarded to a group of scientists for their contribution in biotechnology. One half was attributed to ground-breaking research in the field of enzyme engineering. The properties of enzymes could be adjusted by gene modification in order to catalyze all sorts of reactions, e.g. the enzymatic production of bio-fuel.[20] Huge potential is also seen in the production of biopolymers and in catalyzing organic reactions utilizing renewable resources instead of metal catalysts.[19] Of course, biotechnology bears several uncertainties. The genetic modification of microorganisms creates ethical conflicts and the question arises, how much mankind should interfere with natural mechanisms and if this can be dangerous for humankind.

1.2.2.2 Photosynthesis

Nature has developed the highly sophisticated system of photosynthesis for the conversion of CO_2 and water (H_2O) to oxygen (O_2) and carbohydrates. It is driven by solar energy and can be found within plants, some specific bacteria and protists. In terms of the current energy, fuel and CO_2 issues, we can use it as inspiring model that delivers attractive approaches towards the utilization of a strong, renewable energy source and the reduction and workup of the greenhouse gas CO_2 from the atmosphere. For several decades, the natural mechanisms have been studied and artificial replicas have been created. A developmental stage is reached now, where artificial photosynthesis can be stopped at different levels of the process, *e.g.* after the production of H_2 from H_2O with solar energy or not until the reduction of CO_2 in order to generate carbon-based fuels or building blocks. The dedicated reaction pathways in natural photosynthesis, where light is captured by the plant dye chlorophyll on special antenna arrays, was used as model for the development of dye-sensitized solar cells for the direct conversion of sunlight to electricity.[21]

So far, this chapter has shown that at the current state of our planet, efficient research in green chemistry is required more than ever. The use of renewable materials and the adoption of smart concepts suggested by nature are considered as promising guidelines. It is particularly important to focus green chemistry research on fields bearing high impact. One of the biggest issues in terms of creating greener processes in industry is probably the use of solvents. They are employed in huge quantities and often bear considerable risks to humans and the environment. Hence, the next section addresses the current state of the art in the field of green solvents, especially ionic liquids (ILs) and deep eutectic solvents (DESs).

1.3 Green Solvents

Chemical solvents are generally used in huge amounts in research and industry. It is assumed that they account for approximately 80 % of the total volume of chemicals used in chemical processes,[22] which was around 20 million metric tonnes in 2015.[23] They are used in chemical reactions, extractions, purifications and cleaning operations. In this regard, the sustainability of a certain process highly depends on the choice of solvent and its contribution to the energy requirement, waste production and air pollution caused by this process. In many cases, volatile organic solvents based on petroleum resources are used. They show deficits in terms of safety and environmental compatibility, as they are often non-biodegradable, toxic, flammable, highly volatile and tend to accumulate in the atmosphere. Huge research efforts are in progress to replace them by more sustainable alternatives, as already proposed by the 12 Principles of Green Chemistry, where Warner and Anastas explicitly demand the use of 'safer solvents and auxiliaries'.[24] Accordingly, Jérôme *et al.* proposed 12 criteria that green solvents should fulfil concerning: availability, price, recyclability, grade, synthesis, toxicity, biodegradability, performance, stability, flammability, storage and renewability.[25] In reality, it is an ambitious proposition to find a solvent that fulfils all of these conditions. As a consequence, it is even more challenging to develop green solvents, because the evaluation of their sustainability remains challanging. Predominantly, a new solvent should be 'greener' compared to the conventionally used solvent that is meant to be replaced in a certain process. LCA is a suitable way to estimate the environmental impact of a solvent (see section 1.1.3).[26] Metaphorically, it considers the fate of a solvent from 'cradle to grave', *i.e.* from the manufacturing until its disposal or recycling. This has to be carried out for each specific application of a solvent. It may turn out that a solvent is green (meaning less harmful than another one) only for a special application, but not for another.

In this paragraph, different classes of green solvents will be presented and some promising solubilization concepts will be pointed out. Advantages, drawbacks and applications of ionic liquids (ILs) and deep eutectic solvents (DESs) will be discussed in particular. The present section about green solvents is based on the review 'Some Aspects of Green Solvents'.[27]

1.3.1 No-solvent Systems

In a simplistic, yet often impractical way, the best solvent is no solvent. In several relevant chemical and industrial processes the use of solvents could be completely avoided, which is in full agreement with the fifth Principle of Green Chemistry.[24] For many years, considerable efforts have been spent on the preparation of polymers in the absence of conventional solvents. Indeed, there are industrial polymerization processes avoiding the utilization of solvents, like melt polymerization or solid state polymerization. Exemplarily, polyethyleneterepthalate (PET) is commercially produced by melt polymerization followed by a solid state polymerization process.[28] It is even possible to prepare polymers, such as poly(phenylene vinylene) by ensuring close contact of the reacting molecules in a ball milling process within minutes.[29] The ball milling method is not only known in polymer science, but also in organic synthesis. Besides avoiding the use of organic solvents, it exhibits further advantages like high energy efficiency and reduced reaction times.[30] Solvent-free microwave extraction is another elegant technique worth to mention. Developed in 2004 by Chemat *et al.*, it is used for the extraction of essential oils from fresh plant materials in a microwave-assisted dry distillation process.[31] It is a rapid method that delivers a powerful alternative to the conventional water-consuming and long-lasting hydrodistillation.

1.3.2 Water as Solvent

Some scientists try to replace organic solvents by water, as it bears several advantages, like a low hazard potential, high availability and low cost. It also exhibits interesting aspects concerning reactivity: uncommon selectivities, influences of hydrogen-bond network on reaction behaviour, adjustable pH values, use of salts for salting-in or salting-out effect and the application of biphasic reaction systems. Hence, it is certainly a valuable approach, but it should be kept in mind that water also has some disadvantages: it is liquid only within a temperature range of 0-100 °C; its heat capacity makes distillation processes extremely energy consuming compared to common organic solvents; it tends to hydrolyze specific organic functionalities at certain pH conditions; its final purification for re-use is difficult. Nevertheless, many promising results have been published over the years following this approach.[32] For example, the Diels-Alder-type reactions in water have been widely studied since the 1980s, when Rideout and Breslow reported a certain rate acceleration using water as reaction medium.[33]

1.3.3 Classical Green Solvents

Classical green solvents denote already existing solvents that may already find some applications in chemical industry and formulation and are REACH-registered, which means that they are catalogued according to the previously described regulation of the EU (see section 1.1.2). Most of the classical solvents were declared sustainable, because they are obtained from biomass. Some promising and widely used classical green solvents will be discussed briefly. Their chemical structures are given in Fig. 1.3.3-1.

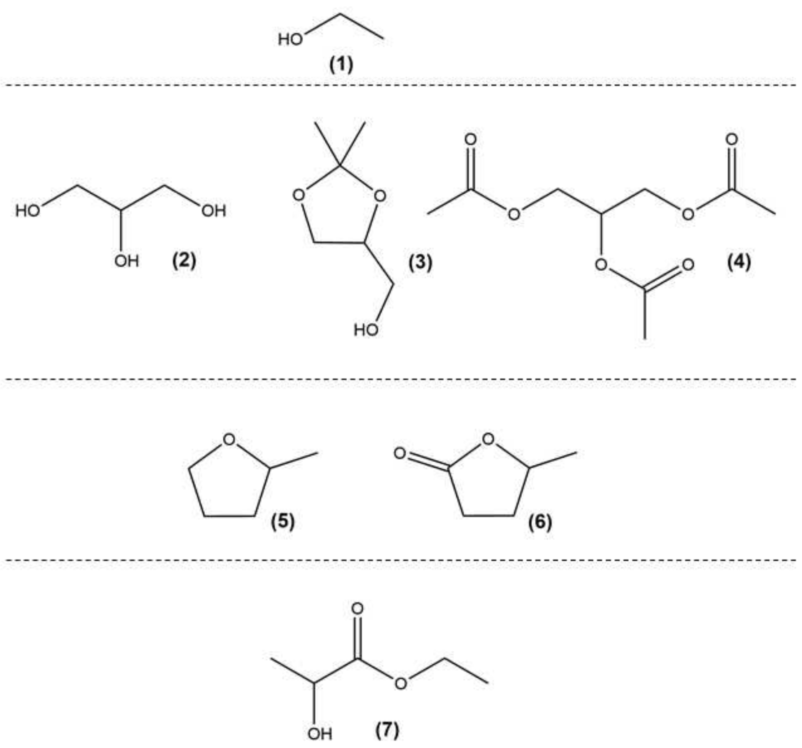

Fig. 1.3.3-1: Chemical structures of some classical green solvents: (1) ethanol, (2) glycerol, (3) solketal, (4) triacetin, (5) 2-methyltetrahydrofuran, (6) γ-valerolactone and (7) ethyl lactate.

1.3.3.1 Bioethanol

Talking about bioethanol, most people might first think about bioethanol as fuel or platform chemical for the production of further value-added chemical products. But of course, ethanol derived from biomass can also be used as green solvent in the chemical industry. Bioethanol is obtained from the fermentation of sugar and starch from agricultural crops, such as corn or sugar cane, but is also generated from lignocellulosic material. Huge amounts of ethanol are for example used in extraction processes.

1.3.3.2 Glycerol-Based Solvents

Glycerol is obtained in huge amounts as by-product in the biodiesel manufacturing process from hydrolysis of vegetable oils. The production of 1 kg of biodiesel generates approximately 0.1 kg of glycerol. In 2008, the glycerol output from the biodiesel production constituted two thirds of the overall glycerol produced and was 1.2 million metric tonnes in Europe.[34,35] The latest glycerol output from biodiesel production is estimated to be even higher. On the one hand, it has been reported that synthetic organic reactions perform well in glycerol itself.[36] On the other hand there is a whole bunch full of bio-based solvents and co-solvents derived from glycerol.[35,37] Among several others, solketal and triacetin belong to these derivatives.[23] Solvent properties of solketal, such as polarity, hydrophobicity and H-bond donor activity have been investigated in order to identify fields where it can be applied as green substitute of conventional solvents. It has been concluded that there are strong similarities with ethanol, propanol, acetonitrile and ethyl acetate. High conversion rates for bio-catalyzed reactions have been reported when triacetin was used as the reaction medium.[38]

1.3.3.3 2-Methyl Tetrahydrofuran (MeTHF) and γ-Valerolactone (GVL)

MeTHF and GVL are obtained from the sugar platform by chemically reacting monosaccharides.[23,39] The dehydration of hexoses, such as glucose in acid media results in the formation of 5-hydroxymethyl furfural and allows for the reaction to levulinic acid. Levulinic acid as a platform chemical gives access to a variety of bio-based chemicals and solvents, including MeTHF and GVL.[39] The aprotic solvent properties of MeTHF are close to those of tetrahydrofuran (THF) and diethyl ether. They are particularly suitable for organometallic and biphasic reactions. In this case, its higher boiling point of 80 °C is an advantage over diethyl ether. In contrast to THF, it is only partially water miscible and therefore favoured for the purification step in organometallic reactions.[40] MeTHF has been reported to be promising as a substitute for hexane in the extraction of fats and oils in food and fuel applications.[41] GVL is obtained in the same reaction line as MeTHF. It is characterized by a low melting as well as a high boiling and flash point. With its pleasant herbal odour it is frequently used in the flavour and perfume industry. Its application as food additive is relatively common. Besides, it proved to be applicable as alternative reaction medium in cross-coupling reactions[42] and for the solubilization of cellulose and lignocellulosic biomass.[43]

1.3.3.4 Lactic Acid-Based Solvents

Lactic acid is formed as a fermentation product from bio-derived carbohydrates, such as glucose. While lactic acid itself is traded as promising monomer for the production of biodegradable polymers (polylactic acid),[44] it also functions as sugar-based platform molecule and opens access to a range of chemicals and solvents. In particular, ethyl lactate raised interest due to several advantageous properties: high boiling point, low vapour pressure, good biodegradability/recyclability, negligible corrosion potential, good solvency of polymers, resins and dyes and its admission in food and pharmaceutical formulations.[45] Besides many other application, it is suitable for the extraction of carotenoids, vitamins and other phytonutrients from plant oils, fruits and vegetables.[46]

In general, the biogenic origin of solvents obtained from natural resource is sometimes not enough to refer to them as ‘green’. There are bio-based substances that are highly toxic or even carcinogenic, *e.g.* furfural. On the other hand, the production of a bio-based solvent can be costly and require large amounts of energy. In many cases where bio-sourced alternatives are potentially applicable, there is still need for process optimization, such as for the separation of lactic acid from the fermentation broth and its subsequent purification.[39] Whether one of these solvents can be finally classified as green, always depends on its application and a comparative study of the solvent conventionally used for the respective application.

1.3.4 Reactions in Subcritical, Supercritical and Switchable Solvents

Apart from ambient conditions, the solvent properties of water can be tuned by its use at elevated pressure and temperature. Similarly, CO_2 is used as sustainable solvent when present in the supercritical state. These solvents convince with high availability, non-toxicity, bio-degradability and sensitive tunability when changing pressure or temperature. However, technical expertise and expensive equipment is required to obtain high-pressure conditions. Switchable solvents are interesting niche-solvents, where pressure, temperature or the presence of CO_2 are used as a trigger to change the solvent properties.

1.3.4.1 Subcritical water

When using water as a solvent, conditions with elevated temperatures are often adopted to reach the so-called subcritical water region, which is in general the liquid water phase above the boiling point at ambient pressure (100 °C) and below the critical point (374 °C, 22.1 MPa). Physical and chemical properties of subcritical water show a significant dependence on temperature and pressure, so that solvent properties, *e.g.* the dielectric constant, are strongly influenced and adjustable. Subcritical water can be considered as a promising solvent for biomass processing, for example, the conversion of lignin-derived compounds into value-added fuel products with and without addition of industrial gases.[47] Furthermore, various organic reactions could be successfully performed under 'hydrothermal' conditions, *i.e.*, in water at temperatures between 150 and 250 °C.[48]

1.3.4.2 Supercritical CO_2

Supercritical conditions of CO_2 are reached at a temperature of 31 °C and a pressure of 7.4 MPa. Supercritical CO_2 turned out to be applicable for the extraction of flavours, fragrances and essential oils from natural materials, as it can be highly selective.[49] The extraction of β-carotene from crude palm oil is only one of many examples. Carotenoides are strong natural dyes and frequently used in food industry.[50] Apart from that, a wide spectrum of natural compounds, such as lipids, oils, terpenes, terpenoids, caffeine, phytochemicals, glycosides and others can be extracted.[51] Due to its great gas solubilization capacity, supercritical CO_2 has been used as reaction medium for hydrogenation reactions. When producing formic acid, its ester derivatives or amide derivatives, CO_2 serves as solvent and reactant at the same time. Good turnover rates were reached with ruthenium (II)-phosphines as homogeneous catalyst.[52]

1.3.4.3 Switchable Solvents

In 2010, Jessop *et al.* introduced the concept of 'switchable solvents'.[53] They could show that depending on the presence or absence of CO_2, certain species can either be water soluble or form a two-phase system with water, respectively. This phenomenon has been observed in water-amidine systems. Because the mixing-demixing process is reversible and can be tuned simply by controlling air and CO_2 pressure, a hydrophobic water-immiscible phase can be temporarily created and removed, when the desired chemical reaction is complete. A resulting non-polar organic product can be collected by separating it from the hydrophilic mixed state of the solvent system. Tremendous advantages of these switchable solvents are the facile isolation of the product and the simple recovery of the organic solvent from water by removing carbonate from the mixture. In this way, an energy-consuming distillation can be avoided completely. On the other hand, the used chemicals such as amines, amides and amidines are not always green. Many of them fail to fulfil the desired properties of green solvents, whereas others are acceptable in this respect. Nevertheless, this is a clever concept and might be helpful in the further development of green solvents and solvent systems.

Instead of using the presence of CO_2 as a trigger, temperature can be used for this purpose, as well. Also here, this change in conditions is accompanied by a transition from a one-phase to a two-phase system. This concept has been used for the extraction of proteins in water/IL mixtures,[54] for carrying out homogeneous reactions in polymeric solvent mixtures[55] and for the removal of heavy metals and organic pollutants from heavily contaminated sediments and sludges.[56]

1.3.5 Ionic Liquids (ILs)

In the last three decades, ILs have been hyped as green designer solvents with an inflationary amount of published literature.[57] Doubtlessly, there was a real hype with ILs starting in the 1990s. In this early period of interest, astonishing potential was attributed to them and the researching community was highly enthusiastic about their extraordinary diversity and properties.[58] The present paragraph about ILs is based on the review paper 'The hype with ionic liquids as solvents'.[57] A brief overview about IL structure and their special properties is given, followed by a discussion of IL applications.

1.3.5.1 Structure and Properties of Ionic Liquids

ILs are defined as organic salts with melting temperatures below 100 °C.[59] Since the middle of the 19th century, such low melting salts were mentioned in research from time to time.[60] The IL hype most probably started in the 1990s, when increasing research effort was made on properties and applications of ILs. This led to the publication of numerous studies and reviews. While common inorganic salts show long-range electrostatic interaction, the crystalline packing of ILs is hindered by the combination of bulky ions with low charge density. The resulting short-range electrostatic interactions deliver salts with moderate melting temperatures, sometimes even below room temperature. The structure and combination of an IL's cation and anion are decisive for its physico-chemical properties. The structures of typical cations and anions are shown in Fig. 1.3.5-1. Most publications deal with ILs containing N,N'-dialkyl-substituted imidazolium cations (Structure (1) in Fig. 1.3.5-1). In a different type of IL, the so-called TOTO-ILs, an oligoether carboxylate anion constitutes the bulky part of the IL. It is combined with smaller cations, such as alkali metal ions or simple quaternary ammonium cations. The low melting temperature is assumed to be a consequence of the flexibility of the ethylene oxide groups.[61]

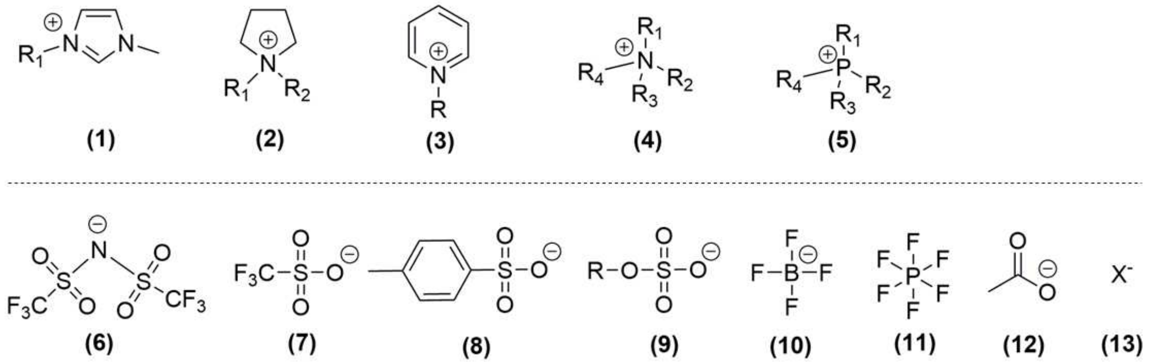

Fig. 1.3.5-1: Molecular structures of cations and anions typically used as IL constituents: (1) 1-alkyl-3-methylimidazolium, (2) 1,1-dialkylpyrrolidinium, (3) 1-alkylpyridinium, (4) tetraalkylammonium, (5) tetraalkylphosphonium, (6) bis-(trifluoromethanesulfonyl) amide, (7) trifluoromethanesulfonate, (8) tosylate, (9) alkylsulphate, (10) tetrafluoroborate, (11) hexafluorophosphate, (12) acetate and (13) halide.

Several special properties are attributed to the unique ionic structure of ILs. They have been considered as green solvents mainly because of their negligible vapour pressure and as such do not contribute to the volatile organic compounds' problematic. In addition, they are usually non-flammable, have extremely low melting temperatures compared to common salts and are highly conductive. They exhibit thermal and electrochemical stability and exist in a liquid state over a wide temperature range.[62] Due to electrostatic interactions, intermolecular van der Waals interaction and the formation of H-bonds, they are often characterized by high viscosities in comparison to conventionally used solvents. The amount of water or other impurities is a key factor influencing the physico-chemical properties of ILs.

Remarkable drawbacks have been detected in recent years of research. Often, the synthesis of (aprotic) ILs is costly and not green at all, many ILs are badly biodegradable and show a significant toxicity.[63] As Jessop pointed out, the synthesis of imidazolium-based cations requires a significant amount of chemical reaction steps, in particular involving non-green reactions.[64] Another dilemma about the greenness of ILs concerns the fact that the term ‘ionic liquid’ comprises a whole bunch of chemically highly different solvent and liquid classes with diverse characteristics, except for their nature as salts and liquids at low to moderate temperature. They are so ‘species-rich’ that the collective term becomes almost meaningless. As pointed out before, the main requirement of green solvents is their superior sustainability compared to the conventionally used solvents. In the huge flood of IL publications, it is often not apparent, if this requirement is fulfilled. While thousands of ‘potential applications’ of ILs have been proposed in literature, only a comparatively small number has finally been implemented into industrial processes. In the following, some of them will be discussed including their advantages over the previously used method.

1.3.5.2 Ionic Liquids in Organic Synthesis

Basic Acidic Scavenging utilizing Ionic Liquids (BASIL) Process: The BASIL process is probably the best-known industrial process implementing an IL. As indicated by its name, the IL functions as acid scavenging agent for the synthesis of alkylphenylphosphines (see Fig. 1.3.5-22). They are important precursors in the production of photoinitiators for UV curing of resins. In the course of this process, 1-methylimidazolium is converted into 1-methylimidazolium chloride, which is an IL with a melting point of 75 °C. This conversion is accompanied by a phase separation and the formation of a biphasic system. The IL bottom phase is removed and recycled for reuse. The upper phase with the alkylphenylphosphine precursor is collected and further processed.[65,66] The surrogated process utilized alkylamines as acid scavenging agents. This resulted in the formation of a thick, insoluble trialkylammonium halide salt slurry, along with inefficiencies and the need for a reaction solvent. The BASIL process was invented by BASF as alternative procedure and introduced to their site at Ludwigshafen in 2002. It is now performed on a multi-ton scale with significantly improved reaction rate and process efficiency compared to the previous method.[67]

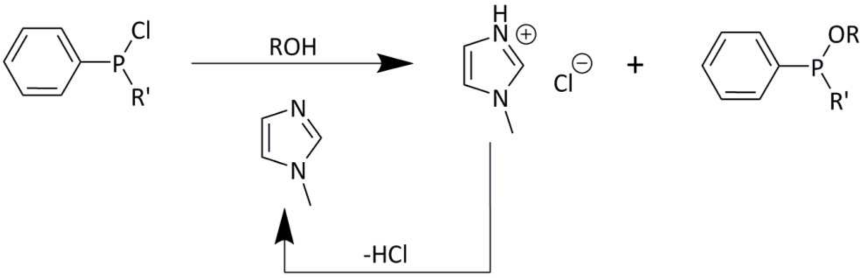

Fig. 1.3.5-2: Reaction scheme of the BASIL process.

Hydrosilylation: Hydrosilylation denotes the addition of a Si-H group to the C=C double bond of an olefin. Degussa reported the synthesis of organo-modified polydimethylsiloxanes by employing a biphasic reaction system with the catalyst dispersed in the IL-phase (see Fig. 1.3.5-3). The pure product phase is easily isolated and the IL containing the catalyst is reused without further purification.[68] As an advantage, no leaching of the catalyst into the product phase is observed and in contrast to the previously used method, the catalyst can be recovered and reused without any decrease in catalyst activity.[67]

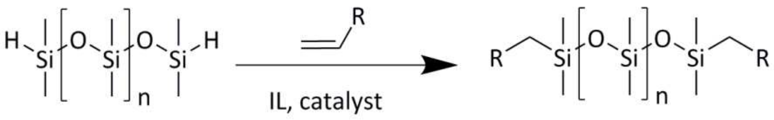

Fig. 1.3.5-3: Reaction scheme of the Degussa hydrosilylation reaction.

Hydroformylation with Supported Ionic Liquid Phase (SILP): The SILP technology employs an IL as solvent for a metal catalyst. A thin film of IL containing the catalyst is applied to an inert porous material, which is added as heterogeneous catalyst material to a reaction.[69] Hydroformylation denotes the conversion of olefins into aldehydes by the addition of syngas. It normally consists of carbon monoxide (CO) and hydrogen, which is associated to significant hazards and risks. In the novel IL process, CO_2 is utilized instead of CO.[70] This minimizes the risk and even transforms an undesirable greenhouse gas. While the IL was first employed as liquid solvent, immobilizing the IL to a solid substrate in terms of the SILP technology requires a considerably lower amount of the expensive IL.[67]

Chlorination of Diols: BASF patented and commercialized a reaction where an IL is employed as solvent.[65,71] It allows for the chlorination of alkyl diols to dichloroalkanes with hydrogen chloride (HCl) gas, in particular, the reaction of butanediol to 1,4-dichlorobutane (see Fig. 1.3.5-44). By using IL solvents instead of conventional organic solvents, the formation of side products could be drastically reduced. During the process, a phase separation occurs and the product phase is easily isolated. The IL can be used for the next run without any further work-up. Compared to the conventional reaction routes, the use of hazardous phosgene can be avoided and the product selectivity is significantly improved.[65]

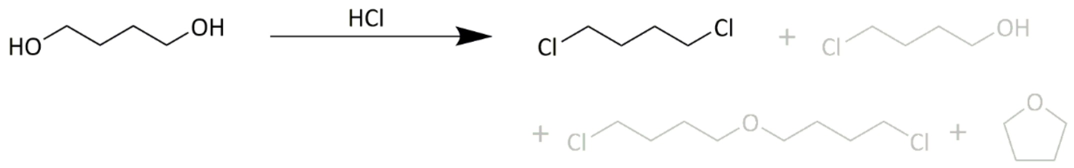

Fig. 1.3.5-4: Reaction scheme of the chlorination of 1,4-butanediol with potential side products indicated in grey.

1.3.5.3 Ionic Liquids for Biopolymer Processing

ILs, in particular those consisting of imidazolium-based cations and halide or acetate anions, were found to be able to dissolve cellulose in relatively mild conditions in concentrations up to 25 wt%.[72] It is reported that the IL anions disrupt the strong intermolecular cellulose network by the formation of H-bonding interactions with the hydroxyl functional groups of cellulose.[73] It can be processed into fibers and films easily from IL solutions. The cellulosic material can be separated by treatment with aqueous or ethanolic solutions, as it is insoluble, while the salt component is solubilized and washed away. There are two conventional processes for cellulose treatment referred to as Viscose process[74] and Lyocell process, respectively.[75] In the former process, cellulose is degraded in alkaline conditions and the cellulose backbone cannot be preserved. The latter one employs *N*-methylmorpholine oxide, which is not only costly, but also thermally instable. An application of ILs in the textile industry is highly interesting. At present, it is questionable, whether the implementation of IL technology to industry is economically feasible, yet. However, it is conceivable as future technology in textile processing.

1.3.5.4 Ionic Liquids for Gas Compression

Linde AG has presented a hydrogen fueling technology where the traditional metal piston is replaced by an IL-based compressor technique.[76] It utilizes the non-solubility of hydrogen in the IL and the non-volatility of the IL. Additional advantages are provided by the good lubrication properties of the IL and the avoidance of corrosion.[77] Linde has commercialized this technology in form of their Ionic Compressor 90 MPa – IC90 for the fast and high-performance fueling of hydrogen vehicles and promote its low operating cost, low energy consumption and high energy conversion efficiency. This compressor is already in operation at more than 100 hydrogen fueling stations.[78]

1.3.5.5 Ionic Liquids in Electrochemical Applications

Due to their high conductivity and their wide electrochemical window, ILs have been considered for applications in electrochemistry. They proved to be applicable for electrodeposition, e.g. for electroplating of chromium, where they showed beneficial effects in terms of energy consumption, waste water production, decreased toxicity and product quality.[65,79] Scionix merchandises IL-based technologies for electroplating and offers expertise and technical support for operators.[80] There is intensive ongoing research considering the use of ILs in batteries and dye-sensitized solar cells. In both cases, the use of an IL as liquid electrolyte is expected to result in elongated lifetimes and enhanced long-term performance of the devices. However, no commercial implantation of the IL technology in batteries or solar cells could be realized, yet.[67,81]

1.3.5.6 Ionic Liquids as Performance Additives

Several applications of ILs as performance additives in chemical formulations or solutions are known. Exemplarily, they are used in cleaning agents developed for the removal of small particles from high value surfaces in the electronic or automotive industry. The advantage in this case is that in contrast to other salts they do not precipitate on the nozzles used for the application of the cleaning agent. In general, ILs seem to be useful as additives in surface treating, air treating and cleaning agents due to their high tunability for the desired application. Accordingly, it must be assumed that such products containing ILs as performance additives are on the market, yet. In this case, the IL is not used as such, but rather as a salt additive. The fact that it is liquid at room temperature is negligible.[67]

In view of the IL hype and the huge inflation of IL research, their implementation to industry almost completely failed to appear. While they were assumed to be the solution for all problems at the beginning of the hype, they are now considered as niche products for specific applications. As shown above, there are a few reactions where they are already used as industrial reaction media. They seem to be promising in the fabrication of cellulose fibres and found commercialized application in gas compressors. Due to their outstanding customizability, they are examined for their application in electrochemistry. However, they did not have their break-through in this industry, so far. In none of the mentioned cases, ILs were used due to their sustainability, but rather because they showed improved performance for the specific application. The fact that they are non-volatile prevents them from being emitted to the atmosphere. Still, this is not enough to generally make this substance class and the processes it is used for, sustainable. In addition, they are often toxic, non-biodegradable and their synthesis is demanding. For a detailed evaluation of their sustainability, a thorough LCA of the process they are used for would be necessary. There are several practical limitations in the use of ILs, such as their yet high costs and their difficult handling: many ILs are hygroscopic and should be kept away from air to prevent water uptake, they are regularly highly viscous and not easy to remove from a reaction mixture, as they are not distillable, so that chemical modification is sometimes required for their separation. To improve the greenness of ILs, researchers replaced the imidazolium cation by more benign compounds, such as amino acids or choline-based cations combined with bio-based (non-fluorinated) anions, *e.g.* saccharides or natural carboxylates.[82] However, these naturally based ILs neither have found vast commercial application, so far.

1.3.6 Deep Eutectic Solvents (DESs)

Since the hype about ILs has slightly subsided, DESs as related substance group or 'the little cousin' of ILs aroused increasing interest. They exhibit similar solvent properties, but additionally several advantages in terms of production effort and cost. However, DESs are in a rather early stage of development and doubtlessly their potential is not yet fully behaviourd. With extensive ongoing research, the output of papers is huge at the moment in the fields of DES basic research and their consideration for a wide spectrum of applications. A selection of promising examples will be given, after some general remarks on DESs.

1.3.6.1 Structure and Properties of Deep Eutectic Solvents

The term 'deep eutectic solvent' is rather broad and the exact definition of the substance mixtures discussed herein not obvious. In theory, an eutectic mixture is characterized by the reduction of the melting temperature to the lowest possible value when combining two or more substances in a certain molar ratio (see Fig. 1.3.6-1). The concept of DES as such has been discussed since the beginning of the 21st century in terms of mixtures of an organic salt (usually a quaternary ammonium compound) with a molecular hydrogen-bond donor (HBD) or a metal chloride.[83,84] The different existing DES categories are listed in Tab. 1.3.6-1. The most widely studied DES consists of choline chloride and urea (see Fig. 1.3.6-2). This special combination results in a considerable reduction of melting temperatures from

302 °C (choline chloride) and 133 °C (urea) to 12 °C (ChCl-urea, 1 : 2) and is caused by the formation of a complex hydrogen-bond (H-bond) network.[84]

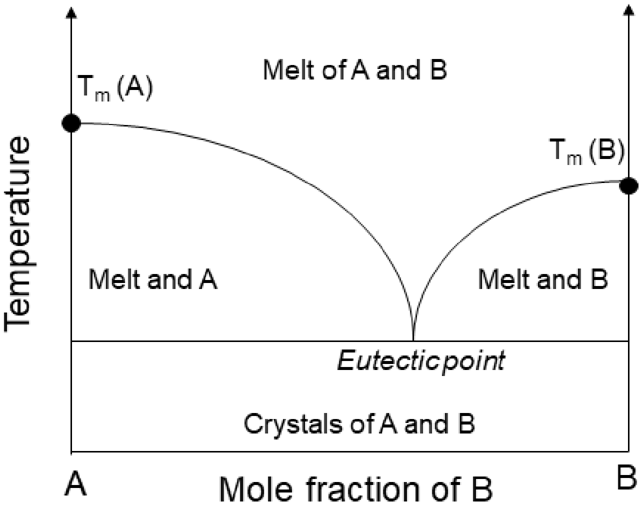

Fig. 1.3.6-1: Binary phase diagram illustrating the formation of a eutectic mixture by combining components A and B.

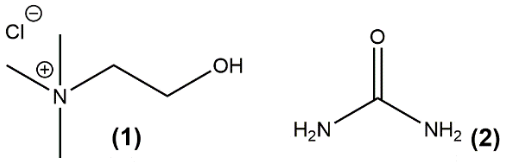

Fig. 1.3.6-2: Molecular structure of choline chloride (1) and urea (2). When combined in a ratio of 2 : 1, they form the most investigated DES.

Tab. 1.3.6-1: Categories of DESs.[85]

Category	**DES components**
Type I	Organic salt + metal salt
Type II	Organic salt + metal salt hydrate
Type III	Organic salt + HBD
Type VI	Metal salt + HBD

Recently, the term ‘Natural Deep Eutectic Solvent’ (NADES) enjoys increasing popularity.[86] It implies that both components (or even more in the case of multicomponent low melting mixtures (LMMs)) are ‘natural’ or of ‘biological origin’.

DESs can be allegorized as the ‘little cousins’ of ILs due to the fact that they share several characteristic properties, such as non-volatility, non-flammability, low melting temperatures, a wide liquid range as well as thermal and electrochemical stability.[85] In contrast to ILs, their preparation is extremely simple, as starting materials are mostly cheap and readily available. Various aspects, such as price, risk-potential, biodegradability etc. are controllable by the choice of the starting materials. This offers potential for designing green, inexpensive solvents for specific applications, just like the kind of designer solvents ILs were supposed to be.

1.3.6.2 Deep Eutectic Solvents in Organic Synthesis

Already well before DESs have gained popularity, eutectic mixtures have been realized to offer special conditions for organic reactions.[87] An obvious advantage is the designability of DESs according to the requirements of the reaction, as they cover a wide range of polarities and are able to dissolve a huge variety of reagents and catalysts.[88] Most DESs are water soluble. When an organic product is synthesized, the addition of water solubilizes the DES and the product phase-separates in form of a precipitate or an organic liquid phase. According to these basic advantages, they have been investigated as reaction media for numerous organic reactions, including redox reactions, addition reactions, cyclizations, substitution reactions, condensation-mediated reactions, multicomponent reactions, organometallic reactions, esterifications and biocatalytic reactions.[22,89] It is not known to the public, if any organic reactions in DESs are conducted on industrial scale, yet. However, several organic synthesis routes implementing DESs have been patented.[90]

1.3.6.3 Deep Eutectic Solvents as Ephemeral Solvents

As mentioned above, the best solvent is, of course, no solvent. This methodology is applicable only in very rare cases. However, there is a way to create an “ephemeral” solvent only during the reaction. If one of the reagents of an organic reaction is, for example, an organic acid, it can occur that it is liquefied by adding a salt such as choline chloride. The second reactant might then be well soluble in this liquid mixture and the reaction can start. In the end, by a mere addition of water, the salt can be separated from the hydrophobic water-insoluble product. This approach has been applied to synthesize caffeic acid phenethyl ester (CAPE), which is a molecule of pharmaceutical relevance.[91] Fig. 1.3.6-3 illustrates the approach: as caffeic acid is almost insoluble in the second reactant phenethyl alcohol, a DES consisting of choline chloride and caffeic acid (molar ratio 2:1) is built in a first step, in which phenethyl alcohol is completely soluble. The reaction is started by the addition of an acid catalyst. When the reaction is complete, the reaction mixture is poured into hot water, where choline chloride and residual phenethyl alcohol solubilize. The CAPE product precipitates upon cooling and can be collected by filtration. However, this smart concept has so far only been tested on laboratory scale.

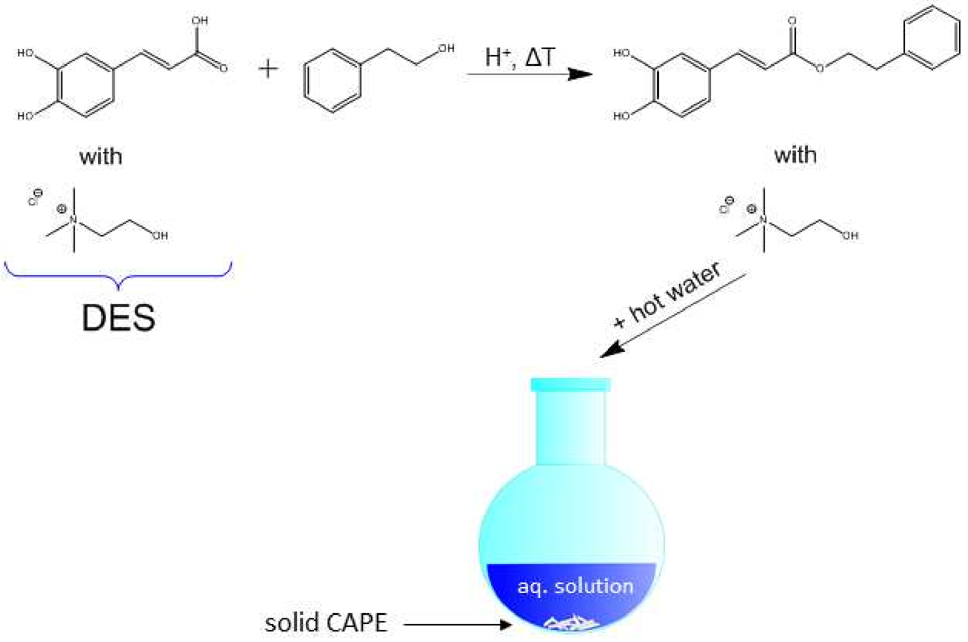

Fig. 1.3.6-3: Acid-catalyzed esterification of caffeic acid with phenethyl alcohol and subsequent collection of CAPE by the addition of water.[27, 91]

1.3.6.4 Deep Eutectic Solvents in Electrochemical Applications

DESs are found to be suitable solvents for electrodeposition of metals on electrode surfaces. Herein, metal salts are dispersed in an electrolyte solution and reduced at the cathode by applying an electric potential to form a solid coating on top of the electrode. DESs are attractive as solvents for this kind of applications, as they exhibit wide electrochemical windows, high conductivities and good solubility for metal salts. For instance, they proved to be promising for electroplating of chromium. They allow for the use of less toxic Cr (III) in replacement of the toxic and carcinogenic Cr (VI) compound.[92] Conventional processes are typically performed in aqueous solution. However, this approach suffers from several drawbacks: narrow electrochemical windows, reactivity towards certain metal derivatives and the resulting passivation of the surface, potential hydrogen evolution and costly waste water recycling. Compared to aqueous solutions, the DES electroplating technique allows for a reduction in energy consumption, avoidance of large volumes of aqueous waste and the formation of a high quality, corrosion resistant product. In addition, DESs can be employed for an extended range of metal-substrate combinations due to their chemical inertness and wider electrochemical windows.[93]

In principle, DESs can be used for a variety of electrochemical processes, especially electrodeposition of metals and metal alloys. However, the accomplishment of these kind of processes in aqueous solution is well established and it is questionable, if DESs can offer a competive advantage over the conventional methods. According to Bernasconi *et al.*, it is not realistic to expect DESs to replace aqueous systems in industry for processing commodity metals, such as iron, copper, nickel etc. Nevertheless, there are several specific cases with high demand for process improvement, in which the performance of DESs can be the method of choice. For instance, aqueous systems are not favourable for the deposition on substrates like aluminium and magnesium, as they tend to be passivated or corroded. Instead the use of DESs has been reported to allow for the deposition of nickel on aluminium.[94] Analogously, the deposition of zinc on magnesium is possible.[95] In addition, the use of DESs in future processes for zinc deposition can be benefitial, since there are issues with cathodic efficiency and substrate embrittlement when using aqueous systems.[96] As mentioned above, DESs are especially interesting for replacing the existing method for chrome electroplating in order to significantly reduce the risk potential of the process.[93]

So far, DESs are not used on a broad industrial scale for electrochemical applications. However, projects on pilot- and semi-industrial scale have been initiated as part of a productive collaboration between the Abbott group (University of Leicester), the IONMET consortium (EU project about 'New Ionic Liquid Solvent Technology to Transform Metal Finishing Products and Processes') and Scionix (the world's largest manufacturer of ILs and DESs).[97]

1.3.6.5 Miscellaneous Applications

Biopolymer processing: As reported earlier in this work (see section 1.3.5.3), ILs are capable of dissolving crystalline cellulose, but likewise they are restricted by high prices and low sustainability. DESs can be considered as their 'little cousins' with similar physico-chemical properties, but the additional advantages of lower prices and higher sustainability. In consequence, they also have a potential as solubilizing agents for cellulose and other biopolymers. In general, they exhibit poorer performance.[98] This makes sense when picturing the mechanism of cellulose dissolution: this process is dominated by the breakage of H-bonds and the formation of new ones between solvent and solute. Strong H-bonding interactions are already present in pure DESs. They compete with the cellulose, so that less H-bond sites are available for the solubilization process. A mixture of choline chloride and urea was not able to dissolve more than 0.2 wt% of crystalline cellulose.[99] However, strategies are being developed to improve the performance. Small successes could be achieved by supporting the cellulose decrystallization by ultrasound or functionalization of the DES with allyl moieties.[100,101] Best results in terms of high solubilities of cellulose (6.48 wt%) were obtained for an allyl-functionalized choline chloride-oxalic acid DES.[100] Unfortunately, this is by far not competitive with the 30 wt% cellulose solutions achieved by *N*-methylmorpholine oxide (Lyocell process)[102] or the 20 wt% cellulose solutions made possible by certain ILs.[103] It is not clarified yet, if the potential of DESs for dissolving cellulose is fully exploited. Future research will shade light on this question.

Extraction: Natural DESs have been thoroughly studied for the extraction of biomolecules in order to replace existing methods, in which volatile, flammable organic solvents are used. DESs show strong ability to dissolve protic molecules due to hydrogen bonding interactions. For instance, several groups reported considerable extraction yields for phenolic compounds in DES-based extraction systems.[104] Best results were obtained when adding a certain amount of water. Simultaneously observed beneficial effects thereof were a decrease in solvent viscosity (improved mass transport) and the reduction of the solvent cost. However, it is not clear, if the improved performance of these DES/water mixtures is really caused by the application of a DES. When combined with certain amounts of water, DESs are nothing else than concentrated salt solutions. Maybe the organic salt component of the DES (choline chloride) would be enough to achieve a similar extraction yield, but it is not reported, whether this kind of experiments were conducted. Finally, the isolation of an extraction product from a DES can cause problems, as the solubility of natural molecules in DESs goes back to strong, mostly H-bonding interactions, which are energetically costly to break. In most cases, researchers do not deliver appropriate information of the selectivity of a DES-based extraction process. This is misleading, as it regularly remains unknown, whether further undesirable substances are extracted as well and if additional efforts were required to remove them from the extract. It is doubted that DESs will be the extracting media of the future. In special cases, they might have a beneficial effect as additive. An evaluation of the future perspective of pure DESs in extraction processes can only be made with the availability of further concrete research results.

CO_2 capture: Several publications relate to the application of DESs as media for CO_2 capture.[105] They purpose the separation and subsequent storage of CO_2 from industrial gas streams. This topic is not to be discussed in detail in the scope of this work. In contrast to what is reported in these papers, techniques like this are believed to remain like a drop in the bucket and – at least in the near future – not to be able to solve the world's CO_2 problem or prevent the planet from the climate change.

It has to be mentioned that the presented DES applications and technologies are just a selection and even more 'potential applications' are reported in literature. As far as it is known publicly, DESs have not found their way to industry, yet. Their high densities and viscosities can be a potential problem for industrial use, especially for continuous flow processes. It is most likely that DESs have the potential to replace certain existing solvent systems in electrodeposition, as they convince with decent performance and reduced toxicity. At the actual state, it is not predictable, if DESs will meet the same fate as ILs or if they will find manifold application in industry in the near future. Practically speaking, the implementation of DESs in industrial applications might be easier, as their availability is better, they are less expensive and easier to prepare. In general, they are considered a good role model for green solvents, but their true environmental impact remains to be evaluated by means of LCA for each process they are used for.

Based on the information available about green solvents and the huge amount of research published every year, some concluding comments can be given:

(1) A solvent is only 'green', when it is more suitable than the present one for a particular application. 'More suitable' means, for example, that more of the criteria proposed by Gu and Jérôme are fulfilled.[25] Of course, it is necessary to also consider its competitiveness in price and performance. It has to be kept in mind that there is no absolutely green solvent. It always depends on the context of its application and 'green' therefore is only a relative term. The best way to study the greenness of a solvent is through LCA, such as regularly carried out for other chemicals and processes.

(2) ILs are widely overestimated as green solvents. DESs can be interesting alternatives. However, they still have to prove their usefulness. Too often, high values of viscosity and density impose significant disadvantages, although there are examples where these issues are overcome by outstanding performance benefits for specific applications.[93] True NADESs, *i.e.*, directly extracted from plants, are not yet used. This will be a challenging topic for the future.

(3) Besides relying on green solvents, it is also worth thinking about alternative solubilization concepts, such as switchable solvents, ephemeral solvents or hydrotropic and surfactant-based solubilization. When using ephemeral[91] and switchable[53] solvents as reaction media, the respective desirable system characteritics are created only during a certain stage of the reaction process. They serve as smart systems for an easy separation of the reaction product. Hydrotropic and surfactant-based aqueous systems are particularly suitable for extraction and purification processes and their use in chemical formulations. They will be discussed further in the next section.

1.4 Amphiphiles

In general, the term 'amphiphilic' describes a structural feature of chemical substances. The molecular structure of an amphiphile consists of a hydrophobic part and a hydrophilic part. Aliphatic hydrocarbon chains or aromatic ring structures regularly constitute the hydrophobic part of an amphiphile. The hydrophilic part typically is a polar head group, either charged or uncharged. Amphiphiles show remarkable properties in solution, as emulsifiers or as solubilization enhancers. As such, they can be divided into two sub-groups: classical surfactants and hydrotropes. This section briefly describes both types, points out some typical features that are relevant for the discussions in the present thesis and interrelates them to green chemistry.

1.4.1 Classical Surfactants

Surface active agents or surfactants belong to a chemical substance class that is ubiquitous in consumer products, such as cosmetics, food, paints or cleaning agents, and industry, such as for polymerization processes or in oilfield applications. They even occur in nature and the human body, *e.g.* as pulmonary surfactants in the lung or as constituents of biological membranes. The term surfactant itself already describes one of their most remarkable characteristics: the ability to decrease surface/interfacial tension at liquid-gas, liquid-liquid or liquid-solid interfaces as a consequence of their surface activity. According to their widespread use, they hold a huge global market volume of 29.9 billion US$ per year (2014) and the demand for surfactants is expected to grow further.[106] In recent years and due to the green chemistry movement, the popular wish for green surfactants emerged. This means that in the ideal case, surfactants should be completely natural or based on natural substances, they should be non-toxic and readily biodegradable.

1.4.1.1 Structure and Regular Classification

Most commonly, surfactants are classified according to their type of head group as anionic, cationic, zwitterionic or non-ionic. Typical surfactant structures for each class are shown in Fig. 1.4.1-1.

Sodium dodecyl sulphate (SDS) is the typical and most often studied anionic surfactant. Anionic surfactants in general are the most abundantly used surfactant class, e.g. in food formulations or as detergents. With their negative charged head group, they are sensitive to changes in the pH of the surrounding medium. Besides the sulphate head group, the sulfonate and carboxylate head groups play a major role.[107]

Cationic surfactants characterized by their positively charged head groups are often used to modify solid surfaces. They are electrostatically attracted by the naturally negatively charged surfaces, where they typically adsorb with their hydrophobic parts oriented away from the surface, so that the surface becomes hydrophobic, *i.e.*, water-repellent. A well-known representative of this group is cetyltrimethylammonium bromide (CTAB), which bears a positively charged quaternary ammonium head group.[107]

Zwitterionic surfactants are the least abundant class of surfactants. They hold both a positively and a negatively charged functional group. Therefore, they are highly pH sensitive and present as zwitterion only at their isoelectric point. Dipalmitoylphosphatidylcholine (DPPC) is a natural, zwitterionic surfactant and present in biological membranes. In research, it is frequently used as a model substance for membrane-related studies. Due to their low potential of skin or eye irritation, zwitterionic surfactants are often used in cosmetic and personal care products.[107]

Non-ionic surfactants constitute a wide group of surfactants. With their uncharged head group, they are compatible with all other surfactant types and non-sensitive to pH changes.

They regularly contain several ethylene oxide or propylene oxide groups. By varying the size of the polyoxyethylenated or polyoxypropylenated moiety and the kind of the hydrophobic part, the properties of the surfactants are well modifiable, *e.g.* in terms of water solubility. Their physico-chemical properties are highly temperature-dependent and their water solubility is decreased with increasing temperature. The so-called Brij and Tween surfactants comprise polyoxyethylene alkylethers and polyoxyethylene sorbate structures, respectively. These types of non-ionic surfactants are typically used as emulsifiers in chemical formulations and consumer products.[107]

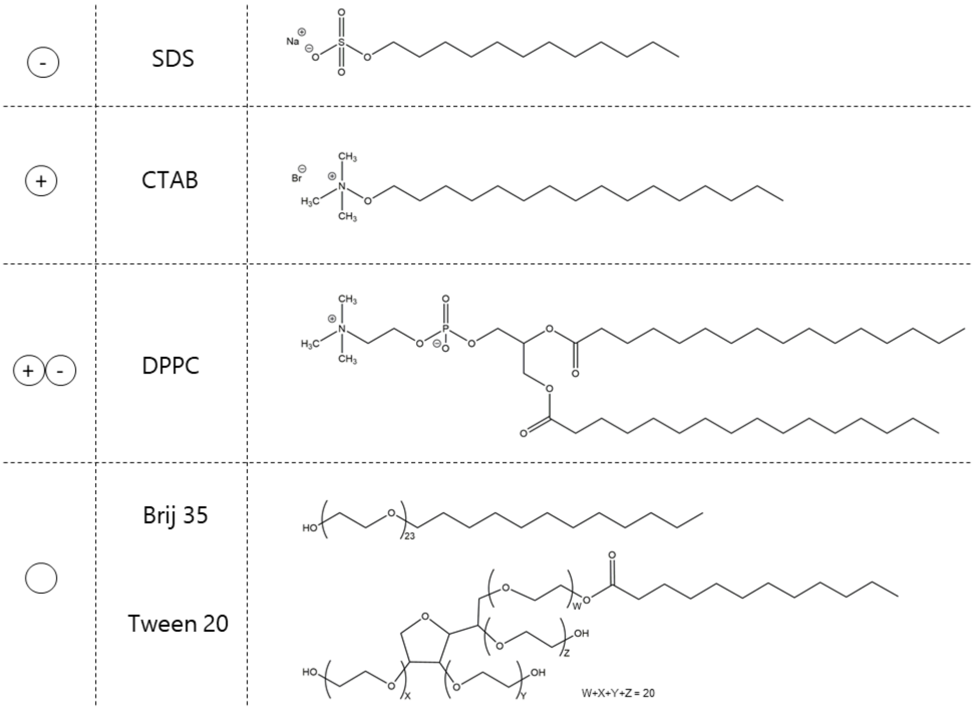

Fig. 1.4.1-1: Molecular structures of typical representatives of commonly used surfactant classes.

1.4.1.2 Special Types of Surfactants

Besides these basic classes of surfactants, halogenated and silicon-based surfactants shall be mentioned. They are characterized by outstanding surface activity compared to hydrocarbon-based surfactants. However, they often suffer from poor biodegradability.[107] Catanionic surfactants represent a further interesting type of surfactant systems. They consist of a cationic surfactant and an anionic surfactant serving as the respective counter-ion. This combination was found to have synergistic effects, which are interesting for applications as detergent or in household formulations. However, they tend to precipitate in aqueous solution and fundamental know-how and experience is required for their beneficial utilization.[108]

1.4.2 Hydrotropes

The term hydrotrope was originally introduced by Neuberg in 1916 to describe a water-soluble, organic compound that increases the solubility of hydrophobic compounds.[109]

However, this definition remains quite vague and applies as well to other substance classes, such as surfactants, co-solvents or salting-in compounds. In the following section, typical hydrotrope structures and possible mechanisms of solubilization enhancement will be described in order to give an overview of hydrotropes and to differentiate them from surfactants.

1.4.2.1 Structure

Typically, hydrotropes feature amphiphilic structure. In contrast to surfactants, their hydrophobic part is smaller. Therefore, they are not able to form micelles in aqueous solution.[110,111] However, molecules such as urea or antagonistic salts were also discussed in terms of hydrotropy, although they are not characterized by pronounced amphiphilicity.[112,113]

Typical representatives of hydrotropes are, for example, sodium salts of short chain alkanoates, alkyl sulphates and alkyl benzene sulfonates.[114,115] In particular, sodium xylene sulfonate (see Fig. 1.4.2-1) is a frequently used hydrotrope with applications in various chemical formulations, such as household products or industrial cleaning agents.[116] Even natural substances, such as sodium salicylate (NaSal) and other natural organic carboxylates were found to exhibit hydrotropic activity.[114] Interestingly enough, many of them have been found to act as antioxidants in the first place.

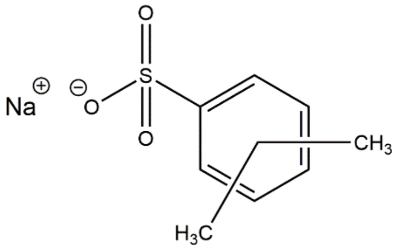

Fig. 1.4.2-1: Molecular structure of sodium xylene sulphonate (SXS).

1.4.2.2 Mechanism of Hydrotropic Solubilization

Generally, three classical hypotheses are discussed for a hydrotrope's mechanism of solubilization: (1) The formation of hydrotrope-solute complexes, (2) the hydrotrope as 'water structure breaker' and (3) self-aggregation of the hydrotrope (similar to micellation of surfactants). It is difficult to 'decide' for one of them as the ultimately valid mechanism. According to a recent review by Kunz, Holmberg and Zemb,[117] hydrotropic solubilization is driven by aggregation, particularly when significantly enhanced by the presence of the hydrophobic solute. In short, this behaviour is determined by a complex interplay of interactions between water, hydrotrope and solute.

The following opinion of the mechanism of hydrotropy has been agreed upon most lately: 'A hydrotrope is a substance whose structuring in water is enforced by the presence of a third, water-immiscible compound'.[117] In contrast to surfactants, hydrotropes do not form microemulsions or lyotropic liquid crystals. The aggregation behaviour in their binary systems is less defined and occurs only at concentrations in the molar range, whereas surfactants are characterized by critical micellar concentrations (CMCs) in the millimolar range (see section 1.4.3.2). Hydrotropes distinguish from co-solubilizers, by not causing a progressive increase in solubility of an organic compound with increasing concentration, but a rather rapid increase after a certain threshold concentration.

1.4.2.3 Natural Hydrotropes

Numerous hydrotropes are found in nature in the form of natural antioxidants, hormones and other metabolites.[118] It is assumed that also in their natural environment, they often play a dual role. On the one hand, they fulfill a commonly recognized task that is well known and established for the respective class of substances, *e.g.* as antioxidant. On the other hand, they might also function as solubility enhancer for other natural molecules, *i.e.* a ‘second purpose’. The following example serves to illustrate this phenomenon: the essential oil of *Nanah* mint is extremely hydrophobic and not water-soluble. However, it can be extracted from fresh leaves in water. It is assumed that the leaves contain a natural solubilizer facilitating the solubilization of the hydrophobic oil in water. These types of ‘solvents’ are considered highly interesting for chemical formulation, *e.g.* in cosmetics, as a certain component could serve a dual purpose: exemplarily both as solubilizer and as antioxidant.

1.4.3 Physico-chemical Properties

1.4.3.1 Adsorption at Liquid/Air Interfaces

In general, molecules located at the surface of a material feature a higher energy compared to those situated in the bulk. Therefore, work is required to hypothetically relocate a molecule from the bulk to the surface. Considering an aqueous amphiphile solution in contact with air as the second phase, the hydrophobic moiety of an amphiphilic molecule exhibits little attraction to the aqueous solvent, while the hydrophilic group shows favourable solvent interactions. In order to decrease the free energy of the overall system, the contact between hydrophobic moieties and solvent is minimized, thereby expelling some of the amphiphilic molecules to the surface. In this process, amphiphiles arrange in a manner where the hydrophilic parts are oriented towards the solvent and the hydrophobic parts towards air. This results in a reduction of the surface tension.[107]

A reduction in the value of surface tension is a typical observation for aqueous solutions of amphiphiles. Typically, this can be measured by means of the Wilhelmy plate or pendant drop technique. In order to compare the performance of amphiphiles in terms of reducing the surface tension of aqueous solutions, their ‘efficiency’ and ‘effectiveness’ can be considered. The efficiency is related to the surfactant bulk concentration required to reduce the surface tension to or by a certain value. For quantitative analysis, the concentration required to decrease the surface tension by 20 mN/m with respect to the pure solvent value is frequently used. In contrast, the effectiveness of a surfactant describes the maximum reduction of surface tension obtainable by the use of a certain surfactant. Regularly, the surface tension value at the CMC is used for quantitative comparison.[119]

The Gibbs adsorption isotherm is a theoretical approach to describe the adsorption of surface active substances at interfaces. In this approach, the molar surface excess concentration Γ_i of an ionic amphiphile i in dilute solution can be related to the concentration-dependent change in surface tension σ and described with the following equations:

$$\Gamma_i = \frac{n_i}{A} = \frac{1}{A_i \cdot N_A} \tag{1}$$

$$\Gamma_i = -\frac{1}{mRT} \cdot \left(\frac{\delta\sigma}{\delta lnc_i}\right) \tag{2}$$

In Eq. 1, n_i denotes the molar amount of solute i at the interfacial area A, A_i represents the mean area that one solute molecule occupies at the surface and N_A is the Avogadro constant. The surface excess concentration can be determined experimentally from surface tension measurements applying Eq. 2 with the following parameters and constants: gas constant R, temperature T and the slope of the concentration dependent surface tension isotherm. The factor m = 2 accounts for the dissociation of an ionic solute and the apparent increase in the particle density in the bulk.[119] It is to be noted that the Gibbs adsorption isotherm is only valid for dilute aqueous solutions, *i.e.* it should only be used for the evaluation of surfactant solutions.

In addition, the adsorption behaviour of amphiphiles at the liquid/air interface and the corresponding formation of monolayers can be studied by means of surface pressure-area isotherms obtainable from the Langmuir trough technique. In most modern setups, the aqueous liquid phase is filled into a Teflon trough and the amphiphile is subsequently spread on the surface. The latter is compressed by a mobile Teflon barrier, whereby the amphiphile density at the interface is varied according to a defined protocol. The surface pressure is determined by means of a Wilhelmy plate. A schematic setup is presented in Fig. 1.4.3-1.

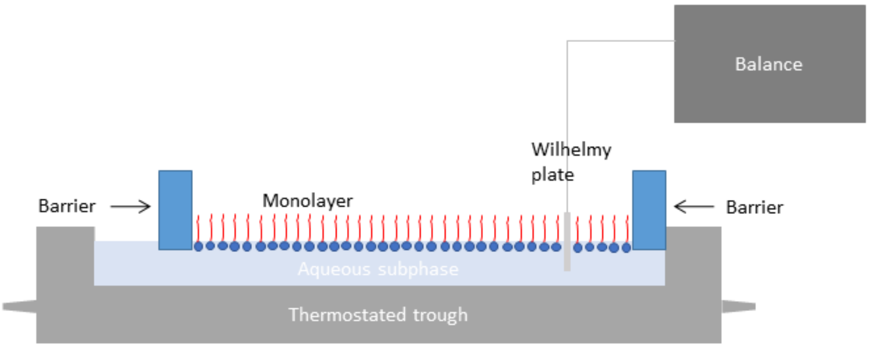

Fig. 1.4.3-1: Setup of a conventional Langmuir trough for investigating monolayers at the water/air interface.

A so-called surface compression isotherm is obtained by plotting the recorded surface pressure π against the mean area A_i per surfactant molecule. The surface pressure is defined as the difference between the surface tension of the pure solvent and the surface tension measured after compressing the surface in presence of the solute ($\pi = \sigma_W - \sigma$).[120]

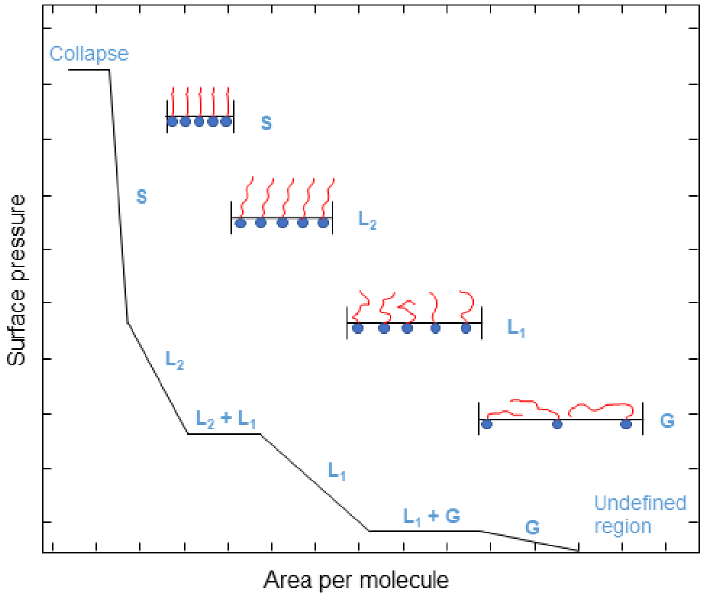

Fig. 1.4.3-2: Typical surface pressure-area isotherm featuring different phases of a Langmuir monolayer and the arrangement of surfactant molecules in the respective phase. This figure is based on Ref. [120].

A typical surface compression isotherm is given in Fig. 1.4.3-2. Kinks in the curve correspond to phase transitions. In regions, where the curve exhibits surface pressure plateaus, two co-existing phases are present. By compressing the surface, gas-like, liquid-like and solid-like monolayer states occur subsequently. The characteristic molecular arragments are shown in Fig. 1.4.3-2 and described in more detail in Tab. 1.4.3-1. At high surface pressure, molecules are squeezed out of the monolayer and the monolayer eventually collapses.[120]

Tab. 1.4.3-1: Overview of characteristic Langmuir phase behaviours of a surfactant monolayer at the water/air interface.

	Phase	Behaviour
G	Gaseous	Molecules are far apart from each other, no interactions (like ideal gas).
L_1	Liquid extended	Low density liquid state, no positional or orientational order.
L_2	Liquid condensed	High density liquid state, long-range orientational order and quasi-long-range positional order.
S	Solid	Densest state before collapse.

1.4.3.2 Self-Assembly in Aqueous Solution

Amphiphilic molecules are able to self-assemble and to form aggregates in aqueous solution. Then, their hydrophobic parts are directed to the interior of the aggregate, while the hydrophilic head groups are in contact with the solvent. The free energy of the overall system is reduced by a reduction of the number of unfavourable interactions between the solvent and the hydrophobic moieties. The resulting hydrophobic effect is dominated by a gain in entropy when water molecules are released from the initial hydration shells to the bulk. The size and shape of the aggregates is determined by the type of amphiphile and other conditions, such as temperature, amphiphile concentration and presence of electrolytes.

Aggregation in aqueous solution is generally found to occur beyond a certain amphiphile threshold concentration, which is referred to as critical aggregation concentration (CAC) and as critical micellar concencentration (CMC) in the case of surfactants. The deviating terminology, *i.e.* CAC and CMC, is due to the shape of the corresponding aggregates. In the easiest case, surfactants are known to form spherical aggregates – micelles – in aqueous solution at concentrations above their CMC. In contrast, amphiphiles featuring smaller hydrophobic moieties aggregate over broader concentration ranges and form aggregates of less defined shapes.

There are several physical properties of an amphiphile solution changing upon the formation of aggregates. They can be used to determine the CAC. Most prominent among them are surface tension and conductivity (see Fig. 1.4.3-3). The surface tension of water is reduced by increasing the amphiphile concentration and remains at a constant value when the CAC is reached. The conductivity of an aqueous ionic amphiphile system increases linearly with increasing amphiphile concentration. Exceeding the CAC, the rise proceeds at a lower slope. This is caused by the ionic amphiphile charge carriers assembling to larger aggregates, which move more slowly compared to the monomers.

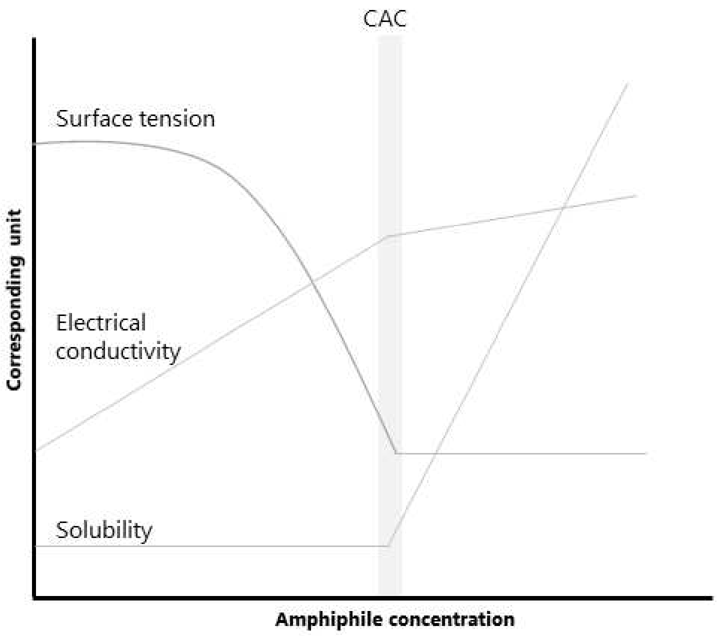

Fig. 1.4.3-3: Evolution of solution properties with increasing amphiphile concentration.[121]

Hopkins *et al.* visualized the different aggregation behaviours of surfactants and hydrotropes relying on surface tension curves of a homologous series of sodium-*p*-*n*-alkylbenzoates.[122] The decrease in the surface tension of aqueous solutions of long-chain homologues was earlier and steeper, *i.e.* it occurred at lower concentrations and over a more narrow concentration range. The break in the curve indicating the CAC/CMC was well-defined. In contrast, the short-chain compounds of the studied series led to a decrease of the surface tension only at higher concentrations and the kink at the CAC was less pronounced. It is assumed that this is due to the formation of less distinct, non-spherical micelles, when the hydrophobic part of the amphiphile is small.

Depending on surfactant shape and concentration, various structural archetypes, besides classical micelles, can be formed in aqueous solution: cylindrical micelles, lamellar phases, bicontinuous phases, vesicles and inverse micelles. The so-called packing parameter N_S (see Eq. 3 for its definition) considers the volume V_h and the length l_h of the hydrophobic tail and the cross-sectional area a_0 of the headgroup to predict the shape of the resulting aggregates.[110,123,124]

$$N_S = \frac{V_h}{l_h \cdot a_0} \qquad \textbf{(3)}$$

Tab. 1.4.3-2 gives an overview of the expected aggregate shapes.

Tab. 1.4.3-2: Aggregate shapes predicted by the packing parameter N_S.

N_S	**Aggregate structure**
<⅓	Spherical micelles
⅓ - ½	Cylindrical micelles
½ - 1	Lamellar structure
>1	Inverse micelles

Sufficiently water-soluble surfactants are – in contrast to hydrotropes – able to form liquid crystalline phases in aqueous solution. The presence of surfactant micelles themselves at a high concentration allows for their assembly to various further ordered arrangements. This is generally accompanied by a considerable increase in the viscosity of the solution. The binary phase diagram shown in Fig. 1.4.3-4 suggests the following simplified evolution of the dominant aggregate structures corresponding to the composition of the aqueous mixture and the temperature upon increasing surfactant concentration: surfactant monomers (below CMC) → micellar solution (L_1) → hexagonal phase (H_1) → cubic bicontinuous phase (V_1) → lamellar phase (L_α) → inverse micelles (L_2). The monomers' arrangement within these structures is illustrated in Fig. 1.4.3-5. Hexagonal and lamellar phases are anisotropic and therefore visible in a polarizing microscope. It is typical for the hexagonal phase to appear in fanlike manner and for the lamellar phase to exhibit maltese crosses in polarized images. In contrast, cubic phases – either cubic arrangements of spherical micelles or cubic bicontinuous phases – are isotropic and for this reason not detectable by means of polarized microscopy.[123,125]

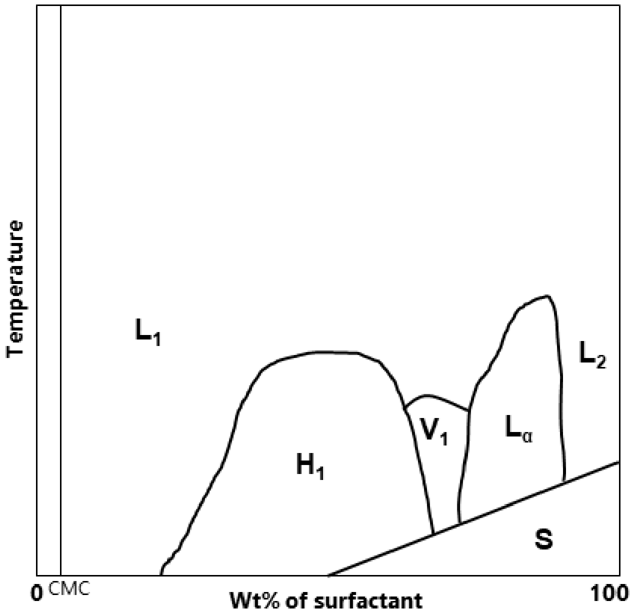

Fig. 1.4.3-4: Binary phase diagram of an aqueous surfactant solution showing different aggregation phases above the CMC: micellar solution (L_1), hexagonal phase (H_1), cubic bicontinuous phase (V_1), lamellar phase (L_α) and inverse micelles (L_2).[125]

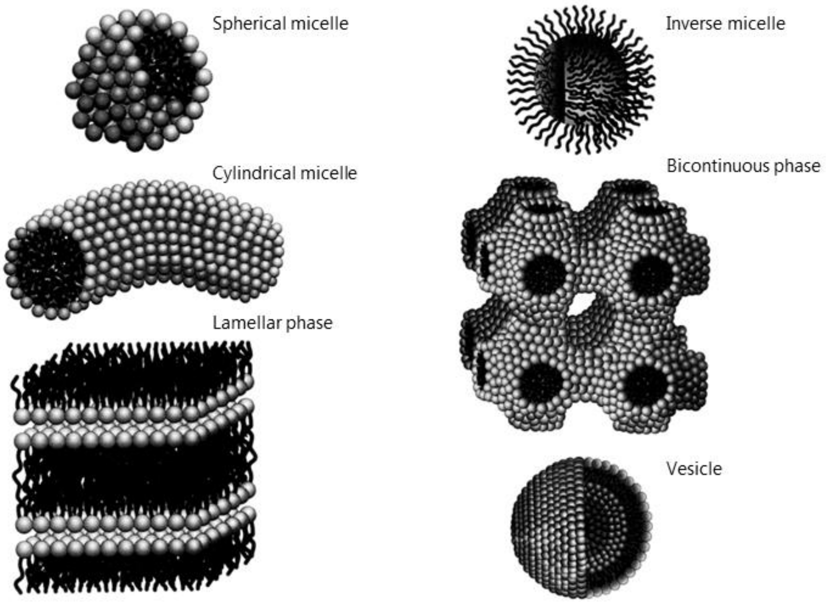

Fig. 1.4.3-5: Different types of surfactant self-assembly in aqueous solution.[123]

The self-assembly of amphiphiles in aqueous solution reveals individual characteristics and creates a colloidal system. Aqueous amphiphile systems promote the solubilization of a third hydrophobic component, which will be described in the following section.

1.4.3.3 Solubilization in Aqueous Amphiphile Systems

An important aspect of amphiphiles is their ability to increase the solubility of a third component – either gaseous, liquid or solid – in an aqueous solution and the compatibility of polar and non-polar components with each other. The system decreases its free energy by incorporating the solute/non-polar component inside the amphiphilic aggregate, where it is still in dynamic interchange with the continuous phase. Thereupon, the amphiphile takes the role of a solubilization enhancer, emulsifier or dispersing agent and enables the formation of clear solutions, microemulsions, emulsions, dispersions or foams.

The ability of amphiphiles to solubilize hydrophobic solutes is referred to as hydrotropic efficiency in the following discussion. It is typically measured by determining the saturation concentration of a hydrophobic solute in a concentration series of aqueous amphiphile solutions. A common sample solute is the hydrophobic dye disperse red 13 (DR13) (see Fig. 1.4.3-6).[113,126] It is added to the amphiphile solution in excess and the amount of solubilized dye is determined by UV/Vis spectrometry. Either the amount of solubilized DR13 or the optical density measured via UV/Vis spectrometry is plotted against the concentration of the amphiphile in the respective solution. For typical hydrotropes, the curve rises steeply beyond a certain threshold amphiphile concentration. The latter is associated with the minimum hydrotropic concentration (MHC), which is a characteristic measure of the hydrotropic efficiency. It is related to the concentration, where self-aggregation allows for the solubilization of the solute. In the case of true surfactants, it corresponds to their CMC. In the case of hydrotropes, the MHC detected by dye solubility measurements is often lower compared to the CAC detected in the binary aqueous system. This is related to the effect of the solute, which obviously promotes the formation of aggregates.[117]

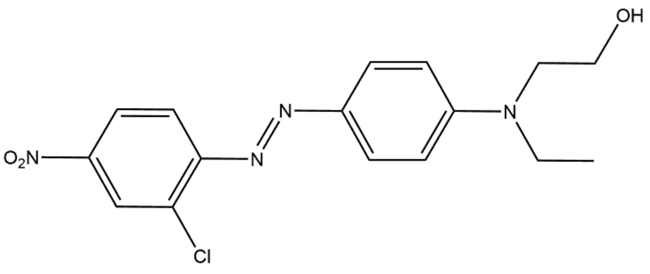

Fig. 1.4.3-6: Molecular structure of the hydrophobic dye DR13.

Salting-in and salting-out effects of additives added to a water/polyethylene glycol (PEG) mixture were originally determined for Hofmeister ions. They caused either an increase (salting-in) or a decrease (salting-out) of the system's homogeneous phase region.[127] More recently, it was shown to be useful for determining the hydrotropic efficiency of organic short-chain molecules: the stronger the salting-in effect, the higher is the hydrotropic efficiency.[128] When the studied amphiphile is of charged nature, this effect is considered to be the result of an interplay of hydrophobic interactions of the hydrophobic tails and ion-specific effects between charged head groups, which will be discussed in the next section.

1.4.3.4 Ion-Specific Effects

The behaviour of charged amphiphiles in solution is significantly influenced by Coulomb-type interactions between charged head groups and counter-ions. Their underlying ion-specific effects are a frequently studied and arbitrarily complex issue in chemical science. The aim of this section is to give a short overview of the fundamentals and to relate the topic to relevant aspects, such as salting-in or -out behaviour.

More than 130 years ago, Hofmeister was the first to systematically study specific ion effects of inorganic salts, particularly the influence on protein solutions. This research eventually resulted in the famous Hofmeister series, which orders inorganic ions according to their 'water withdrawing capability'.[129] Ions initiating strong hydration regularly tend to expel other solutes from the solution (salting-out). On the contrary, weakly hydrated ions promote the solubilization of other solutes (salting-in).

Collins's concept of 'matching water affinities' addresses the interaction strength of ions with water relative to the water-water interactions as a reference point of the interplay.[130–132] Accordingly, ions are classified as kosmotropes and chaotropes. While kosmotropes denote small ions characterized by high charge density and tightly bound hydration shells (high water affinity, 'hard'), chaotropes are large ions with low charge density and loosely bound hydration shells (low water affinity, 'soft') (see Tab. 1.4.3-33).

Tab. 1.4.3-3: Collection of properties and effects of chaotropes and kosmotropes.

Chaotrope	**Kosmotrope**
- Large ions	- Small ions
- Low charge density	- High charge density
- Weakly hydrated	- Strongly hydrated
- Salting-in	- Salting-out
- Destabilizing proteins	- Stabilizing proteins

According to Collins's concept, strong ion association between oppositely charged ions occurs, in case of similar water affinity, *i.e.* both are chaotropes or both are kosmotropes. This finding is rationalized by the formation of inner sphere ion pairs, *i.e.*, one ion pair shares one hydration shell. The ion-ion interaction of kosmotropic, oppositely charged ions in solution is stronger compared to ion-water interactions, so that the associated ion-pair shares one hydration shell. Likewise, the individual hydration shells around two chaotropic, oppositely charged ions break up, when they meet in aqueous solution; only the driving force is different. In this case, the water-ion interactions are weaker in comparison to the water-water interactions, so that one common hydration shell is formed around the chaotropic ion pair. The described effects are less pronounced, when a chaotropic ion encounters an oppositely charged kosmotropic ion in solution. Their tendency to form an ion pair and share a common hydration shell is therefore significantly lower.[130–132]

This principle is applicable not only to inorganic Hofmeister ions, but also to charged molecular head groups of organic macromolecules, such as ionic hydrotropes and surfactants. Carboxylate and phosphate head groups are classified as rather kosmotropic, while sulphate, sulfonate and quaternary ammonium head groups are ranked as chaotropic.[133] With this principle, the degree of association between charged amphiphiles and their counter-ions can be predicted and resulting effects or properties in aqueous solution can be rationalized.

1.4.4 Green Surfactants and Hydrotropes

Surfactants and hydrotropes are widely used in a variety of applications, such as cleaning products, cosmetics, pharmaceutics, food industry, textile industry, mining and oil industry, dyes and coatings, leather and paper industry and polymers and plastics. This leads to a significant precedence of avoiding negative influences of these substance classes on the environment.

A considerable portion is discharged by waste water. In order to avoid ecological issues through amphiphile release and accumulation in aquatic systems or landfills, it is necessary to ensure a sufficiently high degree of biodegradability. A number of standardized test methods is available to obtain quantitative data on the biodegradability of surfactants and hydrotropes. A typical technique to assess the biodegradability in solution is described in the OECD guideline 301 F and ISO 9408. In this test, the oxygen consumption during a 28 day degradation process is measured and used to calculate the biodegradability as the percentage of degraded compound.[110,134] In general, the biodegradability of surfactants with linear alkyl chain is found to be improved compared to branched ones.[135] The biogedradability of cationic quaternary ammonium surfactants can be increased by implementing hydrolyzable ester functions. These kinds of surfactants are known as 'esterquats'.[110]

Especially due to their application in pharmaceutics, health care or cosmetics, it is crucial for hydrotropes and surfactants not to impose any hazard or damage to humans. While their oral toxicity is usually low, eye or skin irritancy caused by surfactants and hydrotropes are a relevant issue.[136] Often, the origin of such irritancies is cell death, i.e. cytotoxicity,[137] so that cell tests are considered to be a suitable method to investigate the toxicity of surfactants and hydrotropes.

With regard to the 12 Principles of Green Chemistry, the use of natural amphiphiles or amphiphiles from renewable resource are favoured over petrochemical substances. Derivatives of natural fats and oils (classical soaps), carbohydrate-based surfactants (alkyl polyglycosides, sorbitan esters, sucrose esters), lecithin – a mixture of phospholipids - and saponines are ranked among these biosurfactants. Requirements for them to be valuable alternatives in industry are competitiveness in terms of price, quality, performance and availability. Exemplarily, lecithin meets these requirements quite well and therefore it is regularly used as emulsifier in the food and feed industries.[138]

1.5 References

[1] E. Heller, *Wie Farben wirken. Farbpsychologie, Farbsymbolik, kreative Farbgestaltung,* 8. Auflage, Rowohlt Taschenbuch Verlag, Reinbek bei Hamburg, **2015**.

[2] P. T. Anastas, J. C. Warner, *Green chemistry. Theory and practice,* 1. ed., Oxford Univ. Press, Oxford, **2000**.

[3] a) "Green Chemistry - A Historical Perspective", to be found under http://www.warnerbabcock.com/green-chemistry/a-historical-perspective/; b) J. A. Linthorst, *Found. Chem.* **2010**, *12*, 55–68; c) M. Poliakoff, J. M. Fitzpatrick, T. R. Farren, P. T. Anastas, *Science* **2002**, *297*, 807–810; d) P. Tundo, F. Aricó, *Chem. Int.* **2007**, *29,* 4–7.

[4] R. Carson, L. Lear, E. O. Wilson, *Silent spring,* 40th anniversary ed., 1st Mariner Books ed., Houghton Mifflin, Boston, **2002**.

[5] "Chronologie umweltpolitischer Meilensteine", to be found under https://secure.bmu.de/service/chronologie/.

[6] M. Ittershagen, *Vorregistrierung für REACH läuft an. Umweltbundesamt unterstützt Unternehmen mit Tipps und Arbeitshilfen bei der REACH Umsetzung*, Dessau-Roßlau, **2008**.

[7] a) "Die Klimakonferenz in Paris", to be found under https://www.bmu.de/themen/klima-energie/klimaschutz/internationale-klimapolitik/pariser-abkommen/; b) *Übereinkommen von Paris*, **2015.**

[8] "India Population 2019", to be found under http://worldpopulationreview.com/countries/india-population/.

[9] " Bruttoinlandsprodukt in Indien (BIP) bis 2018", to be found under https://de.statista.com/statistik/daten/studie/19369/umfrage/bruttoinlandsprodukt-in-indien/, **2019**.

[10] B. Smith, "India: Environmental Issues, Policies and Clean Technology", to be found under www.azocleantech.com, **2015**.

[11] A. A. Koutinas, C. Du, R. H. Wang, C. Webb in *Introduction to Chemicals from Biomass* (Eds.: J. H. Clark, F. E. I. Deswarte), John Wiley & Sons, Ltd, Chichester, **2008**.

[12] R. L. Lankey, P. T. Anastas, *Ind. Eng. Chem. Res.* **2002**, *41*, 4498–4502.

[13] D. Kralisch, D. Ott, D. Gericke, *Green Chem.* **2015**, *17*, 123–145.

[14] M. Secchi, V. Castellani, E. Collina, N. Mirabella, S. Sala, *J. Clean Prod.* **2016**, *129*, 269–281.

[15] W. Keim in *Methanol: The Basic Chemical and Energy Feedstock of the Future* (Eds.: M. Bertau, H. Offermanns, L. Plass, F. Schmidt, H.-J. Wernicke), Springer Berlin Heidelberg, Berlin, Heidelberg, **2014**.

[16] IEA Bioenergy, "Biorefineries: adding value to the sustainable utilisation of bimoass", to be found under https://www.ieabioenergy.com/wp-content/uploads/2013/10/Task-42-Booklet.pdf.

[17] J. H. Clark, F. E. I. Deswarte (Eds.) *Introduction to Chemicals from Biomass*, John Wiley & Sons, Ltd, Chichester, UK, **2008**.

[18] A. Zaid, *Glossary of biotechnology and genetic engineering*, FAO, Rome, **1999**, *Vol. 7*.

[19] M. Fasciotti, *Sust. Chem. Pharm.* **2017**, *6*, 82–89.

[20] The Royal Swedish Academy of Sciences, "Directed evolution of enzymes and binding proteins. Scientifc Background on the Nobel Prize in Chemistry 2018", to be found under https://www.nobelprize.org/prizes/chemistry/, **2018**.

[21] a) K. Kalyanasundaram, M. Graetzel, *Curr. Opin. Biotechnol.* **2010**, *21*, 298–310; b) A. F. Collings, C. Critchley (Eds.) *Artificial photosynthesis. From basic biology to industrial application,* Reprint ed., Wiley-VCH, Weinheim, **2008**.

[22] D. A. Alonso, A. Baeza, R. Chinchilla, G. Guillena, I. M. Pastor, D. J. Ramón, *Eur. J. Org. Chem.* **2016**, 612–632.

[23] J. H. Clark, T. J. Farmer, A. J. Hunt, J. Sherwood, *Int. J. Mol. Sci.* **2015**, *16*, 17101–17159.

[24] P. T. Anastas, J. C. Warner, *Green chemistry. Theory and practice,* 1. ed., Oxford Univ. Press, Oxford, **2000**.

[25] Y. Gu, F. Jérôme, *Chem. Soc. Rev.* **2013**, *42*, 9550–9570.

[26] P. G. Jessop, *Faraday Discuss.* **2018**, *206*, 587–601.

[27] K. Häckl, W. Kunz, *C.R. Chim.* **2018**, *21*, 572–580.

[28] a) S. Chang, M.-F. Sheu, S.-M. Chen, *J. Appl. Polym. Sci.* **1983**, *28*, 3289–3300; b) G. W. Halek, W. T. Freed, J. S. Schaul, R. W. Rupp, S. L. Pauls, US4223128A, **1980**; c) S. A. Wadekar, U. S. Agarwal, W. H. Boon, V. M. Nadkarni in *Solid State Polymerization* (Eds.: C. D. Papaspyrides, S. N. Vouyiouka), John Wiley & Sons, Inc, Hoboken, NJ, **2009.**

[29] J. B. Ravnsbæk, T. M. Swager, *ACS Macro Lett.* **2014**, *3*, 305–309.

[30] A. Stolle, T. Szuppa, S. E. S. Leonhardt, B. Ondruschka, *Chem. Soc. Rev.* **2011**, *40*, 2317–2329.

[31] a) M. E. Lucchesi, F. Chemat, J. Smadja, *J. Chromatogr. A* **2004**, *1043*, 323–327; b) M. E. Lucchesi, F. Chemat, J. Smadja, *Flavour Fragr. J.* **2004**, *19*, 134–138.

[32] a) H. C. Hailes, *Org. Process Res. Dev.* **2007**, *11*, 114–120; b) C.-J. Li, L. Chen, *Chem. Soc. Rev.* **2006**, *35*, 68–82; c) M.-O. Simon, C.-J. Li, *Chem. Soc. Rev.* **2012**, *41*, 1415–1427.

[33] D. C. Rideout, R. Breslow, *J. Am. Chem. Soc.* **1980**, *102*, 7816–7817.

[34] S. Dabbert, I. Lewandowski, J. Weiss, A. Pyka, *Knowledge-Driven Developments in the Bioeconomy. Technological and Economic Perspectives*, Springer International Publishing, Cham, **2017**.

[35] J. I. García, H. García-Marín, J. A. Mayoral, P. Pérez, *Green Chem.* **2010**, *12*, 426–434.

[36] a) A. Wolfson, C. Dlugy, Y. Shotland, *Environ. Chem. Lett.* **2007**, *5*, 67–71; b) A. E. Díaz-Álvarez, J. Francos, P. Croche, V. Cadierno, *CGC* **2013**, *1*, 51–65.

[37] A. Wolfson, A. Snezhko, T. Meyouhas, D. Tavor, *Green Chem. Lett. Rev.* **2012**, *5*, 7–12.

[38] a) A. Mohammad, Inamuddin, *Green solvents*, Springer, Dordrecht, **2012**; b) A. Wolfson, A. Atyya, C. Dlugy, D. Tavor, *Bioprocess. Biosyst. Eng.* **2010**, *33*, 363–366.

[39] A. Corma, S. Iborra, A. Velty, *Chem. Rev.* **2007**, *107*, 2411–2502.

[40] a) D. F. Aycock, *Org. Process Res. Dev.* **2007**, *11*, 156–159; b) V. Pace, P. Hoyos, L. Castoldi, P. Domínguez de María, A. R. Alcántara, *ChemSusChem* **2012**, *5*, 1369–1379.

[41] A.-G. Sicaire, M. Vian, F. Fine, F. Joffre, P. Carré, S. Tostain, F. Chemat, *Int. J. Mol. Sci.* **2015**, *16*, 8430–8453.

[42] a) E. Ismalaj, G. Strappaveccia, E. Ballerini, F. Elisei, O. Piermatti, D. Gelman, L. Vaccaro, *ACS Sustainable Chem. Eng.* **2014**, *2*, 2461–2464; b) G. Strappaveccia, L. Luciani, E. Bartollini, A. Marrocchi, F. Pizzo, L. Vaccaro, *Green Chem.* **2015**, *17*, 1071–1076.

[43] a) D. M. Alonso, S. G. Wettstein, J. A. Dumesic, *Green Chem.* **2013**, *15*, 584–595; b) M. A. Mellmer, D. Martin Alonso, J. S. Luterbacher, J. M. R. Gallo, J. A. Dumesic, *Green Chem.* **2014**, *16*, 4659–4662.

[44] a) J. R. Dorgan, B. Braun, J. R. Wegner, D. M. Knauss in *ACS Symposium Series* (Eds.: K. C. Khemani, C. Scholz), American Chemical Society, Washington, DC, **2006**; b) A.

Jiménez, M. Peltzer, R. Ruseckaite, *Poly(lactic acid) Science and Technology*, Royal Society of Chemistry, Cambridge, **2014.**

[45] C. S. M. Pereira, V. M. T. M. Silva, A. E. Rodrigues, *Green Chem.* **2011**, *13*, 2658–2671.

[46] a) Y. L. Kua, S. Gan, A. Morris, H. K. Ng, *Sustainable Chem. Pharm.* **2016**, *4*, 21–31; b) Y. L. Kua, S. Gan, H. K. Ng, A. Morris, *ISPFVF* **2014**, 244–251.

[47] a) M. A. Hill Bembenic, C. E. Burgess Clifford, *Energy Fuels* **2012**, *26*, 4540–4549; b) M. A. Hill Bembenic, C. E. Burgess Clifford, *Energy Fuels* **2013**, *27*, 6681–6694; c) M. Möller, P. Nilges, F. Harnisch, U. Schröder, *ChemSusChem* **2011**, *4*, 566–579.

[48] a) S. Avola, F. Goettmann, M. Antonietti, W. Kunz, *New J. Chem.* **2012**, *36*, 1568–1573; b) B. Smutek, W. Kunz, F. Goettmann, *C.R. Chim.* **2012**, *15*, 96–101.

[49] a) M. Herrero, J. A. Mendiola, A. Cifuentes, E. Ibáñez, *J. Chromatogr. A* **2010**, *1217*, 2495–2511; b) E. Reverchon, I. de Marco, *J. Supercrit. Fluids* **2006**, *38*, 146–166; c) K.-Y. Khaw, M.-O. Parat, P. N. Shaw, J. R. Falconer, *Molecules* **2017**, *22 (1186),* 1–24.

[50] R. Davarnejad, K. M. Kassim, A. Zainal, S. A. Sata, *J. Food Eng.* **2008**, *89*, 472–478.

[51] C. J. Clarke, W.-C. Tu, O. Levers, A. Bröhl, J. P. Hallett, *Chem. Rev.* **2018**, *118*, 747–800.

[52] a) P. G. Jessop, Y. Hsiao, T. Ikariya, R. Noyori, *J. Am. Chem. Soc.* **1994**, *116*, 8851–8852; b) P. G. Jessop, Y. Hsiao, T. Ikariya, R. Noyori, *J. Am. Chem. Soc.* **1996**, *118*, 344–355; c) P. G. Jessop, T. Ikariya, R. Noyori, *Nature* **1994**, *368*, 231–233.

[53] P. G. Jessop, L. Phan, A. Carrier, S. Robinson, C. J. Dürr, J. R. Harjani, *Green Chem.* **2010**, *12*, 809–814.

[54] Y. Kohno, S. Saita, K. Murata, N. Nakamura, H. Ohno, *Polym. Chem.* **2011**, *2*, 862–867.

[55] D. E. Bergbreiter, P. L. Osburn, T. Smith, C. Li, J. D. Frels, *J. Am. Chem. Soc.* **2003**, *125*, 6254–6260.

[56] Z. Ludmer, T. Golan, E. Ermolenko, N. Brauner, A. Ullmann, *Environ. Eng. Sci.* **2009**, *26*, 419–430.

[57] W. Kunz, K. Häckl, *Chem. Phys. Lett.* **2016**, *661*, 6–12.

[58] a) K. R. Seddon, *J. Chem. Technol. Biotechnol.* **1997**, *68*, 351–356; b) K. Seddon, *Green Chem.* **1999**, *1*, G58–G59.

[59] P. Wasserscheid, T. Welton (Eds.) *Ionic Liquids in Synthesis*, Wiley-VCH,1. ed., Weinheim, **2007**.

[60] a) P. Walden, *Bull. Acad. Imp. Sci. Saint-Petersbourg* **1914**, *8*, 405–422; b) J. S. Wilkes, *Green Chem.* **2002**, *4*, 73–80; c) F. H. Hurley, T. P. WIer, *J. Electrochem. Soc.* **1951**, *98*, 207–212.

[61] O. Zech, M. Kellermeier, S. Thomaier, E. Maurer, R. Klein, C. Schreiner, W. Kunz, *Chemistry* **2009**, *15*, 1341–1345.

[62] a) B. Kirchner (Ed.) *Topics in Current Chemistry, Vol. 290,* Springer Berlin, Berlin, **2013**; b) P. Wasserscheid, T. Welton (Eds.) *Ionic liquids in synthesis,* 2nd, completely rev. and enl. ed., Wiley-VCH, Weinheim, **2008**.

[63] a) T. P. T. Pham, C.-W. Cho, Y.-S. Yun, *Water Res.* **2010**, *44*, 352–372; b) A. Romero, A. Santos, J. Tojo, A. Rodríguez, *J. Hazard. Mater.* **2008**, *151*, 268–273; c) D. Zhao, Y. Liao, Z. Zhang, *Clean Soil Air Water* **2007**, *35*, 42–48.

[64] P. G. Jessop, *Green Chem.* **2011**, *13*, 1391–1398.

[65] M. Maase in *Ionic Liquids in Synthesis* (Eds.: P. Wasserscheid, T. Welton), Wiley-VCH, Weinheim, **2007**, 663–687.

[66] M. Maase, K. Massonne, K. Halbritter, R. Noe, DE10202838A1, **2003**.

[67] K. E. Gutowski, *Phys. Sci. Rev.* **2018**, *3*, 70–79.

[68] B. Weyershausen, K. Hell, U. Hesse in *ACS Symposium Series* (Eds.: R. D. Rogers, K. R. Seddon), American Chemical Society, Washington, DC, **2005**.

[69] a) R. Fehrmann, A. Riisager, M. Haumann, *Supported Ionic Liquids*, Wiley-VCH, Weinheim, **2014**; b) A. Riisager, R. Fehrmann, M. Haumann, P. Wasserscheid, *Eur. J. Inorg. Chem.* **2006**, 695–706.

[70] a) *Evonik demonstrates for the first time that SILP catalyst systems can be used commercially*, Press Release, Essen, Germany, **2015**; b) M. Haumann, A. Riisager, *Chem. Rev.* **2008**, *108*, 1474–1497; c) M. Becker, N. Brausch, A. Christiansen, R. Franke, D. Fridag, M. Haumann, M. Jakuttis, A. Schönweiz, P. Wasserscheid, S. Werner, DE102010041821A1, **2012.**

[71] V. Stegmann, K. Massonne, DE10341308A1, **2005**.

[72] R. P. Swatloski, S. K. Spear, J. D. Holbrey, R. D. Rogers, *J. Am. Chem. Soc.* **2002**, *124*, 4974–4975.

[73] R. C. Remsing, R. P. Swatloski, R. D. Rogers, G. Moyna, *Chem. Comm.* **2006**, 1271–1273.

[74] G. d. Wyss, *Ind. Eng. Chem.* **1925**, *17*, 1043–1045.

[75] a) T. Rosenau, A. Potthast, H. Sixta, P. Kosma, *Prog. Polym. Sci.* **2001**, *26*, 1763–1837; b) D. Eichinger, H. Firgo, C. Rohrer, *MRS Proc.* **2001**, *702*, U.2.2.1–U.2.2.12.

[76] R. Adler, M. Pfandl, G. Siebert, US9109587B2, **2011**.

[77] N. A. Kermani, doctoral thesis, Technical University of Denmark, Kongens Lyngby, **2017**.

[78] Linde AG, "Fuelling the future: Linde's ionic compressor", to be found under https://whyhydrogen.linde.com/lindes-ionic-compressor/.

[79] S. Survilienė, S. Eugénio, R. Vilar, *J. Appl. Electrochem.* **2011**, *41*, 107–114.

[80] Scionix, "Electroplating With Ionic Liquids", to be found under http://www.scionix.co.uk.

[81] D. R. MacFarlane, N. Tachikawa, M. Forsyth, J. M. Pringle, P. C. Howlett, G. D. Elliott, J. H. Davis, M. Watanabe, P. Simon, C. A. Angell, *Energy Environ. Sci.* **2014**, *7*, 232–250.

[82] a) Y. Fukaya, Y. Iizuka, K. Sekikawa, H. Ohno, *Green Chem.* **2007**, *9*, 1155–1157; b) N. Muhammad, M. I. Hossain, Z. Man, M. El-Harbawi, M. A. Bustam, Y. A. Noaman, N. B. Mohamed Alitheen, M. K. Ng, G. Hefter, C.-Y. Yin, *J. Chem. Eng. Data* **2012**, *57*, 2191–2196; c) P. Nockemann, B. Thijs, K. Driesen, C. R. Janssen, K. van Hecke, L. van

Meervelt, S. Kossmann, B. Kirchner, K. Binnemans, *J. Phys. Chem. B* **2007**, *111*, 5254–5263; d) D. Rengstl, B. Kraus, M. van Vorst, G. D. Elliott, W. Kunz, *Colloids Surf., B* **2014**, *123*, 575–581; e) G.-H. Tao, L. He, W.-S. Liu, L. Xu, W. Xiong, T. Wang, Y. Kou, *Green Chem.* **2006**, *8*, 639–646.

[83] a) A. P. Abbott, G. Capper, D. L. Davies, H. L. Munro, R. K. Rasheed, V. Tambyrajah, *Chem. Comm.* **2001**, 2010–2011; b) A. P. Abbott, D. Boothby, G. Capper, D. L. Davies, R. K. Rasheed, *J. Am. Chem. Soc.* **2004**, *126*, 9142–9147.

[84] A. P. Abbott, G. Capper, D. L. Davies, R. K. Rasheed, V. Tambyrajah, *Chem. Comm.* **2003**, 70–71.

[85] E. L. Smith, A. P. Abbott, K. S. Ryder, *Chem. Rev.* **2014**, *114*, 11060–11082.

[86] Y. Dai, J. van Spronsen, G.-J. Witkamp, R. Verpoorte, Y. H. Choi, *Anal. Chim. Acta* **2013**, *766*, 61–68.

[87] R. E. Pincock, *Acc. Chem. Res.* **1969**, *2*, 97–103.

[88] A. Pandey, R. Rai, M. Pal, S. Pandey, *PCCP* **2014**, *16*, 1559–1568.

[89] a) C. Ruß, B. König, *Green Chem.* **2012**, *14*, 2969–2982; b) P. Liu, J.-W. Hao, L.-P. Mo, Z.-H. Zhang, *RSC Adv.* **2015**, *5*, 48675–48704.

[90] a) 张伟霞葛裕华, CN106278824A, **2017**; b) M. Schatte, M. Boenitz-Dulat, US20190040436A1, **2019**; c) J. T. Gorke, R. J. Kazlauskas, F. Srienc, US20090117628A1, **2012**.

[91] V. Fischer, D. Touraud, W. Kunz, *Sust. Chem. Pharm.* **2016**, *4*, 40–45.

[92] a) A. P. Abbott, G. Capper, D. L. Davies, R. K. Rasheed, *Chemistry* **2004**, *10*, 3769–3774; b) A. P. Abbott, G. Capper, D. L. Davies, R. K. Rasheed, J. Archer, C. John, *Transactions of the IMF* **2004**, *82*, 14–17; c) A. P. Abbott, D. L. Davies, G. Capper, R. K. Rasheed, V. Tambyrajah, WO2002026701A2, **2002**; d) E. S.C. Ferreira, C. M. Pereira, A. F. Silva, *J. Electroanal. Chem.* **2013**, *707*, 52–58.

[93] R. Bernasconi, G. Panzeri, A. Accogli, F. Liberale, L. Nobili, L. Magagnin in *Progress and Developments in Ionic Liquids* (Ed.: S. Handy), InTech, London, **2017**.

[94] a) A. P. Abbott, K. El Ttaib, K. S. Ryder, E. L. Smith, *Trans. IMF* **2008**, *86*, 234–240; b) R. Bernasconi, L. Magagnin, *Surf. Eng.* **2016**, *33*, 131–135; c) A. Florea, L. Anicai, S. Costovici, F. Golgovici, T. Visan, *Surf. Interface Anal.* **2010**, *42*, 1271–1275.

[95] A. Bakkar, V. Neubert, *Electrochem. Commun.* **2007**, *9*, 2428–2435.

[96] A. P. Abbott, K. S. Ryder, U. König, *Transactions of the IMF* **2013**, *86*, 196–204.

[97] a) P. Starkey, *Soldering & Surface Mount Tech.* **2007**, *19*; b) E. L. Smith, C. Fullarton, R. C. Harris, S. Saleem, A. P. Abbott, K. S. Ryder, *Trans. IMF* **2013**, *88*, 285–293.

[98] Y.-L. Chen, X. Zhang, T.-T. You, F. Xu, *Cellulose* **2018**, *19*, 2010.

[99] Q. Zhang, M. Benoit, K. de Oliveira Vigier, J. Barrault, F. Jérôme, *Chemistry* **2012**, *18*, 1043–1046.

[100] H. Ren, C. Chen, S. Guo, D. Zhao, Q. Wang, *BioRes.* **2016**, *11 (4)*, 8457-8469.

[101] H. Ren, C. Chen, Q. Wang, D. Zhao, S. Guo, *BioRes.* **2016**, *11 (2)*, 5435-5451.

[102] S. Wang, A. Lu, L. Zhang, *Prog. Polym. Sci.* **2016**, *53*, 169–206.

[103] N. Sun, H. Rodríguez, M. Rahman, R. D. Rogers, *Chem. Comm.* **2011**, *47*, 1405–1421.

[104] a) X. Peng, M.-H. Duan, X.-H. Yao, Y.-H. Zhang, C.-J. Zhao, Y.-G. Zu, Y.-J. Fu, *Sep. Purif. Technol.* **2016**, *157*, 249–257; b) M. Ruesgas-Ramón, M. C. Figueroa-Espinoza, E. Durand, *J. Agric. Food. Chem.* **2017**, *65*, 3591–3601; c) B. Xia, D. Yan, Y. Bai, J. Xie, Y. Cao, D. Liao, L. Lin, *Anal. Methods* **2015**, *7*, 9354–9364; d) H. Zhang, B. Tang, K. Row, *Chem. Res. Chin. Univ.* **2014**, *30*, 37–41; e) L. Duan, L.-L. Dou, L. Guo, P. Li, E.-H. Liu, *ACS Sustainable Chem. Eng.* **2016**, *4*, 2405–2411; f) M. Cvjetko Bubalo, N. Ćurko, M. Tomašević, K. Kovačević Ganić, I. Radojčić Redovniković, *Food Chem.* **2016**, *200*, 159–166.

[105] a) T. J. Trivedi, J. H. Lee, H. J. Lee, Y. K. Jeong, J. W. Choi, *Green Chem.* **2016**, *18*, 2834–2842; b) S. K. Shukla, J.-P. Mikkola, *PCCP* **2018**, *20*, 24591–24601; c) S. Sarmad, J.-P. Mikkola, X. Ji, *ChemSusChem* **2017**, *10*, 324–352; d) C. Ma, S. Sarmad, J.-P. Mikkola, X. Ji, *Energy Procedia* **2017**, *142*, 3320–3325.

[106] "Surfactants Market Analysis By Product (Cationic, Nonionic, Anionic, Amphoteric), By Application (Home Care, Personal Care, Industrial & Institutional Cleaners, Food Processing, Oilfield Chemicals, Agricultural Chemicals, Textiles, Emulsion Polymerization, Paints & Coatings, Construction) And Segment Forecasts To 2022", to be found under https://www.grandviewresearch.com/industry-analysis/surfactants-market, **2015**.

[107] M. J. Rosen, J. T. Kunjappu in *Surfactants and Interfacial Phenomena* (Ed.: M. J. Rosen), John Wiley & Sons, Inc, Hoboken, NJ, **2004,** 235-271.

[108] G. Kume, M. Gallotti, G. Nunes, *J. Surfact. Deterg.* **2008**, *11*, 1–11.

[109] C. Neuberg, *Biochem. Z.* **1916**, *76*, 107–176.

[110] K. Holmberg (Ed.) *Handbook of applied surface and colloid chemistry*, Wiley, Chichester, **2002**.

[111] S. H. Yalkowsky, *Solubility and solubilization in aqueous media*, American Chemical Society, Washington, D.C., **1999**.

[112] J. J. Booth, M. Omar, S. Abbott, S. Shimizu, *PCCP* **2015**, *17*, 8028–8037.

[113] R. Winkler, T. Buchecker, F. Hastreiter, D. Touraud, W. Kunz, *PCCP* **2017**, *19*, 25463–25470.

[114] D. Balasubramanian, V. Srinivas, V. G. Gaikar, M. M. Sharma, *J. Phys. Chem.* **1989**, *93*, 3865–3870.

[115] a) I. Danielsson, P. Stenius, *J. Colloid Interface Sci.* **1971**, *37*, 264–280; b) P. Firman, D. Haase, J. Jen, M. Kahlweit, R. Strey, *Langmuir* **1985**, *1*, 718–724; c) E. C. Lumb, *Trans. Faraday Soc.* **1951**, *47*, 1049–1055.

[116] S. E. Friberg, R. V. Lochhead, I. Blute, T. Wärnheim, *J. Dispersion Sci. Technol.* **2004**, *25*, 243–251.

[117] W. Kunz, K. Holmberg, T. Zemb, *Curr. Opin. Colloid Interface Sci.* **2016**, *22*, 99–107.

[118] a) V. Dhapte, P. Mehta, *St. Petersburg Polytechnic. Un. J. Phys. Math.* **2015**, *1*, 424–435; b) Pan Z., J.-T. Simmenot, US20140107059A1, **2014**; c) A. Patel, L. Malinovska, S. Saha, J. Wang, S. Alberti, Y. Krishnan, A. A. Hyman, *Science* **2017**, *356*, 753–756.;

[119] M. J. Rosen, J. T. Kunjappu in *Surfactants and Interfacial Phenomena* (Ed.: M. J. Rosen), John Wiley & Sons, Inc, Hoboken, NJ, **2004,** 39-122.

[120] R. Kumar, V. Manjuladevi in *Molecular Interactions* (Ed.: A. Meghea), InTech, London, **2012**.

[121] H. Gecol in *Chemistry and Technology of Surfactants* (Ed.: R. J. Farn), Blackwell Publishing Ltd, Oxford, **2006**.

[122] M. H. Hatzopoulos, J. Eastoe, P. J. Dowding, S. E. Rogers, R. Heenan, R. Dyer, *Langmuir* **2011**, *27*, 12346–12353.

[123] D. F. Evans, H. Wennerström, *The colloidal domain. Where physics, chemistry, biology, and technology meet,* 2. ed., Wiley-VCH, New York, **1999**.

[124] a) J. N. Israelachvili, D. J. Mitchell, B. W. Ninham, *J. Chem. Soc., Faraday Trans. 2* **1976**, *72*, 1525–1568.

[125] M. J. Rosen, J. T. Kunjappu in *Surfactants and Interfacial Phenomena* (Ed.: M. J. Rosen), John Wiley & Sons, Inc, Hoboken, NJ, **2004,** 123-201.

[126] K. Häckl, A. Mühlbauer, J. F. Ontiveros, S. Marinkovic, B. Estrine, W. Kunz, V. Nardello-Rataj, *J. Colloid Interface Sci.* **2018**, *511*, 165–173.

[127] P. Bauduin, L. Wattebled, D. Touraud, W. Kunz, *Z. Phys. Chem.* **2004**, *218*, 631–641.

[128] G. Grundl, M. Müller, D. Touraud, W. Kunz, *J. Mol. Liq.* **2017**, *236*, 368–375.

[129] a) W. Kunz, J. Henle, B. W. Ninham, *Curr. Opin. Colloid Interface Sci.* **2004**, *9*, 19–37; b) W. Kunz, R. Neueder in *Specific Ion Effects* (Ed.: W. Kunz), World Scientific Publishing Co. Pte. Ltd., Munich, **2009**, 10–11.

[130] K. D. Collins, *Methods* **2004**, *34*, 300–311.

[131] K. D. Collins, *Biophys. Chem.* **2006**, *119*, 271–281.

[132] W. Kunz, *Curr. Opin. Colloid Interface Sci.* **2010**, *15*, 34–39.

[133] N. Vlachy, B. Jagoda-Cwiklik, R. Vácha, D. Touraud, P. Jungwirth, W. Kunz, *Adv. Colloid Interface Sci.* **2009**, *146*, 42–47.

[134] R. Klein, doctoral thesis, Universität Regensburg, Regensburg, **2011**.

[135] R. D. Swisher, *Surfactant Biodegradation,* 2nd edition, Marcel Dekker, New York, **1987**.

[136] R. Scheer, *Pharm. Unserer Zeit* **1988**, *17*, 58–59.

[137] J. K. Maurer, R. D. Parker, G. J. Carr, *Toxicol. Pathol.* **1998**, *26*, 226–233.

[138] M. Kjellin, I. Johansson (Eds.) *Surfactants from renewable resources*, Wiley series in renewable resources, Wiley, Chichester, **2010**.

Chapter 2
L-Carnitine-Based Ionic Liquids, Hydrotropes and Surfactants

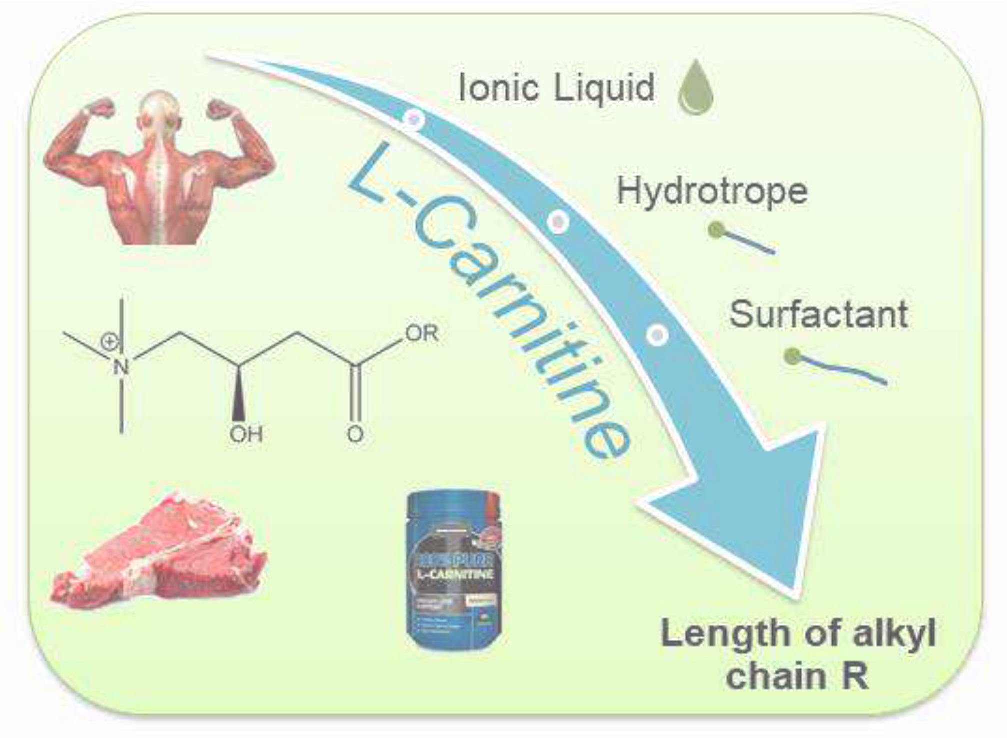
Ionic Liquid
Hydrotrope
Surfactant
L-Carnitine
OR
N
OH
O
L-CARNITINE
Length of alkyl chain R

2 *L*-Carnitine-Based Ionic Liquids, Hydrotropes and Surfactants

2.1 Introduction

L-carntine (*β*-hydroxy-*γ*-trimethylaminobutyrate) is a naturally occurring substance present in a variety of biological materials, such as animal tissue, plants and other microorganisms. It is particularly abundant in mammal muscles.[1] This is probably how its name has been established. It originates from *'carnis'*, which is the Latin word for meat. It was discovered in the early 20th century by the groups of Gulewitsch-Krimberg and Kutscher. Its structure was finally clarified in 1927 by Tomita and Sendju.[2] The substance re-aroused research interest in the 1950s, when Carter *et al.* found that the growth factor vitamin B_T was identical to carnitine.[3] Since then, its metabolism and function in the organism have been studied intensively.[4] On the one hand, carnitine is taken up via nutrition, on the other hand it is bio-synthesized in eukaryotic cells from lysine and methionine. This happens mostly in the liver, the kidney and the brain, from where carnitine is released, distributed and taken up by other tissues, especially cardiac and skeletal muscles.[5] More than 99 % of carnitine in the body is present intracellularly and in dynamic equilibrium with acylcarnitine esters.[6] Long-chain acylcarnitine esters are formed in order to transport fatty acids into the mitochondria, where fatty acid oxidation takes place.[7] This is the main step in the energy metabolism of the cell and the predominant source of energy in mammal muscles.[8] As the transport through the mitochondrial membrane is the rate limiting step, *L*-carnitine plays an important role.[5] The short- and medium-chain acylcarnitine esters are formed inside the mitochondria and peroxisomes in order to remove organic acids from these cell components.[7] In addition to biosynthesis in the body, carnitine can be inserted from nutrition. It is non-toxic for humans up to amounts of several grams when orally consumed. In special cases, it is used as therapeutic agent. In particular, athletes use it as nutritional supplement to enhance their performance by stimulating the energy metabolism of fatty acids. However, it is also reported that the absorption of *L*-carnitine when incorporated through nutrition has low efficiency and most of it is digested by microorganisms in the intestines and subsequently segregated.[5,9]

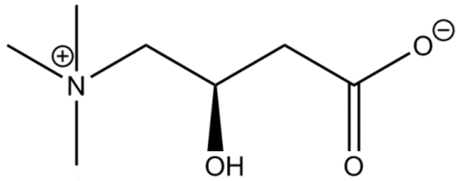

Fig. 2.1.1-1: Molecular structure of L-carnitine.

The structural similarity of carnitine and choline was the reason why *L*-carnitine has initially drawn interest with regard to green chemistry and the development of novel functional molecules. Choline and its derivatives are known to be suitable for their use in green chemistry, *e.g.* for the development of green solvents, surfactants and counter-ions. This is in contrast to other quaternary ammonium moieties, as it is a natural, non-toxic and biodegradable molecule.[5,10,11,12,13] Choline salts and ester derivatives are banned from cosmetic products by the EU.[14] This is not the case for *L*-carnitine and a potential application in cosmetic formulations seems possible. Its beneficial impact on reducing an oily, shiny appearance of human skin has been reported.[15] It is further used in anti-cellulite products and as a conditioning agent for hair and skin applications.[16] According to a statement from 2018 by Lonza, one of the biggest suppliers of *L*-carnitine and related products, there is an increasing market for carnitine as ingredient for weight control products and sports nutrition, in particular energy drinks.[17]

In neutral conditions, *L*-carnitine is a zwitterion with one chiral centre. It features a carboxylate functional group in addition to a hydroxyl group (see Fig. 2.1.1-1). This offers more opportunities for structural modification and derivatisation compared to similar substances, such as choline and betaine. This flexibility enhances the possibilities for an application in green chemistry.

As a consequence of all these aspects, *L*-carnitine was considered as raw material for the development of green, functional molecules. Considering several possibilities for the modification, the formation of ester derivatives was chosen. In general, this should result in compounds with high biodegradability, as the ester function can be hydrolysed.[11] So far, esters of *L*-carnitine are known in association with acylcarnitine compounds that are formed in the organism during fatty acid transport through the inner mitochondrial membrane.[18] Only a few studies from the 1970s and 80s have been published presenting the physical-chemical properties of long-chain acylcarnitines as natural surfactants.[19] One of them investigated the surfactant properties of palmitoylcarnitine, a zwitterionic amphiphile used as a biological detergent. It exhibits a low critical micellar concentration and solubilizes biological membranes.[20] In contrast to acylcarnitine substances, the work in this thesis was based on the esterification of the carboxylic functional group. Only a few publications so far have reported the synthetic modification of carnitine at the carboxylic group. De Maria *et al.* and Cipollone *et al.* have shown the formation of cubic, hexagonal and lamellar phases as well as multilamellar vesicles by different diesters of carnitine.[21] A detailed study of the self-assembly of carnitine dodecyl amide (*i.e.* 3-(dodecylcarbamoyl-2-hydroxypropyl)-trimethylammonium) described the spontaneous formation of cationic vesicles in water and examined the applicability of these aggregates to form complexes with DNA for gene delivery.[22] Another paper of the same group presented the interactions between the cationic carnitine hexadecyl amide surfactant with the protein pepsin.[23]

At first, the formation of short chain carnitine ester derivatives for the development of ionic liquids (ILs) was studied. ILs are highly interesting solvents, as in contrast to most organic solvents they are non-volatile and non-flammable and their use in industry could significantly minimize solvent emission to the atmosphere and risk potential. Due to their ionic character, they exhibit special solvent properties and performance. Detailed information is given in section 1.3.5. It is assumed that the carnitine ester cation has several advantages over imidazolium-based cations, which are most common in ILs. The latter often suffer from long ways of synthesis, toxicity and non-biodegradability.[24–27] In this chapter, it is shown that the carnitine ester cation can be formed in one simple synthesis step. In a second step, the anion can be changed. Two methods for each step (see Fig. 2.1.1-2) are presented and discussed regarding their advantages, disadvantages and in terms of their greenness. The present study further deepens the results found by Andrea Mühlbauer in scope of her dissertation and a previously prepared master thesis.[11,28]

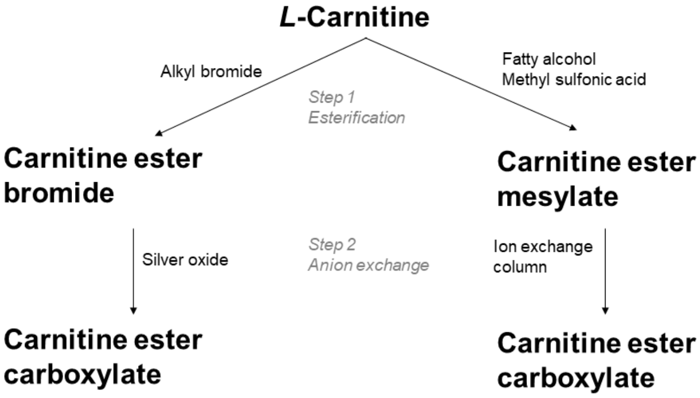

Fig. 2.1.1-2: Tested synthesis methods for carnitine-based ILs.

A variation in the chain length of the carnitine alkyl ester compounds was found to result in the formation of further functional molecules: cationic hydrotropes in the case of medium chain length and cationic surfactants in the case of long alkyl chains. In general, cationic surfactants are important in terms of surface treatment and surface design. They easily adsorb to solid surfaces, which are negatively charged in most cases. For example, they are used as antistatics, fabric softeners or hair conditioning agents.[29,30] Quaternary ammonium compounds are generally regarded as pH-stable cationic surfactants. The so-called 'esterquats' describe a group of cationic surfactants where the hydrophobic moiety is linked to the quaternary ammonium head group via an ester bond. The inclusion of the ester bond promotes biodegradation and reduces ecotoxicity of these cationic surfactants.[31] While synthetic esterquats are usually prepared by the reaction of a tertiary alkanolamine and subsequent alkylation, the quaternary ammonium function is already present in *L*-carnitine, so that it provides an easy access to natural esterquats.

Hydrotropes are also amphiphilic molecules, but in contrast to surfactants they possess smaller hydrophobic moieties (see section 1.4.2). The sub-category of cationic hydrotropes has only scarcely been studied and discussed as separate hydrotrope class, yet. Winkler et al. showed that the antagonistic salt tetraphenylphosphonium chloride can be classified as hydrotrope.[32] A few studies considered cationic hydrotropes as co-surfactants in combination with anionc surfactants.[33] The specific benefit of the presence of a cationic head group in hydrotropes has so far not explicitly been reported. In this thesis, cationic hydrotropes were formed in terms of the esterification of *L*-carnitine with alkyl chains of medium length. They were investigated with regard to their performance in solubilizing two hydrophobic substances.

The results presented in the following are divided into three sections. In the first section, the synthesis of *L*-carnitine-based ILs is described, followed by an overview of the properties determined for the resulting ILs and an evaluation of the applied synthesis methods and the applicability of the synthesized ILs. The second part contains the investigation of a homologous series of carnitine alkyl ester bromides. They are characterized in terms of their thermal properties, self-aggregation behaviour, the ability to dissolve hydrophobic substances and cytotoxicity. The third section reports surfactant properties of carnitine alkyl ester mesylates and discusses differences in comparison to analogous surfactants with bromide counter-ions. The conclusion summarizes the content of this chapter, it evaluates the collected results and gives a prospect on the promises of *L*-carnitine-based functional materials for their application as green alternatives. The experimental part gives rise to the chemicals and measuring techniques used in this study.

2.2 *L*-carnitine-based Ionic Liquids

ILs have been enjoying an image as green solvents for years because of their negligible vapour pressure and their low flammability. However, according to the 12 Principles of Green Chemistry, there are further issues to be considered. Most ILs contain an imidazolium cation. The synthesis of this kind of ILs is costly and the resulting ILs are often toxic and poorly biodegradable.[24–27] *L*-Carnitine was considered in order to obtain greener and 'drinkable' solvents from natural origin and ILs based on carnitine ester derivatives have been formed. Their ethyl esters were synthesized in two different ways and combined with different anions: bromide, mesylate, acetate and levulinate. This section presents the two investigated synthesis routes and critically discusses their advantages and drawbacks. In addition, it includes a study of the thermal properties of the resulting ILs.

2.2.1 Synthesis

It is believed to be not appropriate to declare a product as green, if its synthesis contains high amounts of organic solvents, toxic reagents or intermediates and if it creates non-recylable by-products, although the product itself might be non-toxic and biodegradable. Thus, the way of synthesis is highly important when developing green materials. As the idea of this project was to generate greener ILs, different synthesis routes were tested in order to improve the greenness. While the esterification step was first performed with ethyl bromide, another method was developed which used ethanol and methanesulfonic acid ($MeSO_3H$). A metathesis reaction allowed for the exchange of the initial anions bromide and mesylate, either by a reaction with silver(I)oxide (Ag_2O) or by utilizing an ion exchange column. An overview of the reactions used for the generation of carnitine-based ILs with different counter-anions is shown in Fig. 2.1.1-2 as well as in Tab. 2.2.1-1. The initial (referred to as 'old') way was developed by Andrea Mühlbauer in her dissertation at the University of Lille and included the esterification with alkyl bromides and the ion exchange with Ag_2O.[11] The 'new' route was investigated in order to improve the greenness.

Tab. 2.2.1-1: Overview of the reaction pathways developed for the synthesis of carnitine-based ILs.

	Esterification		***Metathesis***	
	'old'	*'new'*	*'old'*	*'new'*
Resulting Product	$[C_nCar]Br$	$[C_nCar]MeSO_3$	$[C_nCar]OAc$	$[C_nCar]OAc$
Reagent	CH_3CH_2-Br	$MeSO_3H$	Ag_2O	Amberlite IRA 402
Described in section	2.2.1.1	2.2.1.2	2.2.1.3	2.2.1.3

2.2.1.1 *L*-Carnitine Bromide Ionic Liquids

Carnitine ethyl ester bromide, herein referred to as $[C_2Car]Br$, was synthesized in one step using *L*-carnitine and ethyl bromide as starting materials (see Fig. 2.2.1-1).[11,28] *L*-carnitine (1 mole equivalents (eq.)) was combined with ethyl bromide (1.5 eq.) in acetonitrile under nitrogen atmosphere. The reaction mixture was stirred under reflux for at least 12 h. After evaporation of the solvent, the crude product was washed several times with diethyl ether and dried under vacuum. Carnitine ethyl ester bromide was obtained in >90 % yield. The purity of the products was assessed by NMR analysis. The corresponding NMR data can be found in the experimental section (2.6.2).

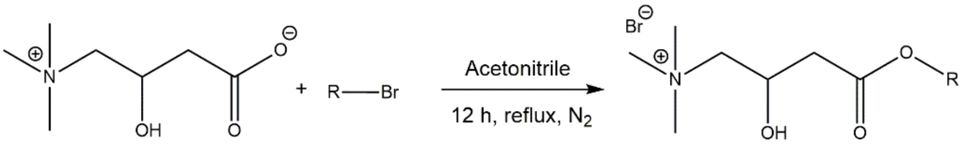

Fig. 2.2.1-1: One-step synthesis of carnitine ethyl ester bromide $[C_2Car]Br$. The same reaction was applicable for the synthesis of carnitine alkyl ester bromides $[C_nCar]Br$, when $R = C_nH_{2n+1}$ and n = 2, 4, 6, 8, 10, 12, 14.

In general, this one-step synthesis was quick and easy to perform. The product isolation was straightforward and the product was obtained in a good yield. However, some aspects caused concerns regarding its greenness. With its boiling temperature of approximately 38 °C under atmospheric pressure, ethyl bromide is very volatile. This caused problems upon addition to the warm reaction mixture. The vapour of this substance is assumed to damage the ozon layer. In addition, it is suspected to cause cancer.[34] In regard of these drawbacks, further options for the formation of carnitine ester ILs were investigated.[28]

2.2.1.2 *L*-Carnitine Mesylate Ionic Liquids

Carnitine ethyl ester mesylate, herein referred to as $[C_2Car]MeSO_3$, was synthesized in one step in a solvent-free manner using *L*-carnitine, ethanol and $MeSO_3H$ as starting materials (see Fig. 2.2.1-2). The aim of investigating this synthesis route was to improve the greenness of the formation of alkyl carnitine ester compounds with an inexpensive and simple approach. As mentioned above, the previous method employing alkyl bromides exhibited some drawbacks and an alternative reaction was wanted.

L-Carnitine was mixed with an excess of ethanol (>10 eq.) and $MeSO_3H$ (1.5 eq.). The solution was stirred at 70 °C for 72 h. After the reaction, excess ethanol could easily be removed at 40 °C using a rotary evaporator at 100 mbar and the product appeared as a white solid. It was washed with diethylether three times to get rid of unreacted acid residues. The resulting solid product was dried in a drying pistol under vacuum for several days. A correlation between reaction time and reaction temperature was observed. The reaction was monitored by NMR analysis. Corresponding NMR data can be found in the experimental section 2.6.2.

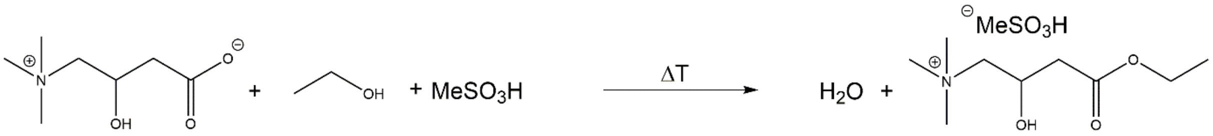

Fig. 2.2.1-2: One-step synthesis of carnitine ethyl ester mesylate [C_2Car]$MeSO_3$.

The successful esterification of the carboxylic group of betaine with fatty alcohols and $MeSO_3H$ for the formation of 'greener cationic surfactants' has been reported in literature.[35,36] The reaction proceeded in one step with an *in situ* activation of the carboxylic group via protonation. The reaction employs only environmentally friendly reactants and is conducted without solvent or, in particular, with one of the reagents serving as solvent at the same time. In contrast to the alkyl bromides, primary alcohols are environmentally less critical. $MeSO_3H$ is a good candidate for acid catalysis, as it is an easy-to-handle liquid, less aggressive than sulfuric acid, biodegradable, recyclable and in a wide sense a natural substance, as it is part of the natural sulfur cycle.[37]

This reaction provides considerable improvement compared to the former synthesis route for the formation of carnitine ester. A reduction of the applied amount of ethanol is assumed to be possible in order to reduce the amount of unreacted material.

Nevertheless, this reaction exhibited some drawbacks, such as longer reaction times and an incomplete conversion, as the ester formation is an equilibrium reaction. The maximum conversion reached was around 90 %. Usually, a 100 % conversion is fostered by withdrawing one of the reaction products, e.g. water, which is produced as a by-product. Practically, this was not possible in case of forming an ethyl ester, as ethanol has a lower boiling point than water and would be removed from the reaction mixture before water. A follow-up problem occurred during product isolation: the polarities of *L*-carnitine and its ethyl ester derivative are too similar, so that recrystallization and column chromatography did not deliver satisfying results for their separation. Therefore, the desired carnitine ester product could not be isolated from unreacted *L*-carnitine.

A relation between the conversion of *L*-carnitine to [C_2Car]$MeSO_3$, reaction time and reaction temperature was observed. This correlation was studied in order to optimize reaction time and temperature. The percentual conversion determined by means of NMR analysis of *L*-carnitine to [C_2Car]$MeSO_3$ at a reaction temperature of 80 °C as a function of the reaction time is illustrated in Fig. 2.2.1-3. It resulted in a saturation curve, where maximum conversion is attained after a certain time. At a temperature of 80 °C, the equilibrium conversion of 90 % was reached within a reaction time of 48 h. Longer reaction times did not further enhance the conversion.

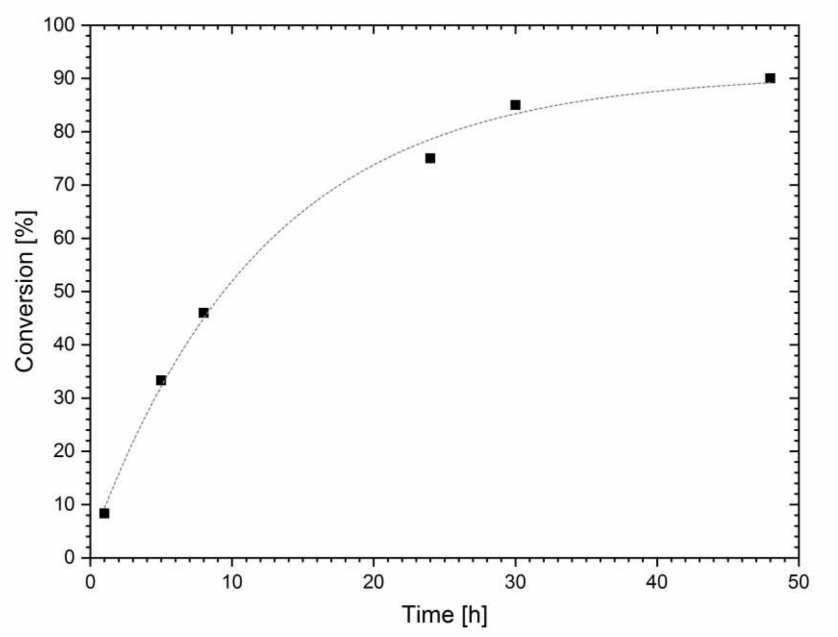

Fig. 2.2.1-3: Conversion of L-carnitine to [C_2Car]$MeSO_3$ as a function of reaction time recorded at a reaction temperature of 80 °C.

Fig. 2.2.1-4 presents the observed linear relation between the reaction temperature and the required time to reach the equilibrium conversion of 90 %. Increasing the reaction temperature allows for a reduction of the reaction time. However, at reaction temperatures above 80 °C, the resulting [C_2Car]$MeSO_3$ product exhibits a considerable smell, which is assumed to be caused by degradation. A reaction temperature of 70 °C was considered as appropriate. This ensures both a high-quality product on the one hand and a reaction time as low as possible on the other hand.

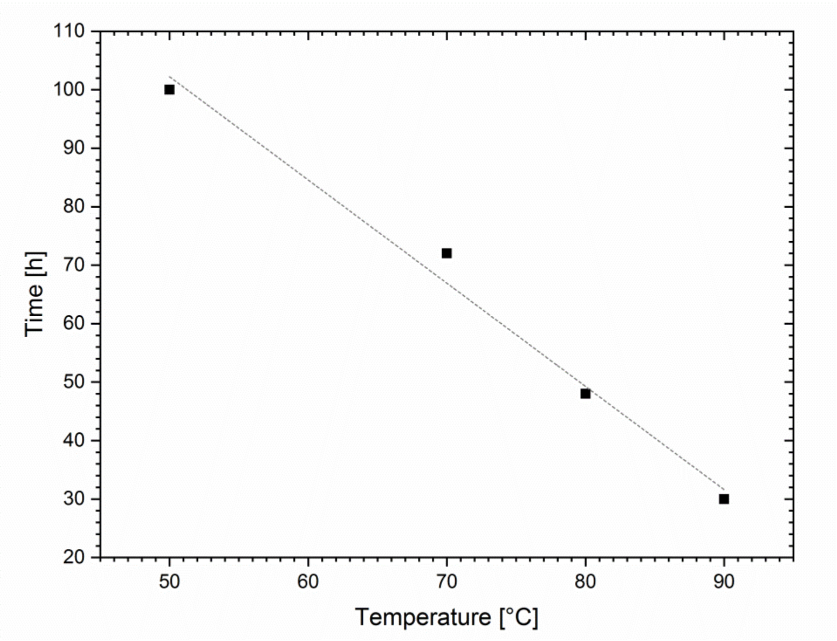

Fig. 2.2.1-4: Reaction time required to reach the 90 % equilibrium conversion as a function of reaction temperature.

2.2.1.3 *L*-Carnitine Carboxylate Ionic Liquids

The properties of ILs can be varied and designed by applying different anion-cation-combinations. In order to obtain a higher diversity of carnitine-based ILs, the bromide or mesylate anion obtained from the first synthesis step was exchanged by a variety of carboxylate compounds. The reaction shown in Fig. 2.2.1-5 proved to be applicable for the formation of carnitine ethyl ester acetate, adipate, citrate, formate, glutarate, glycolate, itaconate, lactate, levulinate, oxalate, propionate and tartrate.[28] However, this reaction can only be used for the metathesis of bromide ILs and there are a few further unfavourable aspects: the high cost of the Ag_2O reagent, the generation of a huge amount of silver bromide waste and the energy consuming removal of water.

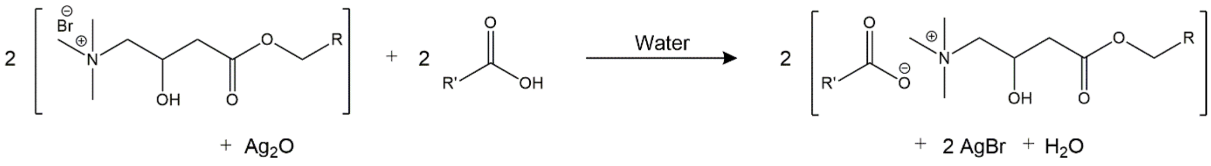

Fig. 2.2.1-5: ‚Old' metathesis reaction for the change of the anion of [C_nCar]Br compounds.[11,28]

This reaction is driven by the precipitation of silver bromide (AgBr). In order to obtain carnitine ethyl ester carboxylates from mesylates, a new approach was required and developed in this thesis.

Amberlite IRA 402 is a chloride-based anion exchange resin with exchange capacity of 1.2 mol/l. 300 ml of this substance were filled into a glass column. The column was rinsed with a substance amount of 2.88 mol sodium carboxylate (acetate or levulinate) in aqueous solution in order to load the column. After washing the column with water, 10.7 g [C_2Car]$MeSO_3$ in concentrated aqueous solution were applied to the column, eluted with water and captured in fractions. The fractions were analysed individually by thin layer chromatography (TLC). The fractions containing carnitine ester carboxylate product were combined. Water was removed by rotational evaporation and the resulting product was dried using a high vacuum pump for at least 48 h. The scheme in Fig. 2.2.1-6 illustrates the described metathesis reaction.

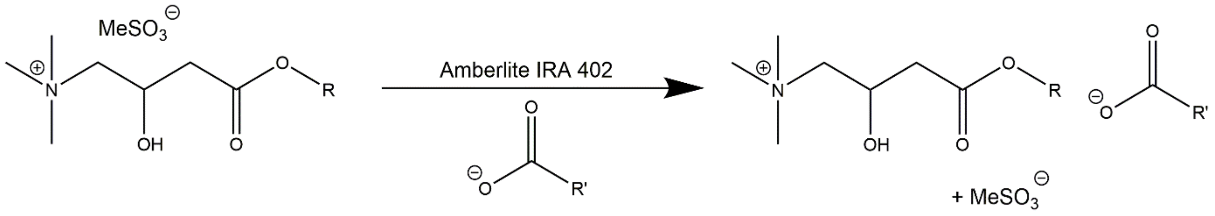

Fig. 2.2.1-6: Reaction scheme for the anion metathesis of [C_nCar]$MeSO_3$.

Along this reaction pathway, carnitine ethyl ester acetate [C_2Car]OAc and carnitine ethyl ester levulinate [C_2Car]Lev were obtained. While sodium acetate was commercially available, sodium levulinate was generated by mixing equimolar amounts of sodium hydroxide and levulinic acid in aqueous solution. The reaction was monitored by NMR analysis. Corresponding NMR data are given in the experimental section 2.6.2.

Two aspects shall be pointed out in view of this metathesis reaction. (1) The used anion exchange resin is characterized by a certain exchange capacity. Regarding this characteristic index, the eightfold molar amount of sodium carboxylate was for loading the exchange material to ensure its saturation with carboxylate anions. Only one eighth of the molar amount of [C_2Car]$MeSO_3$ relative to the indicated capacity was applied to the exchange column in order to obtain full conversion from carnitine ester mesylate to carboxylate. With further investigations it should be tested, if the factor of eight could be reduced to make the reaction more efficient, *e.g.* by varying the temperature or flow rate. (2) After the anion exchange, the product is obtained in dilute aqueous solution. On the one hand, water is a harmless and readily available solvent, on the other hand, the energy consumption for its removal is high and in some particular cases it is difficult to entirely remove all solvent residues from the IL.

2.2.2 Characterization of *L*-Carnitine-Based Ionic Liquids

The viscosity and the thermal properties of ILs, such as degradation temperature, melting temperature and glass transition temperature play a big role when thinking about their application as solvents. Their water content significantly influences these properties. In this section, the determined properties are given under indication of the used synthesis method. This has two reasons: (1) it is virtually impossible to generate two batches of the same product with the same water content, especially when they are produced via different methods; (2) as mentioned in section 2.2.1.2, [C_2Car]$MeSO_3$ contained considerable amounts of unreacted *L*-carnitine. So did the carnitine ester carboxylates that were obtained from [C_2Car]$MeSO_3$. Water as well as other impurities can affect IL properties.

2.2.2.1 Water Content

The indication of IL water contents is required, as they significantly influence characteristic properties of ILs. They vary according to the synthesis pathway and the quality of drying and storage, as most ILs are hygroscopic. The water contents of the studied ILs are given in Tab. 2.2.2-1. There are remarkable differences determined for the pure ILs obtained from the old method and the 90 % pure ILs generated by the new one, although they were dried with the same procedure. There are two possible explanations: either there was a problem with the function of the vacuum drying pump or it was more difficult to remove water from the compounds containing approximately 10 % *L*-carnitine. In theory, it is possible that water is more strongly bound to the IL network by hydrogen bonds in the presence of *L*-carnitine. However, this hypothesis needs to be further investigated.

Tab. 2.2.2-1: Water contents as determined by Karl-Fischer Coulometry for ILs obtained from the 'old' synthesis in almost 100 % purity and from the 'new' synthesis in approximately 90 % purity.

Method:	***old***	***new***
	Water content [wt%]	
[C_2Car]Br	0.03	-
[C_2Car]$MeSO_3$	-	0.1
[C_2Car]OAc	0.07	3.0
[C_2Car]Lev	0.03	1.3

2.2.2.2 Thermal Properties

Typical features of ILs are low melting temperatures below 100 °C and high thermal stabilities.[38] The thermal behaviour of some [C_2Car]X ILs, which were obtained in almost 100 % purity by the old method and approximately 90 % purity by the new method, was studied. Differential scanning calorimetry (DSC) measurements gave information about the melting temperatures (T_m) and glass transition temperatures (T_g) of the studied ILs. A glass transition occurs, when the solid phase is amorphous due to prohibited crystal arrangement of bulky ions. Thermal degradation temperatures (T_{deg}) were determined by thermogravimetric analysis (TGA).

The thermal data is collected in Tab. 2.2.2-2. With a melting temperature of 172 °C, [C_2Car]Br is per definition not an IL. All other compounds exhibited melting or glass transition temperatures below 100 °C and are therefore considered as ILs, whereas [C_2Car]OAc was the only room temperature IL. [C_2Car]Br and [C_2Car]$MeSO_3$ are thermally more stable than the tested carnitine ester carboxylates. The carboxylate ILs had similar degradation temperatures irrespectively of the synthesis method, the water content and the type of carboxylate anion. Also, the glass transition temperatures were located in a rather narrow temperature range between -41 °C and -27 °C. A significant difference was observed for the melting temperatures of [C_2Car]Lev. A melting temperature of 97 °C for the compound formed with the old method was measured, while it was 65 °C, when it was generated according to the new pathway. Most likely this is due to the difference in the water content, as water molecules can influence the crystallization process of the IL. However, there is a chance that the presence of *L*-carnitine generates a reduction in the melting temperature. This hypothesis was tested with [C_2Car]$MeSO_3$ by adding defined amounts of *L*-carnitine and is described in the following.

Tab. 2.2.2-2: Degradation temperature T_{deg}, melting temperature T_m and glass transition temperature T_g of [C_nCar]X ILs obtained from the 'old' synthesis in almost 100 % purity and from the 'new' synthesis in approximately 90 % purity.

Method:	***old***			***new***		
	T_{deg} [°C]	**T_m [°C]**	**T_g [°C]**	**T_{deg} [°C]**	**T_m [°C]**	**T_g [°C]**
[C_2Car]Br	260	172	-16	-	-	-
[C_2Car]$MeSO_3$	-	-	-	296	76	-
[C_2Car]OAc	185	-	-27	187	-	-33
[C_2Car]Lev	188	97	-37	195	65	-41

As the new synthesis method did not allow the formation of 100 % pure IL, the general influence of the presence of *L*-carnitine on the thermal properties of [C_2Car]$MeSO_3$ was determined. Melting temperatures and degradation temperatures of mixtures with different *L*-carnitine contents were measured. At room temperature, all three mixtures appeared as white solids. Fig. 2.2.2-1 shows that there is no obvious trend regarding the degradation temperatures. In contrast, a clear trend is observable for the melting temperatures: the melting temperature of mixtures of [C_2Car]$MeSO_3$ and *L*-carnitine decrease with increasing amount of *L*-carnitine. This gives reason to suggest that a kind of eutectic mixture forms between *L*-carnitine and the respective ethyl mesylate ester. The molar composition of these mixtures can be controlled by the reaction time of the conversion of *L*-carnitine to its ethyl ester with ethanol and $MeSO_3H$ (see Fig. 2.2.1-3). It is to be tested, if the melting temperature of the mixture can be further decreased by higher proportions of *L*-carnitine and if it can even be liquid at room temperature.

As mentioned above, the viscosity is another characteristic feature of ILs. A determination of the studied carnitine-based ILs was not possible due to device-specific limitations of the available rheometer, which could not handle the viscous texture of the ILs, not even at elevated temperature. Only the dynamic viscosity of [C_2Car]OAc (obtained by the old method) has been determined in the scope of the previous master thesis.[28] It revealed a viscosity of 176 Pa·s at room temperature. This is in the same range as the viscosity of peanut butter.[39]

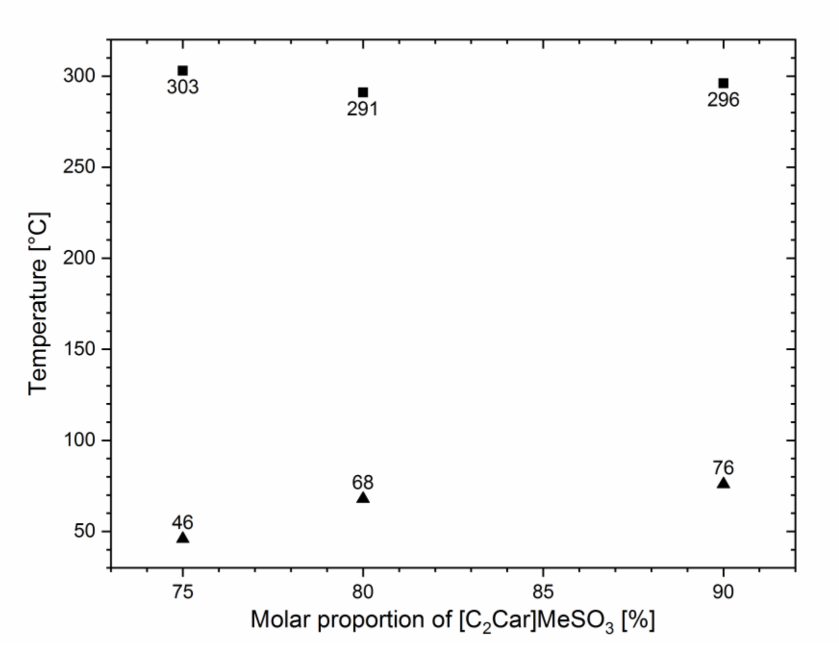

Fig. 2.2.2-1: Degradation temperature T_{deg} (■) and melting temperature T_m (▲) as a function of the molar fraction of [C_2Car]$MeSO_3$ in relation to unesterified L-carnitine.

2.2.3 Critical Discussion of *L*-Carnitine-Based Ionic Liquids

Carnitine has been considered as a promising candidate for generating ILs due to several reasons. It is a natural molecule, which is structurally related to the already established choline. The use of choline for the development of green ILs has been reported.[10,40] The advantage of carnitine over choline is that it is admitted in cosmetics and food industry. This allows for an application in chemical formulation for these industries.

2.2.3.1 Discussion of the Synthesis of *L*-Carnitine-Based Ionic Liquids

Due to the fact that *L*-carnitine is a zwitterionic molecule, it seemed obvious that the esterification of the carboxylate group was an appropriate way to generate a carnitine-based cation for an IL. The presented synthesis routes comprise two different sorts of reaction: (1) the formation of a carnitine ester and (2) an anion exchange reaction. Two methods for each kind of reaction were presented (see also Fig. 2.1.1-2):

(1a) Reaction of *L*-carnitine with ethyl bromide;

(1b) Reaction of *L*-carnitine with ethanol and $MeSO_3H$;

(2a) Anion exchange with Ag_2O;

(2b) Anion exchange with exchange resin Amberlite IRA 402.

In order to assess the applicability and greenness of the tested reactions, they were classified according to five important aspects: cost, energy consumption, type and risk of the solvent, waste generation and hazards. These categories and the colour code are described in more detail in Tab. 2.2.3-1. It has to be mentioned that this is not an entire classification and that there are further aspects to be considered when evaluating chemical reactions. An entire assessment can be reached by life cycle analysis (LCA).[41] Other ways to evaluate the greenness of a reaction are the green star or the green circle method, where all principles of green chemistry are rated.[42] However, the present assessment includes the aspects which are believed to be most important for the practical application of the investigated reactions. It is by far not an absolute assessment, but a comparative evaluation of the reactions presented in this chapter.

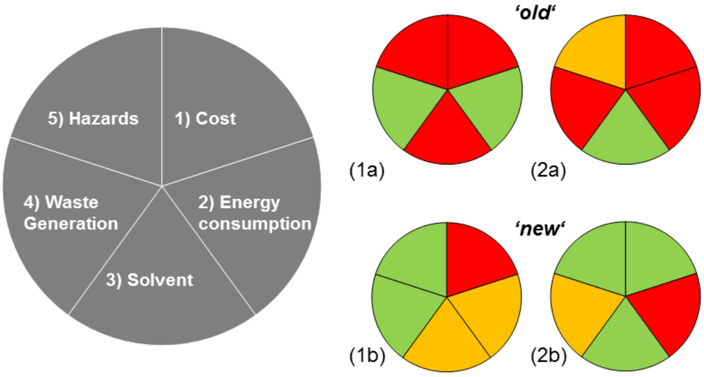

Fig. 2.2.3-1: Classification of the presented reactions 1a, 1b, 2a and 2b according to cost, energy consumption, solvent, waste generation and hazards of the reaction (see. Tab. 2.2.3-1).

The evaluation of the tested reactions is depicted in Fig. 2.2.3-1 by a circular diagram, where each section represents one of the five criteria. The given colour reveals, if this criterium is classified as 'uncritical' (green), 'improvable' (orange) or 'critical' (red). In the following, some explanations regarding the chosen classification will be given.

The cost factor is evaluated in regard of the costs for the starting materials for a synthesis at laboratory scale. As *L*-carnitine with a price of 247 € per 50 g and Ag_2O with a price of 841 € per 500 g (both Alfa Aesar, March 2019) are rather expensive chemicals, reaction (1a), (1b) and (2a) are categorized as critical in terms of the reaction cost. For example, the price for the production of 1 kg [C_2Car]OAc utilizing reaction (1a/b) in combination with (2a) would be more than 4620 € only regarding these two starting materials and assuming that the yield is 100 %.

The energy consumption of the reaction comprises heating and stirring during the reaction and more importantly the removal of the solvent and drying of the product. As the removal of water by evaporation is highly energy consuming, reaction (2a) and (2b) are classified as critical. The long reaction times of (1b) led to its classification as improvable.

Reaction (1a) and (1b) included washing steps with diethylether, which is an organic solvent with high vapour pressure, and easily emitted to the environment. In addition, acetonitrile was used in (1a), while actually no solvent, but ethanol reagent in high excess was used in (1b), so that they were ranked as critical and improvable, respectively. In contrast, reactions (2a) and (2b) did not employ any organic solvent. Although water is used in huge amount, they can be classified as uncritical, as water is non-toxic.

Reactions (1a) and (1b) exhibit favourable profiles in terms of by-product production: while no by-products are created in (1a), only water is formed in (1b). They are both uncritical regarding waste generation. In contrast, reaction (2a) raised concerns, as AgBr is produced in equimolar amounts. For example, the production of 1 kg [C_2Car]OAc would create 0.75 kg AgBr. The anion exchange using the exchange resin is rated improvable, as high amounts of acid and salt solutions are required to load, rinse and regenerate the column.

The category 'hazards' comprises risks for humans and environment caused by the chemicals used in the studied reactions. Due to the properties of ethyl bromide mentioned above (section 2.2.1.1), (1a) is categorized as critical. Reaction (2a) is improvable due to the fact that the silver compounds are toxic for aquatic organisms and Ag_2O being a strong oxidatizing agent. Materials used in (1b) and (2b) are assumed to be uncritical.

Tab. 2.2.3-1: Description of the classification categories for the assessed reactions.

	Description
1) Cost	Includes costs for starting materials.
2) Energy Consumption	Takes into account the energy required during the reaction and for product isolation.
3) Solvent	Considers the kind of solvent and the amount required.
4) Waste Generation	Includes of by-products produced during the reaction and within the purification process.
5) Hazard	Involves risks for humans and environment caused by the reaction educts and products.

🟥 critical 🟨 improvable 🟩 uncritical

It is encouraging to see that in summary the newly developed reactions (1b) and (2b) cause less concerns compared to the 'old' synthesis route in terms of the five aspects considered herein. However, at least with possibilities available in a physical chemical lab, they were not appropriate for the production in high amounts, as the column chromatography-based purification and the anion exchange column were extremely time-consuming.

2.2.3.2 Discussion of the Properties and the Applicability of Carnitine-Based Ionic Liquids

Four [C_2Car]X ILs were investigated in this study: [C_2Car]Br, [C_2Car]$MeSO_3$, [C_2Car]OAc and [C_2Car]Lev. Although treated as IL throughout the present discussion, [C_2Car]Br with a melting temperature of 172 °C is per definition no IL. [C_2Car]$MeSO_3$ and [C_2Car]Lev are solid at room temperature, but exhibit melting points below 100 °C. Only [C_2Car]OAc is a room temperature IL, but features an extremely high viscositiy of 176 Pa*s at 25 °C.[28] Its texture was extremely sticky and unhandy. When considering these ILs as solvents, elevated temperatures are required. This, however, causes stability problems: a change in colour and smell were observed, when the carnitine-based ILs were kept at elevated temperatures. This was attributed to degradation. This and the limitations reported for their synthetic formation extremely restrict them in their applicability. The observation of a lowered melting temperature of [C_2Car]$MeSO_3$ in presence of pure *L*-carnitine holds promise that their properties can be improved by the formation of low-melting mixtures with a second compound. Further investigations regarding this idea can be found in section 3.2.3.

2.3 [C_nCar]Br – Ionic Liquids, Hydrotropes and Surfactants

In the following, the naturally occurring *L*-carnitine has been used for the development of functional bio-based molecules. Its derivatization to form bromide salts of its alkyl esters was conducted in a one-step synthesis. Carnitine alkyl ester bromides [C_nCar]Br have been prepared with alkyl chain lengths ranging from n = 2 – 14. Depending on the length of the alkyl residue, they could be assorted to different substance groups, including ILs, hydrotropes and surfactants. The thermal properties of these novel molecules were determined as well as their interfacial and aggregation behaviour. Their ability to dissolve a hydrophobic dye was studied in order to evaluate their hydrotropic character. The solubility of vanillin as model substance in [C_nCar]Br aqueous solutions was examined in order to demonstrate their applicability as bio-based solubilizers. Their cytotoxicity was compared to conventionally used representatives of each substance group they are addressed to. The results presented in this section are based on the publication 'Carnitine Alkyl Ester Bromides as Novel Biosourced Ionic Liquids, Cationic Hydrotropes and Surfactants' by Häckl *et al.*[69] and previous work conducted by Andrea Mühlbauer at the University of Lille.[11]

2.3.1 Synthesis

Carnitine alkyl ester bromides, abbreviated as [C_nCar]Br, were synthesized in one step using *L*-carnitine and the respective 1-bromoalkane (R = $C_nH_{2n+1}$with n = 2 – 14) as starting materials. The synthesis was conducted analogously to the description in section 2.2.1.1 and Fig. 2.2.1-1 for carnitine ethyl ester bromide ILs.[11,28] NMR data of the prepared [C_nCar]Br compounds are given in the experimental section 2.6.2.

Practically, this synthesis was relatively easy to perform. However, some concerns in terms of greenness have to be admitted: (1) short chain bromoalkanes are volatile (exemplarily, bromoethane evaporates at 38 °C) and hence easily emitted to the atmosphere; (2) safety data reveals that bromoalkanes are labelled with at least one of the following hazard potentials: flammable, carcinogenic, toxic for water organisms or irritant to skin, respiratory tract and eyes.[34] The study was conducted in awareness of these drawbacks of the starting materials and further research efforts aimed to find alternatives (see sections 2.2.1.1, 2.2.3.1 and 2.4.1).

2.3.2 Characterization

2.3.2.1 Temperature-Dependent Phase Behaviour

Typical features of ILs are low melting temperatures below 100 °C and high thermal stabilities.[38] As the [C_nCar]Br compounds were considered as ILs, their temperature-dependent phase behaviour was studied. DSC measurements delivered information about their melting temperatures (T_m) and glass transition temperatures (T_g). Thermal degradation temperatures were determined by TGA. Thermal properties of ILs are typically influenced by their water contents. The latter can be determined by Karl-Fischer coulometry and should always be indicated when discussing thermal properties of ILs.

Tab. 2.3.2-1: Degradation temperature T_{deg}, melting temperature T_m and glass transition temperature T_g of the synthesized [C_nCar]Br compounds for different chain lengths (data partly collected by Mühlbauer A.).[11]

n	T_{deg} [°C]	T_m [°C]	T_g [°C]	Water content [wt%]	Appearance at room temperature
2	260	172	-16	0.03	Solid
4	189	-	-22	1.1	Liquid
6	187	-	-29	2.4	Liquid
8	185	34	-	0.5	Solid/liquid
10	235	59	-	0.1	Solid
12	239	69	-	0.1	Solid
14	241	71	-	0.1	Solid

According to the results shown in Tab. 2.3.2-1, [C_2Car]Br with a melting temperature of 172 °C is per definition no IL.[28] The [C_nCar]Br compounds with n = 4 – 14 belong to the group of ILs, whereas [C_4Car]Br and [C_6Car]Br are even liquid at room temperature and exhibit glass transition temperatures of -22 °C and -29 °C, respectively. The occurrence of such glass transitions is characteristic for ILs and due to the organization into an amorphous solid state upon cooling. The formation of a crystal lattice is sterically hindered.[43] The increase in melting temperatures with alkyl chain length for n = 8 – 14 can be explained by increasing intermolecular van der Waals interactions in the hydrophobic section of the molecule.[44] Interestingly, there is a significant jump in the degradation temperatures between n = 8 and n = 10.

2.3.2.2 Interfacial and Self-aggregation Behaviour of [C$_n$Car]Br Compounds in Aqueous Solution

It shall be mentioned here that the determination of aqueous phase behaviour is not appropriate for characterizing ILs and their solvent properties. Instead, this is more relevant for obtaining information on hydrotropic and surfactant features.

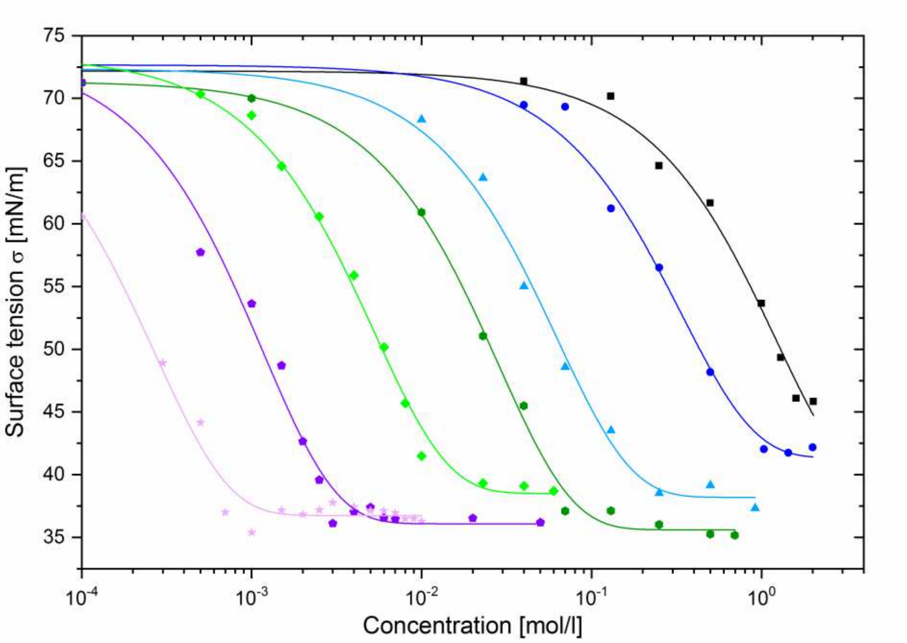

Fig. 2.3.2-1: Concentration dependent surface tension curves of [C$_n$Car]Br compounds with n = 2 (■), 4 (●), 6 (▲), 8 (⬢), 10 (◆), 12 (⬟), and 14 (★) (data partly collected by Mühlbauer A.).[11]

Due to their amphiphilic and ionic character, a certain self-organization of [C$_n$Car]Br in aqueous solution was expected: hydrotrope-like for short alkyl chains and surfactant-like for long alkyl chains. Identifying distinct or fluent transfer from hydrotrope to surfactant when increasing the alkyl chain length n was one of the main interests of the present study. In order to get detailed information, the series of carnitine ester bromides with n in the range from 2 to 14 was studied regarding their equilibrium surface tensions in dilute aqueous solutions at different concentrations. As presented in Fig. 2.3.2-1, all compounds lowered the surface tension of water upon increasing concentration. Their behaviours correspond to the 'regular' surface tension curves of amphiphile solutions: when increasing the [C$_n$Car]Br concentration, the surface tension undergoes a steep decay until a certain point is reached – the so-called critical aggregation concentration (CAC) or the critical micellar concentration (CMC). After this more or less clear curve break, the surface tension value stays constant. The CAC or the CMC denotes the concentration, where amphiphilic molecules self-aggregate in water due to strong hydrophobic interactions, which is energetically more favourable than interactions between water and the hydrophobic tails. The differentiation between CAC and CMC refers to the fact that short chain amphiphilic molecules form less pronounced aggregates in undefined shapes, while long chain amphiphiles (surfactants) form micelles in certain shapes according to their packing parameters. CMCs serve as characteristic qualities of surfactants. In general, they are subject to the kind and charge of the head group and the parameters of the hydrophobic tail.[29] For the sake of consistency, the term CAC will be used in the following discussion.

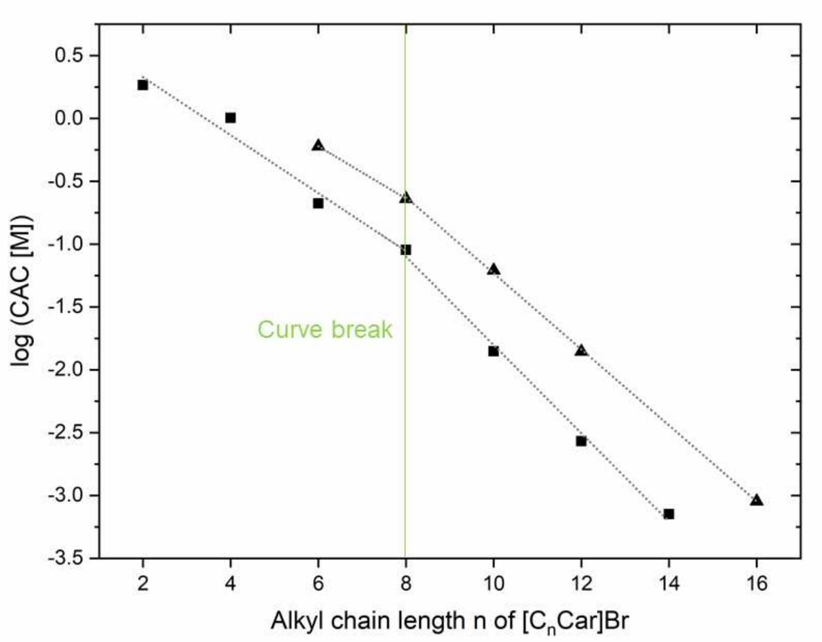

Fig. 2.3.2-2: Log (CAC) as a function of alkyl chain length n of [C$_n$Car]Br (■) and alkyltrimethylammonium compounds C$_n$TAB (literature values from [29,45]) (▲) with a curve break at n = 8 (marked in green).

Water solubilities, CACs and minimum surface tensions σ_{CAC} of the investigated [C$_n$Car]Br compounds are listed in Tab. 2.3.2-2. Especially for n = 2 and n = 4, the water solubility is high and only restricted by the high viscosities of the resulting mixtures. With increasing hydrophobicity of the carnitine derivative, the water solubility decreases. In contrast to other positively charged amphiphiles, the water solubility of all [C$_n$Car]Br agents is fairly high, *e.g.* the water solubility of [C$_{12}$Car]Br is almost six times higher compared to the analogues dodecyltrimethylammonium surfactant.[46] This is ascribed to the bigger size of the carnitine head group, which hinders crystallization, and its higher water compatibility due to the hydroxyl and carboxyl function.

It was found that with increasing alkyl chain length and hence hydrophobicity, the CAC of [C$_n$Car]Br decreases. This corresponds to an increase in 'surfactant efficiency', as less surfactant is required for reducing the surface tension and self-aggregation.[29,30] The CACs of the long-chain carnitine bromides are in the millimolar range with values of 14, 2.7 and 0.71 mM for [C$_{10}$Car]Br, [C$_{12}$Car]Br and [C$_{14}$Car]Br, respectively and therefore similar to other surfactants, such as alkyltrimethylammonium bromides.[29,45] The short-chain compounds have their CACs at higher concentrations in the molar range due to better solvent bulk compatibility and weaker hydrophobic interactions.

Klevens was the first one to investigate the relationship between the logarithmic CAC values and the alkyl chain length of a homologous series of surfactants.[47] He reported a linear relationship and that the slope and the intercept of the linear curve are characteristic for the type of surfactant. In a similar study conducted with *n*-alkylbenzoates, Hatzopoulos *et al.* obtained two distinguishable slopes in the linear log (CAC)-vs.-carbon number curve, one for n = 0 – 3 and another one for n = 4 – 8.[48] This finding was related to a shift from hydrotropic to surfactant behaviour. Fig. 2.3.2-2 shows the log (CAC)-vs.-carbon number plots of $[C_nCar]Br$ and alkyltrimethylammonium bromides C_nTAB (obtained from literature values).[29,45] The curves almost seem to be parallel. They indicate a transition from hydrotrope to surfactant by the visible curve break at n = 8. The position of the transition correlates well with Klevens' results[47] and the above mentioned results obtained by Hatzopoulos *et al.* for the *n*-alkylbenzoates, when considering the hydrophobic contribution of the benzene ring.[48]

In contrast to the efficiency of a surfactant, the 'effectiveness' is not a measure of CAC, but related to the minimum surface tension that can be reached with a certain surface active solute.[30] It is closely related to the packing ability of the solute at the air-liquid interface and influenced by the strength of the van der Waals interactions between the alkyl chains, the kind of head group and in case of ionic surfactants their counter-ion binding.[29] In this study, the surface tension values at the CAC, σ_{CAC} (see Tab. 2.3.2-2 and Fig. 2.3.2-2.), were used for the evaluation of the surfactant effectiveness. Slightly higher values were obtained for n = 2 – 4, while they were similar for n = 6 – 14. This means that middle-chain hydrotropes/surfactants of the type $[C_nCar]Br$ are able to reach minimum surface tensions as low as their long-chain homologues. However, higher concentrations are required to come to these low surface tensions. In summary, this means that the efficiency of the $[C_nCar]Br$ compounds exhibits a strong dependency on the alkyl chain length, while their effectiveness can be similar.[49]

Tab. 2.3.2-2: Water-solubility, critical aggregation concentration (CAC) and minimum surface tension σ_{CAC} of $[C_nCar]Br$ compounds with reference data of alkyltrimethylammonium bromides (data partly collected by Mühlbauer A.).[11]

n	water-solubility [M]	σ_{CAC} [mN/m]	CAC [M]	CMC (C_nTAB) [M]
2	> 10	46	1.84	-
4	> 10	42	1.01	-
6	5.9	37	0.21	0.60[45]
8	5.3	35	0.09	0.23[45]
10	2.4	39	$1.4\text{x}10^{-2}$	$6.2\text{x}10^{-2}$[45] $6.5\text{x}10^{-2}$[29]
12	1.3	36	$2.7\text{x}10^{-3}$	$1.4\text{x}10^{-2}$[45] $1.6\text{x}10^{-2}$[29]
14	0.7	36	$7.1\text{x}10^{-4}$	-
16	-	-	-	$9.0\text{x}10^{-4}$[29]

In summary, the surface tension measurements confirmed that the investigated species are surface active and decrease the surface tension of water. The CACs are highly dependent on the alkyl chain length and decrease with increasing chain length. Alkyltrimethylammonium bromides (C_nTAB) are conventionally used cationic surfactants. Data available in literature (see Tab. 2.3.2-2) reveals that the newly developed carnitine alkyl ester bromides exhibit lower CACs than C_nTAB at analogous chain length. This means that carnitine-based amphiphiles can be taken into consideration as bio-based alternatives to conventional petro-based cationic surfactants. The surfactant effectiveness of $[C_nCar]Br$ is similar for n = 6 – 14 and lower for n = 2 – 4. In addition, a log (CAC)-vs.-carbon number plot showed two different linearities with a break at n = 8. Both findings can be seen as indicators for differentiating aggregation mechanisms and for a potential shift from hydrotrope to surfactant.

Dynamic light scattering (DLS) measurements were carried out in order to gain more information on the self-aggregation behaviour and allow for further statements upon the transition from hydrotrope to surfactant.

2.3.2.3 Characterization of Aggregation by Dynamic Light Scattering

DLS is a method used for analyzing particles and structures in solution. The resulting correlation functions can give information on particle structure, size and polydispersity of the solution. Fig. 2.3.2-3 shows the time-dependent correlation functions of all $[C_nCar]Br$ compounds and some selected reference substances. The measured solutions were prepared in concentrations well above the CAC of the respective compound.

Aqueous solutions of alkyl carnitine esters feature well-defined correlation functions, when $n \geq 6$. The correlation for $n \leq 4$ is low. In total, the correlation decreased with decreasing alkyl chain length. This is in agreement with the theory and suggests that more pronounced, spherical aggregates are formed with longer alkyl chains. Less distinct aggregates are found in short-chain $[C_nCar]Br$ solutions, as hydrophobic moieties are too small for their assembly into proper micelles.[50] Nevertheless, they also have moderate tendency to self-aggregate, as it can be expected for hydrotropes.[51]

In order to evaluate the obtained results, aqueous solutions of 1-butyl-3-methylimidazolium bromide ($[C_4C_1Im]Br$), sodium xylene sulphonate (SXS), $C_{12}TAB$ and $C_{16}TAB$ were analysed and compared. SXS as typical hydrotrope and $[C_4C_1Im]Br$ as typical IL exhibited weak aggregation behaviour similar to $[C_2Car]Br$ in aqueous solution. The correlation of $C_{12}TAB$ lay within the range of the long chain carnitine compounds. The correlation of $C_{16}TAB$ was unexpectedly low. But this can be explained by the low concentration (0.015 M) that had to be used due to $C_{16}TAB$'s restricted water solubility.

In general, the size of the particles in solution can be derived from the correlation function. Hydrodynamic radii can be calculated from the Stokes-Einstein-relation, which takes the diffusion coefficient into account. This operation did not yield physically reasonable results in case of [C$_n$Car]Br solutions. Due to high ionic amphiphile concentrations, the ionic strength of the solutions significantly influenced the diffusion of the aggregates, which is usually dominated by their size.[52] Values obtained by the conventionally applied cumulant analysis led to particle sizes of < 1.5 nm. It must be assumed, however, that the real aggregate size is higher.

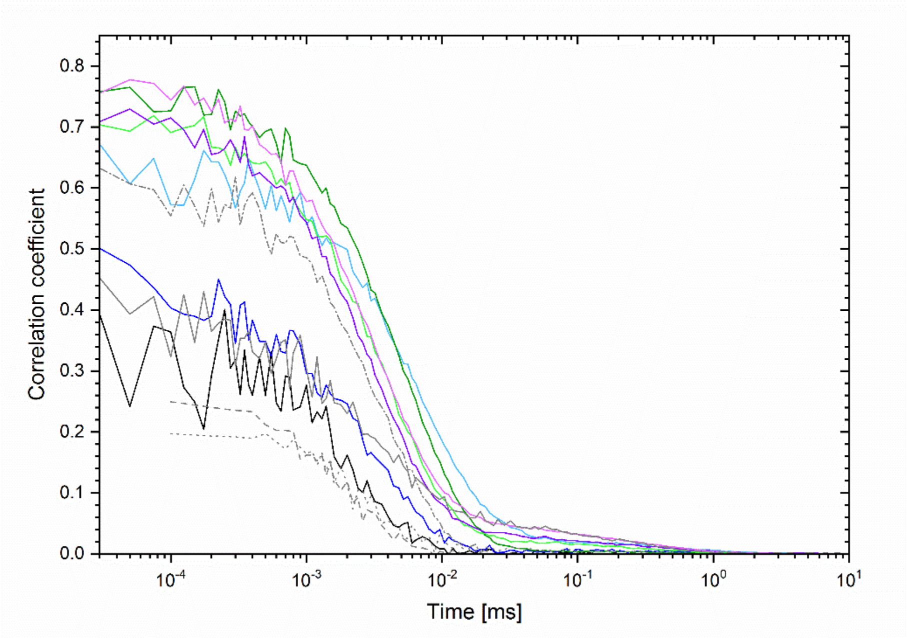

Fig. 2.3.2-3: Time-dependent self-correlation functions as obtained by DLS for the [C$_n$Car]Br/water binary system and several reference substances at 25 °C: 1.946 M [C$_2$Car]Br (—),1.099 M [C$_4$Car]Br (—),0.313 M [C$_6$Car]Br (—), 0.190 M [C$_8$Car]Br (—), 0.114 M [C$_{10}$Car]Br (—), 0.103 M [C$_{12}$Car]Br (—), 0.101 M [C$_{14}$Car]Br (—), 3.5 M [C$_1$C$_4$Im]Br (- -), 0.5 M SXS (••), 0.111 M C$_{12}$TAB (-•-), 0.015 M C$_{16}$TAB (—).

2.3.2.4 Hydrotropic Efficiency of Short- and Medium-Chain [C$_n$Car]Br Compounds (n = 2 – 8)

The solubility of the hydrophobic dye disperse red 13 (DR13) in aqueous [C$_n$Car]Br solutions has been determined by means of UV/Vis spectroscopy. This is an accepted concept for the evaluation of a hydrotrope's efficiency for the solubilzation of hydrophobic substances.[53] Plotting the absorbance at a certain wavelength (near the absorption maximum of DR13) against the concentration of hydrotrope allows for a qualitative analysis and comparison of the studied hydrotropes, as according to Lambert-Beer's Law, the absorbance is proportional to the concentration of solubilized dye.

Fig. 2.3.2-4 illustrates an increase of the DR13 solubility in the studied aqueous solutions, when the corresponding hydrotrope exceeds a certain threshold concentration. This concentration is referred to as minimum hydrotropic concentration (MHC) and quantifies the hydrotrope efficiency for solubilizing hydrophobic solutes. According to the collected data, the hydrotrope efficiency of the [C$_n$Car]Br compounds increases with increasing chain length. Distinct MHC values shall not be given in this work. However, it can be found that estimated MHCs do not correspond exactly to the CACs determined from surface tension measurements. In general, the critical values in the ternary systems were lower compared to the binary systems. This can be rationalized by the assumption that the hydrophobic solute promotes the aggregation, so that self-assembly starts earlier, *i.e.* at lower concentrations, in the presence of a third component.[55] After all, the mechanism of hydrotropic solubilization is still to be clarified and different theories are suggested (see section 1.4.2.2). As self-aggregation of hydrotropes in binary systems was observed via surface tension and DLS measurements, it is believed that the hydrotropic mode of action of carnitine ester derivatives is dominated by a micellar-like mechanism and that the presence of a hydrophobic solute supports aggregation. It is not denied that there are other contributing factors, such as hydration leading to a complex interplay of interactions between hydrotrope, solute and solvent.

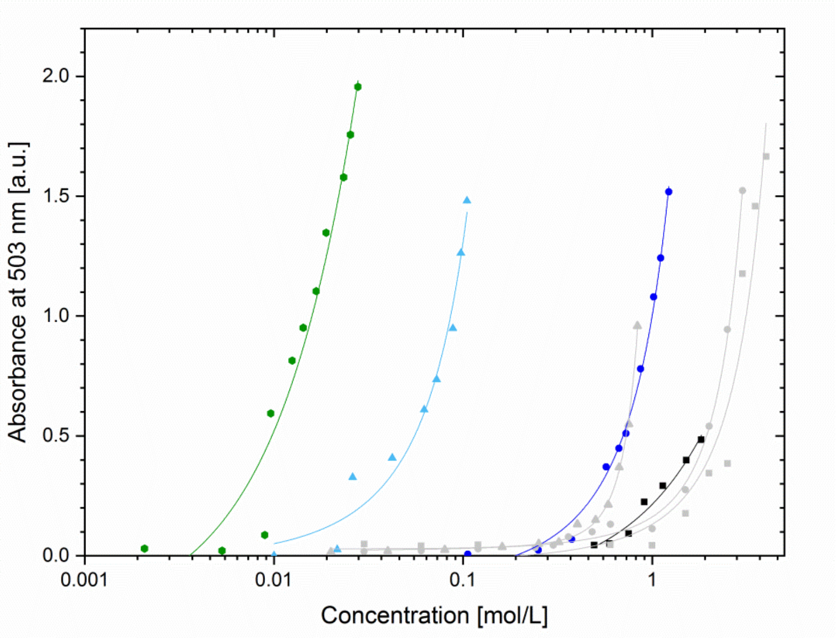

Fig. 2.3.2-4: Hydrotropic solubilization of DR13 in [C$_n$Car]Br compounds with n = 0 (■), 2 (■), 4 (●), 6 (▲), 8 (⬢) and reference substances [C$_1$C$_4$Im]Br (●) and SXS (▲) (data partly collected by Mühlbauer A.).[11]

Besides the carnitine ester derivatives, three reference substances have been studied in terms of their ability to solubilize DR13: *L*-carnitine as unesterified analogue, [C$_1$C$_4$Im]Br and SXS. All [C$_n$Car]Br agents showed higher hydrotropic efficiency than *L*-carnitine and [C$_1$C$_4$Im]Br. The MHC of SXS was similar to the one of [C$_4$Car]Br. However, the performance of the carnitine derivative was better in terms of its ability to dissolve higher amounts of solute. There was an interesting side aspect worth to mention: *L*-carnitine and [C$_1$C$_4$Im]Br did not exhibit a CAC in the binary aqueous systems, though they showed MHCs when investigating the solubility of DR13. Based on the assumption that the hydrotropic solubilization process proceeds in a micellar-like mechanism, it means that *L*-carnitine and [C_1C_4Im]Br only form aggregates in presence of a hydrophobic third component.

2.3.2.5 Cytotoxicity of [C_nCar]Br Compounds

The cytotoxicity was determined by means of an in vitro PrestoBlue assay with human skin keratinocytes (HaCaT cells). The EC_{50} value is a typical measure for the cytotoxicity. It corresponds to the concentration at which 50 % of the contaminated cells survive after a certain time of exposure to the studied contaminant. This characteristic value is obtained from the dose-response fit of the cell viability-vs.-concentration of contaminant plot.

The cytotoxicity of all [C_nCar]Br compounds with n = 2 – 14, [C_1C_4Im]Br and SXS was determined and respective literature values of C_{12}TAB and C_{16}TAB were considered. While [C_2Car]Br, [C_4Car]Br and SXS did not show any impact in the tested concentration range, the EC_{50} values of the other compounds are shown in Fig. 2.3.2-5. [C_1C_4Im]Br and the middle-chain carnitine ester derivatives with n = 6 and n = 8 exhibited moderate cytotoxicity on HaCaT cells with EC_{50} values of $3.3\text{x}10^{-3}$ M, $4.5\text{x}10^{-3}$ M and $1.2\text{x}10^{-4}$ M, respectively. More critical results were obtained for long-chain cationic surfactants of the type [C_nCar]Br and C_nTAB characterized by EC_{50} values ranging from $1.5\text{x}10^{-5}$ M to $3.0\text{x}10^{-5}$ M.[54]

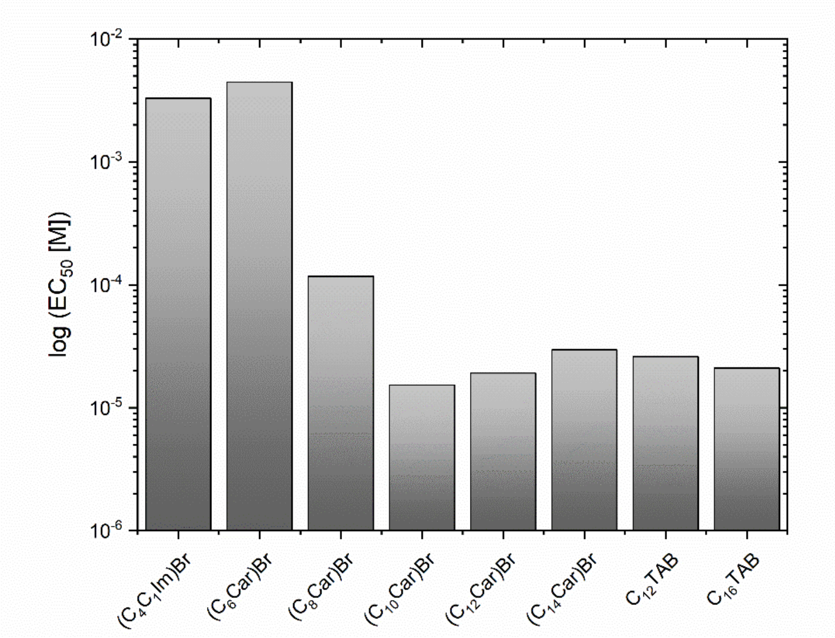

Fig. 2.3.2-5: EC_{50} values (logarithmic scale) for [C_nCar]Br compounds with n = 6 – 14 and [C_1C_4Im]Br including literature values for two alkyltrimethylammonium bromides C_{12}TAB and C_{16}TAB.[54]

These results confirm that the cytotoxicity is mainly determined by the alkyl chain length, as known for a number of other compounds. Several publications report that the cytotoxicity of quaternary ammonium compounds and cationic surfactants originates from their interaction with phospholipid cell membranes.[56,57] Depending on concentration and exposure time, they can affect physical properties and functions of the membranes. An association of surfactant with membrane compounds can occur and leads to cell lysis. Cationic surfactants were also suggested to cause mitochondrial dysfunction.[57] Direct comparison of the EC_{50} of $[C_{12}Car]Br$ with the one of $C_{12}TAB$ obtained from literature, reveals that $[C_{12}Car]Br$ is more toxic. This is attributed to its longer effective carbon chain length, as the carnitine head group itself contains further hydrocarbon groups. However, EC_{50} values reported in literature where obtained with a different method. For better comparability, the cytotoxicity of the C_nTAB compounds should be determined by means of the PrestoBlue assay.

In fact, it is questionable, whether the cytotoxicity of cationic surfactants with quaternary ammonium head group can be avoided at all. Certainly, it takes benefit from a reduction of the alkyl chain length. In this regard, the presented carnitine derivatives deliver an important benefit over conventional alkyltrimethylammonium bromides: they exhibit higher efficiencies with shorter alkyl chains. Therefore, they can be considered as less cytotoxic alternatives for cationic surfactants.

2.3.3 Application for the Solubilization of Vanillin

Vanillin (3-methoxy-4-hydroxy-benzaldehyde) (see Fig. 2.3.3-1) is a biomolecule that can be found in various sorts of vanilla beans. It is one of the main constituents of vanilla extract. Due to its strong flavour, it is added to numerous food products including beverages, bakery goods and desserts as a flavouring ingredient. It is used as a fragrance in cosmetics and occurs as intermediate product in the manufacturing of pharmaceutics, cosmetics or fine chemicals. Due to its widespread use, it is also synthesized from lignin or guaiacol. In addition, vanillin features antioxidant activity and a number of other bioactive functions. Therefore it can also act as a preservative in chemical formulations.[58]

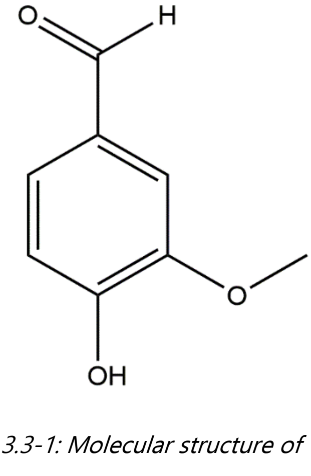

Fig. 2.3.3-1: Molecular structure of vanillin.

Vanillin has a low water solubility in the range of 0.06 M. Accordingly, strategies for making it compatible with aqueous media have to be developed, when needed, *e.g.* for some cosmetic and food formulations or to enhance its extractability. Thus, the solubility of vanillin in aqueous solutions of [C$_n$Car]Br and some selected reference substances has been investigated. The corresponding solubility curves obtained by means of UV/Vis spectrometry and a calibration in ethanolic solution are presented in Fig. 2.3.3-2. While the addition of *L*-carnitine only had negligible effect on the water solubility of vanillin, its esterified derivatives clearly promote the vanillin water solubility. Best results were obtained with [C$_4$Car]Br and [C$_6$Car]Br solutions. With maximum vanillin solubilities of 0.55 M and 0.62 M, achieved by 1.24 mol/kg [C$_4$Car]Br and 1.07 kg/mol [C$_6$Car]Br, respectively, they increased it approximately tenfold compared to pure water. In contrast, long chain alkyl carnitine esters were restricted by their own water solubility. The same was true for C$_{12}$TAB and C$_{16}$TAB. SXS and [C$_1$C$_4$Im]Br turned out to have excellent capacity for solubilizing vanillin. The solubility is suggested to be promoted by π-interactions between the vanillin aromatic ring and the SXS aromatic ring or the imidazolium ring, respectively. Due to the lower water solubility of SXS, [C$_1$C$_4$Im]Br showed improved performance.

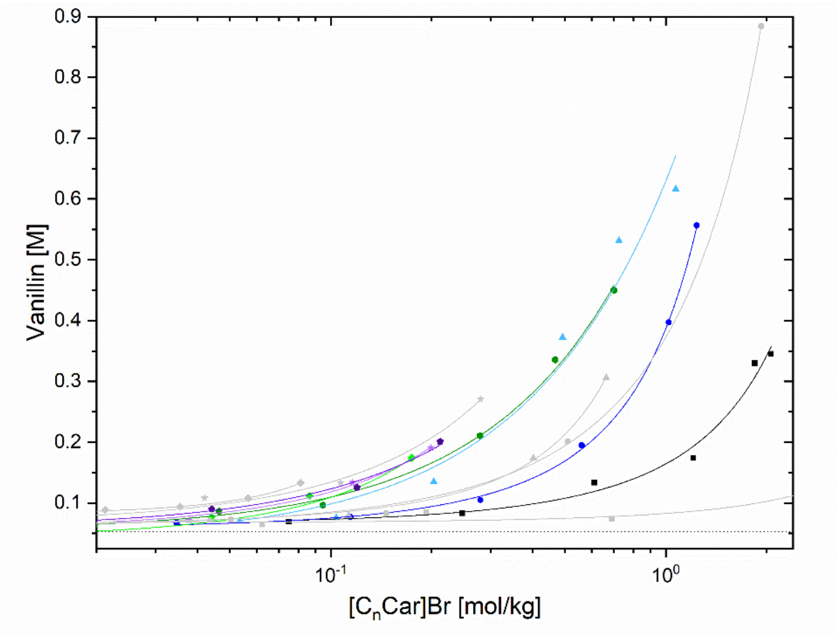

Fig. 2.3.3-2: Solubility of vanillin in aqueous solutions of [C$_n$Car]Br with n = 0 (■), 2 (■), 4 (●), 6 (▲), 8 (●), 10 (◆), 12 (⬟), and 14 (★) and reference substances [C$_1$C$_4$Im]Br (●), SXS (▲), C$_{12}$TAB (◆), and C$_{16}$TAB (★) at room temperature. The dotted horizontal line indicates the solubility of vanillin in pure water.

2.4 [C$_n$Car]MeSO$_3$-Surfactants

The central idea of this study was to improve the synthesis route for the formation of alkyl carnitine ester surfactants with an inexpensive, simple and green approach. As mentioned above, the previous method employing alkyl bromides exhibited some drawbacks (see section 2.2.1.1) and an alternative reaction was desired.

The successful esterification of the carboxyl group of betaine with fatty alcohols and MeSO$_3$H for the formation of 'greener cationic surfactants' has been reported in literature[35,36] and could be reproduced for the formation of carnitine ethyl ester mesylate

ILs (see section 2.2.1.2). An analogous reaction of *L*-carnitine with fatty alcohols catalyzed by $MeSO_3H$ was considered as alternative reaction to obtain carnitine-based surfactants. The surfactant properties and the cytotoxicity of the resulting compounds were investigated herein. This is based on the work conducted by Verena Huber in the course of her Bachelor thesis.[59] In addition, characteristics of carnitine-based surfactants with mesylate as counter-ion are discussed in comparison to those with bromide counter-ions. The specific interaction between a charged surfactant head group and the counter-ion plays a significant role in terms of the surfactant behaviour in aqueous solution and influences parameters, such as CMC, adsorption properties, aggregation size and shape.

2.4.1 Synthesis

Carnitine alkyl ester mesylates, abbreviated as $[C_nCar]MeSO_3$, were synthesized in one step using *L*-carnitine, primary alcohols ($R = C_nH_{2n+1}$ with n = 8 – 14) and $MeSO_3H$ as starting materials (see Fig. 2.4.1-1).

L-carnitine (1 eq.) was combined with $MeSO_3H$ (1.5 eq.) and a primary alcohol (2 eq.) of the desired chain length was added applying an ice bath for cooling. The reaction mixture was subsequently stirred for 72 h at a temperature of 70 °C and under reduced pressure of 100 mbar. The addition of diethylether to the cooled reaction mixture caused a phase separation, with a sticky product phase on the bottom. After the reaction, the product was washed with diethylether three times. The supernatant solution was removed carefully with a syringe. The product was further purified by reversed phase column chromatography. A column of 3 cm diameter was filled with 100 g silica. A concentrated aqueous solution of the product was applied and eluted with a solvent mixture of water and acetonitrile and a solvent gradient ranging from 100 v/v% to 0 v/v% water. Thin layer chromatography (TLC) was used to identify the resulting fractions. The product fractions were combined, the solvent was removed by rotational evaporation and the product was dried with a high vacuum pump for at least 48 h. NMR data of the prepared $[C_nCar]MeSO_3$ compounds are given in the experimental part (see 2.6.2).

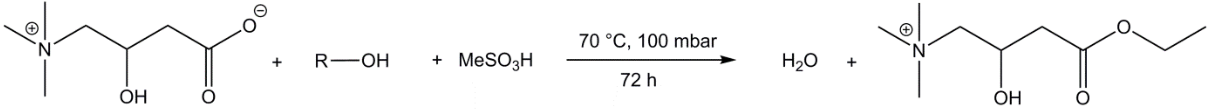

Fig. 2.4.1-1: One-step synthesis of carnitine alkyl ester mesylates; $R = C_nH_{2n+1}$ with n = 8, 10, 12, 14.

In contrast to the esterification with ethanol, the reaction of long-chain alcohols could be stimulated by reducing the pressure. This was meant to remove the generated water and to shift the equilibrium to the product side. Unfortunately, a conversion of more than 90 % could not be attained by this approach. However, the reaction was accelerated, as long-chain alcohols would otherwise react rather slowly. The overall product yield could not be determined exactly, but it is assumed to be around 50 %, as during the column purification a considerable amount of product was lost. Another obvious drawback of this reaction was the high consumption of solvent for product purification. However, it is conceivable to skip the solvent-consuming column chromatography purification according to the desired level of purity.

2.4.2 Characterization

2.4.2.1 Interfacial and Self-Aggregation Behaviour of [C_nCar]$MeSO_3$ Compounds in Aqueous Solution

In order to obtain information on surface- and self-aggregation behaviour, the equilibrium surface tension of a concentration series of each [C_nCar]$MeSO_3$ compound was determined by pendant drop tensiometry. As presented in Fig. 2.4.2-1, all compounds decreased the surface tension of water. All curves exhibit a surface tension minimum, before they reach a constant value. This is attributed to impurities present in the aqueous [C_nCar]$MeSO_3$ solutions originating from ester hydrolysis, which might have been promoted by acid impurities.[60] This means that besides the [C_nCar]$MeSO_3$ surfactant there are fatty alcohols influencing the surface tension of the aqueous solutions. This made the determination of the CMCs less exact. In this case it is deemed appropriate to refer to the critical values as CMCs, as with long hydrophobic tails a micellar aggregation is probable.

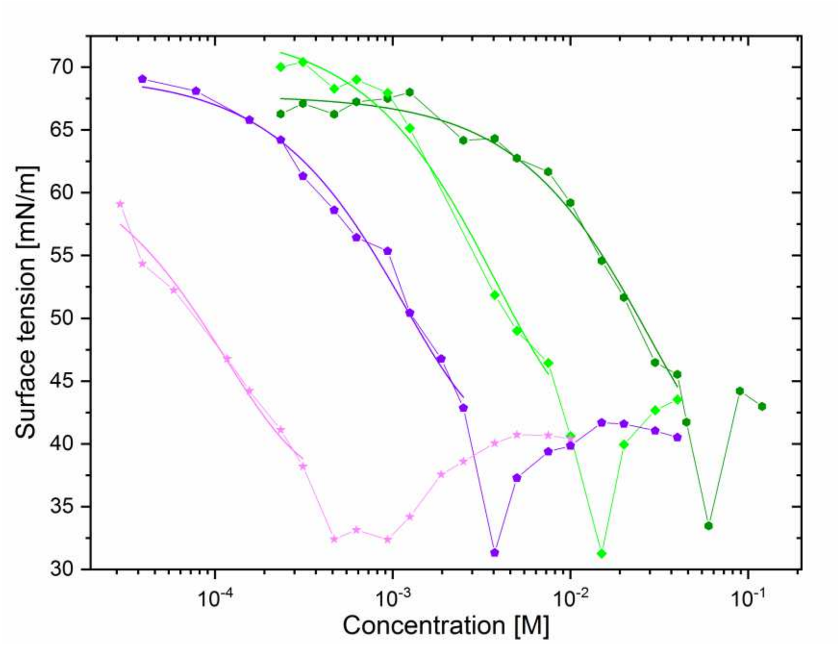

Fig. 2.4.2-1: Concentration dependent surface tension curves of [C_nCar]$MeSO_3$ compounds with n = 8 (⬢), 10 (◆), 12 (⬟), and 14 (★).

As expected, for the series of [C_nCar]$MeSO_3$ surfactants, the CMCs decrease with increasing alkyl chain length. For n = 8 – 14, they range from 4.2×10^{-2} M to 2.4×10^{-4} M (see Tab. 2.4.2-1), respectively and are in the concentration range of other ionic surfactants.[29,45] It is believed that the obtained CMC values are less accurate due to the fatty alcohol impurities.

They are good enough to give orientation values, but they were not analysed according to their logarithmic plot, to avoid false interpretation.

The alkyl chain length in the assessed range did not have a significant influence on the minimum surface tension σ_{CMC} and therefore on the effectiveness of $[C_nCar]MeSO_3$. σ_{CMC} was taken as the constant surface tension that was reached after the minimum. The same problem as for the CMCs applies for these values: their accurate detection was not possible due to impurities.

Tab. 2.4.2-1: Critical micellar concentration (CMC) and minimum surface tension σ_{CAC} of $[C_nCar]MeSO_3$ compounds.

n	**σ_{CMC} [mN/m]**	**CMC [M]**
8	44	$4.2x10^{-2}$
10	44	$8.5x10^{-3}$
12	42	$2.9x10^{-3}$
14	40	$2.4x10^{-4}$

Again, it should be pointed out that the accuracy of the analysis of the surface tension curves of $[C_nCar]MeSO_3$ surfactants was limited by deviations of the normal curve shape due to impurities. Nevertheless, the results were estimated to be fair enough to be used for a qualitative comparison with those obtained for the $[C_nCar]Br$ compounds.

Results revealed that the CMCs of the mesylate species were tendentially lower, *i.e.* their efficiency was higher compared to the above discussed bromide homologues. It is assumed that this effect goes back to Collins's concept of matching water affinities.[62,64] According to this approach, the quaternary ammoninum head group as well as the methyl sulfonate anion can be classified as chaotropic due to big ion size and low charge density.[65] The bromide is assumed to be less chaotropic.[62] In line with the principle 'like seeks like', the degree of counter-ion association in $[C_nCar]MeSO_3$ surfactants will be higher compared to $[C_nCar]Br$ surfactants. Thus, a sort of non-ionic character of $[C_nCar]MeSO_3$ compared to $[C_nCar]Br$ can be claimed. As micellation is easier in non-ionic systems due to lower electrostatic repulsion,[29] the CMC of the more associated $[C_nCar]MeSO_3$ is lower.

$[C_nCar]MeSO_3$ surfactants were less effective in lowering the surface tension and exhibited lower σ_{CAC} values than homologous $[C_nCar]Br$ compounds. This feature is controlled by the ability of the surfactant to adsorb at the water-air interface.[60] In order to explain this finding, the following hypothesis is stated: with its short alkyl moiety, mesylate is inserted into the interfacial region, where it does not contribute to the reduction of the surface tension. It occupies adsorption spaces at the interface which were normally taken by the carnitine ester amphiphile. Therefore, the surface tension is less reduced compared to carnitine bromide surfactants. Lima *et al.* claim similar behaviour for dodecyltrimethylammonium surfactants based on the results they obtained from dielectric relaxation spectroscopy.[63] Measurements with the Langmuir film balance or dielectric relaxation spectroscopy might be appropriate methods for clarifying, whether mesylate counter-ions are indeed inserted into the interface.

2.4.2.2 Characterization of Aggregation by Dynamic Light Scattering

DLS was used to obtain more information on the associates formed by micellation of $[C_nCar]MeSO_3$. As previously mentioned, this study is restricted to the qualitative analysis of the respective correlation functions. From Fig. 2.4.2-2, an overall rather low correlation function can be seen. This is due to the use of lower surfactant concentrations. At elevated concentrations, a clear tendency to form bigger aggregates and bimodal correlation functions was visible (see graph ---). This trend was only weakly observable in the respective bromide homologues, although they were measured in significantly higher concentrations.

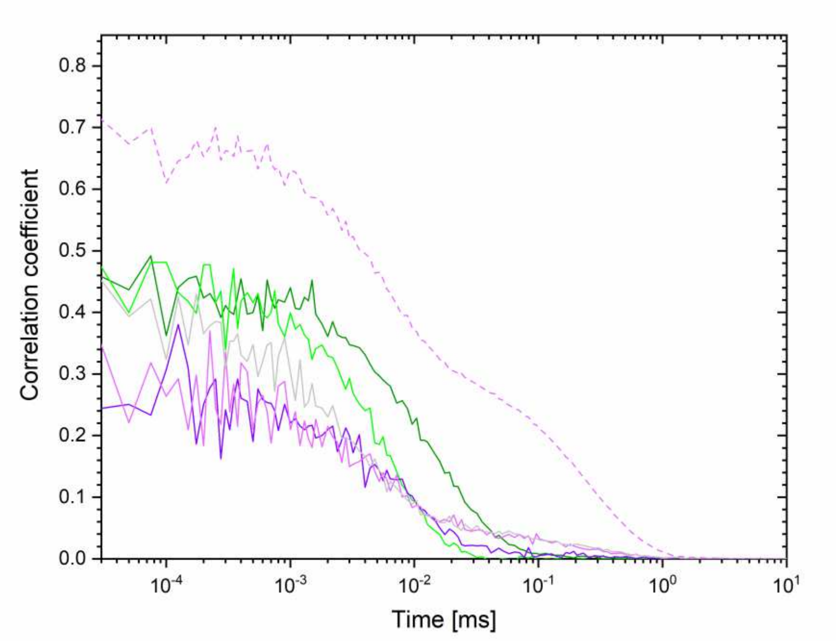

Fig. 2.4.2-2: Time-dependent self-correlation functions as obtained by DLS for the $[C_nCar]Br$/water binary system and several reference substances at 25 °C: 0.06 M $[C_8Car]MeSO_3$ (—), 0.05 M $[C_{10}Car]MeSO_3$ (—), 0.01 M $[C_{12}Car]MeSO_3$ (—), 0.01 M $[C_{14}Car]MeSO_3$ (—), 0.03 M $[C_{14}Car]MeSO_3$ (---) and 0.015 M $C_{16}TAB$ (—).

To explain this observation, one has to go into more detail about specific ion effects and the interactions between charged surfactant head groups and the counter-ion. In general, the size and shape of a surfactant aggregate is determined by its packing parameter (see section 1.4.3.2). Surfactants exhibiting packing parameters below ⅓ regularly self-assemble into spherical micelles in aqueous solution above the CMC. With higher packing parameters, cylindrical or lamellar micelles or vesicles are formed. Furthermore, the packing parameter is influenced by temperature, surfactant concentration, electrolytes, other additives and the type of counter-ion.

As discussed above, the carnitine head group is assumed to be well associated to the mesylate counter-ion in form of a contact ion-pair sharing one hydration shell. In contrast, the carnitine-bromide ion-pair is less associated and strongly hydrated. In consequence, the overall cross-sectional area a_0 of the $[C_nCar]MeSO_3$ surfactants is likely to be higher, so that according to Eq. 3 in section 1.4.3.2 the packing parameter is likely to be >⅓. This in turn means that the tendency for the formation of bigger and non-spherical aggregates is increased.

Static light scattering and small angle X-ray scattering measurements would help to gain further insight in particle shape and size of the studied $[C_nCar]MeSO_3$ systems.

2.4.2.3 Liquid Crystal Characteristics

When investigating the water solubility of the $[C_nCar]MeSO_3$ compounds, no solubility limit could be detected. Instead, viscous, gel-like solutions were formed at high surfactant concentrations. This feature of concentrated aqueous surfactant solutions is often related to the presence of liquid crystal phases. Concentrated $[C_nCar]MeSO_3$ solutions with gel-like texture are depicted in Fig. 2.4.2-3. They exhibited viscosities sufficiently high to render the magnetic stirrer stuck. The 'solution' was viscous enough to avoid a flow even when turned upside down. The surfactant concentration required for this effect decreased with increasing alkyl chain length.

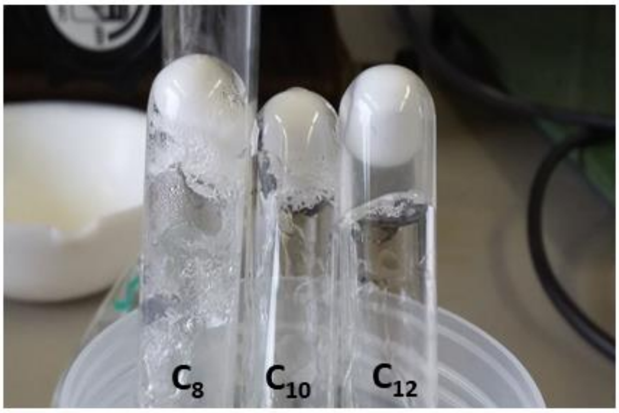

Fig. 2.4.2-3: Gel-like liquid crystal phases of aqueous solutions of $[C_nCar]MeSO_3$ with n = 8 (41 wt% ≙ 1.14 M), n = 10 (32 wt% ≙ 1.06 M) and n = 12 (34 wt% ≙ 0.99 M).

In the subsequent experiment using a polarization microscope, the viscous aqueous $[C_nCar]MeSO_3$ solutions were identified as liquid crystals. Applying the technique of the so-called 'penetration scan' allowed for the visualization of different aqueous phases coming along with the creation of a concentration gradient from low to high surfactant concentration (from right to left side in Fig. 2.4.2-4-A). In this direction, the presence of the following phases is suggested: (1) surfactant monomer solution, (2) micellar solution, (3) two isotropic, cubic phases, (4) anisotropic hexagonal phase, (5) isotropic, cubic bicontinuous phase, (6) lamellar, anisotropic phase. The black spots are ascribed to the presence of air bubbles. In regions of high viscosity, they can have shapes other than spherical. Fig. 2.4.2-4-B shows an optical magnification of the lamellar region (6) of Fig. 2.4.2-4-A. The presence of the typical maltese crosses, as highlighted by the blue ellipse, proves the formation of lamellar liquid crystals at highly concentrated surfactant aqueous solutions.

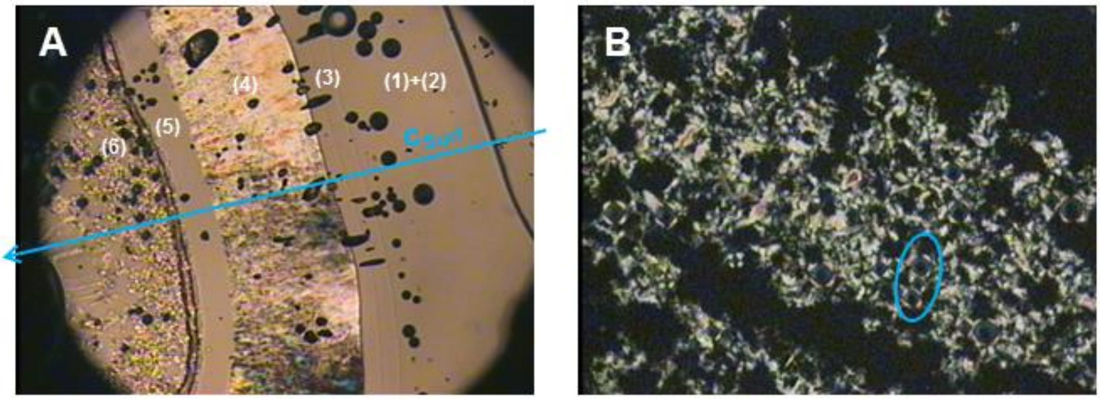

Fig. 2.4.2-4: Images recorded by a polarization microscope in tenfold magnification (left) and 20-fold magnification (right).

The increased water compatibility of [C_nCar]$MeSO_3$ surfactants in contrast to the analogous [C_nCar]Br surfactants, which exhibit solubility limits and are not capable of forming liquid crystals, is remarkable. Whether the surfactant is present in form of crystals or solubilized in form of monomers or micelles is determined by two contributions counter-balancing each other: the free energy of the surfactant in solution and the free energy of the surfactant's crystalline state. While the first one does not change significantly with the type of head group and counter-ion, the latter one is highly dependent on packing effects and therefore the specific interaction between head group and counter-ion.[29] It is assumed that the unsymmetrical, bulky structure of the mesylate anion does not allow for an effective packing into a crystal lattice, so that it features significantly higher water solubilities. This is in accordance with observations made when exchanging the sodium counter-ion of alkylsulphates by a choline cation.[13]

2.4.2.4 Cytotoxicity

As mentioned above, the cytotoxicity of cationic surfactants is dominated by their alkyl chain length and their ability to interact with phospholipid cell membranes. As seen in Fig. 2.4.2-5, EC_{50} values of the studied [C_nCar]$MeSO_3$ surfactants are higher compared to the [C_nCar]Br analogues (with exception of n = 14). Thus, there is obviously only a small influence of the type of counter-ion on the ability of a surfactant to penetrate into the lipid bilayer of a cell membrane. It is suggested that the higher degree of association and the bulky structure of mesylate make the interaction with the cell membrane weaker.

Therefore, $[C_nCar]MeSO_3$ surfactants exhibit slightly lower toxicities than the corresponding $[C_nCar]Br$ amphiphiles. They are even less toxic than C_nTAB, although they have further hydrocarbon groups between the alkyl chain and the quaternary ammonium group increasing the effective carbon chain length.

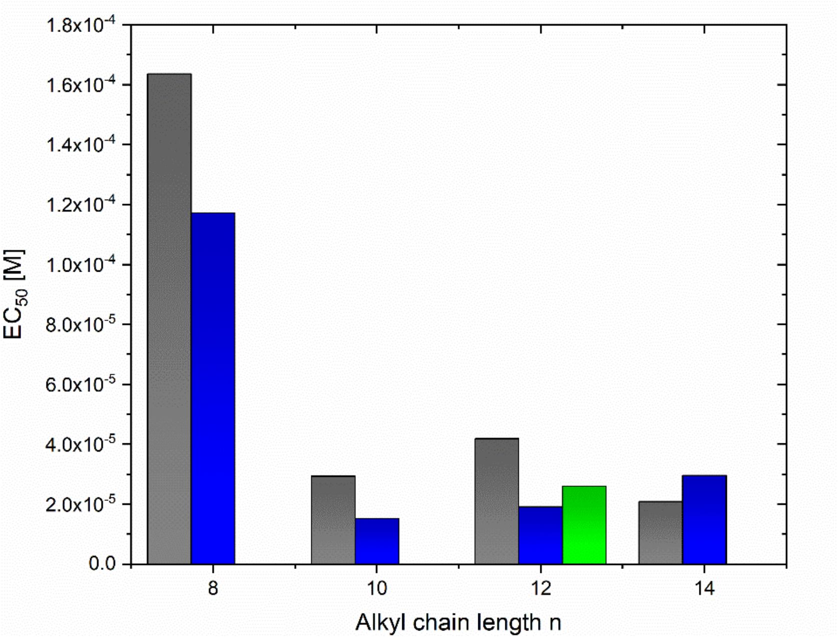

Fig. 2.4.2-5: EC_{50} values for $[C_nCar]MeSO_3$ (grey), $[C_nCar]Br$ (blue) and C_nTAB[54] (green) compounds with n = 8 - 14.

In terms of the determined properties, in particular efficiency in decreasing the surface tension, water solubility and cytotocixity, the $[C_nCar]MeSO_3$ compounds seem to be promising candidates for greener cationic surfactants. However, as a next step it is considered necessary to test their application and performance, *e.g.* in solubilizing hydrophobic biomolecules relevant for chemical applications.

2.5 Conclusion

In this chapter, the applicability of *L*-carnitine as basis for the creation of a variety of functional materials, such as ILs, hydrotropes and surfactants was shown. To this purpose, linear ester-derivatives of *L*-carnitine were synthesized with different alkyl chain lengths ranging from n = 2 to n = 14.

As one of the main ideas was to create functional carnitine-based molecules that can be used as greener alternatives to conventional ones, the first aim was to synthesize them in a simple, cheap and green way. The comparison of the ‘old’, well established route with a newly developed pathway revealed that the ‘new’ method exhibited significant improvements, especially in terms of the hazard potential.

The melting and degradation temperatures of the carnitine ethyl esters either formed by the old or the new pathway were found to be dependent on the type of counter-ion.

According to the determined melting points, [C_2Car]OAc was classified as room temperature IL, [C_2Car]Lev as IL and [C_2Car]Br as non-IL. [C_2Car]$MeSO_3$ could not be obtained in 100 % purity. However, the presence of unreacted *L*-carnitine turned out to have a beneficial effect on decreasing the melting temperature. This led to the idea of combining ILs with a second compound to create low melting mixtures. This concept is further pursued in section 3.2.3. Butyl and hexyl esters of the bromide species were found to be room temperature ILs. In general, the appearance of the developed ILs as sticky and viscous liquids or as solids is believed to lead to a severe limitation of their application as green solvents. It is assumed that the hydroxyl group present in the carnitine molecular structure promotes hydrogen bonding and the formation of highly viscous structures. The use of these ILs at elevated temperatures, especially with carboxylate counter-ions is considered as critical regarding thermal degradation. Although the measured degradation temperatures of all ILs were fairly above 150 °C, solutions became coloured and smelly when heated above room temperature for a while. Although the production of carnitine-based ILs and the resulting product itself might be greener than the conventional imidazolium-based ILs, they are regarded as non-applicable in large-scale applications due to the following reasons: their production is costly; they are extremely viscous; they are temperature-sensitive. However, it is imaginable that they can be used in speciality applications in low amounts, where they exhibit outstanding performance compared to other substances.

A homologous series of carnitine alkyl ester bromides was studied in a range of chain lengths from $n = 2 – 14$. According to the size of the hydrophobic tail, they could be ascribed to different types of functional molecules: ILs with small alkyl chains, hydrotropes with medium alkyl chains and surfactants with long alkyl chains. The transitions were not distinct, but fluent. Exemplarily, compounds with $n = 4$ and 6 exhibited hydrotropic behaviour, at the same time they were room temperature ILs. A log (CAC)-vs.-carbon number plot indicated that the transition from hydrotrope to surfactant might be in the region of $n = 8$. The developed carnitine compounds were compared to conventional hydrotropes and cationic surfactants in terms of their efficiency and effectiveness in decreasing the surface tension of water, their ability to solubilize hydrophobic solutes and their cytotoxicity towards human skin cells. Especially [C_4Car]Br is considered to be a strong hydrotrope. It exhibits high performance as solubilizer without being limited by its own water solubility. At the same time, no cytotoxicity was detected in the measured concentration range. The carnitine-based surfactants were compared to alkyltrimethylammonium bromides. They showed higher surfactant efficiencies (lower CMCs), higher water solubility and similar cytotoxicity. Due to the implementation of an ester function, their biodegradability is expected to be higher. In this respect, they can be considered as greener alternative cationic surfactants.

Specific ion effects were discussed when studying the influence of the type of counter-ion on the behaviour of carnitine-based surfactants. According to Collins's concept, it is assumed that the degree of counter-ion association in [C_nCar]$MeSO_3$ surfactants is higher compared to [C_nCar]Br surfactants. Consequently, they have lower CMCs and tend to form bigger (non-spherical) aggregates. As a result of their high water solubility, they are able to form liquid crystals at room temperature. Compared to the bromides, they are less effective in decreasing the surface tension of water, probably because the counter-ion is partly located at the interface and occupies interfacial space without affecting the surface tension.

At this point it would be interesting to determine the surfactant behaviour of acylcarnitine esters, which naturally occur in the fat metabolism of mammal cells. Depending on the pH, the head group is of zwitterionic or cationic nature. Acylcarnitines are rather expensive when ordering them from usual suppliers, e.g. 10 mg can be purchased for 64.70 €.[66] Several ways of synthesis are given in the literature. Two approaches could be quite accessible: (1) The reaction of carnitine hydrochloride with the respective fatty acid chloride in trifluoroacetic acid.[67] This synthesis was practically adopted in the laboratory, but finally discarded. In addition to the required use of hazardous reagents (fatty acid chloride and trifluoroacetic acid), the purification process was time- and solvent-consuming. Still, the product was not obtained in sufficient purity in the end. All in all, this method was not acceptable in regards of the 12 Principles of Green Chemistry. (2) A more promising and benign way might be an enzymatic approach.[68] A fatty acid vinyl ester can be used as acylating agent and a lipase as enzymatic catalyst. This method seems to be more benign and can be a promising method for obtaining long-chain acyl carnitine ester compounds. Compared to the linear carnitine esters, this type of carnitine ester could give rise to a completely natural surfactant that could be used in chemical formulation. However, even and sometimes especially biological molecules exhibit considerable toxicity, which has to be evaluated thoroughly. In general, studying acylcarnitines in terms of their surfactant properties could deliver further valuable knowledge about carnitine as surfactant or hydrotrope head group. This is assumed to complement the findings and conclusion from the investigations obtained from this thesis.

2.6 Experimental Part

Aqueous solutions were prepared using deionized Millipore water with a resistivity of 18 MΩ·cm. Unless otherwise stated, measurements were conducted at a temperature of 25 °C.

2.6.1 Synthesis

2.6.1.1 Chemicals

The chemicals used in this chapter are listed in Tab. 2.6.1-1 specifying their purity, their supplier and the sections they are relevant for.

Tab. 2.6.1-1: Register of the chemicals used in this chapter, their purity, their supplier and the sections they are relevant for.

	Purity	Supplier	Used in Section
***L*-Carnitine**	99 %	Alfa Aesar	2.2.1.1, 2.2.1.2, 2.3.1, 2.4.1
Ethyl Bromide	98 %	Alfa Aesar	2.2.1.1, 2.3.1
***n*-butyl bromide**	99 %	Sigma Aldrich	2.3.1
***n* -hexyl bromide**	98 %	Sigma Aldrich	2.3.1
***n* -octyl bromide**	98 %	Alfa Aesar	2.3.1
***n* -decyl bromide**	98 %	Alfa Aesar	2.3.1
***n* -dodecyl bromide**	98 %	Alfa Aesar	2.3.1
***n* -tetradecyl bromide**	97 %	Sigma Aldrich	2.3.1
C_{12}TAB	99 %	Sigma Aldrich	2.3.2.3, 2.3.2.5, 2.3.3, 2.4.2.4
C_{16}TAB	>99 %	Fluka	2.3.2.3, 2.3.2.5, 2.3.3, 0, 2.4.2.4
SXS	>90 %	Fluka	2.3.2.3, 2.3.2.4, 2.3.2.5, 2.3.3
[C_1C_4Im]Br	>97 %	Sigma Aldrich	2.3.2.3, 2.3.2.4, 2.3.2.5, 2.3.3
DR13	95 %	Sigma Aldrich	2.3.2.4
Vanillin	>99 %	Roth	2.3.3
$MeSO_3H$	>98 %	Alfa Aesar	2.2.1.2, 2.4.1
Ethanol	≥99.8 %	Sigma Aldrich	2.2.1.2
***n* -Octanol**	>97 %	Merck	2.4.1
***n* -Decanol**	≥99 %	Merck	2.4.1
***n* -Dodecanol**	>95 %	Sigma Aldrich	2.4.1
***n* -Tetradecanol**	97 %	Sigma Aldrich	2.4.1
Amberlite IRA 402		Alfa Aesar	2.2.1.3
RP Column Material		VersaFlash	2.4.1
Sodium acetate trihydrate	99 %	Merck	2.2.1.3
Levulinic acid	98 %	Alfa Aesar	2.2.1.3

2.6.1.2 [C_nCar]Br

[C_nCar]Br compounds have been synthesized according to what has been described in sections 2.2.1.1 and 2.3.1. The synthesis route is depicted in Fig. 2.2.1-1.

2.6.1.3 [C_nCar]$MeSO_3$

[C_nCar]$MeSO_3$ compounds have been synthesized according to what has been described in sections 2.2.1.2 and 2.4.1. The synthesis route is depicted in Fig. 2.2.1-2 and Fig. 2.4.1-1.

2.6.1.4 [C_2Car]OR

[C_nCar]OR compounds have been synthesized according to what has been described in section 2.2.1.3. The synthesis route is depicted in Fig. 2.2.1-6.

2.6.2 Nuclear Magnetic Resonance Spectroscopy

^{1}H- and ^{13}C-NMR analysis was performed by means of an Avance 300 (300 MHz) device supplied by the Bruker BioSpin GmbH in D_2O, d_6-DMSO or $CDCl_3$, as indicated. The chemical shifts (δ) are reported in parts per million (ppm). The following abbreviations were used indicating the multiplicities of the peaks: s = singlet, d = doublet, t = triplet, q = quartet, quint = quintet, sext = sextet, m = multiplet. Relevant NMR data is given in the following.

- **[C_2Car]Br:** (4-Ethoxy-2-hydroxy-4-oxobutyl)-trimethylammonium bromide, [$C_9H_{20}NO_3^+$][Br^-]
  M = 270.17 g/mol
  ^{1}H-NMR (D_2O): δ(ppm): 1.17 (t, 3H), 2.57 (t, 2H), 3.14 (s, 9H), 3.39 (d, 2H), 4.10 (q, 2H), 4.54-4.64 (m, 1H).
  ^{13}C-NMR (D_2O): δ(ppm): 13.3 (CH_3), 40.2 (CH_2), 54.1 (3 CH_3), 62.1 (CH_2), 62.8 (CH), 69.6 (CH_2), 172.5 (C).
- **[C_4Car]Br:** (4-Butoxy-2-hydroxy-4-oxobutyl)-trimethylammonium bromide, [$C_{11}H_{24}NO_3^+$][Br^-]
  M = 298.22 g/mol
  ^{1}H-NMR (D_2O): δ(ppm): 1.04 (t, 3H), 1.43-1.59 (m, 2H), 1.70-1.85 (m, 2H), 2.74-89 (m, 2H), 3.38 (s, 9H), 3.58-3.66 (m, 2H), 4.25-4.37 (m, 2H), 4.75-4.87 (m, 1H).
  ^{13}C-NMR (D_2O): δ(ppm): 13.4 (CH_3), 18.8 (CH_2), 30.2 (CH_2), 40.6 (CH_2), 54.7 (3 CH_3), 63.2 (CH), 66.2 (CH_2), 70.2 (CH_2), 172.5 (C).
- **[C_6Car]Br:** (4-Hexyloxy-2-hydroxy-4-oxobutyl)-trimethylammonium bromide, [$C_{13}H_{28}NO_3^+$][Br^-]
  M = 326.28 g/mol
  ^{1}H-NMR (D_2O): δ(ppm): 0.97-1.07 (m, 3H), 1.39-1.57 (m, 6H), 1.73-1.86 (m, 2H), 2.82 (t, 2H), 3.39 (s, 9H), 3.61-3.68 (m, 2H), 4.24-4.34 (m, 2H), 4.76-4.87 (m, 1H).
  ^{13}C-NMR (D_2O): δ(ppm): 13.8 (CH_3), 22.6 (CH_2), 25.5 (CH_2), 28.3 (CH_2), 31.2 (CH_2), 40.6 (CH_2), 54.7 (3 CH_3), 63.2 (CH), 66.2 (CH_2), 69.9 (CH_2), 172.4 (C).
- **[C_8Car]Br:** (4-Octyloxy-2-hydroxy-4-oxobutyl)-trimethylammonium bromide, [$C_{15}H_{32}NO_3^+$][Br^-]
  M = 354.33 g/mol
  ^{1}H-NMR ($CDCl_3$): δ(ppm): 0.81 (t, 3H), 1.16-1.29 (m, 10H), 1.47-1.61 (m, 2H), 2.64 (d, 2H), 3.42 (s, 9H), 3.68 (d, 2H), 3.98 (t, 2H) 4.58-4.69 (m, 1H), 5.08-5.18 (m, 1H).
  ^{13}C-NMR ($CDCl_3$): δ(ppm): 14.4 (CH_3), 22.6 (CH_2), 25.9 (CH_2), 28.6 (CH_2), 31.7 (CH_2), 32.8 (CH_2), 35.5 (CH_2), 40.8 (CH_2), 53.8 (3 CH_3), 62.7 (CH), 64.7 (CH_2), 69.6 (CH_2), 170.5 (C).

- **[C_{10}Car]Br:** (4-Decyloxy-2-hydroxy-4-oxobutyl)-trimethylammonium bromide, $[C_{17}H_{36}NO_3^+][Br^-]$
  M = 382.38 g/mol
  ^{1}H-NMR ($CDCl_3$): δ(ppm): 0.89 (t, 3H), 1.19-1.40 (m, 14H), 1.62 (quint, 2H), 2.73 (d, 2H), 3.51 (s, 9H), 3.66-3.90 (m, 2H), 4.07 (t, 2H) 4.66-4.84 (quint, 1H), 5.04-5.28 (m, 1H).
  ^{13}C-NMR ($CDCl_3$): δ(ppm): 14.1 (CH_3), 22.7 (CH_2), 25.9 (CH_2), 28.5 (CH_2), 29.3 (2 CH_2), 29.5 (CH_2), 29.6 (CH_2), 31.9 (CH_2), 32.8 (CH_2), 39.4 (CH_2), 55.2 (3 CH_3), 62.7 (CH), 65.4 (CH_2), 70.2 (CH_2), 171.6 (C).
- **[C_{12}Car]Br:** (4-Dodecyloxy-2-hydroxy-4-oxobutyl)-trimethylammonium bromide, $[C_{19}H_{40}NO_3^+][Br^-]$
  M = 410.43 g/mol
  ^{1}H-NMR ($CDCl_3$): δ(ppm): 0.88 (t, 3H), 1.18-1.37 (m, 18H), 1.61 (quint, 2H), 2.72 (d, 2H), 3.49 (s, 9H), 3.64-3.90 (m, 2H), 4.06 (t, 2H) 4.67-4.80 (quint, 1H), 5.14 (d, 1H).
  ^{13}C-NMR ($CDCl_3$): δ(ppm): 14.2 (CH_3), 22.7 (CH_2), 25.9 (CH_2), 28.5 (CH_2), 29.3 (CH_2), 29.4 (CH_2), 29.6 (2 CH_2), 29.7 (2 CH_2), 31.9 (CH_2), 39.4 (CH_2), 55.2 (3 CH_3), 62.7 (CH), 65.4 (CH_2), 70.2 (CH_2), 171.4 (C).
- **[C_{14}Car]Br:** (4-Tetradecyloxy-2-hydroxy-4-oxobutyl)-trimethylammonium bromide, $[C_{21}H_{44}NO_3^+][Br^-]$
  M = 438.49 g/mol
  ^{1}H-NMR ($CDCl_3$): δ(ppm): 0.86 (t, 3H), 1.17-1.38 (m, 22H), 1.60 (quint, 2H), 2.71 (d, 2H), 3.49 (s, 9H), 3.63-3.85 (d, 2H), 4.05 (t, 2H) 4.64-4.78 (m, 1H).
  ^{13}C-NMR ($CDCl_3$): δ(ppm): 14.2 (CH_3), 22.7 (CH_2), 25.9 (CH_2), 28.5 (CH_2), 29.3 (CH_2), 29.4 (CH_2), 29.6 (2 CH_2), 29.7 (4 CH_2), 32.0 (CH_2), 39.4 (CH_2), 55.2 (3 CH_3), 62.7 (CH), 65.4 (CH_2), 70.2 (CH_2), 171.4 (C).

- **[C_2Car]$MeSO_3$:** (4-Ethoxy-2-hydroxy-4-oxobutyl)-trimethylammonium mesylate, $[C_9H_{20}NO_3^+][CH_3SO_3^-]$
  M = 285.36 g/mol
  ^{1}H-NMR (D_2O): δ(ppm): 1.27 (t, 3H), 2.61-2.73 (m, 2H), 2.81 (s, 3H), 3.23 (s, 9H), 3.45-3.53 (m, 2H), 4.15-4.27 (m, 2H), 4.65-4.73 (m, 1H).
  ^{13}C-NMR (D_2O): δ(ppm): 13.4 (CH_3), 38.6 (CH_3), 40.3(CH_2), 54.1 (3 CH_3), 62.2 (CH_2), 62.9 (CH), 69.6 (CH_2), 172.3 (C).
- **[C_8Car]$MeSO_3$:** (4-Octyloxy-2-hydroxy-4-oxobutyl)-trimethylammonium mesylate, $[C_{15}H_{32}NO_3^+][CH_3SO_3^-]$
  M = 369.52 g/mol
  ^{1}H-NMR ($CDCl_3$): δ(ppm): 0.84 (t, 3H), 1.26 (qi, 10H), 1.63 (quint, 2H), 2.65 (d, 2H), 2.78 (s, 3H), 3.21 (q, 9H), 3.47 (m, 2H), 4.15 (m, 2H), 4.67 (qi, 1H).
  ^{13}C-NMR ($CDCl_3$): δ(ppm): 13.6 (CH_3), 22.3 (CH_2), 25.4 (CH_2), 28.0 (CH_2), 28.8 (CH_2), 31.4 (CH_2), 38.5 (CH_2), 40.2 (CH_2), 54.2 (CH_2), 62.9 (CH_2), 65.7 (3 CH_3), 69.7 (CH), 172.1 (C).

- **[C₁₀Car]MeSO₃:** (4-Decyloxy-2-hydroxy-4-oxobutyl)-trimethylammonium mesylate, $[C_{17}H_{36}NO_3^+][CH_3SO_3^-]$
  M = 397.57 g/mol
  ^{1}H-NMR ($CDCl_3$): δ(ppm): 0.73 (t, 3H), 1.14 (m, 14H), 1.50 (quint, 2 H), 2.48 (d, 2H), 2.63 (s, 3H), 3.09 (s, 9H), 3.32 (m, 2H), 3.99 (m, 2H), 4.50 (m, 1H).
  ^{13}C-NMR ($CDCl_3$): δ(ppm): 13.7 (CH_3), 22.4 (CH_2), 25.5 (CH_2), 28.1 (CH_2), 29.0 (CH_2), 29.1 (CH_2), 29.3 (CH_2), 32.0 (CH_2), 38.5 (CH_2), 40.2 (CH_2), 54.2 (CH_2), 62.9 (CH_2), 65.6 (3 CH_3), 69.6 (CH), 172.0 (C).
- **[C₁₂Car]MeSO₃:** (4-Dodecyloxy-2-hydroxy-4-oxobutyl)-trimethylammonium mesylate, $[C_{19}H_{40}NO_3^+][CH_3SO_3^-]$
  M = 425.63 g/mol
  ^{1}H-NMR ($CDCl_3$): δ(ppm): 0.79 (t, 3H), 1.21 (m, 18H), 1.59 (quint, 2 H), 2.60 (d, 2H), 2.74 (s, 3H), 3.16 (s, 9H), 3.42 (m, 2H), 4.07 (m, 2H), 4.10 (m, 2H).
  ^{13}C-NMR ($CDCl_3$): δ(ppm): 13.9 (CH_3), 22.7 (CH_2), 25.8 (CH_2), 29.4 (CH_2), 29.5 (CH_2), 29.7 (CH_2), 29.8 (CH_2), 29.9 (CH_2), 30.0 (CH_2), 32.0 (CH_2), 38.6 (CH_2), 54.2 (CH_2), 62.9 (CH_2), 65.3 (3 CH_3), 69.6 (CH), 171.8 (C).
- **[C₁₄Car]MeSO₃:** (4-Tetradecyloxy-2-hydroxy-4-oxobutyl)-trimethylammonium mesylate, $[C_{21}H_{44}NO_3^+][CH_3SO_3^-]$
  M = 453.68 g/mol
  ^{1}H-NMR ($CDCl_3$): δ(ppm): 0.88 (t, 3H), 1.26 (m, 22H), 1.61 (qi, 2H), 2.70 (d, 2H), 2.76 (s, 3H), 3.38 (s, 9H), 3.59 (d, 1H), 3.82 (dd, 1H), 4.06 (m, 2H), 4.62 (m, 2H).
  ^{13}C-NMR ($CDCl_3$): δ(ppm): 14.2 (CH_3), 22.8 (CH_2), 25.9 (CH_2), 28.5 (CH_2), 29.3 (CH_2), 29.4 (CH_2), 29.6 (2xCH_2), 29.7 (2xCH_2), 32.0 (CH_2), 39.5 (CH_2), 55.3 (CH_2), 63.0 (CH_2), 65.3 (3 CH_3), 68.8 (CH), 171.6 (C).

- **[C₂Car]OAc:** (4-Ethoxy-2-hydroxy-4-oxobutyl)-trimethylammonium acetate, $[C_9H_{20}NO_3^+][C_2H_3O_2^-]$
  M = 249.31 g/mol
  ^{1}H-NMR (D_2O): δ(ppm): 1.22 (t, 3H), 1.86 (s, 3H), 2.54-2.69 (m, 2H), 3.18 (s, 9H), 3.37-3.50 (m, 2H), 4.08-4.23 (m, 2H), 4.61-4.69 (m, 1H).
  ^{13}C-NMR (D_2O): δ(ppm): 13.4 (CH_3), 23.2 (CH_3), 40.1(CH_2), 54.1 (3 CH_3), 62.3 (CH_2), 62.9 (CH), 69.7 (CH_2), 172.3 (C), 181.3 (C).

- **[C₂Car]Lev:** (4-Ethoxy-2-hydroxy-4-oxobutyl)-trimethylammonium levulinate, $[C_9H_{20}NO_3^+][C_5H_7O_3^-]$
  M = 305.37 g/mol
  ^{1}H-NMR (D_2O): δ(ppm): 1.23 (t, 3H), 2.17 (s, 3H), 2.36 (t, 2H), 2.55-2.69 (m, 2H), 2.73 (t, 2H), 3.19 (s, 9H), 3.40-3.50 (m, 2H), 4.09-4.23 (m, 2H), 4.59-4.71 (m, 1H).
  ^{13}C-NMR (D_2O): δ(ppm): 13.4 (CH_3), 29.3 (CH_3), 31.2 (CH_2), 39.5 (CH_2), 40.3 (CH_2), 54.1 (3 CH_3), 62.2 (CH), 63.0 (CH_2), 68.4 (CH), 69.6 (CH_2), 172.3 (C) , 181.6 (C), 215.2 (C).

2.6.3 Determination of Water Solubility

The water solubility was determined visually by adding a carnitine ester compound to a certain amount of water in steps of 10 mg at a temperature of 25 °C. The solution was stirred with a magnetic stirrer. The water solubility limit was expected to be reached, when no clear solution could be formed anymore.

2.6.4 Karl-Fischer Coulometry

The water content of the studied compounds was determined by Karl-Fischer Titration. As measurements have been conducted in the laboratories in Lille and Regensburg, different devices were used: a Mettler Toledo C20 and a Metrohm 899 Coulometer. Hydranal Coulomat AG was used as standard reagent, Aquamicron AKX from API Corporation was relevant for samples with ketone or carboxyl functions. Prior to this, the products were dried with an oil diffusion pump generating pressures lower than 10^{-6} mbar.

2.6.5 Thermal Analysis

2.6.5.1 Differential Scanning Calorimetry

Thermal phase transitions were determined by using a Perkin Elmer DSC 8000. The compound to be studied in a sample size of 4 - 20 mg was placed in a sealed aluminium pan. An empty pan was used as reference. The samples were measured in a temperature range from -60 °C to +180 °C under nitrogen atmosphere. Thermal transitions were obtained in form of sudden changes or jumps in the heat capacity of the heating-cooling cycles. The onset of an endothermic peak during heating was associated with the melting temperature T_m. The midpoint of a small endothermic heat capacity jump was taken as glass transition temperature T_g.

2.6.5.2 Thermal Gravimetric Analysis

A Perkin Elmer TGA 7 unit was used for the determination of the degradation temperatures. The product in a sample size <10 mg was placed in a platinum pan. With a heating rate of 10 °C/min the samples were heated from 30 °C to >300 °C in air atmosphere. Degradation was observed by a loss in mass. The degradation temperatures were obtained from the intersection of the baseline (before decomposition started) and the tangent line placed at the point with the highest slope.

2.6.6 Surface Tension Measurements

As the practical work relevant for this chapter has been simultaneously conducted in the laboratories of Lille and Regensburg, different methods have been used: pendant drop method for $[C_nCar]MeSO_3$ compounds and reference substances and Wilhelmy plate method for $[C_nCar]Br$ compounds.

2.6.6.1 Pendant Drop

The surface tension curves of the $[C_nCar]MeSO_3$ compounds and the reference substances were recorded at 25 °C using the pendant drop technique. A PAT-1M profile analysis tensiometer supplied by SINTERFACE Technologies was used to analyse the shape of a sample drop formed at the tip of a 2 mm stainless steel capillary. The drop was allowed to equilibrate for 900 s, whereas the values recorded during the last 100 s were taken for building an average value. This procedure was repeated twice, so that the mean value of three measurements formed the equilibrium surface tension of one solution.

2.6.6.2 Wilhelmy Plate

A Krüss-K100 tensiometer with Wilhelmy plate geometry has been used for determining the surface tension of the $[C_nCar]Br$ compounds. In order to avoid contamination, the platinum plate has been intensively cleaned and heated before each measurement. Aqueous solutions were prepared with Millipore water. A volume of at least 10 ml was filled into the provided container and the surface tension at equilibrium at 25 °C was measured. The resulting values were calculated by means of the average of at least three measurements.

2.6.7 Dynamic Light Scattering

DLS measurements were performed at 25 °C using a CGS-3 goniometer system from ALV. It comprised an ALV-7004/FAST Multiple Tau digital correlator and a vertical-polarized 22 mW HeNe laser with a wavelength of λ = 632.8 nm. The sample solutions were filtered through a 0.2 μm PTFE filter and approximately 3.5 ml thereof were filled into cylindrical light scattering cells with 10 mm outer diameter. The latter was cleaned and placed in a toluene bath, serving to control the temperature. Each sample was measured for 300 s with the laser set to an angle of 90 ° in regard to the detector. The resulting correlation functions were evaluated qualitatively. It was refrained from calculating the hydrodynamic radii of the particles, as they can be falsified by high ionic strengths of the sample solutions.[52]

2.6.8 Solubility

2.6.8.1 Disperse Red 13

Aqueous stock solutions of the tested hydrotropes were prepared with Millipore water. They were diluted to obtain the desired concentrations. An excess of DR13 was added to at least three samples of each concentration. They were stirred at 25 °C for 24 h, before they were filtered with a 0.2 μm CA filter. The amount of dissolved DR13 was determined by UV/Vis spectrometry at a wavelength of 503 nm using an Agilent Technologies Varian Cary 60 spectrophotometer. Samples were diluted and re-measured, when the absorption was higher than 1.5.

2.6.8.2 Vanillin

Aqueous stock solutions of the tested hydrotropes were prepared with Millipore water. They were diluted to obtain the desired concentrations. An excess of vanillin was added and the solutions were stirred at 25 °C for 72 h to ensure saturation. The samples were centrifuged with an EBA III centrifuge from Hettich for 25 min at maximum speed. The supernatant solution was collected, filled into a quartz cuvette and analysed by UV/Vis spectrometry at a wavelength of 280 nm using a Lambda 18 spectrometer supplied by Perkin Elmer. Where necessary, the sample solutions were diluted with Millipore water. The amount of solubilized vanillin was quantified by means of a calibration curve recorded in ethanol (see Fig. 2.6.8-1) and fitted linearly.

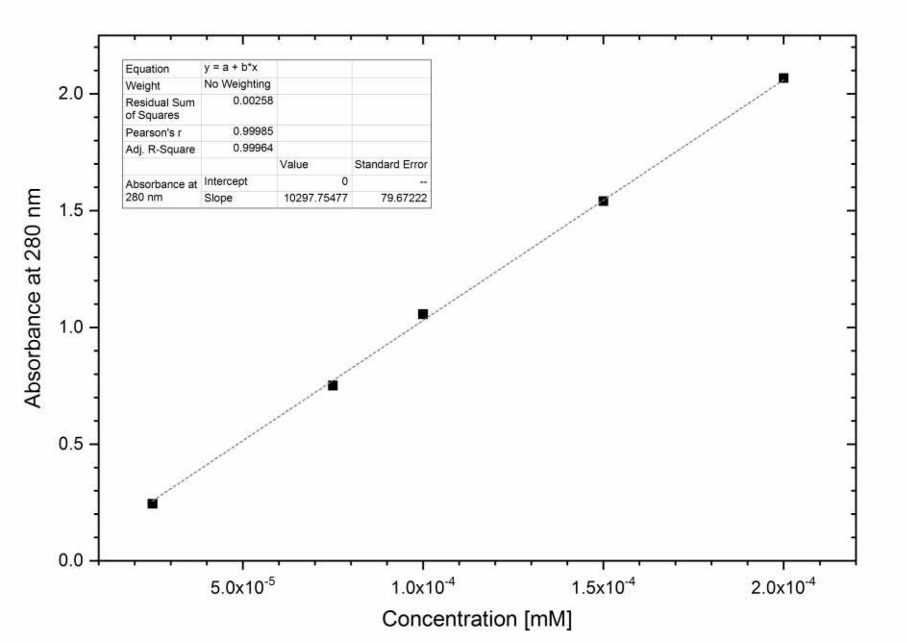

Fig. 2.6.8-1: Calibration curve recorded for vanillin solubilized in ethanol including a linear fit.

2.6.9 Penetration Scan and Polar Microscopy

A penetration scan was used to visualize different liquid crystalline phases occurring in aqueous solutions of $[C_nCar]MeSO_3$. A small amount of pure surfactant powder was placed on a microscope slide. It was covered with a cover slide while leaving some space by putting glass shards in between the two slides. A drop of water was applied next to the created interspace. Water slowly penetrated through the surfactant powder. This led to the in-situ generation of a concentration gradient and enabled the analysis of the aqueous phase behaviour of the surfactant as a function of its concentration. Occurring LC phases were visualized by means of an Orthoplan polarizing optical microscope.

2.6.10 Cytotoxicity

A PrestoBlue Assay with human skin keratinocytes (HaCaT cells) was used to determine the cytotoxicity of the studied compounds. It was kindly conducted by the department of Bioanalytics at the University of Regensburg. The cells were seeded in 96 well plates and incubated with 100 μl sample solution for 24 h. The solutions consisted of the regarding substance solubilized in cell medium in concentrations between 10^{-4} g/L and 1 g/L. Some cells were left untreated as negative control. The sample solutions were removed and 100 μl PrestoBlue solution were applied. This solution is membrane permeable. It contains the blue, non-fluorescent dye resazurin which is reduced to red, fluorescent resorufin when it permeates into the cell. It is applied as 1:10 solution in PBS^{++} with 1 g/L glucose. After 1 h of incubation, the fluorescence was detected with a microplate reader from Tecan with an excitation wavelength of 532 nm and an emission wavelength of 600 nm. In the case of a cytotoxic activity of the tested substance, the fluorescence is reduced. Damaged cells are restricted in their cell metabolism and the production of the required redox equivalents for the generation of the fluorescent dye is inhibited.

2.7 References

[1] G. Fraenkel, *Biol. Bull.* **1953**, *104*, 359–371.

[2] a) M. Tomita, Y. Sendju, *Hoppe-Seylers Z. Physiol. Chem.* **1927**, *169*, 263–277; b) G. Fraenkel, S. Friedman, *Vitam. Horm.* **1957**, *15*, 73–118.

[3] H. E. Carter, P. K. Bhattacharyya, K. R. Weidman, G. Fraenkel, *Arch. Biochem. Biophys.* **1952**, *38*, 405–416.

[4] J. Bremer, *Physiol. Rev.* **1983**, *63*, 1420–1480.

[5] J. L. Flanagan, P. A. Simmons, J. Vehige, M. D. Willcox, Q. Garrett, *Nutr. Metab.* **2010**, *7*, 30.

[6] a) G. Bellinghieri, D. Santoro, M. Calvani, A. Mallamace, V. Savica, *Am. J. Kidney Dis.* **2003**, *41*, S116-22; b) M. C. Cave, R. T. Hurt, T. H. Frazier, P. J. Matheson, R. N. Garrison, C. J. McClain, S. A. McClave, *Nutr. Clin. Pract.* **2008**, *23*, 16–34.

[7] C. J. Rebouche, H. Seim, *Annu. Rev. Nutr.* **1998**, *18*, 39–61.

[8] a) S. Ahmad, *Semin. Dial.* **2001**, *14*, 209–217; b) M. C. Ørngreen, D. B. Olsen, J. Vissing, *Neurology* **2002**, *59*, 1046–1051; c) S. R. Srinivas, P. D. Prasad, N. S. Umapathy, V. Ganapathy, P. S. Shekhawat, *Am. J. Physiol.: GI and Liver* **2007**, *293*, G1046–53.

[9] C. J. Rebouche, *Ann. N.Y. Acad. Sci.* **2004**, *1033*, 30–41.

[10] Y. Fukaya, Y. Iizuka, K. Sekikawa, H. Ohno, *Green Chem.* **2007**, *9*, 1155–1157.

[11] A. Mühlbauer, doctoral thesis, Université de Lille, Universität Regensburg, Lille, **2014**.

[12] a) A. P. Abbott, D. Boothby, G. Capper, D. L. Davies, R. K. Rasheed, *J. Am. Chem. Soc.* **2004**, *126*, 9142–9147; b) R. Klein, D. Touraud, W. Kunz, *Green Chem.* **2008**, *10*, 433–435; c) Q.-P. Liu, X.-D. Hou, N. Li, M.-H. Zong, *Green Chem.* **2012**, *14*, 304–307; d) J. Pernak, A. Syguda, I. Mirska, A. Pernak, J. Nawrot, A. Pradzyńska, S. T. Griffin, R. D. Rogers, *Chemistry* **2007**, *13*, 6817–6827.

[13] R. Klein, M. Kellermeier, D. Touraud, E. Müller, W. Kunz, *J. Colloid Interface Sci.* **2013**, *392*, 274–280.

[14] R. Winter, *A consumer's dictionary of cosmetic ingredients. Complete information about the harmful and desirable ingredients found in cosmetics and cosmeceuticals,* 7th ed., Three Rivers Press, New York, **2009**.

[15] R. I. Peirano, T. Hamann, H.-J. Düsing, M. Akhiani, U. Koop, T. Schmidt-Rose, H. Wenck, *J. Cosmet. Dermatol.* **2012**, *11*, 30–36.

[16] "Carnitine", to be found under https://cosmetics.specialchem.com/inci/carnitine.

[17] "L-Carnitine - "Unquestionable" room for market growth: Lonza", to be found under https://www.nutritioninsight.com/news/l-carnitine-unquestionable-room-for-market-growth-lonza.html.

[18] a) M. Inazu, T. Matsumiya, *Jpn. J. Pharmacol.* **2008**, *28*, 113–120; b) S. E. Reuter, A. M. Evans, *Clin. Pharmacokinet.* **2012**, *51*, 553–572; c) B. Borrebaek, R. Christiansen, B. O. Christophersen, J. Bremer, *Circ. Res.* **1976**, *38*, I16-21; d) M. C. Fonteles, J. J. Cohen, A. J. Black, S. J. Wertheim, *Am. J. Physiol.* **1983**, *244*, 235–246.

[19] a) S. H. Yalkowsky, G. Zografi, *J. Colloid Interface Sci.* **1970**, *34*, 525–533; b) S. H. Yalkowsky, G. Zografi, *J. Pharm. Sci.* **1970**, *59*, 798–802; c) S. V. Pande, *Biochim. Biophys. Acta* **1981**, *663*, 669–673.

[20] F. M. Goñi, M. A. Requero, A. Alonso, *FEBS Letters* **1996**, *390*, 1–5.

[21] a) M. Cipollone, P. de Maria, A. Fontana, S. Frascari, L. Gobbi, D. Spinelli, M. Tinti, *Eur. J. Med. Chem.* **2000**, *35*, 903–911; b) P. de Maria, S. Frascari, P. Mariani, L. Saturni, G. P. Spada, M. O. Tinti, *Liq. Cryst.* **2006**, *19*, 353–365.

[22] T. Patra, S. Ghosh, J. Dey, *J. Colloid Interface Sci.* **2014**, *436*, 138–145.

[23] S. Ghosh, S. Dolai, T. Patra, J. Dey, *J. Phys. Chem. B* **2015**, *119*, 12632–12643.

[24] P. G. Jessop, *Green Chem.* **2011**, *13*, 1391–1398.

[25] T. P. T. Pham, C.-W. Cho, Y.-S. Yun, *Water Res.* **2010**, *44*, 352–372.

[26] A. Romero, A. Santos, J. Tojo, A. Rodríguez, *J. Hazard. Mater.* **2008**, *151*, 268–273.

[27] D. Zhao, Y. Liao, Z. Zhang, *Clean Soil Air Water* **2007**, *35*, 42–48.

[28] K. Häckl, master thesis, Universität Regensburg, Regensburg, **2015**.

[29] K. Holmberg, *Surfactants and polymers in aqueous solution,* 2. ed., Wiley, Chichester, **2007**.

[30] M. J. Rosen, J. T. Kunjappu in *Surfactants and interfacial phenomena,* (Ed.: M. J. Rosen), John Wiley & Sons, Inc, Hoboken, NJ, **2004**, 39-122.

[31] a) S. Mishra, V. K. Tyagi, *J. Oleo Sci.* **2007**, *56*, 269–276; b) K. Holmberg (Ed.) *Surfactant science series*, 2nd ed., rev. and expanded. ed., Marcel Dekker, New York, **2003**.

[32] R. Winkler, T. Buchecker, F. Hastreiter, D. Touraud, W. Kunz, *PCCP* **2017**, *19*, 25463–25470.

[33] a) P. A. Hassan, S. R. Raghavan, E. W. Kaler, *Langmuir* **2002**, *18*, 2543–2548; b) K. Kanan, M. Al-Jabari, I. Kayali, *Arabian J. Chem.* **2017**, *10*, S314-320.

[34] "SDS Search and Product Safety Center", to be found under https://www.sigmaaldrich.com/safety-center.html.

[35] Y. de Gaetano, A. Mohamadou, S. Boudesocque, J. Hubert, R. Plantier-Royon, L. Dupont, *J. Mol. Liq.* **2015**, *207*, 60–66.

[36] F. Goursaud, M. Berchel, J. Guilbot, N. Legros, L. Lemiègre, J. Marcilloux, D. Plusquellec, T. Benvegnu, *Green Chem.* **2008**, *10*, 310–320.

[37] S. C. Baker, D. P. Kelly, J. C. Murrell, *Nature* **1991**, *350*, 627–628.

[38] G. W. Meindersma, M. Maase, A. B. de Haan in *Ullmann's Encyclopedia of Industrial Chemistry* (Ed.: Wiley-VCH), American Cancer Society, **2007**.

[39] V&P Scientific, "Viscosity tables", to be found under http://www.vp-scientific.com/Viscosity_Tables.htm.

[40] a) N. Muhammad, M. I. Hossain, Z. Man, M. El-Harbawi, M. A. Bustam, Y. A. Noaman, N. B. Mohamed Alitheen, M. K. Ng, G. Hefter, C.-Y. Yin, *J. Chem. Eng. Data* **2012**, *57*, 2191–2196; b) P. Nockemann, B. Thijs, K. Driesen, C. R. Janssen, K. van Hecke, L. van Meervelt, S. Kossmann, B. Kirchner, K. Binnemans, *J. Phys. Chem. B* **2007**, *111*, 5254–5263; c) D. Rengstl, B. Kraus, M. van Vorst, G. D. Elliott, W. Kunz, *Colloids Surf., B* **2014**, *123*, 575–581.

[41] R. L. Lankey, P. T. Anastas, *Ind. Eng. Chem. Res.* **2002**, *41*, 4498–4502.

[42] a) M. G. T. C. Ribeiro, A. A. S. C. Machado, *J. Chem. Educ.* **2013**, *90*, 432–439; b) M. G. T. C. Ribeiro, D. A. Costa, A. A. S. C. Machado, *Green Chem. Lett. Rev.* **2010**, *3*, 149–159.

[43] C. A. Angell in *Encyclopedia of Materials: Science and Technology* (Ed.: K. H. J. Buschow, M. C. Flemings, E. J .Kramer, P. Veyssière, R. C. Cahn, B. Ilschner, S. Mahajan), Elsevier, **2004**.

[44] F. Xu, K. Matsumoto, R. Hagiwara, *Chemistry* **2010**, *16*, 12970–12976.

[45] G. D'Errico, O. Ortona, L. Paduano, V. Vitagliano, *J. Colloid Interface Sci.* **2001**, *239*, 264–271.

[46] "MSDS Search & Product Safety Center", to be found under https://www.bio-world.com/pages/msds_search.html.

[47] H. B. Klevens, *J. Phys. Chem.* **1948**, *52*, 130–148.

[48] M. H. Hatzopoulos, J. Eastoe, P. J. Dowding, S. E. Rogers, R. Heenan, R. Dyer, *Langmuir* **2011**, *27*, 12346–12353.

[49] a) W. Kunz, K. Holmberg, T. Zemb, *Curr. Opin. Colloid Interface Sci.* **2016**, *22*, 99–107; b) S. Queste, P. Bauduin, D. Touraud, W. Kunz, J.-M. Aubry, *Green Chem.* **2006**, *8*, 822–830; c) P. Bauduin, L. Wattebled, S. Schrödle, D. Touraud, W. Kunz, *J J. Mol. Liq.* **2004**, *115*, 23–28.

[50] E. C. Lumb, *Trans. Faraday Soc.* **1951**, *47*, 1049–1055.

[51] D. Balasubramanian, V. Srinivas, V. G. Gaikar, M. M. Sharma, *J. Phys. Chem.* **1989**, *93*, 3865–3870.

[52] E. Sutherland, S. M. Mercer, M. Everist, D. G. Leaist, *J. Chem. Eng. Data* **2009**, *54*, 272–278.

[53] P. Bauduin, A. Renoncourt, A. Kopf, D. Touraud, W. Kunz, *Langmuir* **2005**, *21*, 6769–6775.

[54] Y. Zhang, X. Li, H. Yu, *J. Environ. Sci. Health., Part C Environ. Carcinog. Ecotoxicol. Rev.* **2016**, *34*, 204–215.

[55] T. Buchecker, S. Krickl, R. Winkler, I. Grillo, P. Bauduin, D. Touraud, A. Pfitzner, W. Kunz, *PCCP* **2017**, *19*, 1806–1816.

[56] P. Gilbert, L. E. Moore, *J. Appl. Microbiol.* **2005**, *99*, 703–715.

[57] Â. S. Inácio, G. N. Costa, N. S. Domingues, M. S. Santos, A. J. M. Moreno, W. L. C. Vaz, O. V. Vieira, *Antimicrob. Agents Chemother.* **2013**, *57*, 2631–2639.

[58] a) J. Burri, M. Graf, P. Lambelet, J. Löliger, *J. Sci. Food Agric.* **1989**, *48*, 49–56; b) D. J. Charles, *Antioxidant Properties of Spices, Herbs and Other Sources*, Springer, New York, **2013**; c) A. Tai, T. Sawano, F. Yazama, H. Ito, *Biochim. Biophys. Acta* **2011**, *1810*, 170–177; d) A. K. Sinha, U. K. Sharma, N. Sharma, *Int. J. Food Sci. Nutr.* **2008**, *59*, 299–326.

[59] V. Huber, bachelor thesis, Universität Regensburg, Regensburg, **2017**.

[60] M. J. Rosen, *J. Colloid Interface Sci.* **1981**, *79*, 587–588.

[61] R. G. Pearson, *J. Am. Chem. Soc.* **1963**, *85*, 3533–3539.

[62] W. Kunz, *Curr. Opin. Colloid Interface Sci.* **2010**, *15*, 34–39.

[63] F. S. Lima, H. Chaimovich, I. M. Cuccovia, R. Buchner, *Langmuir* **2013**, *29*, 10037–10046.

[64] a) K. D. Collins, *Methods* **2004**, *34*, 300–311; b) K. D. Collins, *Biophys. Chem.* **2006**, *119*, 271–281.

[65] a) N. Vlachy, M. Drechsler, D. Touraud, W. Kunz, *C.R. Chim.* **2009**, *12*, 30–37; b) N. Vlachy, B. Jagoda-Cwiklik, R. Vácha, D. Touraud, P. Jungwirth, W. Kunz, *Adv. Colloid Interface Sci.* **2009**, *146*, 42–47.

[66] "Palmitoyl-L-carnitine", to be found under https://www.sigmaaldrich.com/catalog/product/sigma/61251?lang=de&region=DE.

[67] W. E. M. Lands (Ed.) *Biochemical Preparations*, John Wiley and Sons, New York, **1968**, *Vol. 12*.

[68] P. Lozano, M. Daz, T. de Diego, J. L. Iborra, *Biotechnol. Bioeng.* **2003**, *82*, 352–358.

[69] K. Häckl, A. Mühlbauer, J. F. Ontiveros, S. Marinkovic, B. Estrine, W. Kunz, V. Nardello-Rataj, *J. Colloid Interface Sci.* **2018***, 511,* 165–173.

Chapter 3
Deep Eutectic Solvents

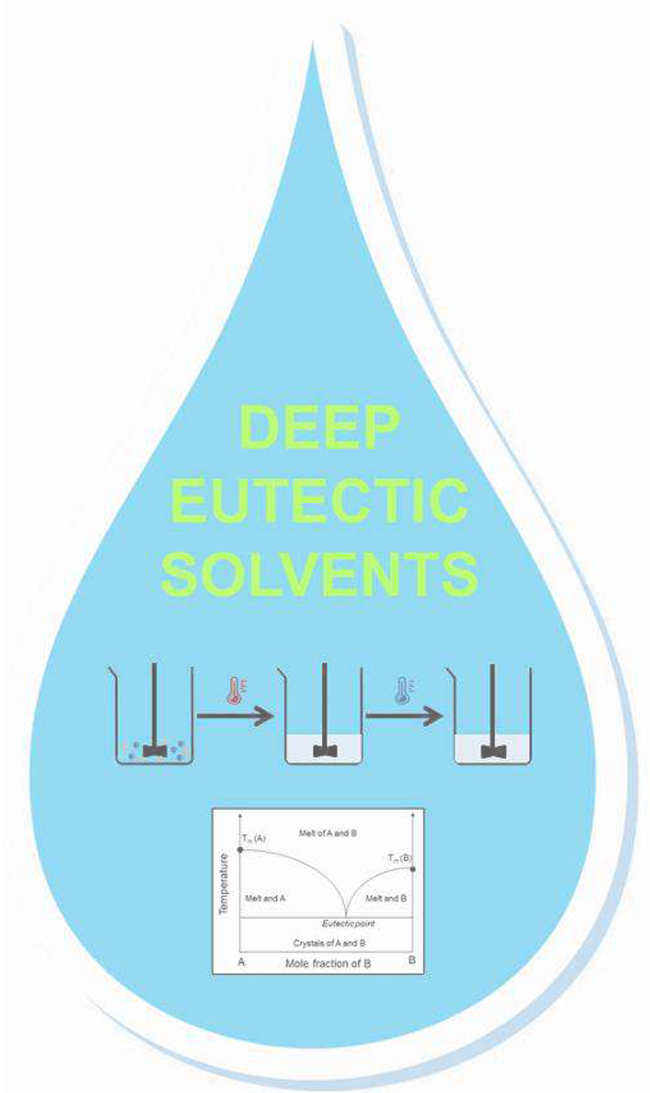
DEEP
EUTECTIC
SOLVENTS
T_m (A)
Melt of A and B
T_m (B)
Temperature
Melt and A
Melt and B
Eutectic point
Crystals of A and B
A
Mole fraction of B
B

3 Deep Eutectic Solvents

3.1 Introduction

Deep eutectic solvents (DESs) have been proposed as a novel class of environmentally benign solvents. In fact, they are composed of a combination of substances and their greenness is determined by the respective properties of the latter. The combination of non-toxic, biodegradable substances from natural origin is expected to result in biogenic, non-toxic, biodegradable solvents. In addition, the variability of constituents offers a great flexibility regarding the desired properties of the resulting green solvent. In general, the properties are similar to those of ionic liquids (ILs). This implies both the advantages for some applications caused by a negligible volatility and a high ionicity of the solvent and disadvantages, such as high viscosities and strong hygroscopicity. A decisive benefit of DESs over ILs is their quick and facile way of preparation. They are formed by combining a Lewis acid and a Lewis base – herein referred to as hydrogen bond acceptor (HBA) and hydrogen bond donor (HBD), respectively – at a defined ratio that leads to a pronounced reduction of the melting temperature of the overall system. While in general different types of DESs are known, this chapter focusses on so-called Type 3 DESs (see section 1.3.6.1), containing a quaternary ammonium salt as HBA and an organic HBD.

The terminology regarding DESs is somewhat difficult and should be clarified beforehand. In Tab. 3.1.1-1, three major terms and their related official definitions are presented. These terms are used synonymously within this study with the following rational: all compounds used are substances that occur in nature. The existence of a homogeneous liquid when stirring the respective compounds at elevated temperature confirmed the formation of a low melting mixture. Whether the tested composition of compounds corresponded to the eutectic composition and resulted in the achievement of maximum melting point depression was not determined. Therefore, it has to be noted that the term DES according to its strict definition might not be accurate for all mixtures.

Tab. 3.1.1-1: Various terms related to the DES topic and their definitions.

Term	**Definition**
Deep eutectic solvent (DES)	Mixture of two or more components in a composition that results in the lowest possible melting temperature.
Low melting mixture (LMM)	Mixture of two or more compounds that shows a melting temperature lower compared to its pure components.
Natural Deep Eutectic Solvent (NADES)	DES entirely formed by components obtained from natural resources.

Two further definition-related issues require clarification in the scope of this work:

(1) Numerous publications report on the application of DESs or NADESs containing considerable amounts of water.[1] It is doubted that these mixtures retain the DES properties considered characteristics for the respective class. Instead, they are rather aqueous solutions of natural substances and the term DES or NADES is believed to be not appropriate.
(2) Similar arguments are to be put forward when discussing mixtures containing at least one component which is already liquid in its pure state, such as ethylene glycol or glycerol-based DESs. The resulting mixture can be argued to be a non-aqueous solution of the respective other compound(s). However, these mixtures are generally accepted as DESs. In the course of this study, the regarding mixtures will be referred to as DESs, too, for the sake of accordance with literature.

The fundamental idea of this study was to (1) create new low melting mixtures in order to obtain novel green solvents, (2) examine different concepts for the creation of low melting mixtures and (3) apply the resulting solvent mixtures to certain applications. The structures of the employed HBA and HBD compounds alongside their abbreviations are illustrated in section 6.1 of the appendix.

The first section of the present chapter comprises primarily the evaluation of new DESs based on betaine, carnitine and their derivatives. This includes the investigation of zwitterionic quaternary ammonium compounds as HBAs and the discussion whether combinations containing a zwitterion and a carboxylic acid are to be considered as ILs or DESs. The respective protonated and esterified analogues are studied in comparison to the zwitterions. Furthermore, the applicability of the betaine- and carnitine-based DESs as solubilization media for melanin is determined.

The combination of biologically relevant HBDs containing a carboxylic acid function with choline chloride and the subsequent formation of DESs is described in the second part. The influence of a third component on their thermal phase behaviour is studied. Three attempts to practically make use of these DESs as ephemeral reaction solvents are presented. This approach describes a sophisticated concept allowing to carry out a reaction involving one of the DES components as a reagent in a temporarily formed solvent. As soon as the reaction is considered completed, the non-reacted part of the DES is, in an ideal case, removable by the addition of water, so that only the pure solid product remains. Herein, this concept is applied to the esterification of biologically relevant carboxylic acids.

The third part is intended to deliver fundamental information on the use of DESs in combination with surfactants in electrochemistry. With their pronounced electric conductivity, their wide electrochemical windows and the capability of dissolving metal salts, DESs are promising candidates as electrochemical solvents.[2] Surfactants are regularly used in electrochemistry to control the ongoing reactions and to modify the electrode surface.[3] The DES-graphite interface and the behaviour and aggregation of ionic surfactants at the latter are studied by means of atomic force microscopy (AFM). Recordings of AFM force-distance curves and images in soft contact mode are used to obtain information on the aggregation behaviour of the surfactants at the interface and the DES environment in nanoscale apart from the aggregates. Furthermore, changes upon the application of electric potential to the electrode are detected.

The conclusion summarizes the content of this chapter. It evaluates the studied concepts for the formation of DESs and the performance of the DESs in the tested applications. The experimental part further details on the chemicals and measuring techniques used in this study.

3.2 Betaine- and Carnitine-Based Deep Eutectic Solvents

Mixing a quaternary ammonium salt (as HBA) with a natural HBD can result in the formation of a natural DES and provides potential for its use as an alternative green solvent. A variety of such quaternary ammonium salts and HBDs is available, so that a huge number of possible combinations is imaginable. Choline chloride has been studied closely in recent years and is known as a typical quaternary ammonium salt forming DESs with numerous HBDs, such as carboxylic acids, alcohols and amides. Other natural HBAs are known, but less investigated, *e.g.* sugars or further quaternary ammonium salts, such as carnitine or betaine. The latter are assumed to be suitable candidates due to their structural similarity to choline chloride. A pool of natural HBDs (mostly carboxylic acids) was selected and combined with betaine and carnitine, with their protonated chloride salts and with their short chain alkyl ester derivatives. Fig. 3.2.1-1 illustrates the various carnitine-based HBA species studied in this section. Likewise, analogous species of betaine were employed. It is hardly predictable, whether or not the combination of a certain HBA with a certain HBD will result in the formation of a liquid. Therefore, the main aim was to determine, which of the tested combinations form a liquid, homogeneous mixture, when stirred at a temperature of 80 – 90 °C and which of them stay liquid at room temperature (rt). As the resulting DESs are characterized by their strong depression in melting point, their most important property clearly is their melting behaviour, which is determined via differential scanning calorimetry (DSC) for several DESs. The question arouse, whether the liquids formed between the zwitterionic HBAs and carboxylic acids are to be classified as DESs or ILs. This issue was investigated by partly replacing betaine and carnitine by their protonated derivatives. Finally, some betaine- and carnitine-based bromide salts were combined with the selected HBDs in order to test their ability in forming DESs and to compare to the regarding zwitterionic compounds. The obtained liquids were considered for the solubilization of melanin, a biopolymer and natural pigment. The addition of 25 wt% water was required for practical reasons, as the pure DESs were too viscous to be processed.

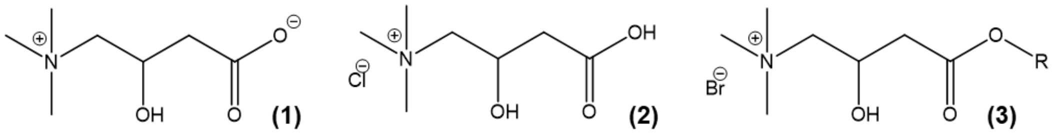

- Proton acceptor
- H-bonding activity

- Proton donor
- H-bonding activity

- H-bonding activity

Fig. 3.2.1-1: Various carnitine-based HBA species studied in this chapter: (1) zwitterionic carnitine, (2) carnitine hydrochloride and (3) carnitine alkyl ester bromide.

3.2.1 Binary Mixtures of Zwitterionic Betaine and Carnitine

Betaine and carnitine were tested regarding their usability for the formation of DESs. In contrast to choline chloride, betaine and carnitine have only been studied scarcely in this context. The formation of DESs has been reported for the combination of betaine with some sugar substances,[4] *DL*-malic acid,[4,5] *L*-tartaric acid,[4] citric acid,[4,5] *L*-lactic acid,[5] glycolic acid[6] and ethylene glycole.[7] Carnitine was found to generate DESs with urea,[6,8] malonic acid,[6] glycolic acid,[6] phenol[9] and ethylene glycol.[7]

A huge number of further combinations has remained unexploited, so far. The range of tested HBDs was extended within this study. Most of the mixtures were prepared under nitrogen atmosphere to avoid water uptake from ambient air. An overview of the considered combinations is given in Tab. 6.2.1-1 in section 6.2.1 of the appendix, alongside the respective molar mixing ratios and an indication, whether a DES was formed or not.

In Tab. 3.2.1-1, those mixtures leading to the formation of DESs are summarized with indication of thermal transition temperatures, if measured. Melting points are given as onset temperatures T_m^{onset} and glass transition temperatures are indicated as T_g, whereas 'n.d.' denotes that the value was not determined. The abbreviations and molecular structures of the HBAs and HBDs are to be found in Fig. 6.1.1-1 and Fig. 6.1.2-1 in section 6.1 of the appendix.

Tab. 3.2.1-1: Summary of betaine- and carnitine-based DESs with indicated visual appearances at room temperature, thermal transition temperatures and water contents.

HBA	**HBD**	**Molar ratio HBA : HBD**	**Appearance at rt**	**Thermal transition**	**Water content [wt%]**
Bet	GlA	1 : 1	clear, colourless liquid	-53 °C (T_m^{onset})	0.7
Bet	LA	1 : 2	clear, colourless liquid	n.d.	prepared with undried starting compounds
		1 : 1	white, sticky solid	n.d.	
Bet	LaA	1 : 2	clear, colourless liquid	n.d.	prepared with undried starting compounds
		1 : 1	white, sticky solid	n.d.	
Bet	ManA	1 : 1	clear, colourless liquid	n.d.	prepared with undried starting compounds

HBA	HBD	Molar ratio HBA : HBD	Appearance at rt	Thermal transition	Water content [wt%]
Car	EG	1 : 2	clear, colourless liquid	n.d.	prepared with undried starting compounds
Car	Gly	1 : 2	clear, yellow liquid	n.d.	prepared with undried starting compounds
Car	LA	1 : 2 1 : 1	clear, colourless liquid white, sticky solid	n.d. n.d.	prepared with undried starting compounds
Car	LaA	1 : 1	clear, colourless liquid	-15 °C (T_m^{onset})	1.3
Car	MA	1 : 1	clear, colourless liquid	n.d.	0.8
Car	MaleA	1 : 1 2 : 1	clear, colourless liquid clear, colourless liquid	n.d. +6 °C (T_m^{onset})	0.4
Car	SA	1 : 1 2 : 1	clear, colourless liquid white, sticky solid	n.d. n.d.	prepared with undried starting compounds
Car	Urea	1 : 2	clear, colourless liquid	n.d.	n.d.

Two general observations are obtained from these experiments: (1) carnitine was compatible with a larger variety of HBDs compared to betaine; (2) betaine was compatible with monocarboxylic acids only, while carnitine formed DESs with dicarboxylic acids, too. This deviating behaviour is assigned to the additional hydroxyl group of carnitine compared to betaine.

Obtaining reliable data on physico-chemical properties appeared to be difficult. At first sight, this was because the water content, which was desired to be as low as possible, could hardly be controlled. Secondly, this was due to tremendous viscosities and densities, which were too high to be measured with the available equipment. Thirdly, the DES substances were very unhandy due to their stickiness and the requirement to keep them away from the atmosphere in order to avoid water uptake.

Thermal transition temperatures of betaine- and carnitine-based mixtures were measured by means of DSC. As generally known, the physico-chemical properties of DESs are influenced significantly by their water contents.[10] It is to be noted that the measured values are not to be compared, as the water contents of the respective DES substances are not consistent.

It has to be mentioned that a set of HBDs listed in Tab. 6.2.2-1 in section 6.2.2 of the appendix was combined with betaine hydrochloride and carnitine hydrochloride, but none of the tested combinations was liquid at room temperature and only two of them (CarHCl-urea (1 : 2) and BetHCl-LA (1 : 2)) formed homogeneous liquids at elevated temperature. This led to the conclusion that the zwitterionic nature of betaine and carnitine plays an important role in the formation of liquid mixtures. The respective zwitterionic component provides the opportunity for a proton exchange with a carboxylic HBD, so that the resulting mixtures might actually feature an IL-like character. This consideration is discussed further in the following paragraph.

3.2.2 Ternary Mixtures of Carnitine, Carnitine Hydrochloride and a Carboxylic Acid

When combining a zwitterionic HBA with an acidic HBD, the question arises, whether the resulting mixture is to be considered as a DES or an IL. An '*in situ* IL' can be formed by proton exchange, as shown in Fig. 3.2.2-1.

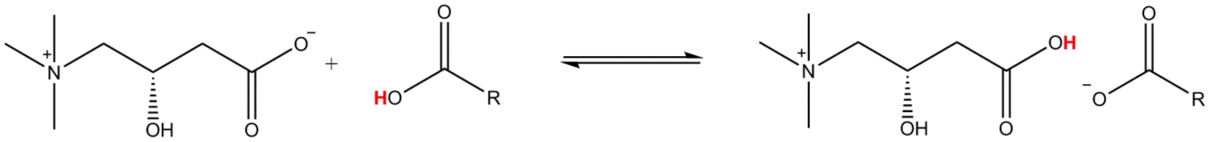

Fig. 3.2.2-1: Formation of 'in situ ILs' by proton exchange when combining carnitine with a carboxylic acid.

A zwitterion-carboxylic acid DES was studied in order to gain information on the role of the carboxylic proton. In particular, two systems comprising carnitine and either lactic acid (monocarboxylic acid) or maleic acid (dicarboxylic acid) were investigated. Both HBDs with pK_a values of 3.86 and 1.92, respectively, are fairly acidic.[11] In a concentration series, carnitine was progressively replaced by carnitine hydrochloride. Thereby, the opportunities for a proton exchange from the acid to the zwitterionic species, as illustrated in Fig. 3.2.2-1, were reduced step by step. The prepared sample series of Car-CarHCl-LaA (HBA : HBD = 1 : 1) and Car-CarHCl-MaleA (HBA : HBD = 2 : 1), where HBA was the sum of carnitine and carnitine hydrochloride, were studied by means of DSC and ^{1}H-NMR analysis. Their water contents were determined in order to take into account its impact on the measured quantities.

Thermal transition temperatures and water contents of the studied systems Car-CarHCl-LaA and Car-CarHCl-MaleA are listed in Tab. 3.2.2-1 and Tab. 3.2.2-2, respectively. Fig. 3.2.2-2 and Fig. 3.2.2-3, respectively, show the corresponding DSC curves.

Tab. 3.2.2-1: Car-CarHCl-LaA series prepared in HBA : HBD ratio of 1 : 1 with the respective appearances at room temperature, thermal transition temperatures and water contents.

Solution	**Molar ratio Car : CarHCl : LaA**	**Appearance at rt**	**Thermal transition**	**Water content [wt%]**
0	1 : 0 : 1	clear, colourless liquid	-15 °C (T_m^{onset})	1.3
1	0.95 : 0.05 : 1	clear, colourless liquid	-21 °C (T_m^{onset})	1.1
2	0.90 : 0.10 : 1	clear, colourless liquid	-18 °C (T_m^{onset})	1.1
3	0.85 : 0.15 : 1	clear, colourless liquid	-18 °C (T_m^{onset})	1.2
4	0.80 : 0.20 : 1	clear, colourless liquid	-15 °C (T_m^{onset})	1.4
5	0.75 : 0.25 : 1	clear, colourless liquid	-39 °C (T_m^{onset})	1.3

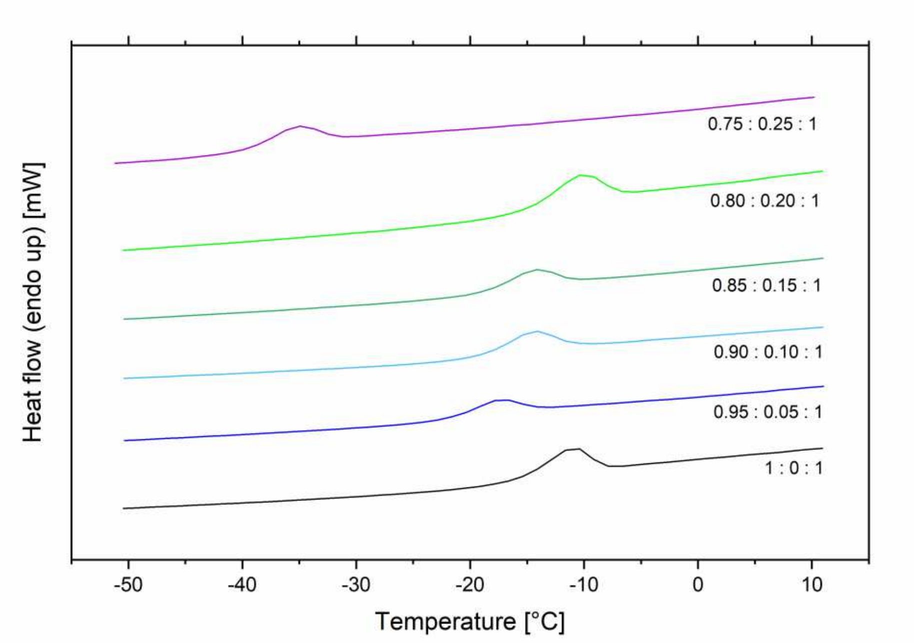

Fig. 3.2.2-2: Qualitative DSC curves of a series of Car-CarHCl-LaA mixtures in HBA : HBD ratio of 1 : 1 including the initial Car-LaA DES (black curve). The plots are offset on the y-scale for clarity in representation.

Mixtures number 0 to 5 of the Car-CarHCl-LaA DESs exhibited water contents in a relatively narrow range from 1.1 to 1.4 wt% and were therefore considered to be comparable. Their melting temperatures as inferred from the respective endothermic peak positions were found between -15 and -39 °C. While no significant trend was observed in samples 0 to 4, the melting temperature of sample 5 was significantly lower. This is indicative for the presence of a eutectic, *i.e.*, lowest melting composition. Further replacement of carnitine by carnitine hydrochloride did not lead to the formation of homogenous solutions.

Tab. 3.2.2-2: Car-CarHCl-MaleA series prepared in HBA : HBD ration of 2 : 1 with the respective appearances at room temperature, thermal transition temperatures and water contents.

Solution	Molar ratio Car : CarHCl : MaleA	Appearance at rt	Thermal transition	Water content [wt%]
0	2 : 0 : 1	clear, colourless liquid	+6 °C ($\mathrm{T_m^{onset}}$)	0.4
1	1.9 : 0.1 : 1	clear, yellowish liquid	-2 °C ($\mathrm{T_m^{onset}}$)	0.4
2	1.8 : 0.2 : 1	clear, yellowish liquid	-3 °C ($\mathrm{T_m^{onset}}$)	0.6
3	1.7 : 0.3 : 1	clear, yellowish liquid	-6 °C ($\mathrm{T_m^{onset}}$)	0.5
4	1.6 : 0.4 : 1	clear, yellowish liquid	-3 °C ($\mathrm{T_m^{onset}}$)	0.4
5	1.5 : 0.5 : 1	clear, yellow liquid	+1 °C ($\mathrm{T_m^{onset}}$)	1.0
6	1.4 : 0.6 : 1	clear, yellow liquid	-1 °C ($\mathrm{T_m^{onset}}$)	0.8

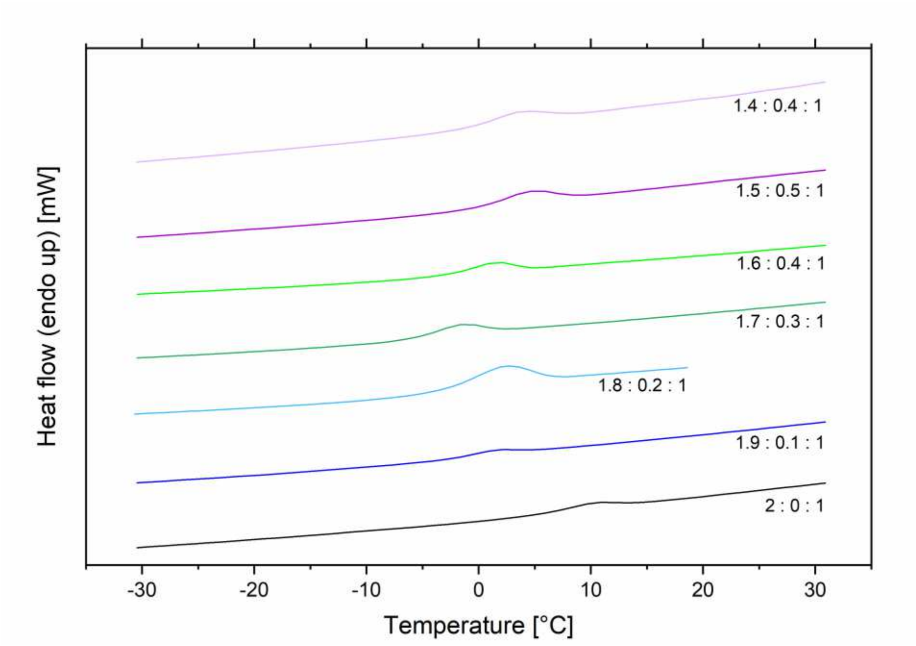

Fig. 3.2.2-3: Qualitative DSC curves of a series of Car-CarHCl-MaleA mixtures in HBA : HBD ratio of 2 : 1 including the initial Car-MaleA DES (black curve). The plots are offset on the y-scale for clarity in representation.

Mixtures 0 to 4 of the Car-CarHCl-MaleA DESs exhibited water contents in a relatively narrow range from 0.4 to 0.6 wt% and were therefore considered to be comparable. The water contents of mixtures 5 and 6 were remarkably higher, so that they were excluded from the ^{1}H-NMR study. The melting temperatures of the Car-CarHCl-MaleA DESs were found to be between -6 and +6 °C. According to the presented DSC data, sample 3 having a composition ratio of 1.7 : 0.3 : 1 constitutes the eutectic, *i.e.*, the lowest melting mixture of the system Car-CarHCl-MaleA. This system exhibited higher melting temperatures compared to Car-CarHCl-LaA. This finding can be ascribed to lower water contents or differences in the H-bond network caused by the presence of a dicarboxylic acid.

In order to obtain further insights in the H-bonding behaviour and the location of the affected carboxylic proton, an ^{1}H-NMR analysis of the Car-CarHCl-MaleA series was conducted. It is to be noted that the respective samples had to be solubilized in a deuterated solvent. Acetonitrile was used, as it is an aprotic solvent which does not interfere with the H-bonding interactions. Still, the samples analysed in the scope of the NMR experiments were dilute solutions and it is not sure to which extent they differ from the pure DESs.

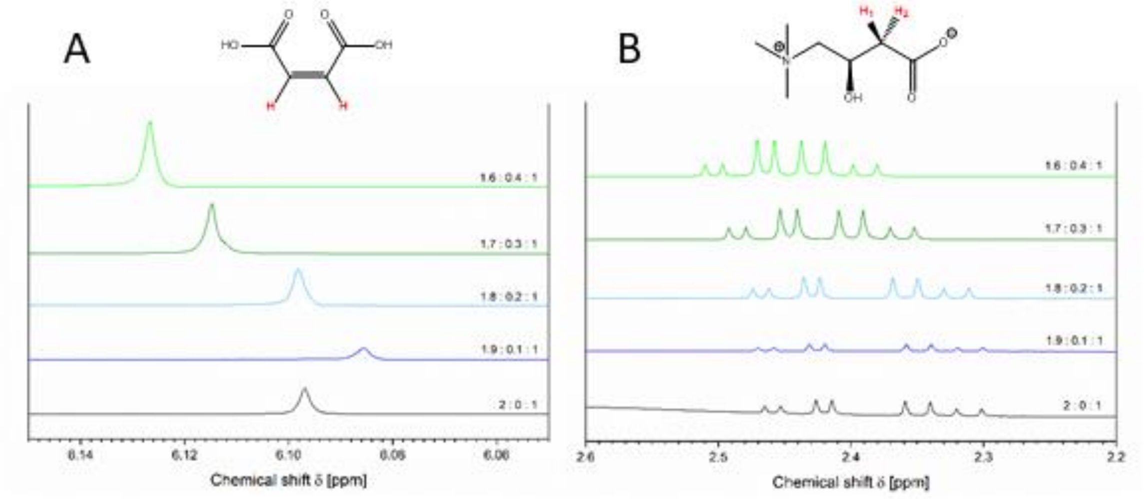

Fig. 3.2.2-4: Selected NMR spectral ranges of a series of Car-CarHCl-MaleA mixtures in HBA : HBD ratio of 2 : 1 including the initial Car : MaleA DES (black curve). The plots are offset on the y-scale for clarity in representation.

The evolution of two selected NMR signals when stepwise replacing carnitine with carnitine hydrochloride and thereby blocking the proton acceptor is illustrated in Fig. 3.2.2-4. Neither of the two signals can be ascribed to the carboxylic proton itself. One of them (Fig. 3.2.2-4-A) is assigned to the alkenyl hydrogens of maleic acid, the other one (Fig. 3.2.2-4-B) corresponds to the protons located at the carbon atom between the hydroxylic and the carboxylic group of carnitine/carnitine hydrochloride. Nevertheless, both types of protons are affected by the replacement of carnitine by carnitine hydrochloride. The effect is caused by changes in the local environment of the examined protons, such as binding parameters, bond length, angles between bonds and H-bonding activity.[12]

The signal of the alkenyl hydrogens of pure maleic acid appeared at a chemical shift of δ = 6.36 ppm (see Fig. 6.3.1-1 in section 6.3.1 of the appendix). As illustrated in Fig. 3.2.2-4-A, the corresponding signal in the binary Car-MaleA DES occurred at δ = 6.10 ppm. The signal shift to higher fields is indicative for a dissociation of the proton and the presence of H-bonds.[13,14] With the progressive replacement of carnitine by carnitine hydrochloride, the opposite effect, *i.e.* the signal shift to lower fields was observable from the presented NMR spectra. Therefore, the H-bonding activity and the degree of deprotonation are assumed to be reduced in presence of carnitine hydrochloride.

Signal B in Fig. 3.2.2-4 represents the peaks of the highlighted carnitine protons. A closer look reveals that H_1 and H_2 are non-equivalent and that two separate signals occur for these protons. A progressive change of the chemical shift δ, the vicinal coupling constants ^3J and the distance $\Delta\delta$ between the signals was observable. The signals of carnitine and carnitine chloride could not be distinguished in the recorded NMR spectra. This implies that they are equally implemented in a H-bond network. The respective signal was shifted towards higher frequencies with the progressive replacement of carnitine by carnitine hydrochloride. The vicinal coupling constant of signal 1 increased with increasing carnitine hydrochloride proportions, while it decreased for signal 2 (see Tab. 3.2.2-3). The difference in the chemical shifts of signals 1 and 2 was reduced simultaneously. These observations suggest a change in the dihedral angle between the vicinal protons and a decrease in the angle between the geminally situated protons H_1 and H_2.[12–14]

So, on the one hand, ^{1}H-NMR analysis revealed a signal shift of the maleic acid protons bound to the carbon atoms, which can be ascribed to the deprotonation of the carboxylic function. On the other hand, proton exchange and formation of H-bonds are expected to result in a change of the orientation and the geometry of the carnitine-bound protons.

Tab. 3.2.2-3: Vicinal coupling constant ^3J of the protons H_1 and H_2 bound to the carbon atom next to the carboxylic group of carnitine/carnitine hydrochloride (see highlighting in Fig. 3.2.2-4) and $\Delta\delta$ between signals 1 and 2.

Solution	**Molar ratio Car : CarHCl : MaleA**	**^3J [Hz] (Signal 1)**	**^3J [Hz] (Signal 2)**	**$\Delta\delta$ [ppm]**
Car		n.d.	8.3	n.d.
0	2 : 1 (Car-MaleA)	4.8	7.5	0.06
1	1.9 : 0.1 : 1	4.7	7.5	0.06
2	1.8 : 0.2 : 1	4.8	7.5	0.05
3	1.7 : 0.3 : 1	5.1	7.3	0.03
4	1.6 : 0.4 : 1	5.3	7.2	0.02

These results suggest at least a partial dissociation of the carboxylic proton in DESs consisting of a zwitterionic compound and a carboxylic HBD. However, the proton is supposed to be not assignable to a distinct position, as it might be interconnected in an advanced H-bond network. Thus, the mixture probably features an IL character to a certain extent, but is at the same time a DES. In short, the boundaries of these substance classes are rather fluent. It might be worthwile to measure the pH values of the ternary Car-CarHCl-MaleA mixtures in order to get more information on the behaviour of the dissociated proton and the H-bond network. In practice, the mixtures are too viscous or sometimes even brittle, so that certain amounts of additional solvent might be required for conducting pH measurements.

3.2.3 Deep Eutectic Solvents Based on Betaine and Carnitine Alkyl Esters

The synthesis of carnitine alkyl ester ILs was presented in the previous chapter (see section 2.2.1). In the course of this study, remaining impurities of carnitine were found to cause a decrease in the melting temperature of the resulting compound. Following this observation, the question arose, whether the addition of a second component with HBD character in general would lead to a reduction of the melting temperatures of such quaternary ammonium salts. It is admittedly not confirmed that the fact of the initial HBA being an IL is important. Instead, the bulkier structure of the quaternary ammonium cation compared to regular HBAs, such as choline chloride, betaine or carnitine is assumed to be relevant.

The betaine and carnitine alkyl ester HBAs studied in this section and their respective melting temperatures are summarized in Tab. 3.2.3-1. De facto, the melting temperatures of the tested HBAs are too high to identify them as ILs according to the classical definition (see section 1.3.5.1).

Tab. 3.2.3-1: Bulky betaine and carnitine ester HBAs and their melting points.

HBA	**Melting temperature [°C]**
[C_2Bet]Br	158
[C_2Car]Br	172
[C_4Bet]Br	100

The tested combinations of HBAs and HBDs are listed in Tab. 6.2.3-1 in section 6.2.3 of the appendix, alongside the respective molar mixing ratios and an indication, whether a DES was formed or not.

A summary of the mixtures, which successfully formed DESs and some of their basic properties can be found in

Tab. 3.2.3-2. The abbreviations and molecular structures of the HBAs and HBDs are to be found in Fig. 6.1.1-1 and Fig. 6.1.2-1 in section 6.1 of the appendix.

Tab. 3.2.3-2: DESs formed from [C_2Bet]Br, [C_2Car]Br and [C_4Bet]Br with indicated visual appearances at room temperature, thermal transition temperatures and water contents.

IL-HBA	**HBD**	**Molar ratio HBA : HBD**	**Appearance at rt**	**Thermal transition**	**Water content [wt%]**
[C_2Bet]Br	EG	1 : 2	solution with white precipitate	n.d.	n.d.
[C_2Bet]Br	GlA	1 : 2	clear, colourless liquid	n.d.	n.d.
[C_2Bet]Br	Gly	1 : 2	clear, colourless liquid	n.d.	n.d.
[C_2Bet]Br	IA	1 : 1	white, sticky solid	n.d.	n.d.
[C_2Bet]Br	LA	1 : 2	white, sticky solid	n.d.	n.d.

IL-HBA	HBD	Molar ratio HBA : HBD	Appearance at rt	Thermal transition	Water content [wt%]
[C_2Bet]Br	LaA	1 : 2	clear, colourless liquid	n.d.	n.d.
[C_2Bet]Br	MA	1 : 1	white, sticky solid	n.d.	n.d.
[C_2Bet]Br	ManA	1 : 2	white, sticky solid	n.d.	n.d.
[C_2Car]Br	EG	1 : 2	solution with white precipitate	n.d.	n.d.
[C_2Car]Br	GlA	1 : 2	clear, colourless liquid	n.d.	n.d.
[C_2Car]Br	Gly	1 : 2	clear, colourless liquid	< -60 °C	n.d.
[C_2Car]Br	LA	1 : 2	white, sticky solid	n.d.	n.d.
[C_2Car]Br	LaA	1 : 2	clear, colourless liquid	n.d.	n.d.
[C_2Car]Br	ManA	1 : 2	white, sticky solid	n.d.	n.d.
[C_2Car]Br	OA	1 : 2	clear, orange liquid	-37 °C (T_m^{onset})	n.d.
[C_2Car]Br	Urea	1 : 2	white solid	-20 °C (T_g) +63 °C (T_m^{onset})	n.d.
[C_4Bet]Br	CiA	1 : 2	clear, colourless liquid	-17 °C (T_m^{onset})	0.7
[C_4Bet]Br	D-Fru	1 : 2	clear, colourless liquid	-25 °C (T_m^{onset})	4.5
[C_4Bet]Br	EG	1 : 1	clear, yellow liquid	n.d.	n.d.
		1 : 2	clear, yellow liquid	< -60 °C	n.d.
[C_4Bet]Br	GlA	1 : 2	clear, colourless liquid	-43 °C (T_g)	2.8
[C_4Bet]Br	Gly	1 : 2	clear, yellow liquid	n.d.	n.d.
[C_4Bet]Br	IA	1 : 1	white, sticky solid	n.d.	n.d.
[C_4Bet]Br	LA	1 : 2	clear, yellow liquid	n.d.	3.8
[C_4Bet]Br	LaA	1 : 2	clear, yellow liquid	-53 °C (T_m^{onset})	3.5
[C_4Bet]Br	MA	1 : 1	clear, yellow liquid	n.d.	1.1
[C_4Bet]Br	MalA	1 : 1	clear, orange liquid	-32 °C (T_m^{onset})	0.8
[C_4Bet]Br	ManA	1 : 2	white, sticky solid	-29 °C (T_m^{onset}) +37 °C (T_m^{onset})	0.1
[C_4Bet]Br	OA	1 : 1	clear, yellow liquid	-37 °C (T_m^{onset})	7.0
[C_4Bet]Br	Urea	2 : 1	white solid	+71 °C (T_g)	n.d.

The compatibility of these HBAs is remarkably higher compared to zwitterionic betaine and carnitine. Especially [C_4Bet]Br delivered promising results when used as HBA, as it formed DESs with most of the tested HBDs. Almost all of the resulting DESs were liquid at room temperature and exhibited melting temperatures fairly below 0 °C. Although the viscosity of those mixtures was not determined, they seemed to be more fluid compared to other betaine- and carnitine-based DESs, as far as this could be estimated from handling them in the labscale. This gives cause to conclude that bulky quaternary ammonium salts, such as betaine and carnitine alkyl esters, have the potential to serve as adequate HBA candidates for the formation of DESs. It confirms the assumption that the melting temperature of quaternary ammonium ILs can be decreased by the addition of a suitable HBD component in a certain ratio.

3.2.4 Betaine- and Carnitine-Based Deep Eutectic Solvents for the Solubilization of Melanin

The term ‘melanin’ describes a group of natural pigments responsible for the colour of hair, skin, feathers and eyes. It is biosynthesized in special cell organelles referred to as melanosomes within the melanocytes. The structures of two basic types of melanin are presented in Fig. 3.2.4-1 – pheomelanin and eumelanin. Melanin exhibits three characteristic properties responsible for its role in the organism: (1) it absorbs UV light, (2) it is a reactive oxygen species scavenger and (3) it complexes metal ions.[15] Natural melanin is insoluble in water, acidic aqueous solution and common organic solvents. For its extraction from plants or animal tissue, protocols including harsh chemical conditions, such as strongly alkaline solutions, are typically used. These can lead to structural modifications of melanin.[16] In cosmetics, melanin presently is a hot topic. On the one hand, the removal of melanin is required for bleaching hair. Bleaches therefore regularly contain oxidizing species which break up the melanin structure. On the other hand, melanin is a valuable natural pigment with potential application in artificial hair or skin colouration.

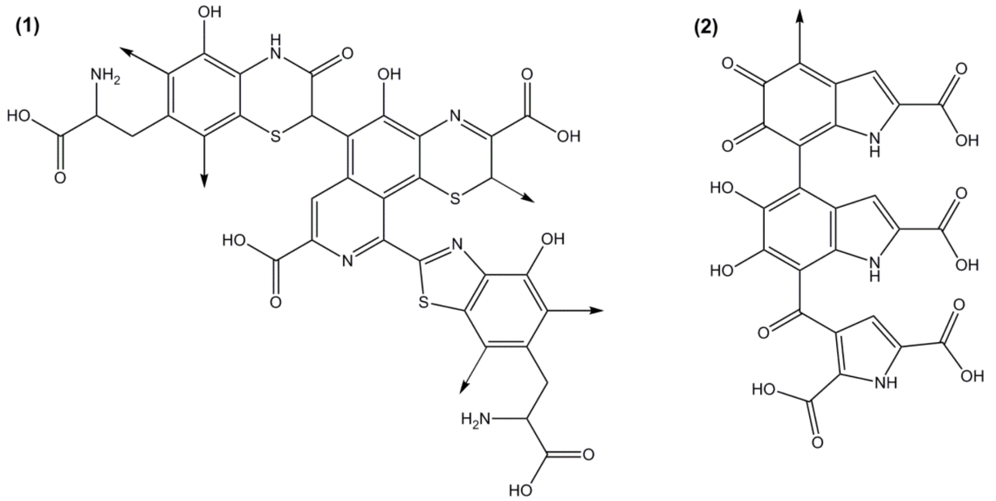

Fig. 3.2.4-1: Molecular structures of (1) pheomelanin and (2) eumelanin. The arrows indicate further connection points for the expansion of the polymer network.

The target of this study was to extract the biopolymer melanin from biomass at neutral or only slightly acidic pH without breaking up the structure in order to access a new source of natural pigments.

DESs containing betaine- or carnitine-based HBAs in combination with organic carboxylic acids as HBDs were evaluated as solvents for the solubilization of melanin. However, strong limitations occurred due to the mixtures’ high viscosities, *e.g.* a magnetic stirrer did not even move in the pure solvents. Therefore, the solubility tests were conducted in the respective DESs containing 25 wt% of water. A linear relation was observed when plotting the absorbance of a concentration series of melanin-DES solutions (after separating solid residues) as a function of the respective initial melanin concentration. The respective relations for the studied solvents are presented in Fig. 3.2.4-2. The so-called 'solubility fraction' for each solvent was determined from the slopes of the respective linear regression lines. It serves as a relative measure of the solubilization capacity of the studied solvent with respect to ethanolamine as a reference solvent. The values for the studied solvents' solubility fractions are compared in Fig. 3.2.4-3 with indication of the measured pH values.

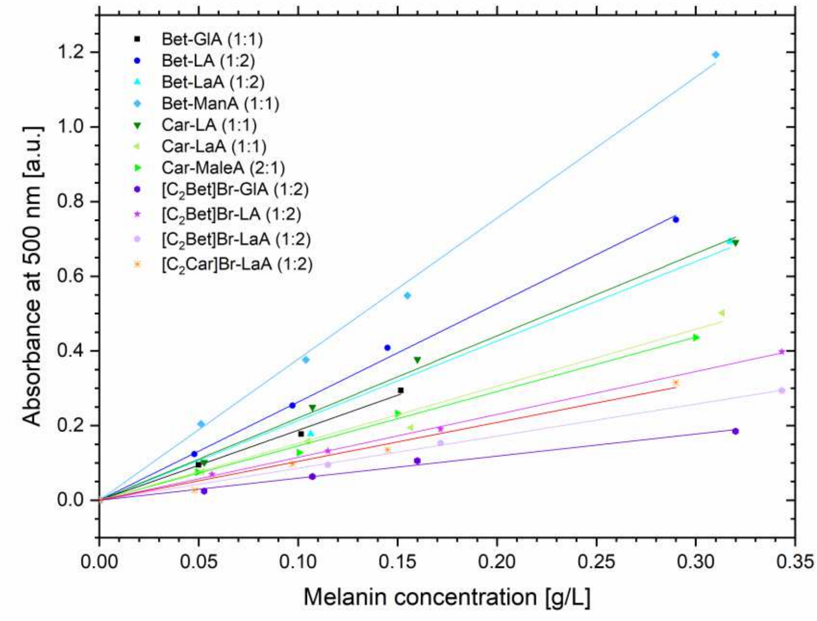

Fig. 3.2.4-2: Absorbance at a wavelength of 500 nm as a function of the initial melanin concentration. The tested solutions contain 25 wt% of water.

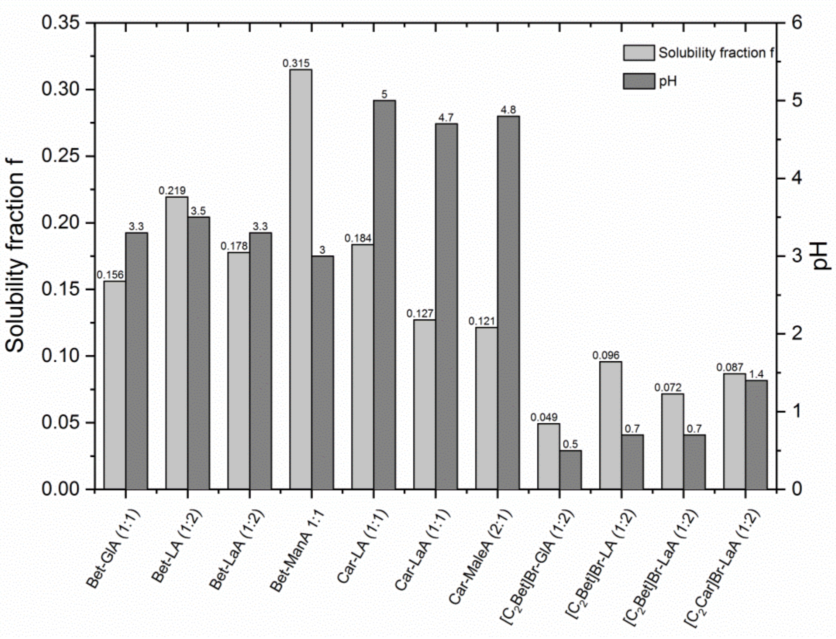

Fig. 3.2.4-3: Solubility fraction and pH values of the tested solvents having a water content of 25 wt% as inferred from the linear regression lines of Fig. 3.2.4-2.

DESs containing zwitterionic betaine or carnitine demonstrated superior performance in solubilizing melanin compared to their esterified derivatives. Higher solubility fractions were determined for the betaine solvents compared to the respective carnitine solvents. The HBAs can be arranged according to the pH values of the respective solutions: Car > Bet > [C_2Car]Br > [C_2Bet]Br. This behaviour is likely to be related to the availability of the carboxylic proton, where a lower pH value corresponds to a higher proton availability. The pH dependence of the solubility fraction was investigated by means of a Bet-ManA (1 : 1) solution containing 25 wt% water. The pH was adjusted by the addition of ethanolamine. The results suggest that the solubility fraction and therefore the relative solubility of melanin increase with increasing pH value (see Fig. 3.2.4-4).

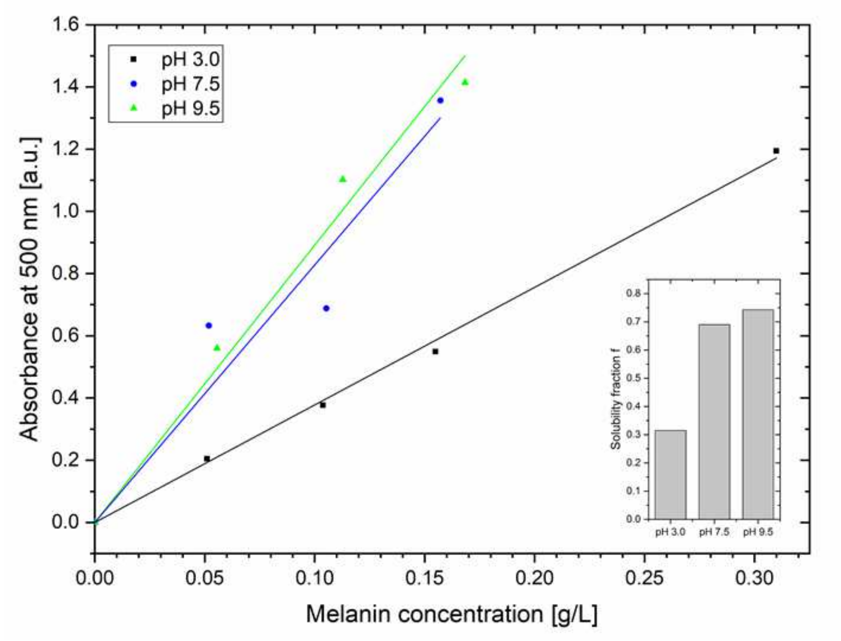

Fig. 3.2.4-4: Absorbance at a wavelength of 500 nm as a function of the initial melanin concentration for Bet-ManA (1 : 1) (25 wt% water) mixtures at pH 3.0, 7.5 and 9.5. The inlay illustrates the respective solubility fractions.

In general, the solubility of melanin in the tested betaine- and carnitine-based solvents was lower in comparison to ethanolamine. Also, amine-based ILs studied by the same approach exhibited improved performance.

Several aspects are to be considered when evaluating the results obtained from the melanin solubility tests in DESs.

(1) The melanin used for the solubility tests was synthetically produced and provided without specification of its exact composition.
(2) When solubilizing melanin in the tested solutions, a considerable part remained undissolved. It can be assumed that the detected absorbance of the solutions is due to the solubilization of only certain melanin components, while others are insoluble.

(3) It remains unknown, whether the polymer structure could be preserved or not.
(4) When using betaine or carnitine, a proton exchange between the carboxylic acid and the zwitterionic quaternary ammonium is likely, so that the resulting solvent exhibits IL character (detailed discussion in section 3.2.2).
(5) A considerable amount of water (25 wt%) was added to the studied DESs in order to decrease the viscosity and enable a decent sample preparation. The resulting solvents can be argued to be equal to concentrated electrolyte solutions.

As known from literature, melanin is soluble in alkaline solutions. The present results confirm a pH dependent solubility, whereby high pH values promoted the solubilization of melanin. The studied DESs did not perform as well as ethanolamine or amine-based solvents, as aqueous solutions of amines in general exhibit higher pH values. In this regard, it is believed that the studied DESs are not suitable for replacing traditional methods of melanin solubilization.

3.3 Deep Eutectic Solvents Containing Biologically Relevant HBDs

The general idea of this approach was to create DESs containing biologically relevant molecules acting as functional, non-aqueous liquid media. This basically means that the resulting DESs were aimed to be applicable as solvents exhibiting additional application-related beneficial properties. A number of biomolecules with HBD activity, including caffeic acid, *p*-coumaric acid, ferulic acid, gallic acid, quinic acid, salicylic acid and shikimic acid were combined with choline chloride and acetylcholine chloride. Caffeic acid, *p*-coumaric acid, ferulic acid, gallic acid and salicylic acid belong to the substance class of polyphenols, more specifically to the subclass of phenolic acids. They are interesting due to their antioxidant activity.[17] In nature, they often occur in glycosylated form or bound to quinic acid, shikimic acid or tartaric acid.[18] Shikimic acid and quinic acid are both natural molecules with carboxylic function and used for applications in pharmaceutics.[19]

This section presents DESs formed by combining quaternary ammonium salts with the above-mentioned biological molecules. Besides binary mixtures, ternary mixtures of choline chloride, gallic acid and one further HBD were studied and compared in terms of their thermal phase behaviours.

As mentioned above, the applied HBDs are biologically relevant substances. All of them exhibit antioxidant activity. In addition, some of them feature antimicrobial or anti-inflammatory characteristics. As a result, these natural carboxylic acids and their derivatives are interesting for applications in chemical formulations and pharmaceutics. In many cases, a chemical modification of these molecules is advantageous or required. The utilization of DES reaction media for the esterification of the respective carboxylic acids was studied. In this kind of reactions they function both as reactant and part of the solvent. This principle was shown for the synthesis of caffeic acid phenethyl ester.[20] The applicability of this reaction pathway to the newly developed DESs was examined.

3.3.1 Binary Deep Eutectic Solvents Containing Biologically Relevant Hydrogen Bond Donors

A number of natural carboxylic acids with biological function exhibit HBD activity. They have been combined with choline chloride in a variety of compositions to determine, if they induce a reduction of the melting temperature and form liquid mixtures. Caffeic acid and gallic acid have been reported to form DESs with choline chloride.[6,21] Further, structurally similar, biologically relevant HBDs are investigated. An overview is given in Tab. 6.2.4-1 in section 6.2.4 of the appendix, alongside the respective molar mixing ratios and an indication, whether a DES was formed or not.

An overview of the combinations, which successfully resulted in the formation of DESs, including their appearance, thermal transition temperatures and water contents is illustrated in Tab. 3.3.1-1. The abbreviations and molecular structures of the HBAs and HBDs are to be found in Fig. 6.1.1-1 and Fig. 6.1.2-1 in section 6.1 of the appendix.

Tab. 3.3.1-1: Overview of DESs formed with choline chloride and biologically active HBDs with indicated visual appearances at room temperature, thermal transition temperatures and water contents.

HBA	HBD	Molar ratio HBA : HBD	Appearance at rt	Thermal Transition	Water content [wt%]
ChCl	CA	2 : 1	white solid	+78 °C ($T_\mathrm{m}^\mathrm{onset}$)	n.d.
		3 : 2	yellowish, sticky solid	-52 °C ($T_\mathrm{m}^\mathrm{onset}$) +80 °C ($T_\mathrm{m}^\mathrm{onset}$)	n.d.
		6 : 5	colourless, viscous liquid	-39 °C ($T_\mathrm{m}^\mathrm{onset}$)	n.d.
ChCl	*p*-CouA	2 : 1	yellowish, sticky solid	n.d.	n.d.
ChCl	FeA	2 : 1	yellowish, sticky solid	n.d.	n.d.
ChCl	GA	2 : 1	yellowish solid	+64 °C ($T_\mathrm{m}^\mathrm{onset}$)	0.1
ChCl	QA	2 : 1	colourless, viscous liquid	-54 °C ($T_\mathrm{m}^\mathrm{onset}$) +73 °C ($T_\mathrm{m}^\mathrm{onset}$)	2.5
ChCl	SalA	1 : 1	yellowish, sticky solid	n.d.	n.d.
ChCl	ShiA	2 : 1	colourless, sticky solid	+78 °C (T_g)	n.d.
		3 : 2	colourless, sticky solid	-52 °C ($T_\mathrm{m}^\mathrm{onset}$) +80 °C ($T_\mathrm{g}$)	n.d.

Only the mixtures ChCl-QA (2 : 1) and ChCl-CA (6 : 5) appeared in a liquid state at room temperature. All other studied DESs solidified upon cooling. It is to be noted that the visual appearance of ChCl-QA (2 : 1) did not correspond to the DSC result, according to which it should be solid at room temperature. This deviation is ascribed to the high viscosity of this DESs. It is to be expected that after a certain period of time, it will become inhomogeneous.

Acetylcholine chloride was used as alternative HBA. At 90 °C, homogeneous mixtures were formed with all tested HBDs, except of shikimic acid. Only for caffeic acid in 2 : 1 molar ratio a room temperature DES was formed (see Tab. 6.2.4-1 in section 6.2.4 of the appendix).

In general, natural antioxidants of the phenolic acid type and related natural carboxylic acids were shown to be able to form DESs when combined with choline chloride in an appropriate molar ratio. Thereby, a non-aqueous liquid medium is created, which is expected to feature antioxidant properties. However, in most cases the reduction of the melting point was not sufficiently pronounced to obtain room temperature DESs. Therefore, attempts to decrease the melting temperatures and alongside eventually the viscosities of these DESs by adding a second HBD component were made. The respective experiments are presented in the next section.

3.3.2 Ternary Mixtures Containing Gallic Acid

Gallic acid is a valuable, natural antioxidant frequently used in cosmetic applications. Implementing gallic acid into a DES grants access to a non-aqueous, antioxidant, liquid medium, which can be interesting for cosmetics and/or the food industry. With a melting point of 64 °C, the binary mixture ChCl-GA (2 : 1) is solid at room temperature. Therefore, a further reduction of the characteristic value was intended to be achieved by the systematical implementation of a second HBD into the mixture. Urea and *D*-fructose were chosen, as they are well studied HBDs and known to form room temperature DESs with choline chloride.[22] In addition, ternary mixtures of Car-LA-GA were investigated. The ternary DESs were prepared in ratios of 2 : 1, 1 : 1 and 1 : 2 in terms of HBA to total HBD, whereas the total HBD amount was taken as the sum of the molar amount of gallic acid and the molar amount of a second HBD. An overview of the considered combinations is given in Tab. 6.2.5-1 in section 6.2.5 of the appendix, alongside the respective molar mixing ratios and an indication, whether a DES was formed or not.

An overview of the combinations, which successfully resulted in the formation of DESs, including their appearance, thermal transition temperatures and water contents is illustrated in Tab. 3.3.2-1.

Tab. 3.3.2-1: Gallic acid-based, ternary DESs with indicated visual appearances, thermal transition temperatures and water contents.

HBA	**HBD1**	**HBD2**	**Molar ratio HBA : HBD1 : HBD2**	**Appearance at rt**	**Thermal transition**	**Water content [wt%]**
ChCl	Urea	GA	2 : 0.75 : 0.25	white, sticky solid	+79 °C (T_m^{onset})	0.2
ChCl	Urea	GA	2 : 0.50 : 0.50	white, sticky solid	+66 °C (T_m^{onset}) +78 °C (T_m^{onset})	0.2
ChCl	Urea	GA	2 : 0.25 : 0.75	white, sticky solid	-29 °C (T_g) +80 °C (T_m^{onset})	0.2
ChCl	Urea	GA	1 : 0.75 : 0.25	clear, colourless liquid	-39 °C (undef.) +83 °C (undef.)	0.1

HBA	HBD1	HBD2	Molar ratio HBA : HBD1 : HBD2	Appearance at rt	Thermal transition	Water content [wt%]
ChCl	Urea	GA	1 : 0.50 : 0.50	clear, yellowish liquid	-26 °C (undef.)	0.1
ChCl	Urea	GA	1 : 1.50 : 0.50	clear, colourless liquid	-24 °C (T_g)	0.1
ChCl	D-Fru	GA	1 : 0.75 : 0.25	clear, orange liquid	-30 °C (T_g)	4.6
ChCl	D-Fru	GA	2 : 0.75 : 0.25	clear, orange liquid	+40 °C (T_m^{onset})	3.8
ChCl	D-Fru	GA	2 : 0.50 : 0.50	clear, orange liquid	+30 °C (T_m^{onset})	3.0
ChCl	D-Fru	GA	2 : 0.25 : 0.75	clear, orange liquid	+18 °C (T_m^{onset})	1.7
Car	LA	GA	2 : 1.50 : 0.50	clear, yellow liquid	-9 °C (T_m^{onset})	0.5
Car	LA	GA	1 : 1.50 : 0.50	clear, yellow liquid	-20 °C (T_m^{onset}) +27 °C (T_m^{onset})	0.5

In case of the Car-LA-GA system, only two of the nine tested combinations formed homogeneous liquid mixtures. The implementation of *D*-fructose as second HBD resulted in the formation of DESs with visually lower viscosities compared to the other ternary mixtures. However, they suffered from elevated susceptibility towards thermal degradation, which was reflected by dark brown appearances of the mixtures.

The system ChCl-urea-GA formed liquid mixtures in a variety of different compositions. Mixtures with 1 : 1 and 1 : 2 overall HBA : HBD ratio were liquid at room temperature. Interestingly enough, the respective mixtures without urea did not result in the formation of DESs. In contrast, 2 : 1 ternary mixtures were solid at room temperature. Fig. 3.3.2-1 illustrates their thermal transition temperatures in comparison with the binary mixture ChCl-GA in two relevant ranges of temperature. The ternary ChCl-urea-GA DESs at overall HBA : HBD ratios of 2 : 1 do not show a thermal transition in the temperature range from -50 °C to 0 °C (see Fig. 3.3.2-1-A), but an endothermal - albeit in some cases unpronounced - peak between 40 °C and 100 °C (see Fig. 3.3.2-1-B). In contrast, ChCl-urea-GA DESs in ratios of 1 : 1 and 1 : 2 do exhibit transitions in the former, but not in the latter temperature range. According to this finding, the thermal behaviour of the 2 : 1 ternary mixtures is similar to the 2 : 1 binary ChCl-GA DES. Aroso *et al.* suggested that choline chloride contained in excess is sometimes not completely included within the DES network.[23] In this case, it causes an endothermic DSC peak between 75 °C and 85 °C, which is proposed to be due to its crystallographic arrangement during the increase in temperature. The 2 : 0.25 : 0.75 and 1 : 0.75 : 0.25 ChCl-urea-GA mixtures exhibit – albeit rather indistinct - thermal transitions in both the low and the high temperature range and seem to be intermediate cases. The exothermic peak appearing in the DSC curve of the 1 : 1.50 : 0.50 mixture at a temperature of 78 °C is probably an artefact or caused by impurities.

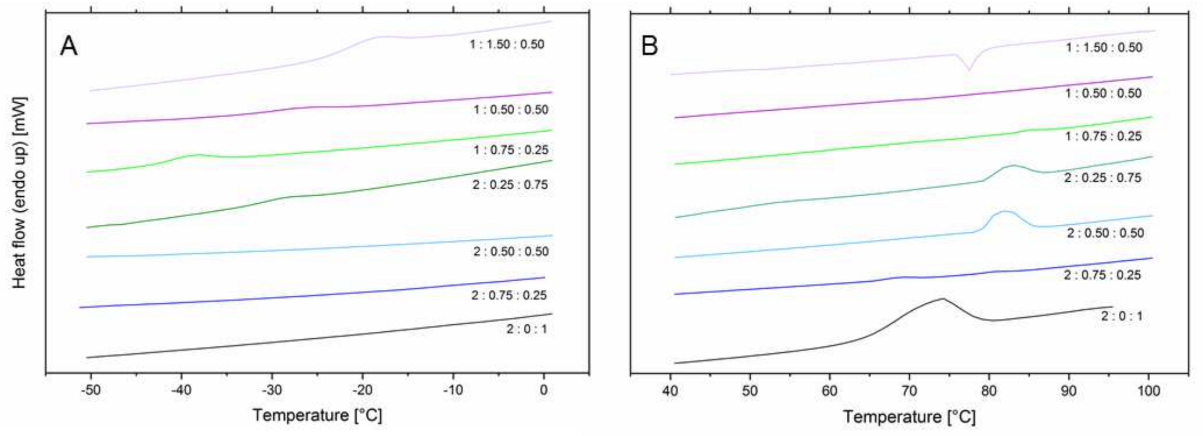

Fig. 3.3.2-1: Thermal transitions of the ternary mixture ChCl-urea-GA measured by means of DSC presented in two characteristic temperature ranges. The plots are offset on the y-scale for clarity in representation.

In summary, the replacement of a certain amount of GA by urea in a ChCl-GA DES and the corresponding formation of ternary ChCl-urea-GA DESs was found to be an appropriate method to further decrease the melting temperature and create room temperature liquid media. A change in the solvent viscosity, in particular the desired reduction in viscosity was not clearly identifiable. The resulting solvents are expected to exhibit antioxidant activity due to the presence of GA. Therefore, they can be referred to as functional, non-aqueous liquid media and might be interesting for chemical formulations.

3.3.3 Application of Deep Eutectic Solvents as Ephemeral Reaction Solvents

The former paragraphs described the use of several biomolecules with carboxylic function as HBDs for the formation of DESs and the creation of functional, non-aqueous liquid media. They were considered as ephemeral solvents for the esterification of carboxylic acids. This concept proved to be applicable for the synthesis of caffeic acid phenethyl ester (CAPE).[20] In this case, a DES consisting of choline chloride and caffeic acid was used as reaction medium. Caffeic acid was not only part of the solvent, it also functioned as reactant in the ester reaction. The second reactant, phenethyl alcohol, was soluble in the DES and the desired product CAPE was obtained in good yields, when adding an acid catalyst. The ease and elegance associated with is approach is obtained from the way of isolating the product: upon mere pouring of hot water to the reaction mixture, CAPE precipitated as white solid. The remaining compounds were water soluble and could be easily separated from the product.

In this project, the previously described reaction concept was intended to be repeated by three different approaches: (1) the esterification of gallic acid to obtain gallic acid alkyl esters, (2) the esterification of caffeic acid with quinic acid to obtain chlorogenic acid and (3) the esterification of shikimic acid with ethanol.

3.3.3.1 Synthesis of Gallic Acid Alkyl Ester

Due to its antioxidant activity and further therapeutic effects, gallic acid is an interesting substance for the use in pharmaceutics and in chemical formulations, e.g. as food preservative.[24] However, it is rather hydrophilic, but hardly water soluble. By esterifying the carboxylic group, it becomes more hydrophobic and oil soluble, while maintaining its antioxidant properties.[25] As a result, gallic acid esters are more compatible with certain chemical formulations. A further advantage of the corresponding esters is their lower sensitivity towards changes in the pH value. The concept of ephemeral reaction media was considered an elegant way of synthesizing this class of antioxidants.

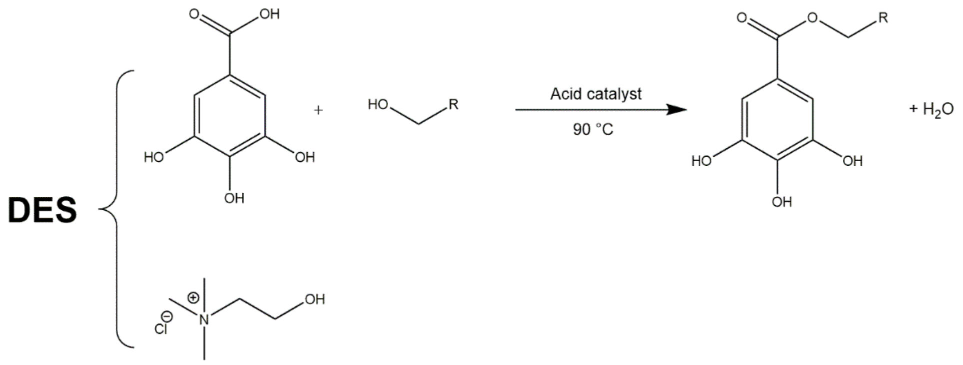

Fig. 3.3.3-1: Esterification of gallic acid to form a gallic acid alkyl ester in a DES reaction medium.

The proposed reaction scheme of the acid catalyzed esterification of gallic acid with a linear alkyl alcohol to yield alkyl gallates is demonstrated in Fig. 3.3.3-1. A DES comprising gallic acid was used as a reaction medium, so that gallic acid was on the one hand part of the solvent and on the other hand the reactant. The binary ChCl-GA (2 : 1) DES exhibits a melting temperature of 64 °C. Further reduction of the melting temperature was possible by the addition of a third component, either urea or *D*-fructose (see section 3.3.2). A stoichiometric amount of alkyl alcohol was added to the reaction mixture and stirred in the presence of an acid catalyst for a defined period of time. High pressure liquid chromatography (HPLC) and nuclear magnetic resonance (NMR) analysis were utilized to detect the presence or absence of the desired GA ester. The tested reaction parameters are summarized in Tab. 3.3.3-1.

Tab. 3.3.3-1: Assessed reaction parameters of the gallic acid esterification.

Reaction medium	ChCl-GA ChCl-urea-GA ChCl-*D*-Fru-GA No solvent
Linear alkyl alcohol	Butanol Octanol
Acid catalyst	No catalyst Amberlyst 15 H_2SO_4

In a first step, the solubility of the tested linear alkyl alcohols butanol and octanol in the applied DESs was determined. The respective values are compared in Fig. 3.3.3-2. Butanol exhibited high solubilities both in the binary mixture ChCl-GA and in the ternary ChCl-*D*-Fru-GA DESs. Octanol, however, was poorly soluble in the tested DESs. Its solubility in ChCl-GA, ChCl-*D*-Fru-GA and some of the ChCl-urea-GA mixtures was too low to be detected with the method applied. Minor octanol solubility was found only in ChCl-urea-GA in overall HBA : HBD ratios of 1 : 1 and 1 : 2 and not in 2 : 1 ratio. This implies that high amounts of choline chloride inhibit the solubilization of octanol in the studied systems.

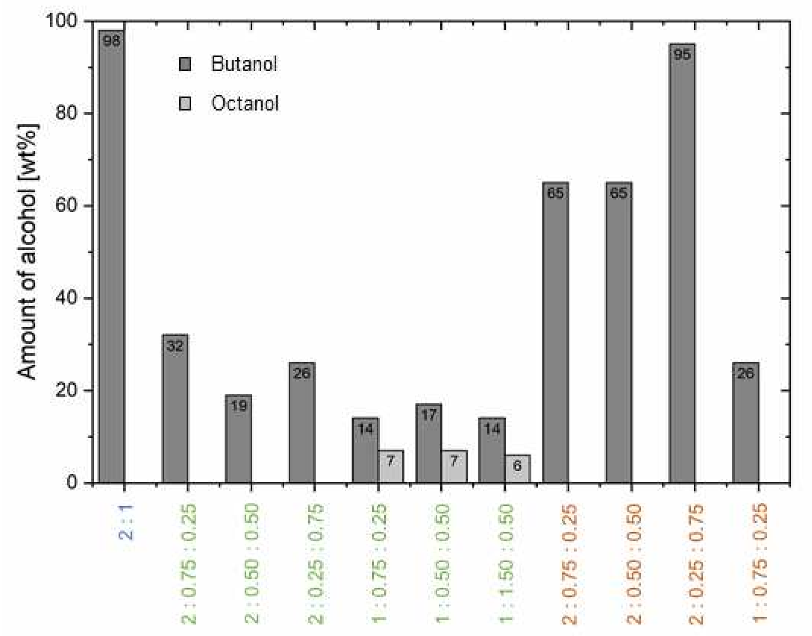

Fig. 3.3.3-2: Solubility of butanol and octanol in ChCl-GA (indicated in blue), ChCl-urea-GA (indicated in green) and ChCl-D-Fru-GA (indicated in orange) DESs of various molar ratios.

The particular DESs for the investigation of the desired esterification reaction were chosen on the basis of the solubility experiments, whereas the highest chance of success was assumed to occur, when the alcohol is solubilized in the solvent.

Tab. 3.3.3-2: Screened reaction systems for the esterification of gallic acid with n-alcohols and the resulting conversion either without catalyst, in presence of Amberlyst 15 or in presence of H_2SO_4.

Reaction medium	**Reactant**	**Conversion**		
		Without cat.	Amberlyst 15	H_2SO_4
ChCl-GA (2 : 1)	Butanol	5 %	54 %	60 %
ChCl-*D*-Fru-GA (2 : 0.25 : 0.75)	Butanol	n.d.	n.d.	n.d.
ChCl-urea-GA (2 : 0.75 : 0.25)	Butanol	<1 %	<1 %	<1 %
ChCl-GA (2 : 1)	Octanol	1 %	13 %	18 %
ChCl-*D*-Fru-GA (2 : 0.25 : 0.75)	Octanol	n.d.	n.d.	n.d.
ChCl-urea-GA (1 : 0.75 : 0.25)	Octanol	<1 %	<1 %	<1 %
No solvent	Octanol	<1 %	4 %	22 %

The alcohol was added to the DES in equimolar amount to gallic acid in order to start the reaction. For each system, one sample was reacted without catalyst, one with Amberlyst 15 and one with concentrated sulfuric acid as catalysts. The samples were stirred at 80 °C for 20 h, cooled to room temperature and analysed by means of HPLC. The tested systems and the respective results are listed in Tab. 3.3.3-2.

The ternary DESs were found to be not adequate as reaction media for the esterification of gallic acid. The presence of urea completely hindered the formation of the desired ester. In ChCl-*D*-Fru-GA DESs, considerable degradation occurred, so that besides a certain amount of the desired product, a multitude of degradation products was found and the mixtures turned black.

The formation of gallic acid butyl ester and gallic acid octyl ester could be achieved in the binary ChCl-GA DESs. Integration of the educt and product peak from the chromatograms (see Fig. 3.3.3-3-A and –B) revealed values of the relative conversions, which are indicated in Tab. 3.3.3-2. In general, the reaction without catalyst resulted in negligible conversion. Thus, the necessity of an acid catalyst was concluded. The esterification with butanol resulted in a higher conversion compared to octanol, probably due to increased butanol solubility in the DESs.

In order to have a reference, the reaction of gallic acid with octanol was conducted without solvent, *i.e.* without choline chloride. The desired ester was formed in the presence of an acid catalyst. The values of the relative conversions obtained from the chromatograms (see Fig. 3.3.3-3-C) were compared with the respective reactions in the DESs. This revealed a comparatively lower conversion with Amberlyst 15 and a higher conversion with sulfuric acid as catalyst.

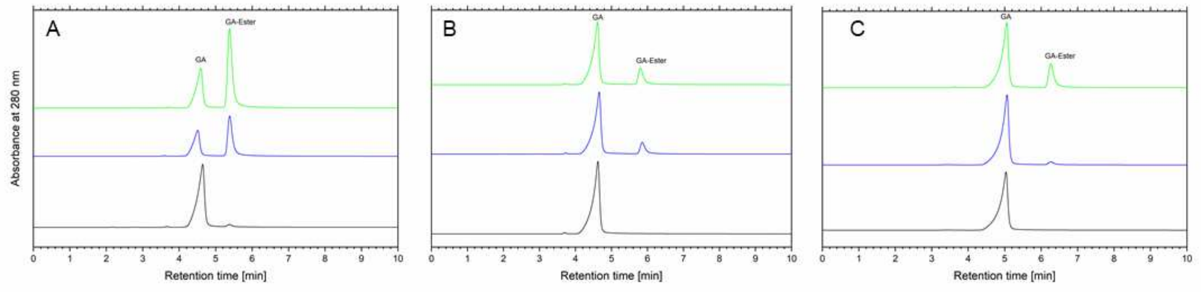

Fig. 3.3.3-3: HPLC chromatograms of the esterification of gallic acid with (A) butanol in ChCl-GA, (B) octanol in ChCl-GA and (C) octanol without solvent. Each chromatogram has the following colour code: black curve – without catalyst, blue curve – with Amberlyst 15, green curve – with H_2SO_4. The plots are offset on the y-scale for clarity in representation.

As mentioned above, the simple product isolation is the main advantage of using an ephemeral solvent in synthesis. Exemplarily in the synthesis of CAPE, the product precipitated upon the addition of water and is readily separated by filtration.[20] The addition of water to the gallic acid reaction mixture, however, led to a kinetically stable emulsion and after centrifugation to a phase separation into aqueous and organic phases. NMR analysis confirmed the presence of the product in the organic phase together with remaining *n*-alcohol and a certain amount of unreacted gallic acid.

Reflecting upon these findings, it is not evident that the presence of choline chloride and the DESs adds considerable value to the synthesis of gallic acid alkyl ester, as the formation of gallic acid octyl ester could equally be conducted without a DES type solvent at a similar conversion rate. Furthermore, the principle of an ephemeral solvent was not immaculately applicable in this reaction. The addition of water did not facilitate the precipitation of the targeted product. Instead, a more elaborate separation is required compared to the standard approach.

3.3.3.2 Further Approaches towards Deep Eutectic Solvents as Ephemeral Solvents

Chlorogenic acid (3-caffeoylquinic acid) (see Fig. 3.3.3-4) is an ester of caffeic acid and quinic acid. It is reported to exhibit antioxidant and anti-inflammatory properties as well as further properties beneficial to health, e.g. for the treatment of cardiovascular diseases, diabetes type 2 and Alzheimer's disease.[17] It is biosynthesized from phenylalanine in many plants.[26]

Both caffeic acid and quinic acid were found to be able to form a DES with choline chloride (see section 3.3.1). So, the idea was to combine these two acids within a ternary DES with choline chloride thereby providing a reaction medium for the synthesis of chlorogenic acid. The ternary mixture was an orange homogeneous liquid after heating. However, NMR and HPLC analysis revealed the presence of numerous degradation products, so that this attempt was rated unsuccessful.

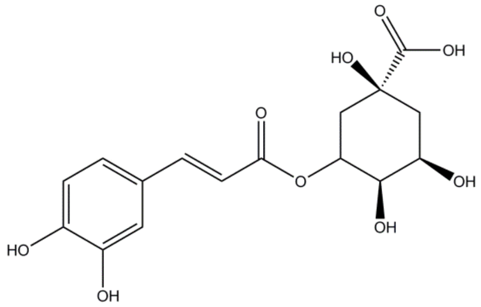

Fig. 3.3.3-4: Molecular structure of chlorogenic acid.

A further approach was directed towards the synthesis of shikimic acid ethyl ester within a DES reaction medium containing choline chloride and shikimic acid. This compound serves as a precursor for the synthesis of Tamiflu, which is used for the medical treatment and prevention of influenza virus infections.[27] The respective chemical structures are illustrated in Fig. 3.3.3-5.

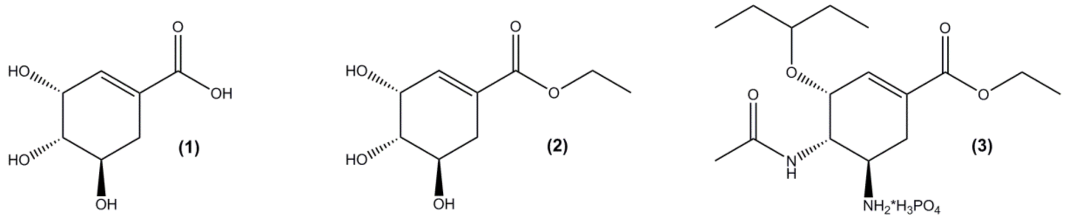

Fig. 3.3.3-5: Molecular structures of (1) shikimic acid, (2) shikimic acid ethyl ester and (3) oseltamivir phosphate (Tamiflu).

Shikimic acid was shown to form DESs with choline chloride at several molar ratios. First pre-tests revealed that ChCl-ShiA (2 : 1) is compatible with ethanol. After stirring the DES with ethanol for several hours at elevated temperature, recorded NMR spectra demonstrated a new signal, which possibly belongs to the newly formed ester species. However, further investigations, in particular HPLC analysis, will be necessary to confirm these assumptions.

3.4 Atomic Force Microscopy Study of the Behaviour of Surfactants at a Deep Eutectic Solvent-Graphite Interface

3.4.1 General Considerations

Nanostructuration at the electrode-liquid interface turned out to be one of the key parameters in electrochemistry. ILs have been extensively discussed regarding their potential for application in electrochemistry and so the composition and structure of the interfacial layers they form with an electrode surface. DESs have been reckoned promising as solvents in electrochemical processes, including electrochemical extraction,[28] electropolishing[29] and electrodeposition.[2,30] This is due to their electrochemical stability with wide electrochemical windows and their ability to dissolve metal ions.[31] As the structure and behaviour of solvents in close proximity to solid surfaces differs widely from the solvent bulk behaviour, studying solid-liquid interfaces is imperative for understanding electrochemical processes in detail.

The liquid nanostructure formed between several ILs and various types of surfaces has been studied thoroughly.[32,33,34] In contrast, DESs are less investigated and only few studies are available, where atomic force microscopy (AFM) proved to be an appropriate method for visualizing the layered nanostructure of the DES near the surface.[35–37] Their behaviour was shown to depend on the composition of the DESs. On the one hand, it is governed by the cation alkyl chain length, when the salt component is an alkyl ammonium bromide salt.[35] On the other hand, it depends on the type of hydrogen bond donor (HBD) used.[36,37] Regularly, force-distance curves are analysed to predict the constitution of the interfacial liquid layers. Force steps are observed due to liquid layers that are pierced through by the tip of the AFM sampling unit. They are observable in molecular solvents as well as in ILs, with the distinction that IL nanostructure is more pronounced. This is inferred from a higher number and more precise steps, which even increases when a surface potential is applied.[33,34,38] From the step width, information on the constitution of the layers is obtained. However, in DESs the presence of a molecular component in addition to an organic salt makes the interpretation complex. Chen *et al.* reported the presence of an ion rich Stern layer closest to a graphite surface, which is not replaceable by the AFM tip, followed by a molecular component layer. At open circuit potential and negative potential, the Stern layer is rich in choline cations, at positive potential, it is rich in chloride anions. The latter case enhances H-bonding with the molecular component and therefore increases the force required to push through the molecular layer. In general, the number of layers and the push through forces for DESs were lower compared to ILs.[36] Only recently, the interfacial nanostructure of DESs on platinum was investigated as a function of its water content. Up to an amount of ~40 wt%, the addition of water was found to increase the interfacial nanostructure. Considering similar experiments for ILs, where the addition of small amounts of water diminished nanostructuration significantly, these were surprising results.[39] They reveal the participation of water in the H-bond network, thereby supporting interfacial layering.

DESs have been recognized as media promoting self-assembly of amphiphilic solutes. Recent studies investigated the self-aggregation of sodium dodecyl sulphate (SDS) in choline chloride-based DESs including ChCl-urea, ChCl-EG and ChCl-Gly and observed the formation of spherical and elongated micelles, depending on the kind of HBD.[40,41] It was found that the critical micellar concentration (CMC) of SDS in DESs was smaller than in aqueous solution,[42] while the CMC of cationic cetyltrimethylammoniumbromide (CTAB) was similar in ChCl-Gly and water.[43,44] These findings are surprising, as DESs are less polar than water.[45] This indicates that other forces contribute to surfactant self-assembly in DESs. Sanchez-Fernandez *et al.* studied the 'interactive self-assembly', *i.e.* the participation of solvent components in the aggregation.[44] The bulk aggregation behaviour of dodecyl sulphate in ChCl-urea and ChCl-Gly depending on the counter-ion was investigated with the result that the counter-ion influences the bulk CMC and the limiting surface tension.[41] However, the nature of counter-ions plays an at least equally important role in inter-micellar interactions. The so-called Stern layer is formed due to electrostatically-driven attachment of oppositely charged ions to the micelle surface and has several consequences: reduction of interfacial charge density, change in the packing parameter of surfactant monomers, control over headgroup and micelle repulsion.[46,47] The Stern layer composition in DESs is not evident, as dissociated choline cations or chloride anions compete with the original counter-ions. In addition, hydration and co-surfactancy effects are involved.[41]

In general, the presence of a solid surface leads to an even more complex system. Besides surfactant-solvent and surfactant-surfactant interactions, the surfactant-surface and solvent-surface interactions are involved. In electrochemistry, surfactants are regularly used to modify the electrode surface, template the structure of deposited material, extend electrochemical windows and reduce the surface tension of electroplating solutions to facilitate bubble detachment and prevent pitting.[3] Several groups have studied the adsorption and self-aggregation behaviour of non-ionic and ionic surfactants on different surfaces in aqueous solution and ILs. They showed hemicylindrical micelles to arrange parallel across a hydrophobic graphite surface.[48–52,53] The proposed mechanism of a first adsorption monolayer with surfactant tails orientated parallel to the substrate plane in head-to-head orientation and the subsequent formation of hemimicellar micelles was generally accepted and confirmed by AFM images.

Having information on the nanostructuration of DESs at the graphite surface and aggregation of surfactants at aqueous-graphite and IL-graphite interfaces, this study is intended to obtain fundamental information on the behaviour of ionic surfactants at the DES-graphite interface. Concretely, SDS as well as CTAB are dissolved in concentrations fairly above their bulk CMC in DESs consisting of choline chloride and ethylene glycol (ChCl-EG) and choline chloride and glycerol (ChCl-Gly), both in (1:2) molar ratio. The latter mixtures are conventional DESs and known under the trade-names Ethaline and Glyceline. They appear to have potential as solvents in electrochemistry, as they are non-aqueous, conductive, low-viscous solutions and additionally cheap compared to other DESs and ILs. Beyond, they are readily available and easy to prepare. This study aimed to investigate the surfactant aggregate structure at the DES-graphite interface via AFM soft-contact imaging and AFM force curves. The obtained images are discussed in terms of changes in the surface pattern considering the following parameters: (1) choice of DES, (2) choice of surfactant, (3) surfactant concentration and (4) application of a surface potential. Force curves are analysed in order to gain information on the nanostructural surrounding of the surface and the aggregates, taking into account the parameters mentioned above.

3.4.2 Interfacial Behaviour of Deep Eutectic Solvents at a Graphite Surface

The nanostructuration of DESs at a graphite surface has been reported and discussed by Chen and co-workers.[36] In order to check the reliability of the complex (electrochemical) AFM system, analogous experiments were conducted with ChCl-Gly and ChCl-EG.

3.4.2.1 Force-Distance Curves Recorded at Open Circuit Potential

The recorded force-distance curves (see Fig. 3.4.2-1) showed oscillatory force steps when the tip was approaching the highly oriented pyrolytic graphite (HOPG) surface. This is characteristic of the presence of nanostructured liquid layers. The width of the force steps can provide valuable information on the composition of the corresponding liquid layer. It is important to point out that the zero separation of the force-distance curve does not always correspond to the distance from the solid surface, as in some cases the AFM tip is not able to replace dense liquid layers. This is taken into account by referring to the distance as 'apparent distance'.

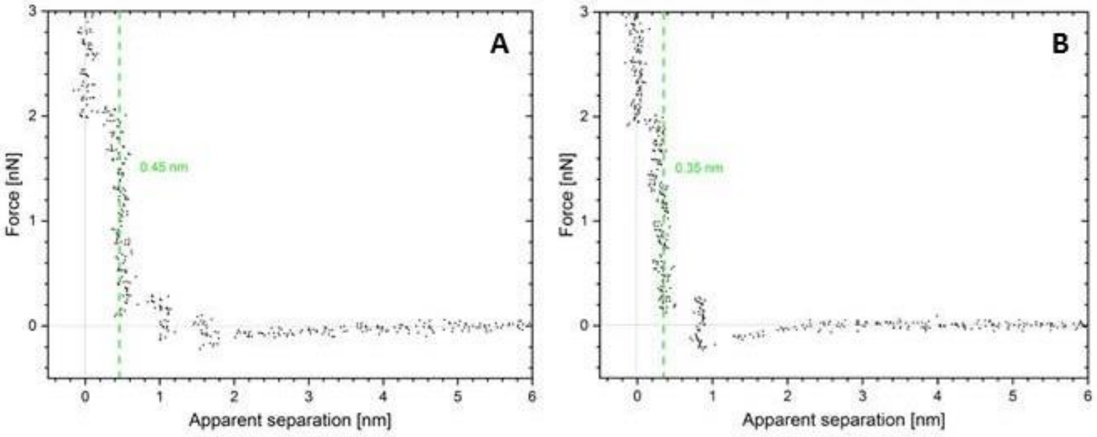

Fig. 3.4.2-1: Force-distance curves showing the normal force as a function of the apparent separation between tip and surface upon the AFM tip approaching the HOPG surface in pure ChCl-Gly (A) and pure ChCl-EG (B). The apparent nearest surface layers have thicknesses of 0.45 nm and 0.35 nm, respectively. The corresponding values are marked with green, dashed lines.

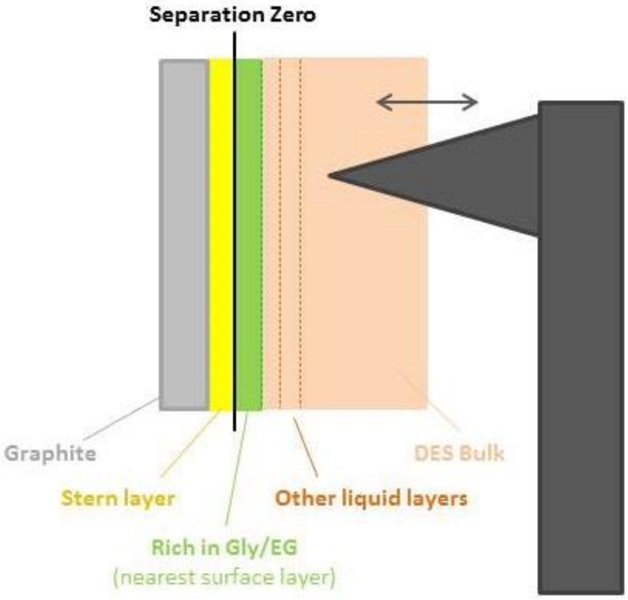

Fig. 3.4.2-2: Suggested interface model of the interface between graphite and a deep eutectic solvent with a barrier for the AFM tip between the ion rich Stern layer (yellow) and a layer rich in molecular component (green).

The nearest surface layer detected in the force-distance curves of pure DESs was evidenced as a nearly vertical repulsive wall at an apparent separation of 0.45 nm for ChCl-Gly (see Fig. 3.4.2-1-A) and 0.35 nm for ChCl-EG (see Fig. 3.4.2-1-B). According to literature, this corresponds to an incompressible layer of the molecular DES component, *i.e.* glycerol or ethylene glycol, respectively. An interfacial model as depicted in Fig. 3.4.2-2 was reported, where the so-called Stern layer (yellow) covers the graphite surface. This layer is dominated by ionic components, either choline or chloride, depending on the surface electric potential. However, this layer cannot be penetrated by the AFM tip and therefore acted as apparent zero separation. The adjacent layer was assumed to be rich in the molecular DES component, as the width matched the molecular dimension of the respective substances, 0.45 nm for glycerol and 0.35 nm for ethylene glycol. Further force steps are caused by less distinct nanostructured layers.[36]

3.4.2.2 Influence of the Electric Surface Potential on the Deep Eutectic Solvent-Graphite Interfacial Behaviour

A set of force curves recorded at a (ChCl-Gly)-graphite interface at varying electric surface potential is shown in Fig. 3.4.2-3. The width of the nearest surface step remains constant at all measured potentials. This suggests that the composition of this layer does not change. The normal force on the tip when pushing through the apparent nearest surface layer (rich in glycerol), *i.e.* the height of the first step was tendentially higher at positive electric potential compared to neutral and negative potential. This was rationalized by a change in the composition of the underlying Stern layer. At positive potential, it is rich in chloride ions, while at negative potential, it is rich in choline ions.[36] When the Stern layer is dominated by chloride, strong H-bonding interactions are formed with the adjacent glycerol layer, so that a higher force is required to replace this layer.[36] The corresponding set of force curves of ChCl-EG is given in Fig. 6.4.1-1 in section 6.4.1 of the appendix.

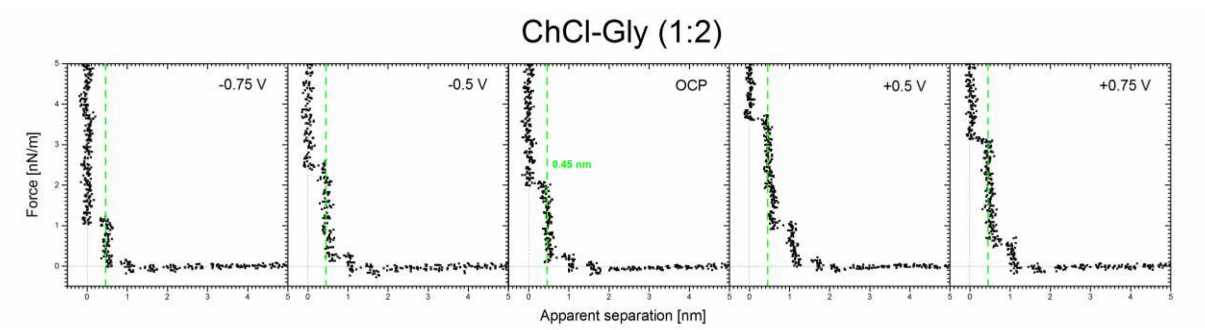

Fig. 3.4.2-3: Force-distance curves (normal force as a function of apparent separation) upon the AFM tip approaching the HOPG surface in pure ChCl-Gly at a molar ratio of 1 : 2. The apparent nearest surface layer has a thickness of 0.45 nm at OCP. It is marked with a green, dashed line.

3.4.3 Surfactant Aggregation at a Deep Eutectic Solvent-Graphite Interface

In order to study the aggregation behaviour of ionic surfactants at DES-graphite interfaces, SDS and CTAB were solubilized in both ChCl-Gly or ChCl-EG. While SDS was soluble in both solvents, CTAB could only be dissolved in ChCl-Gly. AFM was used to analyse the interfacial region and the formation of surface aggregates via force-distance curves and deflection images in soft-contact mode.

3.4.3.1 Proposed Mechanism for the Adsorption of Ionic Surfactant at a Graphite Surface

The presence of surface aggregates at a graphite surface has been confirmed by AFM deflection images by the appearance of a regular pattern with periodic, parallel stripes.[48–52] A mechanism for its evolution was proposed: a flat monolayer of surfactant adsorbs at the graphite surface with the alkyl chains epitaxically arranged along one of the three graphite symmetry axes (Fig. 3.4.3-1-A). At sufficiently high surfactant concentrations, hemimicellar shapes can form (Fig. 3.4.3-1-B), which infinitely spread along the surface as hemicylindrical aggregates (Fig. 3.4.3-1-C).

In general, there are two main driving forces guiding the adsorption of a monolayer: (1) minimization of the interfacial area between hydrophobic graphite and the polar regions of solvent and surfactant; (2) a strong specific interaction between the crystalline structure of graphite and the alkyl chains of the surfactant molecules.[54]

Indeed, Zettlemoyer proposed a surface model according to which amphiphilic molecules assemble evenly on a water-graphite surface.[55] It is supported by the fact that the change in enthalpy for this adsorption in water was found to be -15 k_BT per molecule, whereas the change in free energy, additionally accounting for an entropic contribution, for micellation in aqueous solution is -8 k_BT per molecule and hence the adsorption is energetically favoured.[46,48] The epitaxial alignment of the alkyl chains parallel to one of the symmetry axes of graphite results from the graphite anisotropic structure, where carbon atoms are arranged in two-dimensional graphene layers in a honeycomb lattice. Hydrogen atoms attached to the alkyl chains of the adsorbent were found to match the hexagon centres of this lattice, when the alkyl chains are located in parallel orientation.[56] The special head-to-head (synonymously tail-to-tail) arrangement of the surfactants templates the formation of the hemimicellar aggregates.[57] A low degree of dissociation and the presence of additional electrolyte from the solvent reduce the effective charge and hence the head group repulsion.[58]

In an early model, the adsorbate density was believed to increase with surfactant concentration, due to the gradual desorption of the two-dimensionally adsorbed alkyl chains and their orientation perpendicular to the substrate.[55] However, this theory was disproved by AFM images, showing the presence of regular adsorption patterns. As a consequence, the formation of surfactant hemimicelles was suggested.[48]

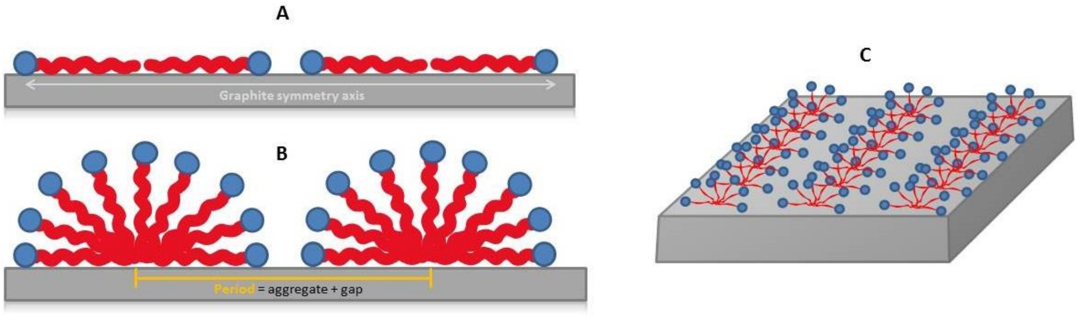

Fig. 3.4.3-1: Scheme of the proposed mechanism for the formation of surfactant surface aggregates on graphite consisting of the adsorption of a flat surfactant monolayer (A), the formation of hemimicellar aggregates (B), which infinitely spread along the graphite surface in form of hemicylindrical aggregates (C).

3.4.3.2 Atomic Force Microscopy – Force-Distance Curves

Fig. 3.4.3-2 shows the force distance curve recorded for the system (ChCl-Gly) + CTAB (2.5 mM) at neutral surface potential. Its shape is similar to the curve obtained for pure ChCl-Gly, with an identical thickness of the nearest surface layers. The force jumps appeared over a wider distance, *i.e.* were less vertical, which is ascribed to a higher compressibility of the layers. The curve does not exhibit features typical for the presence of aggregates. As the presence of surface aggregates was confirmed by AFM images, it is assumed that the aggregate layer covering the graphite surface cannot be penetrated by the AFM tip. The corresponding force curves of (ChCl-EG) + SDS and (ChCl-Gly) + SDS are given in Fig. 6.4.2-1 and Fig. 6.4.2-2 in section 6.4.2 of the appendix, respectively.

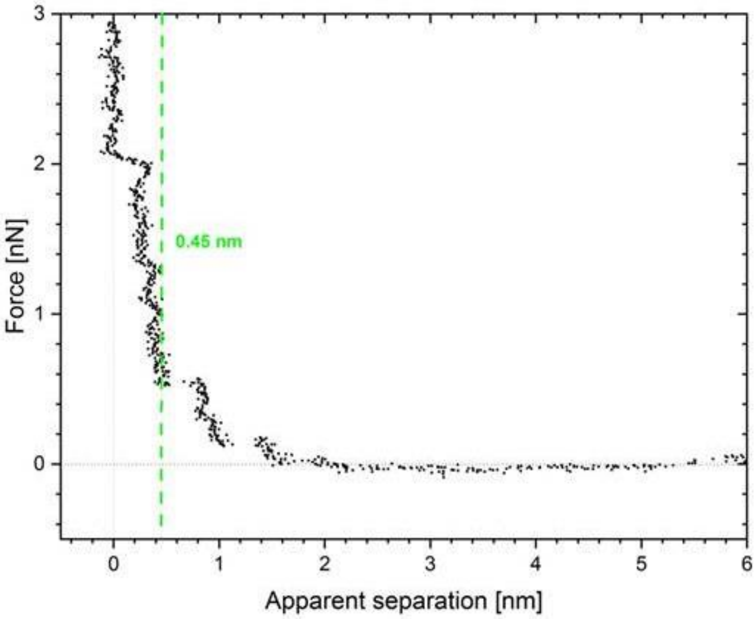

Fig. 3.4.3-2: Force-distance curve (normal force as a function of apparent separation) upon the AFM tip approaching the electrically neutral HOPG surface in a solution of CTAB (2.5 mM) in ChCl-Gly. The apparent nearest surface layer has a thickness of 0.45 nm. It is marked with a green, dashed line.

On extremely rare occasions, force-distance curves in a shape characteristic of surface aggregates could be recorded (Fig. 3.4.3-3), in which the AFM tip was subject to a jump-in from a distance of approximately 2 nm. This was in approximate agreement with the expected length of a CTAB molecule and the respective height of a hemimicelle.[48,59] In addition to the aggregate feature, less distinct force steps were observed corresponding to the nanostructured liquid layers of ChCl-Gly on top of the aggregate layer. The thickness of the first liquid layer of the DES solvent was only 0.35 nm, *i.e.,* thinner compared to the usual apparent nearest surface layer. It matches the ion diameter of chloride ions and is therefore ascribed to a liquid layer rich in chloride.[60] This layer was followed by further liquid DES layers apparent in the normal forces-distance curves.

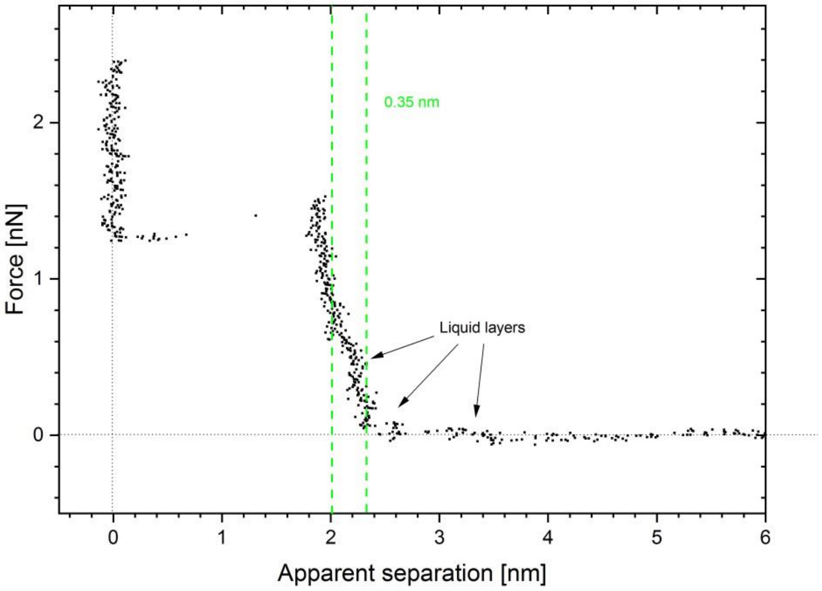

Fig. 3.4.3-3: Force-distance curve (normal force as a function of apparent separation) upon the AFM tip approaching the HOPG surface in a solution of CTAB (2.5 mM) in ChCl-Gly at a potential of -0.75 V. The shape of the curve is typical for the presence of surface aggregates. The first liquid layer of DES has a thickness of 0.35 nm and is marked with a green, dashed line.

Apart from these exceptional cases, the force-distance curves recorded for DES-graphite interfaces in the presence of surfactants strongly resembled those obtained for pure DESs at a graphite interface. They revealed information on the nanostructured surrounding of the self-assembled surfactants, but were not suitable for analysing the behaviour of the surface aggregates.

3.4.3.3 Atomic Force Microscopy – Deflection Images

AFM deflection images delivered valuable information on the aggregation behaviour of ionic surfactants at a DES-graphite interface. They were recorded when scanning the surface in soft-contact mode. The tip was placed at a constant distance from the surface, so that it was not in physical contact with the hard surface. Instead, it was in a pre-contact region a few nanometres above, allowing for sensing of aggregates.

AFM deflection images recorded at a (ChCl-Gly)-graphite interface in the presence of SDS or CTAB in the solvent are illustrated in Fig. 3.4.3-4. Likewise, AFM deflection images recorded at a (ChCl-EG)-graphite interface for solubilized SDS at different concentrations are shown in Fig. 3.4.3-5. Two parameters are used to characterize the images and the corresponding aggregation behaviour of the surfactants: (1) the so-called aggregation period taking into account the aggregation size and the inter-aggregation separation, and (2) the deflection height scale, which corresponds to the depth, *i.e.*, height of the surface features normal to the solid surface.

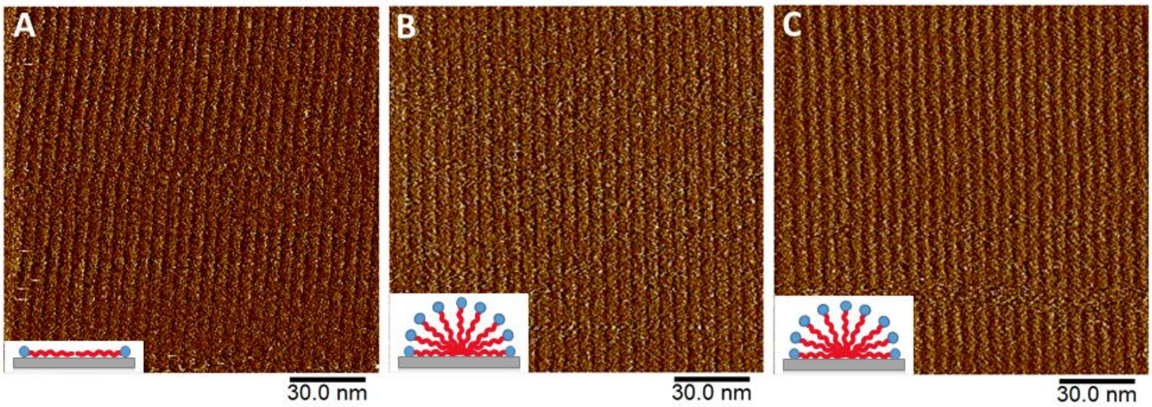

Fig. 3.4.3-4: AFM deflection images showing adsorbed surfactant aggregates at the (ChCl-Gly)-graphite interface with indicated shape of surfactant. Image A was recorded for a 21 mM SDS solution, its height scale is 0.5 nm. Image B was recorded for a 2.5 mM CTAB solution, its height scale is 1.0 nm. Image C was recorded for a 21 mM CTAB solution, its height scale is 0.85 nm.

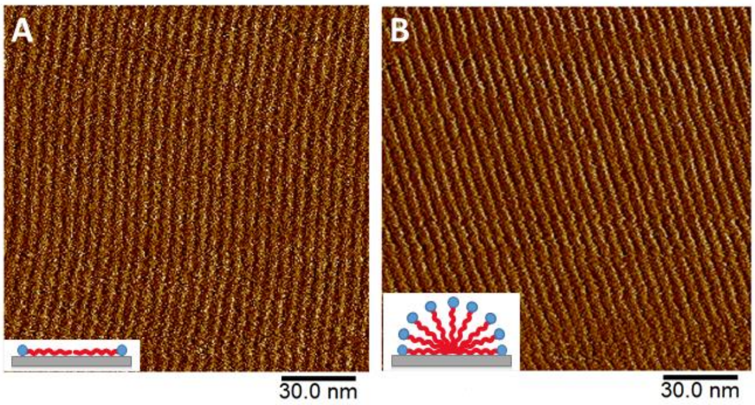

Fig. 3.4.3-5: AFM deflection images showing adsorbed SDS aggregates at the (ChCl-EG)-graphite interface with indicated shape of surfactant. Image A was recorded for a 25 mM SDS solution, its height scale is 0.3 nm. Image B was recorded for a 132 mM SDS solution, its height scale is 1.0 nm.

At a first glance, the images in Fig. 3.4.3-4 and Fig. 3.4.3-5 appear similar. However, a closer look at the parameters mentioned above allows for a differentiation. An overview of the extracted parameters and the data for aqueous solutions reported in the literature is presented in Tab. 3.4.3-1. In aqueous solution, the aggregation period was found to decrease with increasing surfactant concentrations until a constant minimum value was reached. The addition of an electrolyte reduced the aggregation period for low surfactant concentrations, but had no influence for high surfactant concentrations.[50,52] For systems 2 and 3, as well as systems 4 and 5, respectively (see Tab. 3.4.3-1), the aggregation period of the surfactants adsorbed on a DES-graphite interface were found to be not influenced by the surfactant concentration. They were in the range, where a minimum value had been reached. Solubilizing both surfactants in ChCl-Gly, SDS formed aggregates characterized by a smaller aggregation period compared to CTAB (see systems 1, 2 and 3 in Tab. 3.4.3-1). This is ascribed to the longer alkyl chain of CTAB.

Considering the height scales of the recorded AFM deflection images, clear deviations were observable. Systems containing SDS at concentrations below 25 mM were found to form surface assemblies of lower height, compared to the other studied systems. Findings of this kind, however, have to be treated with caution. Besides the morphology of the aggregation layer, further factors are likely to influence the apparent vertical height of the studied surface features. The ability of the AFM tip to access the narrow gap between the aggregates is affected by the individual elasticity of the cantilever and the normal force that is set to the tip arbitrarily, when operating in soft-contact mode. As the results were reproducible and a clear trend was identified, SDS at concentrations below 25 mM is suggested to be unable to form full aggregates. Instead, the surface is proposed to be covered by a monolayer of SDS molecules arranged in head-to-head orientation or loosely packed, less dense aggregates. However, these results require further clarification by additional methods.

Tab. 3.4.3-1: Height scale of the presented AFM deflection images and aggregation period determined from power spectral density (PSD) analysis of the AFM deflection images for the studied surfactant solutions at a graphite interface.

System No.	Solvent	Surfactant	Conc. [mM]	Period [nm]	Height scale [nm]
1	ChCl-Gly	SDS	21	5.2	0.5
2	ChCl-Gly	CTAB	2.5	5.5	1.0
3	ChCl-Gly	CTAB	21	5.5	0.85
4	ChCl-EG	SDS	25	5.0	0.3
5	ChCl-EG	SDS	132	5.0	1.0
6	Water	SDS	2.8	7.0[50]	-
7	Water	SDS	>20	5.3[50]	-
8	Water	CTAB	1.8	9.1[51]	-
9	Water	CTAB	5.0	4.2[48]	-

3.4.4 Influence of Electric Surface Potential on the Aggregation Behaviour of Surfactants at a Deep Eutectic Solvent-Graphite Interface

The adsorption and aggregation behaviour of ionic surfactants at the DES-graphite interface upon the application of an electric potential to the graphite surface was studied. Images and force-distance curves were recorded at open-circuit potential (OCP), ±0.5 V and ±0.75 V. Interestingly enough, upon applying surface potentials, shapes of the recorded force-distance curves did not remarkably differentiate from those obtained for pure solvent upon visual inspection (see Fig. 6.4.3-1 and Fig. 6.4.3-2 in section 6.4.3 of the appendix). At the same time, a quantitative analysis of AFM images revealed valuable results. As to be inferred from the periodic striped pattern of the recorded images, the cationic surfactant CTAB solubilized in ChCl-Gly adsorbed to graphite at negative, neutral and positive potential (see Fig. 3.4.4-1). On the contrary, no regular pattern in the AFM images at negative potential was obtained for SDS solubilized in ChCl-EG (see Fig. 3.4.4-2).

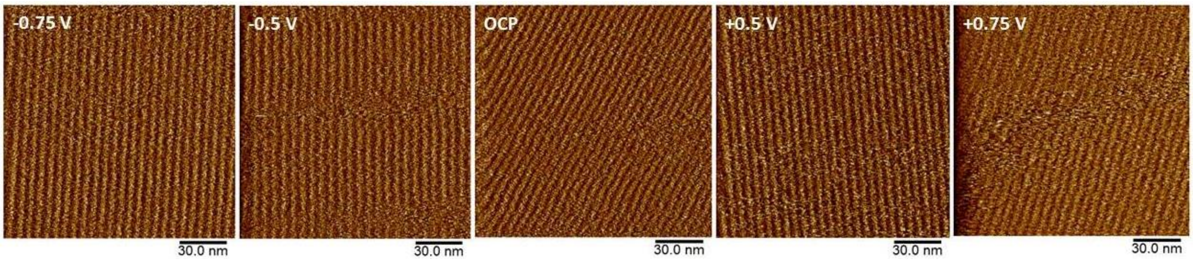

Fig. 3.4.4-1: AFM deflection images of adsorbed CTAB aggregates at the (ChCl-Gly)-graphite interface as a function of electric surface potential.

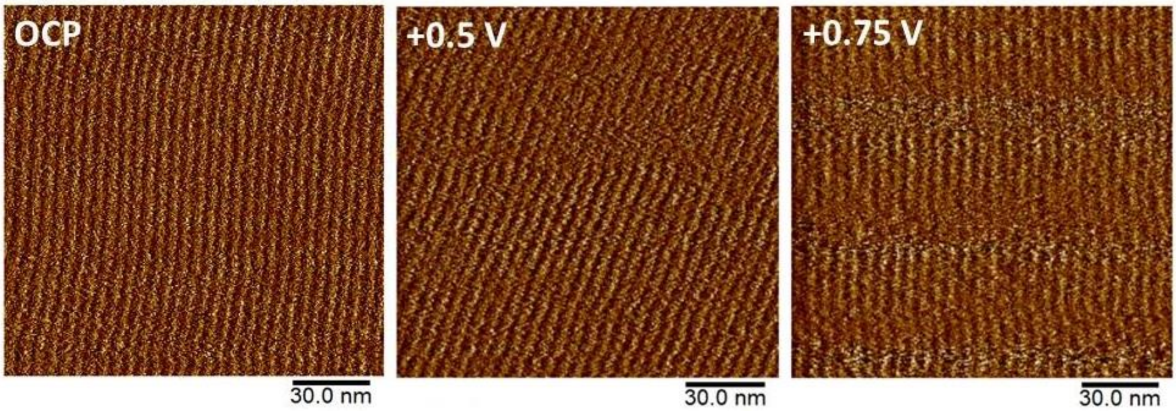

Fig. 3.4.4-2: AFM deflection images of an adsorbed SDS monolayer at the (ChCl-EG)-graphite interface as a function of electric surface potential.

The fact that CTAB with its positively charged head group adsorbed to graphite even at positive surface potential illustrates the strength of the hydrophobic interactions between the hydrocarbon chains of the surfactant and graphite. It apparently outweighs the electrostatic repulsion between the charged head group and the charged surface. Furthermore, electrostatic interactions in DESs are suggested to be only of short-range nature due to the high ionic strength of the solvent and its extraordinary ability to screen charges. On the other hand, the electrostatic repulsion of SDS caused by the application of negative surface potential overcame the hydrophobic attraction. Accordingly, no adsorption was observed in this case. This is probably due to less pronounced van der Waals interactions of the shorter C_{12} alkyl chain (SDS) compared to the C_{16} alkyl chain (CTAB).

AFM results in terms of the aggregate period as a function of surface potential are summarized in Tab. 3.4.4-1. When applying negative potential to the system comprising DES and CTAB and *vice versa,* when applying a positive potential to the system comprising DES and SDS, an increase in the aggregation period was observed. Apparently, the counter-ions surrounding the surfactant head groups are repelled from the surface so that charge screening is reduced. Simultaneously, ions with charges opposite to the surface and equal to the surfactant are attracted, so that repulsion between the surfactants is increased. This induces an increasing inter-aggregate separation.

Tab. 3.4.4-1: Aggregation periods determined from PSD analysis of the AFM deflection images in the presence of an applied electric surface potential.

System	-0.75 V	-0.5 V	OCP	+0.5 V	+0.75 V
(ChCl-Gly) + CTAB (2.5 mM)	6.0 nm	6.0 nm	5.5 nm	5.6 nm	5.6 nm
(ChCl-EG) + SDS (25 mM)	x	x	5.0 nm	5.5 nm	5.5 nm

3.4.5 Summary of the Results Obtained from the Atomic Force Microscopy Study of the Deep Eutectic Solvent-Graphite Interface

This study presented the formation of surface aggregates of SDS and CTAB at DES-graphite interfaces. The initial driving force for adsorption is attributed to strong van der Waals interactions between the hydrophobic graphite surface and the respective hydrophobic surfactant tails. Charge screening between the surfactant head groups is promoted by the ionic DES medium.

CTAB was shown to adsorb in form of hemimicelles at relatively low concentrations (2.5 mM), while SDS requires significantly higher concentrations (≫25mM) for this effect to occur. SDS is adsorbed to graphite in form of a head-to-head monolayer at concentrations below 25 mM.

Upon applying a surface potential to the graphite surface, CTAB remains attached at the screened potentials (OCP, ±0.5 V, ±0.75 V). In contrast, SDS is repelled from the surface at negative potentials. This finding led to the assumption that the van der Waals interactions of the C_{12} alkyl chain of SDS are weaker compared to those of the CTAB C_{16} chain. Consequently, electrostatic interactions can overcome the van der Waals interactions of a C_{12} alkyl chain with graphite, thereby determining the overall system behaviour.

3.5 Conclusion

This chapter addressed the development of novel DESs. Their thermal phase behaviour and potential applications for solubilizing melanin and as ephemeral solvents were evaluated. The behaviour of surfactant-DES solutions at the graphite interface was examined in order to extend the fundamental knowledge and the range of applicability of DESs in electrochemical processes.

In general, several characteristics of DESs imparted substantial difficulty and inconvenience on the handling of these substances. In particular, they are highly viscous and sticky in the majority of cases. Sometimes they are even solid at room temperature requiring a usage at elevated temperatures. Due to their strongly hygroscopic behaviour, they are to be treated preferably at air-free environment, *e.g.* nitrogen atmosphere, in order to avoid water uptake from the air.

While choline chloride-based DESs have been extensively studied in literature, herein, the structurally related betaine- and carnitine-based DESs were examined in combination with several organic acids, urea, glycerol, ethylene glycol and *D*-fructose. Three different types of betaine and carnitine compounds were investigated.

(1) The zwitterions betaine and carnitine formed DES with some particular HBDs, whereas most of them were liquid at room temperature. However, starting materials were used without drying. Therefore, the resulting DESs might contain considerable amounts of water.
(2) Betaine hydrochloride and carnitine hydrochloride were combined with the respective HBDs. Only in two cases of the conducted screening, this resulted in the formation of homogenous liquids in the measured temperature range up to 90 °C.
(3) The bromide salts of betaine and carnitine alkyl esters formed liquid mixtures with a strikingly large variety of HBDs.

This led to the conclusion of melting point depression in the formation of DESs being not only controlled by the formation of H-bonds, but also by the size of the involved HBA and the capability of proton exchange between HBA and HBD. In fact, this proton exchange was found to impart a certain IL character to the respective mixtures of the zwitterionic HBAs with carboxylic acid HBDs. Some of the prepared betaine- and carnitine-based DESs were employed as solubilization medium for the natural biopolymer pigment melanin. However, their performance was not comparable to amine-based solvents. Consequently, the evaluated DESs are considered to have no prospect as media for the solubilization of melanin.

A special type of DES with antioxidant activity implementing biologically relevant HBDs, mainly natural phenolic acids was established. They were shown to form liquid homogeneous mixtures with choline chloride at elevated temperature. In order to further decrease the thermal phase transition temperature, a second HBD, in particular urea or *D*-fructose, was incorporated into the DES. Thereupon, gallic acid-based DESs, liquid at room temperature, were prepared in various compositions. The application of the latter as ephemeral solvents for the esterification of the respective biologically relevant HBD was evaluated. The presence of a DES did not convey any considerable advantage in the esterification of gallic acid. The formation of chlorogenic acid within a DES containing choline chloride, caffeic acid and quinic acid was not further investigated, after the observation of considerable degradation of the incorporated compounds. Finally, the esterification of shikimic acid ethyl ester in a ChCl-ShiA DES was confirmed by NMR. In general, DESs containing constituents with antioxidant activity, are expected to exhibit antioxidant properties. Therefore, they might be interesting as ingredients in chemical formulations, such as in cosmetics or food industry, as the implementation of further additional ingredients can be avoided.

For the first time, the behaviour of surfactants at a DES-electrode interface has been studied by means of AFM force-distance curves and deflection images. The presence of nanostructured DES layers at the graphite surface, which had been reported before, could be confirmed. In the presence of an ionic surfactant, in particular SDS and CTAB, parallel stripes formed by a surfactant monolayer arranged in head-to-head orientation or infinitely elongated hemimicelles were observed. SDS was found to form monolayers at low concentration and to require higher concentrations for the formation of hemimicellar aggregates. In contrast, CTAB assembled into hemimicelles even at low concentrations. Comparable surface structures have been observed in water and IL media, before. The aggregation period corresponding to the aggregate size and the inter-aggregate separation is a characteristic measure and varied depending on the type of solvent, type of surfactant and the surface electric potential. Finally, the general driving force for the formation of these surface aggregates was concluded to be a strong attractive hydrophobic interaction between the hydrophobic graphite surface and the hydrocarbon chain of the surfactants. Due to electrostatic repulsion, SDS surfactants were released from the surface, when negative electric potential was applied. In contrast, strong van der Waals interactions due to CTAB's C_{16} alkyl chain were able to outweigh the electrostatic repulsion even at positive electric surface potential. These investigations are intended to deliver further knowledge on the applicability of DESs as solvents for electrochemistry.

Finally, it should be noted that the all-encompassing approach in this study was not ideal. Having at hand novel DESs, it is not readily apparent to identify suitable applications. Rather, it makes sense to approach this issue from the other direction and develop DESs for a particularly required application and leave the real application tests to the designated specialists, as they are in a better position to evaluate, where and if a DES is able to deliver benefits for a certain application. A research chemist in this field can play an interesting role by examining fundamental parameters of a great variety of DESs and providing the respective data and characteristic properties of interest to a more application-focused audience in a way so that it is available, and more importantly useful, for application chemists, e.g. in form of a powerful data base. The conductor-like screening model for realistic solvation (COSMO-RS) might be a useful tool for predicting the behaviour of DESs. It is believed that a computer-assisted working mode can help to prevent the waste of resources, money, time and research effort in order to provide a more efficient approach towards developing applications for DESs as green solvents.

3.6 Experimental

3.6.1 Chemicals

Tab. 3.6.1-1: Chemicals used in this chapter, their purity, their supplier and the sections they are relevant for.

	Purity	**Supplier**	**Used in Section**
ChCl	≥98 %	Sigma Aldrich	3.3, 3.4
L-Carnitine	99 %	Alfa Aesar	3.2, 3.3.2
Betaine	98 %	Alfa Aesar	3.2
CarHCl	>98 %	Alfa Aesar	3.2
BetHCl	99 %	Sigma Aldrich	3.2
AChCl	>98 %	TCI Europe	3.2
Urea	≥99.5 %	Merck	3.2, 3.3
EG	≥99.8 %	Sigma Aldrich	3.2, 3.4
Gly	≥99 %	Sigma Aldrich	3.2, 3.4
GA	≥98 %	Merck	3.3
LA	98 %	Alfa Aesar	3.2, 3.3.2
D-Fru	≥99 %	Merck	3.2, 3.3.2
MA	≥99 %	Merck	3.2
MaleA	≥99 %	Sigma Aldrich	3.2
LaA	98 %	Alfa Aesar	3.2
GlA	99 %	Merck	3.2
CA	>98 %	TCI Europe	3.3
QA	98 %	Alfa Aesar	3.3
ShiA	≥97 %	TCI Europe	3.3
EtOH	absolute	Labochem International	3.3.3
BuOH	≥99 %	Merck	3.3.3
OctOH	≥99 %	Merck	3.3.3
Amb15		Sigma Aldrich	3.3.3
H_2SO_4 (conc.)	97 %	Merck	3.3.3
Melanin		Provided by L'Oréal	3.2.4
SDS	>99 %	Merck	3.4
CTAB	>99 %	Fluka	3.4

If not stated otherwise, the starting materials for the preparation of the DESs prepared for thermal characterization were dried under high vacuum and stored in a glove box under nitrogen atmosphere.

3.6.2 Synthesis of Betaine- and Carnitine-Based Alkyl Esters

Carnitine alkyl ester compounds, herein referred to as [C_nCar]Br, were prepared according to the reaction scheme in Fig. 2.2.1-1 in section 2.2.1.1.

Betaine ethyl ester compounds, herein referred to as [C_nBet]Br, were synthesized analogously to the carnitine ester in one step using betaine and alkyl bromide as starting material (see Fig. 3.6.2-1).[61] Betaine (1 eq.) was combined with alkyl bromide (1.5 eq.) in acetonitrile under nitrogen atmosphere. The reaction mixture was stirred under reflux for at least 12 h. After evaporation of the solvent, the crude product was washed several times with diethyl ether and dried under vacuum. Betaine alkyl ester bromides were obtained in yields above 90 %. The purity of the products was assessed by NMR analysis.

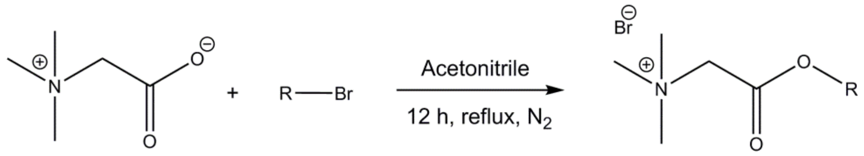

Fig. 3.6.2-1: One-step synthesis of betaine alkyl ester bromide [C_nBet]Br.

3.6.3 Preparation of Deep Eutectic Solvents

Two different techniques were used for the preparation of the studied DESs:

(1) The corresponding amounts of starting compounds were combined in hermetically sealable glass vials within a glovebox. The overall amount of each sample was approximately 1.5 g. They were heated under stirring until a homogeneous solution was visually observable. This method was used for the DESs to be characterized thermally.
(2) The corresponding amounts of starting compounds were combined in a round bottom flask or another glass vial. They were heated under stirring until a homogeneous solution was visually observable. The resulting solvents were dried after the preparation, if this was required for the corresponding application.

The first method delivered DESs with less water contamination. The former method was used for the preparation of the DESs meant to be characterized thermally, as therefore the purity of the DES is highly important. The latter approach was used for application-based studies.

The heating temperature and duration required for the formation of the DESs depended on the respective starting compounds. Several mixtures formed within an hour at 50 °C, others were heated to 90 °C for more than one day.

3.6.4 Differential Scanning Calorimetry

The measuring system and sample preparation was equal to the description in section 2.6.5.1. The samples were measured in a temperature cycle from (1) 25 °C to 100 °C, (2) 100 °C to -60 °C and (3) -60 °C to 100 °C under nitrogen atmosphere.

Thermal transitions, as obtained from DSC, were categorized as melting point T_m, glass transition T_g or undefined transition (undef.). The temperature corresponding to the onset of an endothermic peak during heating was associated with the melting temperature T_m. The temperature corresponding to the midpoint of a small endothermic heat capacity jump was taken as glass transition temperature T_g. When the occurring peak could neither be classified as melting point nor glass transition temperature, it was classified as 'undefined' and temperatures corresponding to the maximum of the peak are indicated as the phase transition temperatures.

3.6.5 Karl-Fischer Coulometry

The water content was determined according to the procedure described in section 2.6.4.

3.6.6 Atomic Force Microscopy

AFM force measurements and imaging were performed using a Nanoscope IV multimode atomic force microscope (Bruker Instruments) in contact mode. The setup consisted of a standard silicon tip (NSC36, MikroMasch) with a radius of 32.5 nm and a spring constant between 0.2 and 0.8 N/m, a polytetrafluoroethylene (PTFE) O-ring and an AFM liquid cell. The 10x10x2 mm HOPG surface of ZYB quality was supplied by TipsNano with a mosaic spread of 0.8 ± 0.2°. Prior to use, the tip was rinsed with Millipore water and ethanol (analytical grade), dried and applied to a UV-ozon cleaner for at least 20 minutes. The graphite surface was prepared by cleaving the top layer with adhesive tape. An Autolab potentiostat was used to apply potential to the graphite surface. Each system was evaluated at open-circuit potential (OCP), OCP±0.5 V and OCP±0.75 V. Before each measurement, the system was allowed to reach equilibrium for at least 10 min. Force curves were detected at a scan rate of 0.2 Hz and a ramp size of 30 nm. The presented force curves are chosen from a pool of more than 75 curves recorded over several days representing the mean number of force steps and the mean push-through force. Deflection images of the aggregates were taken in soft contact mode without physical contact between the surface and the tip by setting the deflection setpoint to a precontact region when scanning the surface.[48,62] Scanning angles were varied to ensure the validity of the observed images. Imaging was repeated to assure reproducibility. All measurements were conducted at room temperature of 22±1 °C.

The spacing of the apparent periodic surface features was determined by power spectral density (PSD) analysis using the Bruker NanoScope Analysis software. Measuring periods of images with scanning angle not perpendicular to the aggregate symmetry axis, results in considerable errors. Therefore, only images with deviations below ±5° from perpendicular were analysed. The values for the aggregate period given in this work represent the average of at least 3 measured values. The respective errors were below 0.1 nm.

3.6.7 Procedure for the Solubilization of Melanin

The DESs were prepared according to the procedure outlined in section 3.6.3, point (2). Their water content was determined and adjusted to 25 wt% by the addition of Millipore water. The preparation of the melanin solutions was conducted at 40 °C to ensure adequate fluidity and avoid errors caused by unevenly emulsified melanin. A standard melanin solution of 30 g/L in a DES volume of 3 ml was prepared. Further solutions with concentrations at 15 g/L, 10 g/L and 5 g/L were produced by diluting the standard solution. These solutions were stirred at 40 °C in sealed glass tubes for 15 h. Subsequently, the non-dissolved melanin residues were separated by centrifugation with a SIGMA 2-16 PK device for 20 min at 3000 rpm. The resulting melanin-DES solutions were analysed by means of an Agilent Technologies Varian Cary 60 UV/Vis spectrometer. The absorbance at a wavelength of 500 nm was plotted against the initial melanin concentration. The slope a was extracted from the corresponding linear fits to calculate the solubility fraction f as:

$$f = \frac{a}{12} \tag{4}$$

The factor 1/12 takes into account the respective slope obtained from the same experiment with ethanolamine. Accordingly, the solubility factor f describes the solubility of melanin in a medium relative to the reference substance ethanolamine.

3.6.8 Solubilization of *n*-Alkyl Alcohols

The solubility of butanol and octanol in DESs was examined by the stepwise addition of the respective alcohol. The solutions were subsequently heated to 90 °C and 70 °C, respectively, for DES containing urea and *D*-fructose. The respective amount of alcohol was considered soluble, if the solution appeared as homogeneous liquid.

3.6.9 Synthesis of Gallic Acid Alkyl Ester

The DESs were prepared in a total sample size of approximately 2 g by mixing the components in the respective molar ratio under nitrogen atmosphere and stirring them at at least 80 °C until a homogeneous liquid is visually observable. The reaction was started by the addition of an *n*-alcohol in equimolar amount to gallic acid. For each system, three samples were tested: one without catalyst, one with 10 wt% Amberlyst 15 and one with 50 µl H_2SO_4 (conc.) as acid catalyst. The reaction mixture was stirred for 20 h at 80 °C. The reaction was stopped by cooling. HPLC was used to analyse the samples.

3.6.10 High Performance Liquid Chromatography (HPLC)

The individual constituents of a DES reaction mixture were determined by means of a Waters HPLC system including a Waters 515 HPLC pump, a Waters 717 plus autosampler, a Waters 2487 UV/Vis detector and the Waters Empower 3 software. A Knauer Eurosphere C18-column (100 Å, 250 x 4.6 mm) served as HPLC column. The HPLC system was operated at 30 °C and a flow rate of 0.5 ml/min. HPLC samples were prepared by diluting 5 to 50 mg of the reference or a DES in 5 ml methanol. Thereof, 10 µl were injected to the HPLC system. The resulting chromatograms show the absorbance at 280 nm as a function of the retention time. The relative conversion of the studied reaction mixture was calculated by integration of the characteristic, separated educt and product peaks.

3.7 References

[1] a) W. Bi, M. Tian, K. H. Row, *J. Chromatogr. A* **2013**, *1285*, 22–30; b) H. E. Park, B. Tang, K. H. Row, *Anal. Lett.* **2014**, *47*, 1476–1484; c) Z.-F. Wei, X.-Q. Wang, X. Peng, W. Wang, C.-J. Zhao, Y.-G. Zu, Y.-J. Fu, *Ind. Crops Prod.* **2015**, *63*, 175–181; d) B. D. Ribeiro, M. A. Z. Coelho, I. M. Marrucho, *Eur. Food Res. Technol.* **2013**, *237*, 965–975;

[2] E. L. Smith, A. P. Abbott, K. S. Ryder, *Chem.Rev.* **2014**, *114*, 11060–11082.

[3] R. Vittal, H. Gomathi, K.-J. Kim, *Adv. Colloid Interface Sci.* **2006**, *119*, 55–68.

[4] Y. Dai, J. van Spronsen, G.-J. Witkamp, R. Verpoorte, Y. H. Choi, *Anal. Chim. Acta* **2013**, *766*, 61–68.

[5] S. Bajkacz, J. Adamek, *Food Anal. Methods* **2018**, *11*, 1330–1344.

[6] V. Fischer, doctoral thesis, Universität Regensburg, Regensburg, **2015**.

[7] K. Zhang, S. Ren, Y. Hou, W. Wu, *J. Hazard. Mater.* **2017**, *324*, 457–463.

[8] F. Ilgen, B. König, *Green Chem.* **2009**, *11*, 848–854.

[9] C. Yao, Y. Hou, S. Ren, Y. Ji, W. Wu, *Fluid Phase Equilib.* **2017**, *448*, 116–122.

[10] X. Meng, K. Ballerat-Busserolles, P. Husson, J.-M. Andanson, *New J. Chem.* **2016**, *40*, 4492–4499.

[11] W. M. Haynes, D. R. Lide (Eds.) *CRC handbook of chemistry and physics. A ready-reference book of chemical and physical data,* 91. ed., CRC Press, Boca Raton, **2010**.

[12] M. Hesse, H. Meier, B. Zeeh, S. Bienz, L. Bigler, T. Fox, *Spektroskopische Methoden in der organischen Chemie,* 9., überarbeitete und erweiterte Auflage ed., Georg Thieme Verlag, Stuttgart, New York, **2016**.

[13] Y. Wei, A. E. McDermott in *ACS Symposium Series* (Eds.: J. C. Facelli, A. C. de Dios), ACS, Washington, DC, **1999**.

[14] B. Bernet, A. Vasella, *HCA* **2000**, *83*, 995–1021.

[15] J. D. Simon, L. Hong, D. N. Peles, *J. Phys. Chem. B* **2008**, *112*, 13201–13217.

[16] S. Ito, *Biochim. Biophys. Acta* **1986**, *883*, 155–161.

[17] M. Sova, *Mini-Rev. Med. Chem.* **2012**, *12*, 749–767.

[18] M. N. Clifford, *J. Sci. Food Agric.* **1999**, *79*, 362–372.

[19] a) S. Abrecht, M. C. Federspiel, H. Estermann, R. Fischer, M. Karpf, H.-J. Mair, T. Oberhauser, G. Rimmler, R. Trussardi, U. Zutter, *CHIMIA* **2007**, *61*, 93–99; b) C. J. Besset, A. T. Lonnecker, J. M. Streff, K. L. Wooley, *Biomacromolecules* **2011**, *12*, 2512–2517; c) E. Padmini, L. Inbathamizh, *Asian J. Pharm. Clin. Res.* **2013**, *6*, 106–112.

[20] V. Fischer, D. Touraud, W. Kunz, *Sust. Chem. Pharm.* **2016**, *4*, 40–45.

[21] Z. Maugeri, P. Domínguez de María, *RSC Adv.* **2012**, *2*, 421–425.

[22] a) A. P. Abbott, G. Capper, D. L. Davies, R. K. Rasheed, V. Tambyrajah, *Chem. Commun.* **2003**, 70–71; b) A. Hayyan, F. S. Mjalli, I. M. AlNashef, T. Al-Wahaibi, Y. M. Al-Wahaibi, M. A. Hashim, *Thermochim. Acta* **2012**, *541*, 70–75.

[23] I. M. Aroso, A. Paiva, R. L. Reis, A. R. C. Duarte, *J. Mol. Liq.* **2017**, *241*, 654–661.

[24] S. Choubey, L. R. Varughese, V. Kumar, V. Beniwal, *Pharm. Pat. Anal.* **2015**, *4*, 305–315.

[25] I. Kubo, N. Masuoka, T. Joung Ha, K. Shimizu, K.-i. Nihei, *Open Bioact. Compd. J.* **2010**, *3*, 1–11.

[26] P. A. Tuan, D. Y. Kwon, S. Lee, M. V. Arasu, N. A. Al-Dhabi, N. I. Park, S. U. Park, *nt. J. Mol. Sci.* **2014**, *15*, 14743–14752.

[27] M. Karpf, R. Trussardi, *Angew. Chem. Int. Ed.* **2009**, *48*, 5760–5762.

[28] G. R.T. Jenkin, A. Z.M. Al-Bassam, R. C. Harris, A. P. Abbott, D. J. Smith, D. A. Holwell, R. J. Chapman, C. J. Stanley, *Miner. Eng.* **2016**, *87*, 18–24.

[29] W. O. Karim, A. P. Abbott, S. Cihangir, K. S. Ryder, *Trans. IMF* **2018**, *96*, 200–205.

[30] a) A. P. Abbott, K. S. Ryder, U. König, *Trans. IMF* **2008**, *86*, 196–204; b) A. P. Abbott, K. El Ttaib, G. Frisch, K. J. McKenzie, K. S. Ryder, *PCCP* **2009**, *11*, 4269–4277.

[31] a) B. Xuân, *Ionic Liquids*, Nova Science Publishers Incorporated, Hauppauge, **2017**; b) Q. Li, J. Jiang, G. Li, W. Zhao, X. Zhao, T. Mu, *Sci. China Chem.* **2016**, *59*, 571–577.

[32] a) F. Endres, N. Borisenko, S. Z. El Abedin, R. Hayes, R. Atkin, *Faraday Discuss.* **2012**, *154*, 221–233; b) R. Hayes, N. Borisenko, B. Corr, G. B. Webber, F. Endres, R. Atkin, *Chem. Comm.* **2012**, *48*, 10246–10248; c) S. Maolin, Z. Fuchun, W. Guozhong, F. Haiping, W. Chunlei, C. Shimou, Z. Yi, H. Jun, *J. Chem. Phys.* **2008**, *128*, 134504-1–7; d) B. McLean, H. Li, R. Stefanovic, R. J. Wood, G. B. Webber, K. Ueno, M. Watanabe, G. G. Warr, A. Page, R. Atkin, *PCCP* **2015**, *17*, 325–333; e) M. Mezger, H. Schröder, H. Reichert, S. Schramm, J. S. Okasinski, S. Schöder, V. Honkimäki, M. Deutsch, B. M. Ocko, J. Ralston et al., *Science* **2008**, *322*, 424–428; f) O. Werzer, E. D. Cranston, G. G. Warr, R. Atkin, M. W. Rutland, *PCCP* **2012**, *14*, 5147–5152.

[33] R. Hayes, N. Borisenko, M. K. Tam, P. C. Howlett, F. Endres, R. Atkin, *J. Phys. Chem. C* **2011**, *115*, 6855–6863.

[34] H. Li, F. Endres, R. Atkin, *PCCP* **2013**, *15*, 14624–14633.

[35] Z. Chen, M. Ludwig, G. G. Warr, R. Atkin, *J. Colloid Interface Sci.* **2017**, *494*, 373–379.

[36] Z. Chen, B. McLean, M. Ludwig, R. Stefanovic, G. G. Warr, G. B. Webber, A. J. Page, R. Atkin, *J. Phys. Chem. C* **2016**, *120*, 2225–2233.

[37] O. S. Hammond, H. Li, C. Westermann, A. Y. M. Al-Murshedi, F. Endres, A. P. Abbott, G. G. Warr, K. J. Edler, R. Atkin, *Nanoscale Horiz.* **2019**, *4*, 158–168.

[38] a) R. Atkin, G. G. Warr, *J. Phys. Chem. C* **2007**, *111*, 5162–5168; b) S. J. O'Shea, N. N. Gosvami, L. T. W. Lim, W. Hofbauer, *Jpn. J. Appl. Phys.* **2010**, *49*, 08LA01-1–9.

[39] a) R. G. Horn, D. F. Evans, B. W. Ninham, *J. Phys. Chem.* **1988**, *92*, 3531–3537; b) J. A. Smith, O. Werzer, G. B. Webber, G. G. Warr, R. Atkin, *J. Phys. Chem. Lett.* **2009**, *1*, 64–68; c) Z. Wang, H. Li, R. Atkin, C. Priest, *Langmuir* **2016**, *32*, 8818–8825.

[40] a) T. Arnold, A. J. Jackson, A. Sanchez-Fernandez, D. Magnone, A. E. Terry, K. J. Edler, *Langmuir* **2015**, *31*, 12894–12902; b) M. Pal, R. Rai, A. Yadav, R. Khanna, G. A. Baker, S. Pandey, *Langmuir* **2014**, *30*, 13191–13198; c) A. Sanchez-Fernandez, K. J. Edler, T. Arnold, R. K. Heenan, L. Porcar, N. J. Terrill, A. E. Terry, A. J. Jackson, *PCCP* **2016**, *18*, 14063–14073; d) R. M. M. Azaga, doctoral thesis, University of Leicester, Leicester **2018.**

[41] A. Sanchez-Fernandez, O. S. Hammond, K. J. Edler, T. Arnold, J. Doutch, R. M. Dalgliesh, P. Li, K. Ma, A. J. Jackson, *PCCP* **2018**, *20*, 13952–13961.

[42] J. Zhao, B. M. Fung, *Langmuir* **1993**, *9*, 1228–1231.

[43] N. Nazir, M. S. Ahanger, A. Akbar, *J. Dispersion Sci. Technol.* **2009**, *30*, 51–55.

[44] A. Sanchez-Fernandez, T. Arnold, A. J. Jackson, S. L. Fussell, R. K. Heenan, R. A. Campbell, K. J. Edler, *PCCP* **2016**, *18*, 33240–33249.

[45] A. Pandey, R. Rai, M. Pal, S. Pandey, *PCCP* **2014**, *16*, 1559–1568.

[46] J. N. Israelachvili, *Intermolecular and surface forces,* 3. ed., Academic Press, Burlington, **2011**.

[47] a) J. N. Israelachvili, D. J. Mitchell, B. W. Ninham, *J. Chem. Soc., Faraday Trans. 2* **1976**, *72*, 1525–1568; b) Y. C. Liu, S. H. Chen, R. Itri, *J. Phys.: Condens. Matter* **1996**, *8*, A169–A187.

[48] S. Manne, J. P. Cleveland, H. E. Gaub, G. D. Stucky, P. K. Hansma, *Langmuir* **1994**, *10*, 4409–4413.

[49] S. Manne, H. E. Gaub, *Science* **1995**, *270*, 1480–1482.

[50] E. J. Wanless, W. A. Ducker, *J. Phys. Chem.* **1996**, *100*, 3207–3214.

[51] J.-F. Liu, W. A. Ducker, *J. Phys. Chem. B* **1999**, *103*, 8558–8567.

[52] E. J. Wanless, W. A. Ducker, *Langmuir* **1997**, *13*, 1463–1474.

[53] a) R. Atkin, G. G. Warr, *J. Am. Chem. Soc.* **2005**, *127*, 11940–11941; b) H. N. Patrick, G. G. Warr, S. Manne, I. A. Aksay, *Langmuir* **1997**, *13*, 4349–4356.

[54] G. Srinivas, S. O. Nielsen, P. B. Moore, M. L. Klein, *J. Am. Chem. Soc.* **2006**, *128*, 848–853.

[55] A. C. Zettlemoyer, *J. Colloid Interface Sci.* **1968**, *28*, 343–369.

[56] A. J. Groszek, *Proc. R. Soc. London, Ser. A* **1970**, *314*, 473–498.

[57] a) J. J. Kipling, E. H. M. Wright, *J. Chem. Soc.* **1962**, 855; b) J. P. Rabe, S. Buchholz, *Science* **1991**, *253*, 424–427; c) Y. H. Yeo, K. Yackoboski, G. C. McGonigal, D. J. Thomson, *J. Vac. Sci. Technol., A* **1992**, *10*, 600–602.

[58] R .M. Pashley, P. M. McGuiggan, R. G. Horn, B. W. Ninham, *J. Colloid Interface Sci.* **1988**, *126*, 569–578.

[59] G. C. McGonigal, R. H. Bernhardt, D. J. Thomson, *Appl. Phys. Lett.* **1990**, *57*, 28–30.

[60] R. D. Shannon, *Acta Cryst. A* **1976**, *32*, 751–767.

[61] a) K. Häckl, master thesis, Universität Regensburg, Regensburg, **2015**; b) A. Mühlbauer, doctoral thesis, Université de Lille, Universität Regensburg, Lille, **2014.**

[62] a) W. A. Ducker, T. J. Senden, R. M. Pashley, *Nature* **1991**, *353*, 239–241; b) T. J. Senden, C. J. Drummond, P. Kekicheff, *Langmuir* **1994**, *10*, 358–362.

Chapter 4
Amphiphilic Hormones: Physical-Chemical Characterization

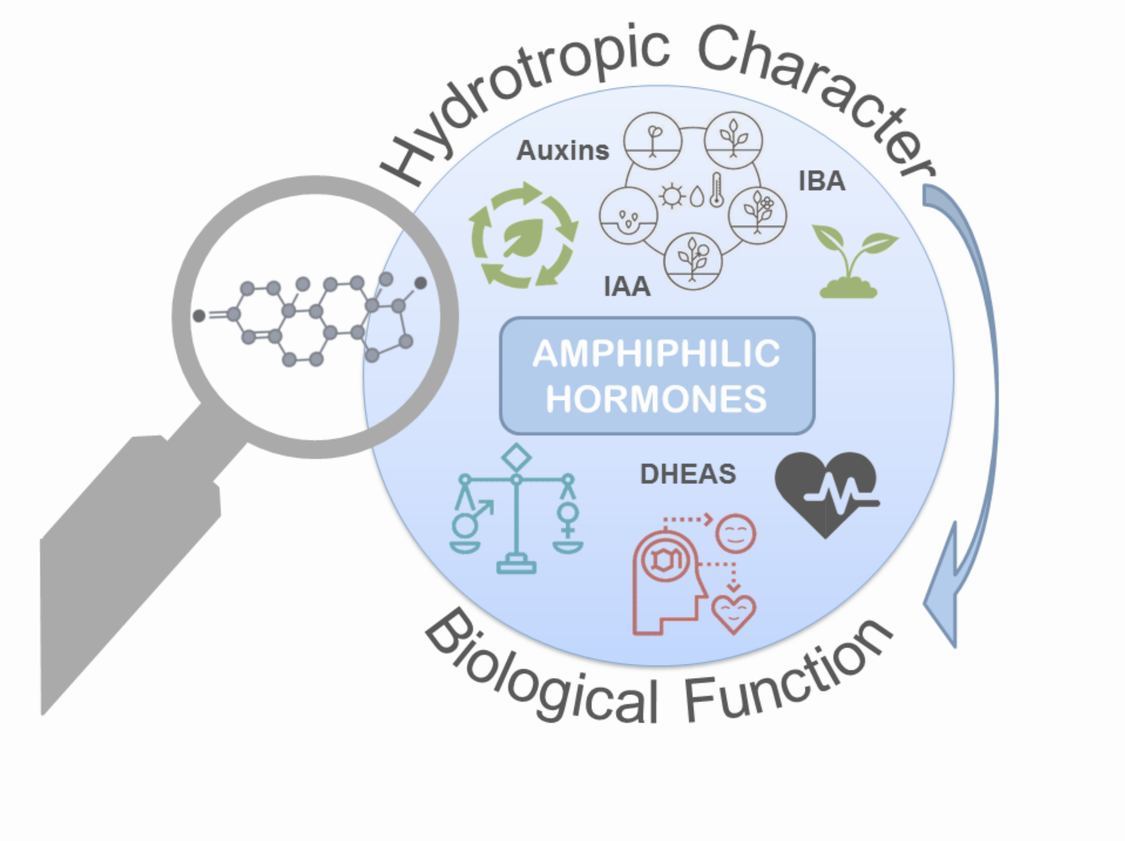
Hydrotropic Character
Auxins
IBA
IAA
AMPHIPHILIC HORMONES
DHEAS
Biological Function

4 Amphiphilic Hormones: Physical-Chemical Characterization

4.1 Introduction

Nature has developed marvellous concepts, systems and mechanisms to ensure perfectly synergistic processes in nature. One of these systems is undoubtedly the hormonal system (in mammalian beings also referred to as endocrine system) for the regulation of a high number of biological events in natural organisms. While such processes have gained high interest from the side of biological research, they can be relevant for green chemistry, too. Numerous originally biological concepts proved to be applicable in chemistry and resulted in an improvement of ecological aspects. A prominent example for such concepts is enzymatic catalysis. On the one hand, catalysis is a powerful tool to enhance chemical reactions and reduce unwanted side-products. On the other hand, the enzymatic pathway helps to avoid expensive, synthetic metal catalysts. Both aspects of the idea of enzymatic catalysis are adopted from nature: the concept catalysis itself and the enzyme as corresponding catalyst material of natural origin. The second motivation of this project was the physical-chemical characterization of the selected hormones in order to clarify biological mechanisms and to identify unrevealed side functions of biomolecules, such as just recently discovered for adenosine triphosphate (ATP).[1] Besides being an energy supplier for the organism, ATP is suggested to act as hydrotrope for the solubilization of hydrophobic biomolecules in a natural system.

Three hormones of human and plant origin were in the focus of this investigation: dehydroepiandrosterone (DHEA), or rather the related sodium salt of dehydroepiandrosterone sulphate (DHEAS), indole-3-acetic acid (IAA) and indole-3-butyric acid (IBA). They are powerful molecules that affect and regulate biological processes when present in very low concentrations. Their molecular structures are shown in Fig. 4.1.1-1. All three of them feature an amphiphilic character. The key questions were, if this feature is relevant for their biological action as hormones or another function in the organism and, whether these biomolecules could play a role for green chemistry.

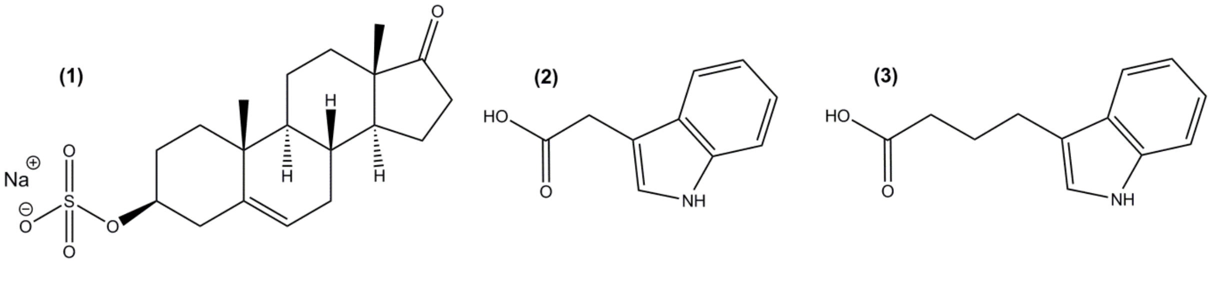

Fig. 4.1.1-1: Molecular structure of the sodium salt of dehydroepiandrosterone sulphate (DHEAS) ***(1)****, indole-3-acetic acid* ***(2)*** *and indole-3-butyric acid* ***(3)****.*

The steroid hormone DHEA has multiple functions in mammalian organisms. It is present in an enzymatically controlled equilibrium with its sulphated form DHEAS. On the one hand, it plays a key role in the biosynthetic pathway of sex hormones, on the other hand it holds functions as neurosteroid in the brain. It is believed to be present in even higher concentrations in certain parts of the brain as compared to the serum.[2] This is important, as the function of hormones, either in form of specific receptor interactions or in form of non-specific interactions is highly dependent on the concentration.

IAA and IBA belong to the group of auxins. They are plant hormones and essential for growth and developmental processes in basically all parts of the plant. In contrast to mammalian hormones which are produced in a certain organ and function in a certain tissue, an auxin is ubiquitously distributed in the plant and exhibits particular functions at each location. Auxin levels vary drastically depending on plant tissue and the cell type, respectively. This heterogenous distribution is decisive for its various functions.[3]

For the tested hormones, their biological functions and mechanisms of action are not entirely clarified. Exemplarily, a correlation between DHEAS levels and Alzheimer's disease has been detected, however, the exact correlation is unknown.[4,5] So far, Alzheimer's is an incurable disease and research is in full progress in order to find effective therapeutic methods.[6] In regard of developing new approaches, it is an urgent matter to study the relation between DHEAS and Alzheimer's disease and to figure out, if DHEAS deficiency plays a role in the precipitation of proteins in the brain, potentially causing neuronal diseases. In case of the plant hormones, a synergistic interplay of auxins and other plant constituents relevant for plant growth was found, *e.g.* with mostly water-insoluble cytokinins.[7,8] If a hydrotropic character of the hormones can be confirmed, it is imaginable that they contribute to the solubility of such substances (insoluble proteins, enzymes, hormones etc.) in biological media and regulate their action.

The present study is of physical-chemical nature and aims to examine the respective properties of these hormones, in particular their interfacial, self-aggregation and solubility characteristics. It is to be pointed out that this will not enable to draw a clear picture or allow for clear statements about the biological mechanisms and functions of the hormones. However, it will screen their properties and possible ways of mechanisms from a physical-chemical point of view. The results can be helpful to evaluate and support or disprove existing theories. They might be useful for researchers from other disciplines, such as biology or biochemistry, to explain certain observations or for developing new approaches and theories. In addition, this study was meant to investigate, if these powerful biomolecules are promising for green chemistry, either as natural materials or conceptually.

In the first part, this chapter provides some further information on hormones in general and DHEA and auxins in particular. The second part presents the results obtained from surface tension measurements, conductivity measurements and dynamic light scattering of the hormones in aqueous solution. Based thereon, the interfacial and aggregation behaviour of the hormones is discussed. The hydrotropic character of the hormones is investigated in the subsequent section. The solubility of a hydrophobic dye in aqueous hormone solutions and the influence of the hormones on water/propylene glycol ether mixtures give information on their hydrotropic efficiency. The relation between DHEAS and protein precipitation is studied in terms of solubility tests with hen egg white. In the fourth part, the impact of small amounts of hormone on a phospholipid monolayer is investigated and the possible mechanism of interaction is discussed. The conclusion summarizes the content of this chapter and evaluates the collected results regarding their usefulness in green chemistry and their biological function in the organism. The experimental part gives further details about the chemicals and measuring techniques used in this study.

4.2 Hormones

4.2.1 General Function of Hormones

Hormones are often defined as ‘substances produced in one tissue that affect the functions of other tissues’.[9] The term hormone was originally coined by E. Sterling at the beginning of the 20th century and is derived from the Greek meaning ‘to arouse or excite’.[10] Besides the nervous system, the hormone or endocrine system is the second important facility for the response to internal and external stimuli in the mammalian organism. Hormones are chemical messengers, that are produced in the endocrine glands. From there, they are released to the bloodstream and transported to the target tissue. They play a key role in reproduction and growth, but also in other important processes, like metabolism and immune system.[11] Their function is based on a signaling pathway controlled by specific receptor-ligand binding. There are two possible mechanisms: (1) the hormone binds to a cell-surface receptor, usually a G protein-coupled receptor or a receptor tyrosinase kinase. This binding creates a signal that is transferred to the cell interior, where it triggers the activation of a protein or the production of a second messenger. The activated protein or the messenger will then initiate or inhibit a certain process within the cell. (2) If the hormone has a lipid character (e.g. steroids), it can cross the cell membrane to directly interact with intracellular receptors. The receptor-ligand complex moves to the nucleus, where it binds to a hormone response element of the DNA. It controls the adjacent genes and their level of expression of a special protein.[9] In this way, hormones control physiological processes at extremely low concentrations, far below those where nutriants or vitamins would have an effect. The overall outcome is usually controlled by an interplay of agonists and antagonists and a net effect of hormonal balance. Improper hormone levels can be the reason for serious diseases. For example, the widespread diabetes disease is caused by a hormone (insulin) deficiency or a dysfunction in hormone response, so that the body's glucose level cannot be controlled.[12]

4.2.2 Dehydroepiandrosterone and its Sulphate

DHEA as well as its sulphated form DHEAS belong to the group of steroid hormones. Approximately 85 % of DHEA is biosynthesized in the adrenal cortex, the other part mostly in the gonads and the brain. Cholesterol serves as the parent substance for the steroid biosynthetic pathway. DHEA is generated in two steps from pregnenolone, a central intermediate in steroid formation. DHEA itself acts as a precursor for the biosynthesis of androgens and estrogens, which are sexual hormones.[13,14] DHEA is present in the organism in an equilibrium with its sulphated form DHEAS (see Fig. 4.2.2-1). This equilibrium is controlled by the sulfotransferase enzyme SULT2A1. DHEAS is the inactive form of DHEA and meant for storage and transport.[14] More than 99 % of the overall DHEA/DHEAS amount in the organism is present as DHEAS. Compared to other hormones, this steroid is highly abundant with a blood concentration in the range from 3 to $10\text{x}10^{-6}$ M in human adults.[15][16] Its level in blood is approximately two-fold higher in males. Maximum concentrations of DHEAS usually occur at an age of 20 to 30 and decrease steadily after.[17]

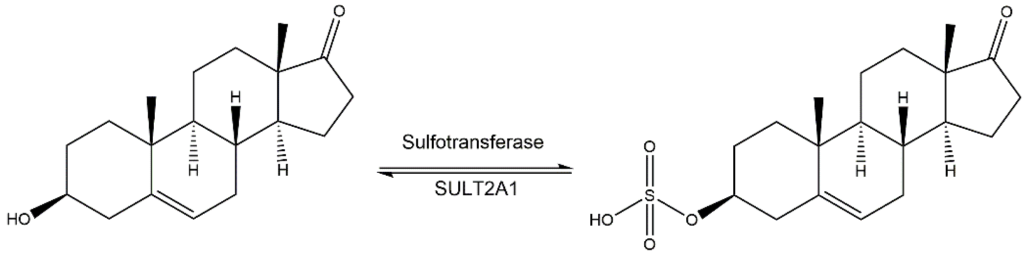

Fig. 4.2.2-1: Enzymatically controlled equilibrium between DHEA and its sulphated form DHEAS.

Considerable amounts of DHEA/DHEAS are produced in the mammalian brain, independently from the peripheral endocrine system and higher DHEAS levels are found in the brain than in the serum.[2] As DHEA and other steroid hormones are neuroactive by affecting neurotransmitter receptors in the brain, they are also referred to as 'neurosteroid' in this context.[18] The age-related decrease in cognitive function as well as neuronal degeneration and dysfunction have been related to decreasing DHEAS concentrations in elderly people.[19] This is why DHEA is known as anti-aging hormone and believed to have neuroprotective activity.[20] In addition, reduced levels of DHEAS have been found in patients suffering from schizophrenia, dementia and Alzheimer's disease.[4,21,22] In numerous publications, it is considered as remedy for neuropsychiatric and neurodegenerative disorders.[23] The neuroprotective impact of DHEA is reported to originate from the effect on and prevention of oxidative stress, neuroinflammation and excitoxicity. This is a result of its multifunctional activity in the brain. Two of these functions shall be mentioned exemplarily here: (1) DHEA suppresses the activity of *N*-methyl-*D*-

aspartate receptors. These are neuron receptors for glutamate and play a central role in excitoxicity (cell death caused by persistent over-activation). DHEA counteracts excitoxicity caused by high levels of extra-cellular glutamate levels via controlling the receptor activity and thus exhibits neuroprotective action in the brain.[18] (2) DHEA contributes to the regulation of brain-derived neurotrophic factors.[24] They are produced in different parts of the central nervous system and responsible for cell proliferation and differentiation. With its function in the potentiation of synaptic transmissions, it is essential for learning processes and the memory of mammalian brains.[18] Many neuronal processes where DHEA is involved can be related to neuropsychiatric and neurodegenerative disorders, but the role of DHEA and other steroid hormones is far from being clarified. Numerous research groups concentrate on the investigation of the role of neurosteroids in Alzheimer's disease, where patients experience progressive memory loss and cognitive deterioration for which no therapies are available so far.[6]

4.2.3 Auxins

Auxins are a group of plant hormones, which are also referred to as phytohormones. Although plant hormones affect physiological processes when present in very low concentrations, they are often believed to be a unique type of biological compounds, as their biosynthesis, metabolism and regulation differentiates from mammalian hormones. They are produced in a wide range of different tissues within the plant. Sometimes, they are transported to the location of action, sometimes they act in the same cell/tissue where they were produced. In addition, plant organisms lack a neuronal regulation system and therefore hormone function and homeostasis is even more essential for the plant machinery.[8] Auxins were the first plant hormones structurally identified with indole-3-acetic acid (IAA) as the main active auxin. It was first called 'Wuchsstoff' (English literal translation: 'growing substance') by its discoverer F.W. Went, who found a strong correlation between the growth rate of special parts of the plant and the auxin content at the regarding location.[25] Since then, auxins are known to stimulate the plant growth at several locations, such as roots, leaves and flowers. Accordingly, highest levels of auxin are found in these parts of the plant.[26] Their mechanism of action is similar to mammalian hormones: by interacting with special receptor proteins at the cell membrane, they control the gene expression responsible for growth and developmental processes.[27] They are responsible for several other plant processes, such as the response towards environmental stimuli.[8] IAA is biosynthesized from the amino acid tryptophan.[27] There is evidence of auxin activity of some biomolecules structurally related to IAA, e.g. indole butyric acid (IBA) or 4-chloroindole-3-acetic acid. Auxins also occur in so-called auxin conjugates, in which they are linked to sugars, amino acids or peptides. All these related substances can be transformed into IAA, e.g. by hydrolysis or β-oxidation. It is not clarified to which extent they take an active role in plant processes or if they are only formed for storage, transport and protection of IAA. Several auxins play a significant role in cell and tissue culture of plants as well as in plant propagation for the development of modern crop varieties.[27,28]

4.3 Interfacial and Self-Aggregation Behaviour of Hormones in Aqueous Solution

In order to evaluate the hydrotropicity of the studied hormones, their surface activity and self-aggregation behaviour was studied in terms of surface tension measurements, conductivity measurements and dynamic light scattering (DLS).

4.3.1 Surface Tension

Due to the amphiphilic structure of the studied hormones, they were expected to be surface active and to decrease the surface tension of water. The surface tension of a concentration series of aqueous solutions of each hormone sodium salt have been measured. The resulting surface tension curves are shown in Fig. 4.3.1-1. Surface tension curves of sodium salicylate (NaSal) and sodium dodecyl sulphate (SDS) are included as characteristic types of a hydrotrope and a surfactant for reference.[29–31] The critical aggregation concentration (CAC) is a characteristic feature of surface-active substances. Unfortunately, the present surface tension curves do not allow for an accessibility of this feature due to the restricted water solubility of the investigated hormone compounds. Only the curves of NaDHEAS and NaSal give indication that the CAC is almost reached, as they are levelling off at the end. Although not shown in Fig. 4.3.1-1, the true surfactant SDS exhibits a critical micellar concentration (CMC) at a concentration of $8x10^{-3}$ M.[30]

From the surface tension curves, it is obvious that NaIAA, NaIBA and NaSal have moderate surface efficiency and induce the reduction of the surface tension only at rather high concentrations in the molar range. Less NaIBA is required to cause a reduction compared to NaIAA and NaSal. This is due to the larger hydrophobic part of NaIBA and the resulting higher surface activity. NaIAA and NaSal behave similarly in this regard. But differences were observable in terms of surface effectiveness. While NaSal was not able to decrease the surface tension of water by more than 14 mN/m in the measured concentration range, the sodium salts of the auxins led to a reduction of >20 mN/m, even if applied in smaller concentrations. The terms surface efficiency and effectiveness are explained in detail in section 1.4.3.1.

The surface tension of NaDHEAS was measured at 37 °C in order to mimic physiological conditions. Simultaneously, this enhanced its limited water solubility. It started to decrease the surface tension of water at much lower concentrations compared to NaIAA, NaIBA and NaSal. In the measured concentration range until 0.075 M, it decreased the surface tension to a value of 54 mN/m.

In total, the following order of surface activities of the studied compounds was determined: SDS > NaDHEAS > NaIBA > NaIAA ≈ NaSal. Basically, NaDHEAS behaves as an intermediate case between hydrotrope and surfactant. The surface efficiency is much higher compared to hydrotropes, the effectiveness is similar. On the other hand, surface efficiency and effectiveness are lower compared to SDS. The extremely slow drop of NaDHEAS's surface tension and the resulting low negative slope of the curve were remarkable.

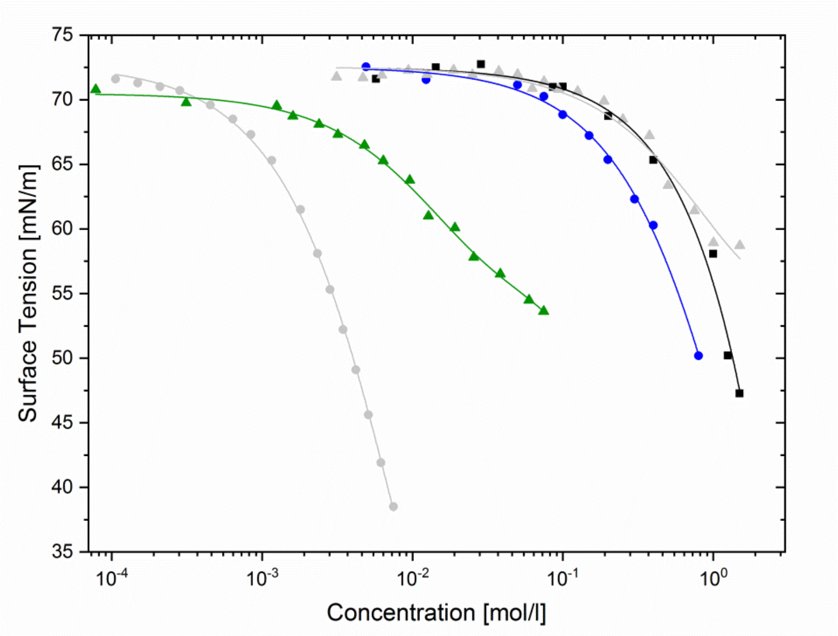

Fig. 4.3.1-1: Surface tension curves of NaDHEAS (▲) (measured at 37 °C), NaIAA (■), NaIBA (●), NaSal (▲) and SDS (●) (measured at 25 °C). Data for the surface tension of SDS is adopted from Lunkenheimer et al.[31]

The slope of a surface tension curve can be related to the area required per molecule of surfactant at the surface utilizing the Gibbs adsorption theory. The surface excess concentration Γ_i gives information on the molar amount of adsorbed solute i per unit area of surface and can be expressed by Eq. 1 and Eq. 2 in section 1.4.3.1. Accordingly, the cross-sectional area required per surfactant molecule can be determined experimentally from the concentration dependent surface tension curves. It has to be noted that this calculation is only valid for dilute systems. High solute concentrations require the consideration of the solute activity coefficient. Therefore, the calculation was only conducted for NaDHEAS and compared to existing literature values for SDS (see Tab. 4.3.1-1). Although no directly comparable data on SDS at physiological temperature was available, it is observable that the space requirement of NaDHEAS at the water/air interface is roughly three times as high as the one of SDS. This is assigned to the bulky hydrophobic steroid part of the hormone and explains its lower effectiveness in decreasing the surface tension. Similar results were found, when the behaviour of other steroid hormones at the water/dodecane interface has been studied, and distinctly higher A_i values were found for progesterone and testosterone compared to SDS.[32]

Tab. 4.3.1-1: Surface excess concentration Γ_i and mean surface area per molecule A_i obtained from the Gibbs isotherm with indication of the measuring temperature T.

	T [°C]	Γ_i x10^{-6} [mol/m^2]	A_i [Å^2]
NaDHEAS	37	0.93	179
SDS	25	3.2[33]	53[33]
SDS	60	2.6[33]	63[33]

As known from literature and exemplarily represented by the reference substances SDS and NaSal, true surfactants exhibit a rapid decrease of surface tension and associate in form of micelles, while the decrease in surface tension caused by hydrotropes and self-assembly are less pronounced and occur in a molar concentration range.[29] The surface tension plateau of hydrotropes indicating a CAC is less distinct and not always apparent, as short amphiphilic molecules are less capable of self-assembly due to limited hydrophobic interactions. According to the data obtained from surface tension measurements and in view of the reference hydrotrope and surfactant, it is expected that the sodium salts of auxins are hydtrotropes. NaDHEAS instead is an intermediate case and cannot be clearly classified as true hydrotrope or true surfactant. As the surface tension results for NaDHEAS did not allow for an obvious categorization, conductivity measurements were carried out in order to detect an onset of aggregation or obtain a probable CAC.

4.3.2 Conductivity

The specific conductivity κ of a concentration series of NaDHEAS was measured at 37±0.5 °C by dilution of a stock solution. Plotting the specific conductivity κ against the surfactant concentration of an aqueous surfactant solution typically results in a distinct break of the curve slope at the CMC.[34] In case of NaDHEAS (see Fig. 4.3.2-1), the breakpoint is determined by the intersection of a linear fit of the beginning of the curve (low NaDHEAS concentrations) and a linear fit of the end of the curve (high NaDHEAS concentration). It appears at a concentration of 0.034 M. As the curve break is rather indistinct, it might not be suitable to associate it with a CMC. However, it suggests the occurrence of a certain grade of self-assembly which causes the non-linearity of the conductivity curve. In contrast to the 'sharp' micellar aggregation, it might happen in a more continuous, *i.e.* gradual aggregation process.

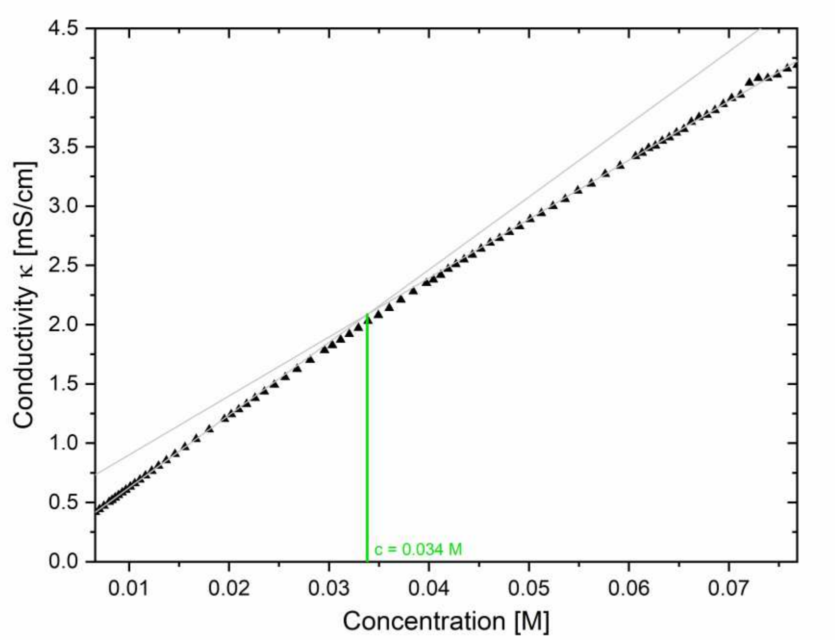

Fig. 4.3.2-1: Specific conductivity κ as a function of the NaDHEAS concentration in aqueous solution with indication of a breakpoint of the curve slope.

4.3.3 Dynamic Light Scattering

Performing DLS measurements of aqueous hormone solutions delivered information on their aggregation behaviour. First, concentration dependent correlation functions of NaDHEAS, NaIAA and NaIBA were studied. Second, time dependent correlation functions of NaDHEAS solutions were investigated. Fig. 4.3.3-1 shows the concentration dependent correlation functions of aqueous solutions of NaDHEAS (left, green), NaIAA (middle, violet) and NaIBA (right, blue). A NaDHEAS solution at a concentration of 0.038 M is the first one to feature a correlation function above 0.6, so that a reasonable degree of aggregation can be expected. This threshold concentration matches the breakpoint observed in the conductivity measurements, as described above. The NaDHEAS solutions appear to have remarkably long delay times (compare to carnitine surfactants in section 2.3.2.3). This is indicative for the presence of large aggregates. In addition, some of the correlation functions of NaDHEAS exhibit moderate bimodality, observable from the irregular curve shapes. This is a characteristic behaviour of solutions comprising particles in different sizes or non-spherical shape. This might be caused by the bulky hydrophobic part of the NaDHEAS molecule. In contrast to NaDHEAS, the sodium salts of the auxins do not show pronounced correlation. Although they increase with increasing auxin concentration, self-aggregation of the auxins is much less pronounced compared to NaDHEAS. This is a typical behaviour of hydrotropes, as their tendency to self-aggregate in aqueous solution is unincisive.

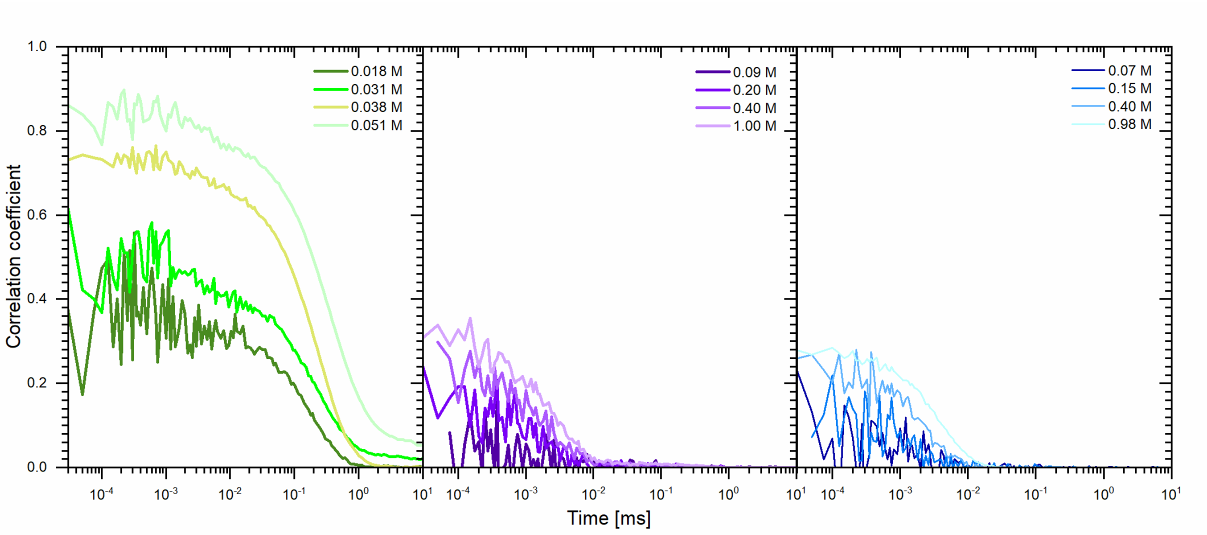

Fig. 4.3.3-1: Time-dependent self-correlation functions as obtained by DLS for aqueous solutions of NaDHEAS (left, green, measured 2 h after preparation, 37 °C), NaIAA (middle, violet, 25 °C) and NaIBA (right, blue, 25 °C).

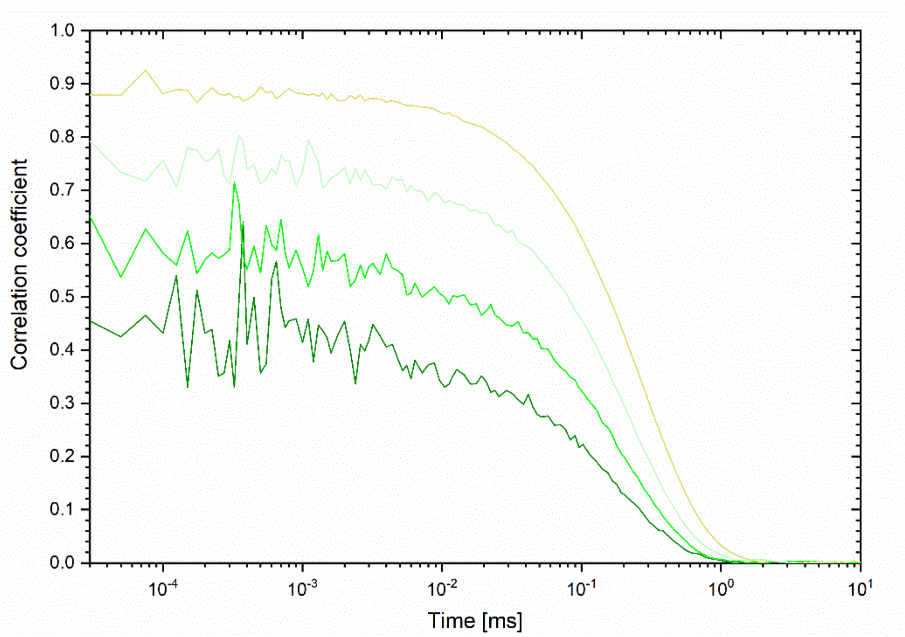

Fig. 4.3.3-2: Time-dependent self-correlation functions as obtained by DLS for a 0.026 M aqueous NaDHEAS solution 2 h (–), 8 h (–), 16 h (–) and 24 h (–) after preparation of the solution at 37 °C.

When performing DLS measurements of NaDHEAS solutions, it was noted that the resulting correlation functions were correlated to the time that had passed between the preparation of the solution and the DLS measurement. Fig. 4.3.3-2 shows the correlation functions of a 0.026 M NaDHEAS solution obtained 2 h, 8 h, 16 h and 24 h after preparation. The correlation function increases with the age of the solution and so does the tendency of NaDHEAS towards self-aggregation. It is assumed that NaDHEAS undergoes hydrolysis in aqueous solution. As the amount of hydrolysis product (DHEA) in the solution increases, the correlation function as well as the delay time and the related aggregate size increase. At a certain point, the solutions even became turbid and a white precipitate was observed. The promotion of aggregation and the increase in aggregate size is expected to be due to the implementation of hydrolysis product inside the aggregates.[35] The presence of hydrolysis product could be proved by mass spectrometry.

Investigating the interfacial and self-aggregation behaviour of hormones in aqueous solution and two reference substances revealed that the studied compounds were surface active with surface efficiencies in the following order: SDS > NaDHEAS > NaIBA > NaIAA ≈ NaSal. The surface effectiveness of NaDHEAS, NaIAA, NaIBA and NaSal was much lower compared to SDS. Conductivity measurements of NaDHEAS as a function of concentration revealed a curve with a slight breakpoint. This was related to a certain grade of NaDHEAS aggregation. The intersection of the linear fits of the start and the end of the curve corresponded well to the threshold concentration of aggregation found by DLS. Below this concentration, the correlation functions and the related tendency for self-aggregation were low, while above this concentration pronounced correlation functions were obtained. The sodium salts of the auxins showed minor correlation in the DLS measurements and their tendency to self-assemble is expected to be lower.

4.4 Evaluation of the Hydrotropic Efficiency of Hormones

The hydrotropic efficiency is related to the ability of hydrotropes to enhance the solubility of hydrophobic substances (see section 1.4.3.3). This feature has been studied in two different ways: (1) the solubility of the hydrophobic dye disperse red 13 (DR13) has been determined by UV/Vis spectrometry. (2) The salting-behaviour of the hormones in water/propylene glycol ether mixtures has been investigated.

4.4.1 Solubilization of Disperse Red 13

Dye solubility experiments were performed with a concentration series of each of the three sodium hormone salts and the two reference substances SDS and NaSal. The resulting solubility curves are shown in Fig. 4.4.1-1. The shape of the curves is similar for each compound: after a certain threshold concentration, a sudden increase in the DR13 solubility is observed. The solubilization efficiency follows the same order as the efficiency to decrease the surface tension: SDS > NaDHEAS > NaIBA > NaIAA ≈ NaSal. However, the solubilization power of IAA and IBA is much higher compared to the other substances. The performance of NaDHEAS is limited by its own water solubility. The measurement at even higher concentrations of NaSal and SDS in view of its ability to dissolve DR13 seems possible and should be done to improve the comparability of the results. It has been shown in another publication that further increasing the SDS concentration results in a slow increase of the amount of solubilized DR13.[36] In the case of SDS, the threshold concentration, where DR13 solubility starts to increase rapidly, corresponds to its CMC, reported in literature.[30] NaDHEAS's threshold concentration obtained from the solubility experiments approximately matches the possible CAC determined by conductivity measurements and DLS. While no critical or threshold concentrations were obtained for NaIAA, NaIBA and NaSal in other experiments, a so-called minimum hydrotropic concentration (MHC) is accessible by the DR13 experiment. Approximate values are 0.5 M, 0.9 M and 1.0 M for NaIBA, NaIAA and NaSal, respectively.

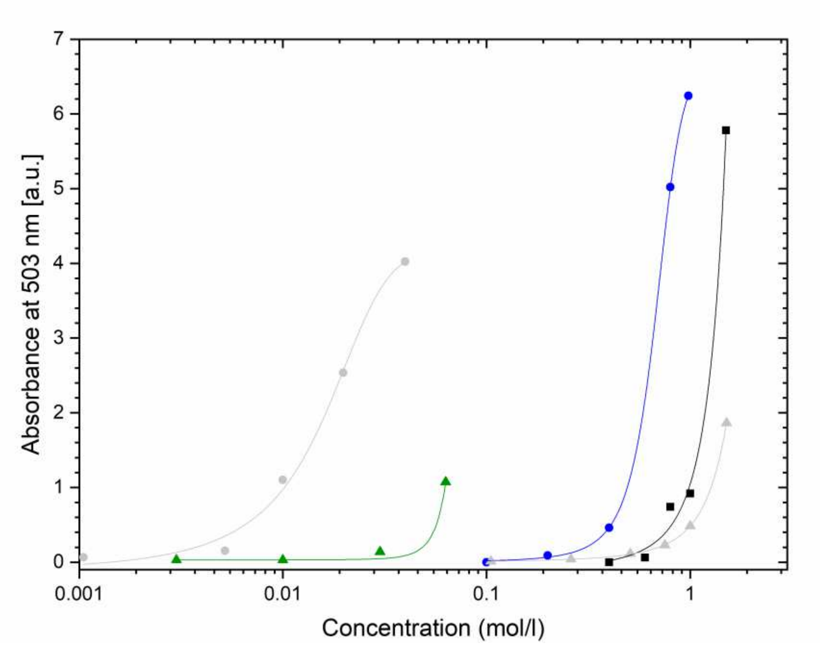

Fig. 4.4.1-1: Hydrotropic solubilization of DR13 in aqueous solutions of NaDHEAS (▲) (measured at 37 °C), NaIAA (■), NaIBA (●), SDS (●) and NaSal (▲) (measured at 25 °C) as evidenced from the absorbance of DR13 at a wavelength of 503 nm.

The results obtained from the DR13 solubility experiments confirm the assumption that NaIAA and NaIBA are hydrotropic compounds. The fact that no clear critical concentration of aggregation was found in binary aqueous systems, but in the presence of a hydrophobic solute, supports the concept that aggregation of hydrotropes is promoted in the presence of a hydrophobic third component.[35] The behaviour of NaDHEAS is again located inbetween hydrotropes and anionic surfactant.

4.4.2 Influence of Hormone Sodium Salts on Water/Propylene Glycol Ether Mixtures

4.4.2.1 General Considerations

Due to the structural features of the studied hormones, they are assumed to influence the behaviour of water/oil mixtures. On the one hand, they are organic salts, on the other hand they have an amphiphilic character. They are expected to exhibit certain solubility in both phases of a water/oil mixture, and the specific contribution of the ions of the head group will be considered. A special phenomenon occurring in water/propylene glycol ether (PGE) mixtures is used for this investigation: their formation of homogeneous mixtures below and heterogeneous mixtures above a certain threshold temperature, which depends on the composition. Throughout this study, this demixing temperature will be termed 'lowest solution temperature' (LST), as the composition exhibiting the minimum demixing temperature is taken for the investigations. The presence of a one-phasic system is energetically favoured at low temperatures and stabilized by a network of hydrogen-bonds. Higher temperatures induce increased molecular motion of the flexible PGE molecules, dehydration and the formation of a heterogeneous system. The phase diagrams can be influenced by organic salts depending on their structure and ion composition. There are two possible opposite effects: (1) So-called '*salting-in*' additives increase the one-phasic region and the LST. (2) '*Salting-out*' additives promote demixing and lower the LST.[37,38]

This concept originally goes back to Hofmeister, who studied ion-specific effects on the solubility of proteins.[39] He developed the so-called Hofmeister series classifying inorganic ions according to their ability to enhance or reduce the solubility of proteins in water. This concept has later been applied to aqueous solutions of polymers[40] and non-ionic surfactants.[41] However, the mechanism is arbitrarily complex and several existing concepts can be taken into account. They are listed in Tab. 4.4.2-1 assigned to the effect they have on the LST of a water/PGE mixture. Whether an additive is salting-in or salting-out is closely related to their interaction with water and the formation of hydration shells. It can be related to Collins's concept and the classification of ionic species as chaotrope or kosmotrope.[42] Elsewhere, descriptions such as 'structure-breaking' or 'structure-making' can be found according to the extent of hydrogen-bonding induced by the contemplated additive.[43,44] Anyway, the salting-effect originates from a complex interplay of hydrogen-bonding interactions, hydrophobic interactions, dipole-dipole interactions and changes in the system's entropy caused by changes in water structure.[37,43]

Tab. 4.4.2-1: List of concepts and properties characterizing LST increasing and decreasing compounds.

↑ LST	**↓ LST**
- Salting-in	- Salting-out
- Chaotrope	- Kosmotrope
- Structure-breaking	- Structure-making
- Destabilizing proteins	- Stabilizing proteins

The use of PGEs is highly convenient in terms of studying the salting behaviour of ionic and non-ionic additives. Some have LSTs close to room temperature, they are low-toxic and available at low cost and highly pure state (just keeping isomers in mind).[37] In particular, propylene glycol propyl ether (PnP) and di(propylene glycol) propyl ether (DPnP) have been used in this study (see Fig. 4.4.2-1). The LST of the binary water/PnP mixture was found to be at 33 °C and a PnP mass fraction of 0.45.[37] This system was employed for the investigation of NaDHEAS to ensure its water solubility at the LST. A system consisting of water and DPnP with a DPnP mass fraction of 0.55 had a LST of 14 °C.[37] This was the system of choice for the auxin sodium salts.

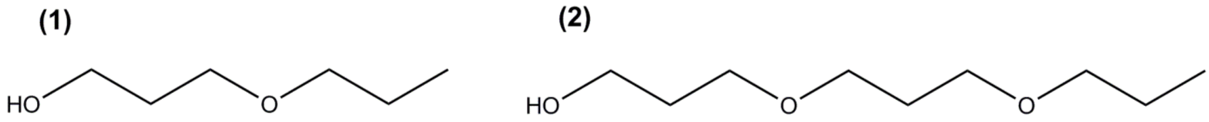

Fig. 4.4.2-1: Molecular structures of PnP (1) and DPnP (2).

As mentioned above, the addition of certain amounts of (organic) salts results in an increase or decrease of the LST of a water/PGE mixture. A correlation between the change in LST and the added salt concentration is described by the linear relation:

$$\mathrm{LST}\ (\mathrm{c}) = \ \mathrm{LST}(\mathrm{c} = 0) + ac \qquad \textbf{(5)}$$

wherein, *LST(c = 0)* is the demixing temperature of the binary water/PGE mixture, *LST(c)* the demixing temperature after the addition of the salt, *c* is the concentration of additive in [mmol per 1 mol of water/PGE mixture] and *a* is a comparable coefficient assigned to each salt as an indicator for its salting behaviour and given in [°C per mmol of additive in 1 mol of water/PGE mixture]. Positive *a* values imply a salting-in effect and negative values a salting-out effect.

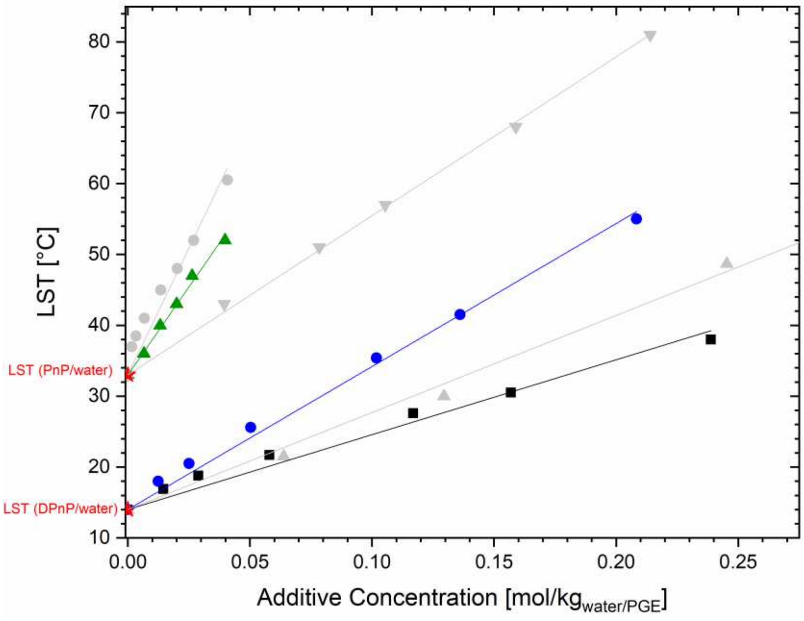

Fig. 4.4.2-2: Shifts of the LST of water/PnP upon the addition of NaDHEAS (▲), NaSal (▼) and SDS (●) and the LST of water/DPnP upon the addition of NaIAA (■), NaIBA (●) and NaSal (▲) with linear fits indicating the salting-in activity of the tested substance.

While originally only the ionic effects and the salting behaviour of inorganic salts have been examined,[39,45,46] Grundl *et al.* were the first ones to investigate charged and uncharged organic substances.[38] Using water/PGE mixtures, organic acids, sodium salts of organic acids and biomolecules, such as amino acids, sugars and natural sweeteners were studied regarding their LSTs. The sodium salts of organic acids, sugars, ammonium organic salts, sugars and amino acids were found to be salting-out, while organic carboxylic acids and natural sweeteners were salting-in. Relevant results are summarized in Tab. 4.4.2-2.

4.4.2.2 Influence of Sodium Dehydroepiandrosterone Sulphate on the Lowest Solution Temperature of a Water/Propylene Glycol Propyl Ether Mixture

When investigating the evolution of the LST of a water/PnP mixture upon the addition of NaDHEAS, the mass fraction of PnP was kept constant at 0.45. The corresponding amount of PnP was then mixed with an aqueous NaDHEAS solution in concentrations of 0 - 0.04 $\text{mol/kg}_{\text{water/PGE}}$. The behaviour of NaSal and SDS as characteristic types of a hydrotrope and a surfactant was tested, too, for reference. The results are presented in Fig. 4.4.2-2 and reveal that all studied sodium salts increase the LST of a water/PnP mixture. Therefore, they can be classified as salting-in. The respective coefficients *a* are listed in Tab. 4.4.2-2, whereas higher values of *a* are indicative for stronger salting-in effects. All substances investigated in the water/PnP mixture showed stronger salting-in activity than NaSCN, which was the strongest salting-in salt determined by Bauduin et al.[37] The corresponding *a* coefficients follow the order SDS > NaDHEAS > NaSal > NaSCN. However, it remains questionable, if NaSCN, which is a salt consisting of small, inorganic ions, can be compared with the tested sodium salts exhibiting non-neglectable organic moieties and amphiphilicity. For the studied substances NaDHEAS, NaSal and SDS, the coefficient *a* appears to increase with the hydrophobicity of the compound.

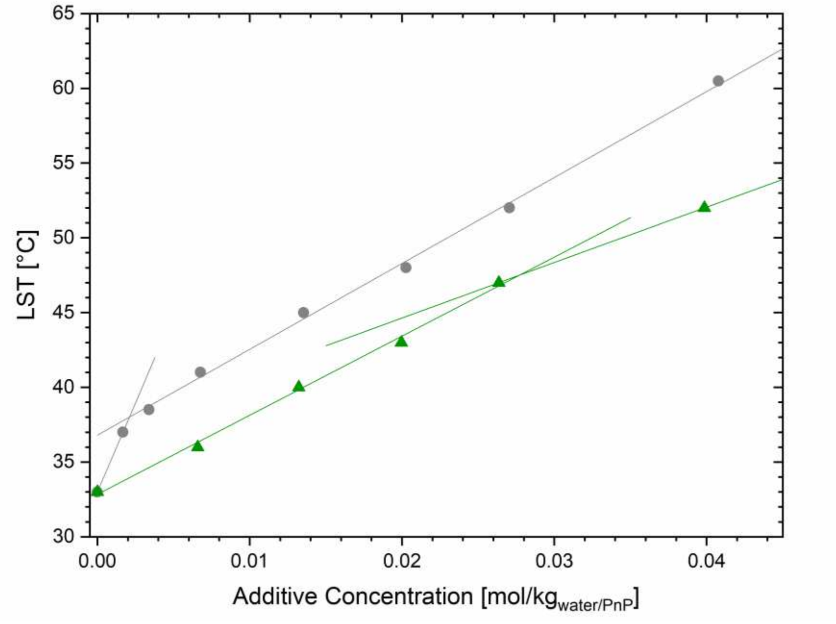

Fig. 4.4.2-3: Shifts of the LST of water/PnP upon the addition of NaDHEAS (▲) and SDS (●) and the change of the curve linearity.

At this point it has to be argued if the concept of ion specificity is suitable for large organic salts and if the term 'salting' is actually appropriate for molecules with amphiphilic structure. It is assumed that there is a significant difference between ion specific effects and the effects exhibited by ionic head groups (when there is a considerably large organic rest).[46,47] A particular example is sulphate. When present as SO_4^{2-} ion, it has high charge density and is classified as kosmotrope. Sulphate as head group connected to an organic rest carries only one negative charge and is known to be chaotropic. In the first case, sulphate is even more kosmotropic than an acetate ion, while in the latter case the acetate head group is more kosmotropic. Although substances tested in this study do exhibit charged moieties, their behaviour will be significantly influenced by the hydrophobic part of the molecule. The resulting hydrophobic interactions are assumed to considerably contribute to the phase behaviour of the water/PGE mixture. Taking a closer look at the LST curves of SDS and NaDHEAS (see Fig. 4.4.2-3) allows for the detection of two linearities for each curve. The change in the slope of the curve is assumed to be caused by the start of aggregation. It is not clear, however, to which extent micellar solubilization or the formation of a microemulsion will play a role. To further investigate this observation and gain precise knowledge on the complex interactions guiding the behaviour of this system, the aggregation of ionic amphiphiles in water/PGE mixtures should be studied. It will be more convenient to start with well-known ionic amphiphiles instead of hormones.

Tab. 4.4.2-2: Coefficient a in units of [°C per mmol of additive in 1 mol of water/PGE mixture] for systems with a PnP mass fraction of 0.45 and a DPnP mass fraction of 0.55.

	Water/PnP	**Water/DPnP**
NaDHEAS	16.6	-
NaIAA	-	2.6
NaIBA	-	5.2
NaSal	7.4	3.6
SDS	21.1	-
NaSCN	3.4[37]	3.2[37]
NaNic	-	-1.6[38]
NaOAc	-	-3.3[38]

4.4.2.3 Influence of the Sodium Salts of Indole-3-Acetic Acid and Indole-3-Butyric Acid on the Lowest Solution Temperature of a Water/di(Propylene Glycol) Propyl Ether Mixture

When investigating the evolution of the LST of a water/DPnP mixture upon the addition of auxin sodium salts, the mass fraction of DPnP was kept constant at 0.55. The respective amount of DPnP was then mixed with aqueous solutions of NaIAA (0 - 0.26 $mol/kg_{water/PGE}$) or NaIBA (0 - 0.23 $mol/kg_{water/PGE}$). NaSal was studied as reference hydrotrope. The results are presented in Fig. 4.4.2-2. They reveal that all studied sodium salts increase the LST of a water/DPnP mixture and that they can be classified as salting-in. The determined coefficients *a* are listed in Tab. 4.4.2-2, whereas higher values for *a* indicate stronger salting-in effects. In accordance with the measurements of water/PnP, all substances studied in the water/DPnP mixture showed stronger salting-in activity than NaSCN.[37] In addition, Grundl *et al.* have investigated two other sodium salts of organic carboxylic acids: sodium acetate (NaOAc) and sodium nicotinamide (NaNic) and found that they, in contrast to the hormones, exhibited salting-out activity with negative *a* coefficients.[38] The overall order of *a* was: NaIBA > NaSal > NaSCN >NaIAA > NaNic > NaOAc. According to these data, NaOAc is a kosmotrope with salting-out effect. In contrast, other organic salts with carboxylate head group, such as NaIAA, NaIBA and NaSal have the opposite effect on a water/DPnP mixture. This confirms the assumption that the behaviour of true ions is not equal to the same ion connected to an organic rest and that the organic rest plays an important role in the salting-in mechanism.

4.4.2.4 Salting-in and the Hydrophobic Efficiency of Hormones

Unequivocally and disregarding the above-mentioned critical considerations, this experiment confirmed the hydrotropic activity of the studied hormones. They showed salting-in effects on water/PGE mixtures and promoted a mixing of aqueous and oil phases. As this method has so far been mainly used for the investigation of the salting effect of true Hofmeister salts, the comparability with former results is expected to be rather low. However, the results from the experiments conducted for the hormones can be compared to each other. The efficiency for increasing the compatibility of an aqueous and an oil phase can be evaluated and related to the hydrotropic efficiency of the hormones. According to the experimental series with water/PnP mixtures, the efficiency follows the order SDS > NaDHEAS > NaSal. This reveals that the efficiency of NaDHEAS lies inbetween the one of a hydrotrope and the one of a true surfactant. According to the experimental series with water/DPnP mixtures, the following order for the hydrotropic efficiency was found from the respective coefficients *a*: NaIBA > NaSal > NaIAA. Basically, the results derived from the investigation of the salting behaviour correspond to what has been found in the previous experiments. Regarding the salting-in mechanism, it is assumed that the salting behaviour of the studied molecules is dominated by their hydrophobicity rather than by specific ion effects, although they will contribute to a certain extent.

4.4.3 Influence of Sodium Dehydroepiandrosterone Sulphate on an Aqueous Egg White Solution

Proteins are natural macromolecules consisting of a defined sequence of amino acids connected by peptide bonds and a characteristic three-dimensional structure of the polypeptide-chain. The protein structure is a significant feature for its accurate function in the organism, where proteins act in different roles and are responsible for manifold processes, including stabilization, transport, catalysis, signaling, etc. The whole organism is dependent on defect-free performance of all proteins.[48] The dysfunctionality of only one protein can have severe consequences for the organism and lead to serious diseases or death. Protein denaturation could be linked to several diseases, such as Alzheimer's, Parkinson's and Huntington's. In particular, protein precipitation and the accumulation of protein aggregates were found to play a major role.[49,50] Decreased levels of DHEAS in the brain were related to such diseases.[4,5,51] In this context, the question arose, whether neurosteroids contribute to the stabilization of proteins and inhibit protein precipitation in the brain. Therefore, the influence of NaDHEAS on the denaturation of egg white has been investigated. Natural egg white is easily accessible from hen eggs and consists of a mixture of proteins. Its major constituents are ovalbumin (54%), ovotransferrin (12%), ovomucoid (11%), ovomucin (3.5%) and lysozyme (3.5%).[52] Thermal treatment of an aqueous egg white solution leads to a conformational change of the proteins, they partially unfold and precipitate.[53]

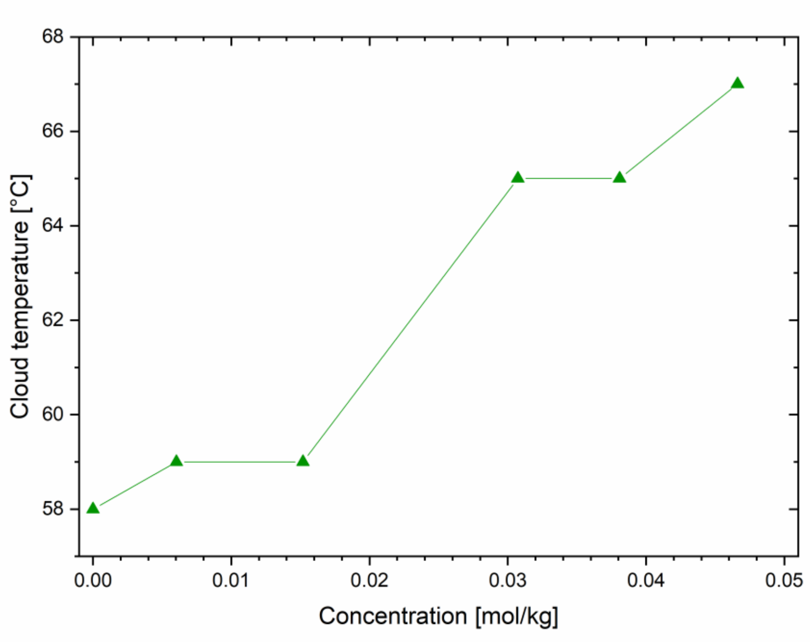

Fig. 4.4.3-1: Cloud temperature of egg white solutions containing NaDHEAS at different concentrations.

According to the conducted experimental protocol, an aqueous solution of egg white (without the addition of physiological buffer) becomes turbid at a temperature of 58 °C upon heating. In presence of certain amounts of NaDHEAS, this so-called cloud temperature could be increased (see Fig. 4.4.3-1). This observation supports the assumption that DHEAS is involved in protein solubilization and prevents proteins from precipitation. Similar to what has been reported about adenosine triphosphate (ATP) by Patel *et al.*, DHEAS could function as a biological hydrotrope in the organism.[1] However, the results should be treated with caution and the experiment should be rather seen as preliminary test for further investigations. The use of a buffer is required to mimic physiological conditions more closely. A detailed investigation and discussion of the 'mechanism' will be necessary. From this experiment it is not evident, if the hormone really prevents the denaturation of the proteins or if it only inhibits precipitation and clouding by solubilization of the denaturated protein polypeptide-chains. Furthermore, one might argue that DHEAS concentrations in the millimolare range are biologically not realistic to occur in the brain. However, the formation of protein pockets and cavities might create local environments facilitating DHEAS concentrations much higher than its standard concentration in the organism. Only a detailed chemical and biological study finally allows for assessing an existing association between the DHEA hormone and protein-related human diseases. From a physico-chemical point of view a relation seems possible in view of the very pronounced effect.

4.5 Interaction with a Dipalmitoylphosphatidylcholine Monolayer

The studied hormones were found to be surface active to a certain extent. Due to the fact that they are present in biological organisms, it is important to clarify, if they are able to interact with biological membranes, such as the cell membrane. In this section, the interaction of the hormones with a dipalmitoylphosphatidylcholine (DPPC) monolayer at the water/air interface was investigated. It has to be admitted that this is not an ideal model for biological membranes, but suitable to get first information on interactions with a biological phospholipid.

4.5.1 General Considerations

Recording surface pressure-area isotherms with a Langmuir trough is a common method to study surfactant monolayers at the water/air interface and goes back to the beginning of the 19th century and the research of Irving Langmuir.[54] In most modern setups, the aqueous subphase is filled into a Teflon trough and the surfactant is spread on the surface. The latter is compressed by a mobile Teflon barrier, whereby the surfactant density at the surface is varied (see Fig. 1.4.3-1 in section 1.4.3.1). A typical surface pressure isotherm is shown in Fig. 1.4.3-2 in section 1.4.3.1. By compressing the surface, gas-like, liquid-like and solid-like monolayer phases occur. They are described in Tab. 1.4.3-1 in section 1.4.3.1. At high surface pressure, molecules are squeezed out of the monolayer and the monolayer eventually collapses.[55]

The phospholipid DPPC (see Fig. 4.5.1-1) is known as natural constituent of biological membranes. They usually consist of a phospholipid bilayer matrix including a variety of other chemicals, such as proteins, glycolipids and carbohydrates.[56] Their role in interacting with toxins, drugs, pollutants or other substances is of utmost importance and interest. In biochemical research, DPPC is frequently used as a model substance to probe such interactions. A DPPC monolayer at the water/air interface is the simplest model and was used in this study to get insights into the hormone-membrane interactions of hormone sodium salts, when they were present in the aqueous subphase. DPPC was assumed to be suitable, as it is of zwitterionic nature and therefore interactions will not be completely dominated by strong coulomb interactions. In addition, its monolayer at the water/air interface is well characterized and reference literature is readily available.

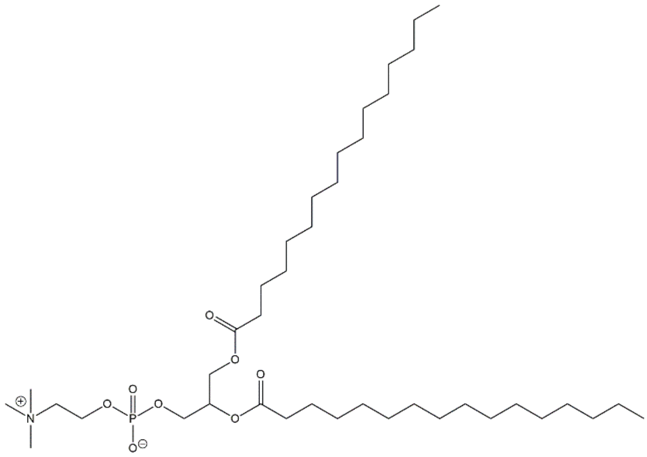

Fig. 4.5.1-1: Molecular structure of DPPC.

4.5.2 Surface Pressure-Area Isotherms

The recorded surface pressure-area isotherms of DPPC with DHEAS (left, green), NaIAA (middle, violet) and NaIBA (right, blue) added to the aqueous subphase are presented in Fig. 4.5.2-1. The difference in the curve shape of the NaDHEAS concentration series compared to the NaIAA and NaIBA concentration series is assumed to be mainly due to the difference in temperature. The former system was measured at 37 °C, the latter at 25 °C. For reasons of simplicity, the curves recorded for NaIAA and NaIBA will be discussed first, as they correspond well to the theoretical curve shape shown in Fig. 1.4.3-2 in section 1.4.3.1. The DPPC monolayer recorded with pure water as subphase at 25 °C passes through the following phases upon compression: **L_1 + G** ($A_m > 1.05$ nm^2), **L_1** (1.05 nm$^2 > A_m > 0.80$ nm^2), **L_2 + L_1** (0.80 nm$^2 > A_m > 0.60$ nm^2), **L_2** and **S** without visible transition (0.60 nm$^2 > A_m > 0.40$ nm^2). The monolayer collapse occurs at $A_m = 0.40$ nm^2.

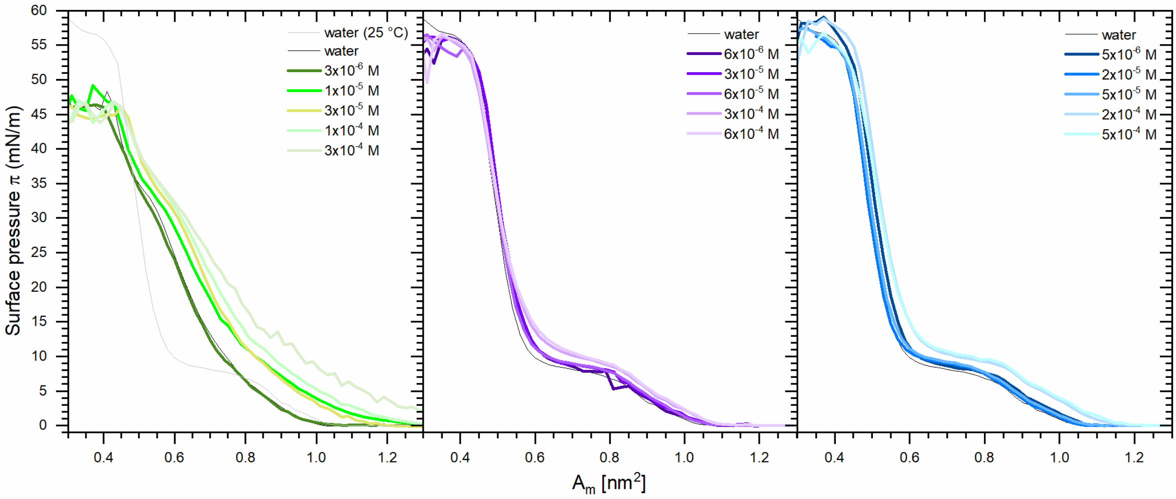

Fig. 4.5.2-1: Surface pressure-area isotherms of DPPC with different concentrations of NaDHEAS (left, green, 37 °C), NaIAA (middle, violet, 25 °C) and NaIBA (right, blue, 25 °C) as additive in the aqueous subphase.

The presence of NaIAA and NaIBA in the subphase was found to increase the surface pressure at a fixed area per molecule. The higher the concentration of auxin, the stronger was the increase. This effect was most pronounced in certain regions of the diagram, in particular the $\mathbf{L_1}$ and the $\mathbf{L_1 + L_2}$ phase. The total increase in surface pressure was higher for NaIBA than for NaIAA. In addition, the $\mathbf{L_1}$, $\mathbf{L_1 + L_2}$ and $\mathbf{L_2}$ phases were shifted to the right, *i.e.* the surface pressure started to increase earlier. The curves converged at high surface pressure.

A different curve shape was observed for a DPPC monolayer with pure water as subphase at 37 °C. In accordance to what has been reported in the literature,[57,58] the DPPC isotherm was shifted to higher surface pressure at fixed area per molecule. In general, the phase transitions were less visible. The flat coexistence region $\mathbf{L_1 + L_2}$ was dramatically decreased and less horizontal. In contrast, the liquid expanded phase $\mathbf{L_1}$ was significantly increased. The surface collapse occurred at lower surface pressure compared to the isotherms recorded at room temperature. The observed behaviour is attributed to increased thermal motion of the surfactant chains causing increased surface pressures at the same calculated value of molecular surface area and thereby an extended $\mathbf{L_1}$ phase.[58]

Similar to the findings for the auxins, the presence of NaDHEAS in the subphase increased the surface pressure at a fixed area per molecule. It led to a curve shift to the right and an expansion of the $\mathbf{L_1}$ phase towards higher area per molecule.

A specific interaction of Hofmeister anions with DPPC monolayers at the water/air interface has been reported by Aroti et al.[59] The presence of chaotropic anions in the aqueous subphase was observed to result in an increase of the surface pressure at a fixed area per molecule depending on the amount of added salt. The increase followed the Hofmeister series with a stronger impact on the surface pressure caused by more chaotropic anions. Minor influences on the liquid condensed $\mathbf{L_2}$ phase were observed, while the liquid extended $\mathbf{L_1}$ phase was found to be strongly affected by penetration of the ions into the interfacial region. An entropic gain by the release of water molecules from the interface was assumed to be the main driving force.

The addition of the studied hormones to the aqueous subphase in concentrations several magnitudes lower than the Hofmeister salts caused similar effects. Just as Hofmeister salts, the sodium salts of the studied hormones influenced the $\mathbf{L_1}$ and the coexisting $\mathbf{L_1 + L_2}$ phase much more than the $\mathbf{L_2}$ phase, subject to the following difference: the addition of Hofmeister salts led to an expansion of the $\mathbf{L_1}$ phase and the $\mathbf{L_1 + L_2}$ phase was decreased. In contrary, the hormones caused a shift of the whole curve, which means an earlier start of $\mathbf{L_1}$, but also $\mathbf{L_1 + L_2}$ and $\mathbf{L_2}$ when compressing the surface. It is assumed that the hormones penetrate into the interfacial area. Analogous to the salts, it is driven by the release of bound hydration water through ion specific interactions of the interfacial ions.

According to Collins's concept and the chaotropicity of the headgroups, the interaction between the sulphate group of NaDHEAS and the choline head group of DPPC will be energetically more favoured compared to the same interaction with the acetate group of NaIAA and NaIBA. Another significant driving force (and maybe the dominating one) is the hydrophobic effect caused by the amphiphilicity of the hormone compounds and the resulting surface activity. In contrast to Hofmeister salts, amphiphilic hormones can interact not only with the DPPC head group, but also with the hydrophobic tails. Especially in the low-density regime, *i.e.* the disordered liquid extended state of the monolayer, the hormones are able to adsorb to the surface, join the present DPPC molecules and increase the surface pressure. With increasing DPPC density at the interface, it is expected that the hormone molecules are suppressed into the bulk solution. As a result, the isotherms are changed in the above-mentioned phase regions, but not at very high surface pressures near the collapse. The fact that the hormones can cause significant changes in the monolayer at low concentrations compared to the salts, underlines the high significance of the hydrophobic effect in the interfacial hormone-monolayer interaction.

Fig. 4.5.2-2 shows the surface pressure π as a function of the square root of the additive concentration in the subphase at a constant molecular area of $A_m = 0.75$ nm^2. Nearly linear correlations were found for NaIAA and NaIBA with a higher slope for NaIBA. In contrast, the curve of NaDHEAS was rather sigmoidal. This difference is probably caused by the stronger surface activity of NaDHEAS and a higher influence of the hydrophobic interactions. It might also be attributable to the elevated temperature. According to Aroti *et al.*,[59] the values obtained for the slopes of the linear curves of such a plot are ion specific. They increase with increasing chaotropic character of the anion. Accordingly, they obtained the highest slope for SCN^- and an order corresponding to the Hofmeister series. The same plot was applicable for the hormones and resulted in linear curves for NaIAA and NaIBA. In this respect, it is believed that the determination of monolayer interactions is another suitable method for evaluating the salting-in ability of hydrotropes and their hydrotropic efficiency. It revealed a hydrotropic efficiency of the hormones in the following order (neglecting the non-linearity of the NaDHEAS curve): NaDHEAS > NaIBA > NaIAA, which corresponds to findings of the former experiments.

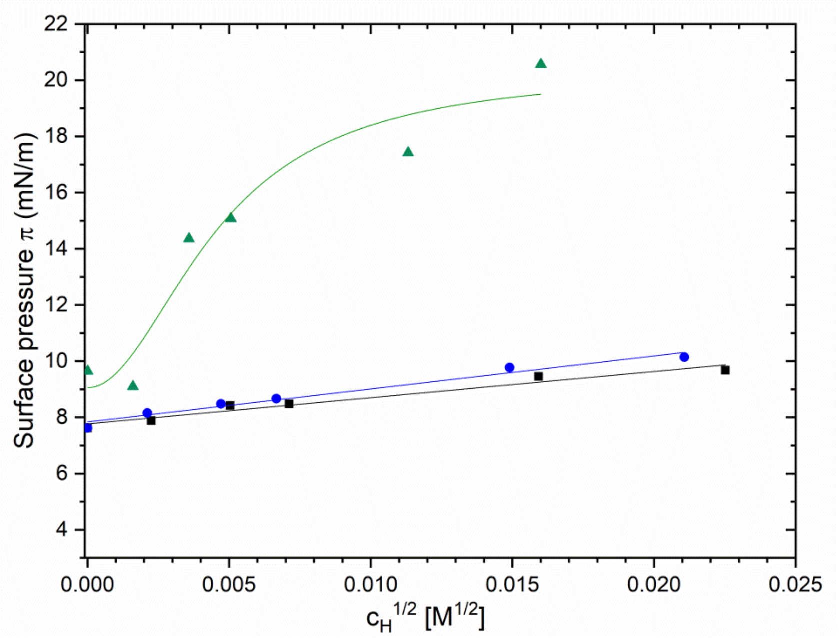

Fig. 4.5.2-2: DPPC monolayer surface pressure as a function of the square root of hormone concentration of NaDHEAS (▲),NaIAA (■) and NaIBA (●) in the subphase. The area per molecule A_m *is 0.75* nm^2 *and the temperature is 37 °C for NaDHEAS and 25 °C for NaIAA and NaIBA.*

From the Langmuir trough experiments with hormones in the aqueous subphase, NaDHEAS concentrations of 10^{-5} M were found to be required to exhibit effects on a phospholipid monolayer, while a concentration of 10^{-4} M was necessary for an analogous effect of the auxins. In case of NaDHEAS, this result corresponds to the findings for other steroid hormones in terms of surface pressure isotherms.[60] A previous study about the influence of plant hormones on phospholipid monolayers reported monolayer destabilization in the presence of only 10^{-6} M IAA, when the surface pressure was left to equilibrate for a while.[61] In addition, IAA in concentrations above 10^{-5} M was found to inhibit plant growth.[62] This roughly corresponds to the experimentally determined concentrations, upon which auxins influence DPPC monolayers. The inhibition of plant growth at high auxin concentrations is concluded to be a result of the rigidification of the cell membrane by auxin penetration, occurring at concentrations, where the receptor and growth activity is already saturated.

For both hormone classes, it is imaginable and even probable that they occur in biological systems in concentrations sufficiently high for phospholipids to be influenced. In this regard, the phospholipid monolayer interaction is relevant for the prediction of interactions of hormones with biological membranes. In contrast to specific hormone-receptor interactions, which are observed at even lower concentrations, the monolayer interactions are of non-specific nature.

4.6 Conclusion

Predominantly, this study revealed that the amphiphilic structure of the tested hormones NaDHEAS, NaIAA and NaIBA provided them with surface activity, a more or less intense tendency to self-assemble, hydrotropic efficiency and the ability to interact with phospholipid monolayers. Throughout this study, the hormones were compared to the typical surfactant SDS and the typical hydrotrope NaSal. Repeatedly, the following order was found in the strength of the observed effects: SDS > NaDHEAS > NaIBA > NaIAA ≈ NaSal. It holds true for the ability to decrease the surface tension of water, the hydrotropic efficiency in terms of solubilizing the hydrophobic dye DR13 and the salting-in ability on a water/PGE mixture. The resulting implication was that NaIAA and NaIBA are natural hydrotropes, whereas NaDHEAS is to be understood as an intermediate case between a hydrotrope and a surfactant. It is imaginable that they promote the solubilization of hydrophobic components in the organism and that this is a relevant side-function of the studied hormones. However, it should be considered that threshold concentrations in 10^{-2} M range for NaDHEAS and 10^{-1} – 10^{0} M range for auxins are required. The presence of such high concentrations in biology has not been confirmed, so far. However, it is believed that these high concentrations are not impossible at specific locations in the cell. Lower concentrations of 10^{-5} M for NaDHEAS and 10^{-4} M for auxins were sufficient to interact with a phospholipid monolayer. The change in surface pressure as a function of additive concentration was found to be suitable to evaluate the hydrotropic efficiency of the hormones. It delivered the same trend in results as all other experiments.

As shown in section 4.4.3, NaDHEAS inhibited egg white precipitation compared to a reference sample and could play a role in protein stability in the brain. In this way, the theory that NaDHEAS plays a role in Alzheimer's disease is maintained from a physical-chemical point of view. The mental disorder in affected patients is related to increased protein precipitation in the brain and could be promoted by decreased levels of DHEAS in elderly people.[22,50,51] In the same manner, it is possible that auxins promote the solubilization of other biomolecules in the plant, such as cytokinins and in this way control their action. As expected, the physical-chemical screening of DHEAS, IAA and IBA does not deliver a full clarification of the open questions about their biological functions and mechanisms. However, it could be shown that besides specific receptor interactions at low hormone concentrations, they are potentially able to non-specifically interact at interfaces, *e.g.* with biological membranes and in terms of self-aggregation and the solubilization of hydrophobic substances. The obtained results will be helpful for further biological investigations.

It has to be mentioned that the stability of the aqueous hormone solutions was limited. This was observed from a time-dependent DLS study of NaDHEAS and the occurrence of turbidity of the solutions after approximately two days. It is most likely that this is caused by progressing hydrolysis and the formation of desulfonated DHEA. Furthermore, this finding indicates that the organism has developed a subtle way to control hydrolysis and stabilize the DHEA/DHEAS equilibrium. The assumption of DHEA inclusion into DHEAS aggregates in aqueous solution is an interesting point that could be further investigated in order to find out, if this is also true for biological fluids. Discolouration of the auxin solutions was observed after a few days and can be rationalized by their light- and oxidation-sensitivity.[7]

It is suggested that not all of the studied hormones as such are promising natural materials for green chemistry. As the biological functions of hormones are not entirely clarified, the consequences of humans and environment coming into contact with hormones are unknown in some respects. The DHEA/DHEAS system is classified as potentially toxic and carcinogenic. IBA is toxic if swallowed. IAA in turn is rated as a harmless chemical and a promising candidate as green and natural hydrotrope, e.g. for agrochemical formulations or for the extraction of other biomolecules from biomaterial. More interesting in terms of green chemistry is the following concept: as generally known, hormones are capable of forming specific receptor interactions at very low concentrations. It is suggested that they are also able to interact non-specifically when present in higher concentrations. This can happen in form of self-aggregation, solubilization enhancement and interfacial or membrane interactions. IAA, for example, was found to act as growth promoter in plants, when present in low concentrations adequate for specific receptor interactions. In contrast, when present at higher concentrations, it inhibits plant growth. However, if and when in particular this principle is used by nature has to be investigated further by biological research. Possibly, this might be applicable as green chemistry concept, *e.g.* in sensor techniques.

4.7 Experimental Part

In general, aqueous solutions of DHEAS were prepared using deionized Millipore water with a resistivity of 18 MΩ·cm. The pH of the auxin solutions was adjusted to a value of 7 with sodium hydroxide solution. Calculations of NaDHEAS solution concentrations were conducted with the molar mass of the anhydrous compound. NaIAA and NaIBA concentrations were calculated with the molar mass of the protonated compound, as an equilibrium between protonated and deprotonated auxins was expected. Unless stated otherwise, the physical-chemical analysis of the auxins was conducted at 25 °C. When possible, measurements with NaDHEAS were performed at 37±0.5 °C in order to resemble physiological conditions and to increase its otherwise limited water solubility.

4.7.1 Chemicals

The chemicals used in this chapter are listed in Tab. 4.7.1-1 specifying their purity and their supplier.

Tab. 4.7.1-1: Chemicals used in this chapter, their purity and their supplier.

	Purity	Supplier
NaDHEAS	>98 %	TCI
IAA	98 %	Sigma Aldrich
IBA	≥99 %	Sigma Aldrich
NaSal	99.5 %	Merck
SDS	ultrapure	AppliChem
DR13	95 %	Sigma Aldrich
PnP	99 %	Sigma Aldrich
DPnP	≥98.5 %	Sigma Aldrich
DPPC	>99 %	Avanti Polar Lipids

4.7.2 Surface Tension Measurements

Surface tension curves of NaDHEAS, NaIAA, NaIBA and NaSal were recorded at 37 °C and 25 °C, respectively. The pendant drop technique utilizing a PAT-1M profile analysis tensiometer supplied by SINTERFACE Technologies (see section 2.6.6.1) was used. The drop was allowed to equilibrate for 300 s, whereas the values recorded during the last 100 s were taken for calculating an average equilibrium surface tension value. This procedure was repeated twice, so that the average of three measurements formed the equilibrium surface tension of one solution. In the course of measuring the equilibrium surface tension of highly concentrated solutions (NaIAA, NaIBA and NaSal), a density adjustment has been conducted by the provided tensiometer software.

4.7.3 Conductivity Measurements

The conductivity of a NaDHEAS solution was measured as a function of its concentration at 37±0.5 °C in order to get information on the self-aggregation behaviour. A volume of 15 ml at a concentration just below the solubility limit was filled into a tempered measuring cell with a magnetic stirrer. It was diluted stepwise by the addition of Millipore water. After each addition, it was left to mix and equilibrate for 30 s, before the conductivity value was read off. The conductivity was determined by means of a WTW Cond730 conductivity meter with TetraCon325 electrode.

4.7.4 Dynamic Light Scattering

Concentration dependent DLS measurements were conducted at temperatures of 37 °C for NaDHEAS and at 25 °C for NaIAA and NaIBA. The measuring system and sample preparation was equal to what has been reported in section 2.6.7.

4.7.5 Solubility

4.7.5.1 Disperse Red 13

Aqueous stock solutions of the tested hydrotropes were prepared with Millipore water. They were diluted to obtain the desired concentrations. An excess of DR13 was added to at least three samples of each concentration. NaDHEAS and auxin solutions were stirred at 37 °C and 25 °C, respectively, for 2 h, before they were filtered with a 0.2 μm CA filter. The amount of dissolved DR13 was determined by UV/Vis spectrometry at a wavelength of 503 nm using an Agilent Technologies Varian Cary 3E spectrophotometer. Samples were diluted and re-measured, when the absorption was above 1.5.

4.7.5.2 Chicken Egg-White

A volume of 0.6 ml NaDHEAS solution was mixed with 0.4 ml aqueous egg-white solution without biological buffer at 40 °C. The mixtures were heated and cloud points were determined. The egg-white solution was kindly provided by Johannes Mehringer. It was prepared by cracking a fresh egg and isolating the egg-white portion. A 50 wt% aqueous solution of egg-white was centrifuged for 10 min. The supernatant was taken and diluted in a ratio of 1 : 2 with Millipore water. The final protein content of the solution was assumed to be 1.8 wt%.

4.7.6 Determination of the Lowest Solution Temperatures of Water/Propylene Glycole Ether Mixtures

Mixtures of PGE with aqueous hormone solution were prepared in a total sample amount of 3 g. PnP in a mass fraction of 0.45 was used in combination with NaDHEAS solutions; DPnP in a mass fraction of 0.55 was mixed with the sodium auxin solutions.

A NaDHEAS stock solution was prepared at 37 °C and diluted to obtain the desired concentrations. Mixtures containing NaDHEAS aqueous solutions and PnP were slowly heated from 27 °C, until the cloud point was reached.

NaIAA and NaIBA stock solution were prepared at room temperature. Mixtures containing sodium auxins and DPnP were cooled to a temperature of approximately 0 °C with an ice bath and slowly heated until the cloud point was reached.

The temperature was monitored by a digital thermometer. The cloud points were determined visually and referred to as LSTs.

4.7.7 Langmuir Film Balance

After extensive cleaning with water and chloroform, approximately 300 ml of the respective aqueous hormone solution was filled into a 20x25 cm tempered (37 °C for DHEAS and 25 °C for auxins) trough of a type 601 Langmuir film balance, provided by Nima Technology. A DPPC monolayer was formed by the dropwise distribution of 50 μl of a respective 0.86 g/L solution in chloroform. To ensure complete evaporation of chloroform, the solvent was left to equilibrate for at least 5 min, before the surface area was decreased at a rate of 20 cm^2/min by moving the designated barrier. The Wilhelmy plate technique with a filter paper platelet was used to measure the surface pressure as the difference in surface tension to the pure solvent. The curves presented in the corresponding Figure represent the average of two or more measurements.

4.8 References

[1] A. Patel, L. Malinovska, S. Saha, J. Wang, S. Alberti, Y. Krishnan, A. A. Hyman, *Science* **2017**, *356*, 753–756.

[2] N. Maninger, O. M. Wolkowitz, V. I. Reus, E. S. Epel, S. H. Mellon, *Front. Neuroendocrinol.* **2009**, *30*, 65–91.

[3] S. Paque, D. Weijers, *BMC Biology* **2016**, *14*, 67–71.

[4] S. Aldred, P. Mecocci, *Arch. Gerontol. Geriatr.* **2010**, *51*, e16–18.

[5] M. Bo, M. Massaia, P. Zannella, G. Cappa, E. Ferrario, I. Rainero, E. Arvat, R. Giordano, M. Molaschi, *Int. J. Geriatr. Psychiatry* **2006**, *21*, 1065–1070.

[6] P. Scheltens, K. Blennow, M. M. B. Breteler, B. de Strooper, G. B. Frisoni, S. Salloway, W. M. van der Flier, *Lancet* **2016**, *388*, 505–517.

[7] E. F. George, M. A. Hall, G.-J. D. Klerk, *Plant Propagation by Tissue Culture*, Springer Netherlands, Dordrecht, **2007**.

[8] P. J. Davies (Ed.) *Plant hormones. Biosynthesis, signal transduction, action!,* 3., rev. ed., Springer, Dordrecht, **2010**.

[9] C. W. Pratt, K. Cornely, *Essential biochemistry,* 3. ed., Wiley, Hoboken, **2014**.

[10] E. H. Starling, *Lancet* **1905**, *166*, 339–341.

[11] C. Taylor, *The Kingfisher science encyclopedia*, Kingfisher, London, **2000**.

[12] "Diabetes", to be found under https://www.encyclopedia.com/medicine/diseases-and-conditions/pathology/diabetes.

[13] C. E. Marx, W. T. Trost, L. Shampine, F. M. Behm, L. A. Giordano, M. W. Massing, J. E. Rose, *Psychopharmacol.* **2006**, *186*, 462–472.

[14] B. N. Chimote, N. M. Chimote, *Vitam. Horm.* **2018**, *108*, 223–250.

[15] N. V. Bhagavan, *Medical biochemistry,* 4th ed., Harcourt/Academic Press, San Diego, **2002**.

[16] S. J. Webb, T. E. Geoghegan, R. A. Prough, K. K. Michael Miller, *Drug Metab. Rev.* **2006**, *38*, 89–116.

[17] a) W. E. Rainey, B. R. Carr, H. Sasano, T. Suzuki, J. I. Mason, *TEM* **2002**, *13*, 234–239; b) W. L. Miller, *Acta Paediatr.* **1999**, *88*, 60–66.

[18] T. A. Quinn, S. R. Robinson, D. Walker in *Sex Hormones in Neurodegenerative Processes and Diseases* (Ed.: G. Drevenšek), InTech, London, **2018**.

[19] a) C. Berr, S. Lafont, B. Debuire, J. F. Dartigues, E. E. Baulieu, *PNAS* **1996**, *93*, 13410–13415; b) A. Weizman, M. S. Ritsner (Eds.) *Neuroactive steroids in brain functions, behavior, and disorders. Novel strategies for research and treatment*, Springer, Dordrecht, **2008.**

[20] a) A. J. Morales, J. J. Nolan, J. C. Nelson, S. S. Yen, *J. Clin. Endocrinol. Metab.* **1994**, *78*, 1360–1367; b) H. Nawata, T. Yanase, K. Goto, T. Okabe, K. Ashida, *Mech. Ageing Dev.* **2002**, *123*, 1101–1106.

[21] a) P. Gallagher, S. Watson, M. S. Smith, A. H. Young, I. N. Ferrier, *Schizophr. Res.* **2007**, *90*, 258–265; b) M. Ritsner, A. Gibel, E. Ram, R. Maayan, A. Weizman, *Eur.*

Neuropsychopharmacol. **2006**, *16*, 137–146; c) M. Ritsner, R. Maayan, A. Gibel, A. Weizman, *Eur. Neuropsychopharmacol.* **2007**, *17*, 358–365; d) R. D. Strous, R. Maayan, R. Lapidus, R. Stryjer, M. Lustig, M. Kotler, A. Weizman, *Arch. Gen. Psychiatry* **2003**, *60*, 133–141.

[22] T. Yanase, M. Fukahori, S. Taniguchi, Y. Nishi, Y. Sakai, R. Takayanagi, M. Haji, H. Nawata, *Endocr. J.* **1996**, *43*, 119–123.

[23] a) S. Bastianetto, C. Ramassamy, J. Poirier, R. Quirion, *Brain Res. Mol. Brain Res.* **1999**, *66*, 35–41; b) J. Grimley Evans, R. Malouf, F. Huppert, J. K. van Niekerk, *Cochrane Database Syst. Rev.* **2006**, CD006221; c) R. R. Watson, A. Huls, M. Araghinikuam, S. Chung, *Drugs aging* **1996**, *9*, 274–291; d) E. B. Strauss, D. E. Sands, A. M. Robinson, W. J. Tindall, W. A. H. Stevenson, *Br. Med. J.* **1952**, *2*, 64–66.

[24] a) N. Pluchino, M. Russo, A. N. Santoro, P. Litta, V. Cela, A. R. Genazzani, *Neuroscience* **2013**, *239*, 271–279; b) H. F. Sakr, K. I. Khalil, A. M. Hussein, M. S. A. Zaki, R. A. Eid, M. Alkhateeb, *J. Physiol. Pharmacol.* **2014**, *65*, 41–53.

[25] F. W. Went, K. V. Thimann, *Phytohormones*, The Macmillan Company, New York, **1937**.

[26] A. C. Leopold, *Auxins and Plant Growth*, University of California Press, Berkeley, **1955**.

[27] P. M. Dey, J. B. Harborne (Eds.) *Plant biochemistry*, Acad. Press, San Diego, **1997**.

[28] A. W. Woodward, B. Bartel, *Ann. Bot.* **2005**, *95*, 707–735.

[29] D. Balasubramanian, V. Srinivas, V. G. Gaikar, M. M. Sharma, *J. Phys. Chem.* **1989**, *93*, 3865–3870.

[30] P. H. Elworthy, K. J. Mysels, *J. Colloid Interface Sci.* **1966**, *21*, 331–347.

[31] K. Lunkenheimer, G. Czichocki, R. Hirte, W. Barzyk, *Colloids Surf., A* **1995**, *101 (2)*, 187–197.

[32] S. Feng, P. M. Bummer, *Langmuir* **2012**, *28*, 16927–16932.

[33] M. J. Rosen, *Surfactants and Interfacial Phenomena*, John Wiley & Sons, Inc, Hoboken, NJ, USA, **2004**.

[34] a) A. Dominguez, A. Fernandez, N. Gonzalez, E. Iglesias, L. Montenegro, *J. Chem. Educ.* **1997**, *74*, 1227–1231; b) A. Khan, S. Shah, *J. Chem. Soc. Pak.* **2008**, *30*; c) D. López Díaz, M. M. Velázquez, *J. Chem. Educ.* **2007**, *12*, 1–4.

[35] T. Buchecker, S. Krickl, R. Winkler, I. Grillo, P. Bauduin, D. Touraud, A. Pfitzner, W. Kunz, *PCCP* **2017**, *19*, 1806–1816.

[36] R. Winkler, T. Buchecker, F. Hastreiter, D. Touraud, W. Kunz, *PCCP* **2017**, *19*, 25463–25470.

[37] P. Bauduin, L. Wattebled, D. Touraud, W. Kunz, *Z. Phys. Chem.* **2004**, *218*, 631–641.

[38] G. Grundl, M. Müller, D. Touraud, W. Kunz, *J. Mol. Liq.* **2017**, *236*, 368–375.

[39] F. Hofmeister, *Archiv f. experiment. Pathol. u. Pharmakol* **1888**, *24*, 247–260.

[40] a) G. Karlstroem, A. Carlsson, B. Lindman, *J. Phys. Chem.* **1990**, *94*, 5005–5015; b) N. Pandit, T. Trygstad, S. Croy, M. Bohorquez, C. Koch, *J. Colloid Interface Sci.* **2000**, *222*, 213–220.

[41] a) C. Holtzscherer, F. Candau, *J. Colloid Interface Sci.* **1988**, *125*, 97–110; b) H. Schott, *J. Colloid Interface Sci.* **1998**, *205*, 496–502; c) H. Schott, A. E. Royce, *J. Pharm. Sci.* **1983**, *72*, 1427–1436.

[42] K. D. Collins, M. W. Washabaugh, *Q. Rev. Biophys.* **1985**, *18*, 323–422.

[43] P. Ball, J. E. Hallsworth, *PCCP* **2015**, *17*, 8297–8305.

[44] Y. Marcus, *Chem. Rev.* **2009**, *109*, 1346–1370.

[45] a) W. Kunz, J. Henle, B. W. Ninham, *Curr. Opin. Colloid Interface Sci.* **2004**, *9*, 19–37; b) Y. Zhang, P. S. Cremer, *Curr. Opin. Colloid Interface Sci.* **2006**, *10*, 658–663.

[46] W. Kunz, *Curr. Opin. Colloid Interface Sci.* **2010**, *15*, 34–39.

[47] N. Vlachy, B. Jagoda-Cwiklik, R. Vácha, D. Touraud, P. Jungwirth, W. Kunz, *Adv. Colloid Interface Sci.* **2009**, *146*, 42–47.

[48] C. M. Dobson, *Semin. Cell Dev. Biol.* **2004**, *15*, 3–16.

[49] C. M. Dobson, *Philos. Trans. R. Soc. London, Ser. B* **2001**, *356*, 133–145.

[50] P. J. Thomas, B. H. Qu, P. L. Pedersen, *Trends Biochem. Sci.* **1995**, *20*, 456–459.

[51] S. Majd, J. H. Power, H. J. M. Grantham, *BMC Neuroscience* **2015**, *16:69*, 1–13.

[52] a) E. D. N. S. Abeyrathne, H. Y. Lee, D. U. Ahn, *Poultr. Sci.* **2013**, *92*, 3292–3299; b) J. Kovacs-Nolan, M. Phillips, Y. Mine, *J. Agric. Food. Chem.* **2005**, *53*, 8421–8431.

[53] Y. Mine, T. Noutomi, N. Haga, *J. Agric. Food. Chem.* **1990**, *38*, 2122–2125.

[54] I. Langmuir, *J. Am. Chem. Soc.* **1917**, *39*, 1848–1906.

[55] R. Kumar, V. Manjuladevi in *Molecular Interactions* (Ed.: A. Meghea), InTech, London, **2012**.

[56] S. J. Singer, G. L. Nicolson, *Science* **1972**, *175*, 720–731.

[57] a) H. Yun, Y.-W. Choi, N. J. Kim, D. Sohn, *Bull. Korean Chem. Soc.* **2003**, *24*, 377–383; b) D. D. Baldyga, R. A. Dluhy, *Chem. Phys. Lipids* **1998**, *96*, 81–97; c) J. M. Crane, G. Putz, S. B. Hall, *Biophys. J.* **1999**, *77*, 3134–3143.

[58] S. L. Duncan, R. G. Larson, *Biophys. J.* **2008**, *94*, 2965–2986.

[59] A. Aroti, E. Leontidis, E. Maltseva, G. Brezesinski, *J. Phys. Chem. B* **2004**, *108*, 15238–15245.

[60] N. L. Gershfeld, *J. Gen. Physiol.* **1971**, *58*, 650–666.

[61] B. Gzyl-Malchera, M. Filek, G. Brezesinski, A. Fischer, *Z. Naturforsch., C: Biosci.* **2007**, *62*, 55–60.

[62] R. J. Foster, D. H. McRae, J. Bonner, *PNAS* **1952**, *38*, 1014–1022.

Chapter 5
Concluding Remarks

5 Concluding Remarks

The presented thesis comprising three individual studies is intended to develop chemical solvents and solubility concepts according to the principles of green chemistry.

The first study aimed to design green, functional substances on the basis of the naturally occurring *L*-carnitine. Carnitine esters resulting from the esterification of the carboxylic group of this basic substance were found to grant access to ionic liquids, hydtrotropes and surfactants. In particular, an alternative reaction pathway employing *L*-carnitine, methylsulfonic acid and *n*-alkyl alcohols as starting materials was developed. An anion exchange was shown to be feasible by an exchange column. Advantageously, an evaluation of this synthesis route regarding cost, energy consumption, solvent consumption, waste generation and hazard potential revealed an improvement compared with the previously used method. Taking into account the thermal properties of the resulting compounds, carnitine alkyl ester bromides characterized by their alkyl chain lengths from C_4 to C_{14} were classified as ionic liquids in view of their melting temperatures below 100 °C. The butyl and hexyl homologues were found to belong to the subclass of room temperature ionic liquids. The same holds for carnitine ethyl ester acetate. As a drawback, they suffer from extremely high viscosities and a sticky texture, which made them rather unhandy and inconvenient to use. Although working at elevated temperatures was able to remedy these practical issues, this approach is in contradiction with the carnitine ionic liquids' sensitivity towards thermal degradation. As the incorporation of the alkyl ester function imparted a certain amphiphilicity to the carnitine-based substances, they exhibited hydrotropic or surfactant character, depending on the alkyl chain length. More specially, a transition from hydrotropic to surfactant-like character was determined to be around C_8 from investigating the interfacial and aggregation behaviour of the homologues series of carnitine alkyl ester bromides in aqueous solution. Comparing carnitine alkyl ester surfactants with either a bromide or a mesylate counter-ion revealed a higher 'surfactant efficiency' of the mesylate species, but a more pronounced 'surfactant effectiveness' of the respective bromide compounds, which was ascribed to specific ion effects. An evaluation of cytotoxicity and solubilizing performance of the model solute vanillin in comparison to conventional hydrotropes and surfactants led to the assumption that the investigated carnitine ester compounds hold promise as green alternatives. However, it remains to be pointed out that the *L*-carnitine used in this study was manufactured synthetically and that the application of starting compound extracted from natural sources will be more cost-intensive.

The second part of this thesis dealt with a rather new solvent class referred to as deep eutectic solvents. They offer considerable variability and the possibility to modify the resulting solvent properties, as they are composed of two or more compounds. Two types of deep eutectic solvents were studied:

(1) Betaine- and carnitine-based quaternary ammonium compounds in combination with carboxylic acids and several further H-bond donors: Employing betaine and carnitine zwitterions or their alkyl ester derivatives resulted in the formation of a number of novel deep eutectic solvents. In contrast, almost none of the mixtures containing betaine or carnitine hydrochloride were found to form homogeneous liquids. A proton exchange was evidenced for the particular combination of a quaternary ammonium zwitterion with a carboxylic acid. Therefore, the presence of a certain IL character of the resulting deep eutectic solvents was concluded. The betaine- and carnitine-based deep eutectic solvents were finally evaluated for their ability to solubilize the natural biopolymer pigment melanin. They exhibited lower performance compared to amine-based solvents. Therefore, they were considered to have no prospect for this particular application.

(2) Deep eutectic solvents containing biologically relevant components: In particular, the combination of choline chloride with a natural carboxylic acid exhibiting antioxidant activity, such as caffeic acid or gallic acid, resulted in the formation of liquid homogeneous mixtures. The melting temperature of the gallic acid-based solvents could be decreased further by the addition of a second H-bond donor. The application of these newly formed antioxidant deep eutectic solvents as ephemeral solvents in the synthesis of pharmaceutically relevant ester-type substances was investigated. Of the three tested reactions, only the formation of shikimic acid ethyl ester is still in consideration to benefit from the presence of the deep eutectic solvents, but requiring further investigations. In addition, the antioxidant solvents are considered to be interesting ingredients in chemical formulations, such as cosmetics or food. It allows for keeping such formulations more simple, as the addition of further antioxidant ingredients can be avoided.

The addition of a third component and the application of a bulkier quaternary ammonium derivative, such as a carnitine alkyl ester instead of *L*-carnitine, were found to be suitable methods for decreasing the melting temperatures of the studied types of deep eutectic solvents even further.

The interfacial behaviour of surfactants at the deep eutectic solvent-graphite interface was studied with the intention to add to the general knowledge in the application of this solvent class in electrochemistry. The formation of infinitely elongated parallel surfactant aggregates, either in form of a flat surfactant monolayer or hemicylindrical micelles, at the graphite surface was observed by atomic force microscopy. Attractive van der Waals interactions between the hydrophobic graphite surface and the surfactant alkyl chains were concluded to be the dominant driving force for these findings. This is further supported by screening effects of the deep eutectic solvent environment.

The interfacial properties and aggregation behaviour of natural hormones, in particular sodium salts of dehydroepiandrosterone sulphate, indole-3-acetic acid and indole-3-

butyric acid in aqueous solution were investigated. These substances were found to decrease the surface tension of water, to exhibit hydrotropic efficiency in terms of solubilizing a hydrophobic dye and a salting-in ability on a water/PGE mixture. In addition, a dipalmitoylphosphatidylcholine probe interfacial monolayer was found to be influenced by the presence of the studied hormones in the aqueous subphase, above a certain concentration threshold. All in all, a hydrotropic character was ascribed to the auxin hormones, while the behaviour of dehydroepiandrosterone sulphate was found to be in between typical hydrotropes and surfactants. The conductance of egg white solubility tests in aqueous solutions of dehydroepiandrosterone sulphate revealed a protein stabilizing effect of this hormone. This could lead to a precipitation of stabilized proteins when the hormone level decreases, which is regularly the case for dehydroepiandrosterone in elderly people. Consequently, its suggested involvement in Alzheimer's disease is possible, in view of the propagated accumulation of proteins in the brain. The hydrotropic character of auxins might rationalize the synergistic effect occurring with cytokinins, under the assumption of an involvement of auxins in their solubilization in biological systems. In nature, hormones typically occur at concentrations lower than the concentrations of the studied aqueous solutions. However, the presence of local environments, such as protein pockets, characterized by concentrations significantly above the nominal concentrations cannot be excluded. The integration of the studied hormones into a dipalmitoylphosphatidylcholine monolayer, which often functions as simplified membrane model, was observed at concentrations even below the millimolar range. The reported growth inhibitory effect of auxins at concentrations exceeding 10^{-5} M can therefore be related to the rigidification of the cell membrane by auxin penetration. The conducted study of the amphiphilic hormones provided information on their physical-chemical properties in aqueous solution, which can be valuable for further investigations of their biological functions.

When finally evaluating the usability of the studied substances, substance classes and concepts, several points are to be mentioned:

- As described in the context of the theoretical framework of this thesis, ionic liquids were strongly hyped in recent decades. However, extensive research in this field resulted merely in a few valuable applications in industry. This minor applicability is - among other aspects - ascribed to limitations in terms of elevated viscosity, sticky texture, hygroscopicity and thermal degradation sensitivity, which was equally confirmed for the ionic liquids and deep eutectic solvents studied in this work. It remains to be clarified, whether the solvent class of deep eutectic solvents will experience the same fate as ionic liquids, as their research is only emerging. In general, their odds for being used in industry are believed to be higher compared to ionic liquids due to lower cost and easier preparation.

- In view of the above-mentioned drawbacks of pure ionic liquids and deep eutectic solvents, it might be worth considering the use of co-solvents to ease their practical applicability in industry. Most probably, this will change the specific, but impart other interesting characteristics to these solvents. A review article of Douglas MacFarlane and co-workers published in 2017 discusses these solvent mixtures in detail as the '4th evolution of ionic liquids'.[1]
- Hydrotropes and surfactants are generally applied for increasing the compatibility between hydrophobic and hydrophilic substances. Therefore, they are particularly interesting for applications in chemical formulations or extraction processes. The use of a hydrotrope or surfactant solution for a chemical reaction only makes sense, when the presence of aggregates adds a special value to the reaction. The modification of *L*-carnitine via esterification resulted in the availability of novel cationic hydrotropes and surfactants with moderate cytotoxicity and eminent performance in enhancing the water compatibility of hydrophobic substances. It remains to be evaluated in direct comparison with the conventionally used substance, whether substances of the new class are applicable as greener standard ingredients in presently used formulations or extraction processes.
- The studied amphiphilic hormones as such are rather uninteresting for their direct use in chemical formulations and consumer products, as the long-term consequences of interactions of hormones with humans and the environment are unknown in some respects. However, indole-3-acetic acid being classified as harmless substance is assumed to be useful in the extraction of particular functional molecules from plant material, as it is expected to be involved in the solubilization of such in nature. Studying the physical-chemical properties of these natural functional molecules, demonstrated their potentially manifold action in several functions in the biological system respective to the given concentration, and as such provide a potentially valuable concept for green chemistry and technology.

The general idea of the research conducted within the scope of this thesis was to contribute to the ongoing progress of green chemistry, which intends to develop more sustainable alternatives for traditional chemicals, products and processes. This work consisted of three individual approaches. The first one focused on the chemical modification, characterization and evaluation of the applicability of a naturally resourced substance. As a second approach, a whole substance class was examined in order to broaden the general knowledge on the characteristics and the applicability of these solvents. The third strategy comprised the investigation of particular biomolecules regarding their mode of action in nature. Eventually, none of these strategies is – from the present point of view – believed to be the 'non-plus-ultra' technique to achieve revolutionary progress in green chemistry. The fact that the greenness of a substance or solvent always depends on the specific application it is used for, significantly complicates fundamental research in the field of green chemistry. In contrast, application-oriented research in green chemistry is considered to be more efficient, *i.e.,* starting with a particular issue/application and searching for a greener alternative. Successful scientific research in the field of green chemistry is considered to require the cooperation of researchers and members of different disciplines and facilities. In particular, theoretical considerations might complement experimental research to identify possible regions of interest. On the other hand, it makes sense to incorporate specialists from industry, who have an improved idea about the feasibility of certain visions and approaches. To conclude, 'green chemistry' and the associated underlying issues have been identified as crucial challenges of present times and first steps have been taken. Nevertheless, an ever-growing joint effort of the research community, industry, politics and, most importantly, 'the consumer' will be required for a sustainable progress of green chemistry.

References

[1] D. R. MacFarlane, A. L. Chong, M. Forsyth, M. Kar, R. Vijayaraghavan, A. Somers, J. M. Pringle, *Faraday Discuss.*, **2018**, *206*, 9–28.

Chapter 6
Appendix

6 Appendix

6.1 Chemical Structures of Deep Eutectic Solvent Components

6.1.1 Hydrogen Bond Acceptors Based on Quaternary Ammonium Compounds

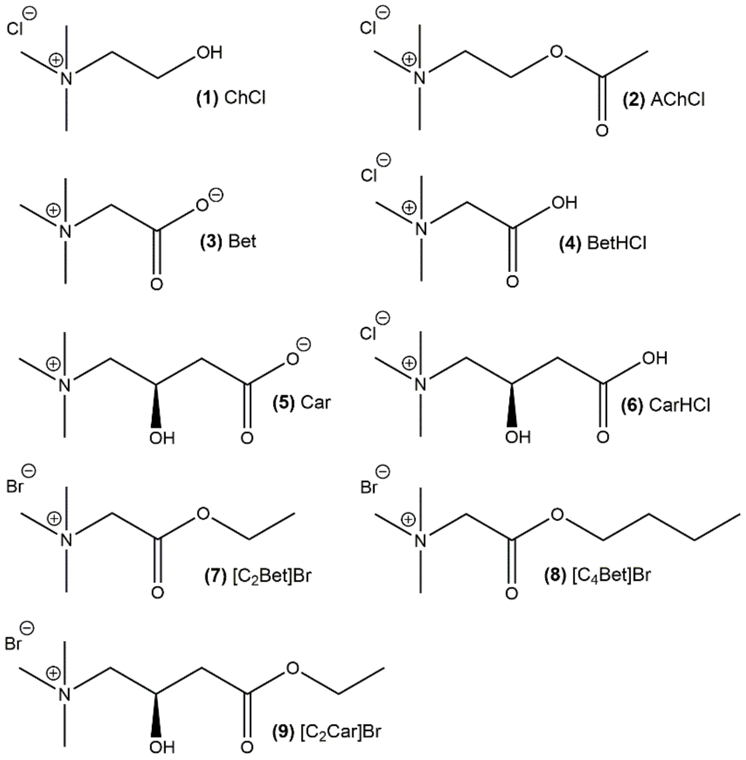
(1) ChCl
(2) AChCl
(3) Bet
(4) BetHCl
(5) Car
(6) CarHCl
(7) [C2Bet]Br
(8) [C4Bet]Br
(9) [C2Car]Br

Fig. 6.1.1-1: Molecular structures of the quaternary ammonium compounds and the respective abbreviations used in the course of chapter 3: (1) choline chloride, (2) acetylcholine chloride, (3) betaine, (4) betaine hydrochloride, (5) carnitine, (6) carnitine hydrochloride, (7) betaine ethyl ester bromide, (8) betaine butyl ester bromide and (9) carnitine ethyl ester bromide.

6.1.2 Hydrogen Bond Donors

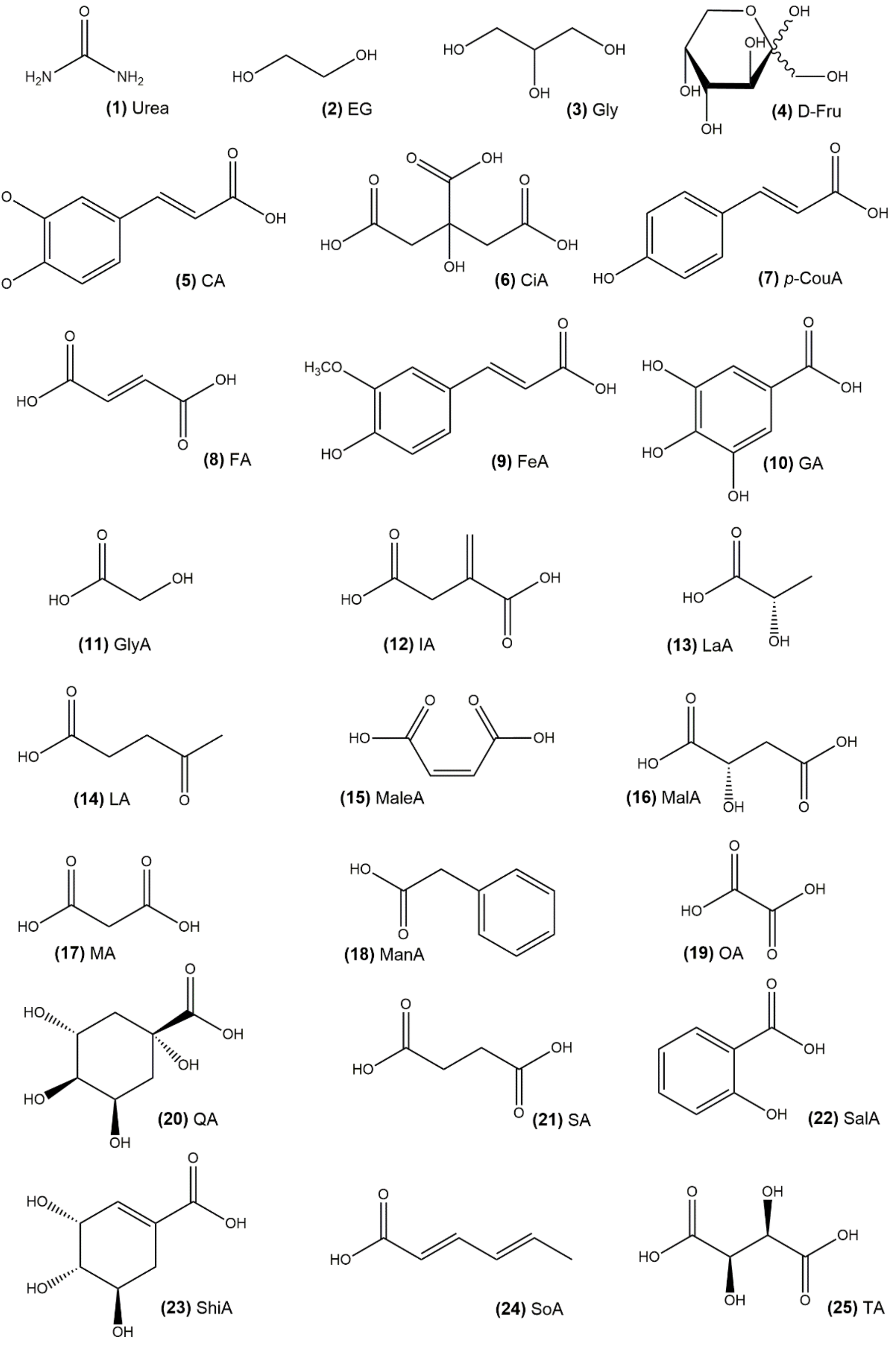

(1) Urea
(2) EG
(3) Gly
(4) D-Fru
(5) CA
(6) CiA
(7) *p*-CouA
(8) FA
(9) FeA
(10) GA
(11) GlyA
(12) IA
(13) LaA
(14) LA
(15) MaleA
(16) MalA
(17) MA
(18) ManA
(19) OA
(20) QA
(21) SA
(22) SalA
(23) ShiA
(24) SoA
(25) TA

Fig. 6.1.2-1: Molecular structures of the hydrogen bond donors and the respective abbreviations used in the course of chapter 3: (1) urea, (2) ethylene glycol, (3) glycerol, (4) D-fructose, (5) caffeic acid, (6) citric acid, (7) p-coumaric acid, (8) formic acid, (9) ferulic acid, (10) gallic acid, (11) glycolic acid, (12) itaconic acid, (13) lactic acid, (14) levulinic acid, (15) maleic acid, (16) malic acid, (17) malonic acid, (18) mandelic acidm (19) oxalic acid, (20) quinic acid, (21) succinic acid, (22) salicylic acid, (23) shikimic acid, (24) sorbic acid and (25) tartaric acid.

6.2 Collection of Mixtures Considered for the Formation of Deep Eutectic Solvents

In the following, several tables summarizing binary and ternary compositions considered for the development of DESs are presented. The formation of a homogeneous, liquid mixture is indicated by the sign '✓'. On the contrary, '✗' represents the experimental observation that no homogeneous mixture was formed.

6.2.1 Binary Mixtures Containing Betaine or Carnitine Zwitterions

Tab. 6.2.1-1: Binary mixtures containing betaine or carnitine considered for the formation of DESs.

HBA	HBD	Molar ratio HBA : HBD	Liquid at rt	Liquid at 90 °C
Bet	CiA	1 : 2	✗	✗
Bet	D-Fru	1 : 1	✗	✗
Bet	FA	1 : 1 2 : 1	✗ ✗	✗ ✗
Bet	GlA	1 : 1	✓	✓
Bet	IA	1 : 2 1 : 1	✗ ✗	✗ ✗
Bet	LA	1 : 2 1 : 1	✓ ✗	✓ ✓
Bet	LaA	1 : 2 1 : 1	✓ ✗	✓ ✓
Bet	MA	1 : 1	✗	✗
Bet	MaleA	1 : 1 2 : 1	✗ ✗	✗ ✗
Bet	ManA	1 : 1	✓	✓
Bet	OA	1 : 2	✗	✗
Bet	SA	1 : 1 2 : 1	✗ ✗	✗ ✗
Bet	SoA	1 : 1	✗	✗
Bet	TA	1 : 1 2 : 1	✗ ✗	✗ ✗
Bet	Urea	1 : 2	✗	✗
Car	CiA	1 : 2	✗	✗
Car	D-Fru	1 : 1	✗	✗
Car	EG	1 : 2	✓	✓
Car	FA	1 : 1 2 : 1	✗ ✗	✗ ✗
Car	GlA	1 : 1	✗	✗
Car	Gly	1 : 2	✓	✓
Car	IA	1 : 2 1 : 1	✗ ✗	✗ ✗
Car	LA	1 : 2 1 : 1	✓ ✗	✓ ✓
Car	LaA	1 : 1	✓	✓
Car	MA	1 : 1	✓	✓

HBA	HBD	Molar ratio HBA : HBD	Liquid at rt	Liquid at 90 °C
Car	MaleA	1 : 1 2 : 1	✓ ✓	✓ ✓
Car	ManA	1 : 1	✗	✗
Car	OA	1 : 2	✗	✗
Car	SA	1 : 1 2 : 1	✓ ✗	✓ ✓
Car	SoA	1 : 1	✗	✗
Car	TA	1 : 1 2 : 1	✗ ✗	✗ ✗
Car	Urea	1 : 2	✓	✓

6.2.2 Binary Mixtures Containing Betaine or Carnitine Hydrochloride

Tab. 6.2.2-1: Binary mixtures containing betaine or carnitine hydrochloride considered for the formation of DESs.

HBA	HBD	Molar ratio HBA : HBD	Liquid at rt	Liquid at 90 °C
CarHCl	CA	1 : 2	✗	✗
CarHCl	CiA	1 : 1	✗	✗
CarHCl	*D*-Fru	1 : 2	✗	✗
CarHCl	GA	1 : 2	✗	✗
CarHCl	IA	1 : 2 1 : 1	✗ ✗	✗ ✗
CarHCl	LA	1 : 4 1 : 3 1 : 2	✗ ✗ ✗	✗ ✗ ✗
CarHCl	MA	1 : 1	✗	✗
CarHCl	TA	1 : 1 2 : 1	✗ ✗	✗ ✗
CarHCl	Urea	1 : 2	✗	✓
BetHCl	CA	1 : 2	✗	✗
BetHCl	CiA	1 : 1	✗	✗
BetHCl	*D*-Fru	1 : 2	✗	✗
BetHCl	GA	1 : 2	✗	✗
BetHCl	IA	1 : 2 1 : 1	✗ ✗	✗ ✗
BetHCl	LA	1 : 4 1 : 3 1 : 2	✗ ✗ ✗	✗ ✗ ✓
BetHCl	MA	1 : 1	✗	✗
BetHCl	TA	1 : 1 2 : 1	✗ ✗	✗ ✗
BetHCl	Urea	1 : 2	✗	✗

6.2.3 Binary Mixtures Containing Betaine or Carnitine Alkyl Esters

Tab. 6.2.3-1: Binary mixtures containing betaine or carnitine alkyl ester salts considered for the formation of DESs.

HBA	**HBD**	**Molar ratio HBA : HBD**	**Liquid at rt**	**Liquid at 90 °C**
[C$_2$Bet]Br	EG	1 : 2	✗	✓
[C$_2$Bet]Br	GlA	1 : 2	✓	✓
[C$_2$Bet]Br	Gly	1 : 2	✓	✓
[C$_2$Bet]Br	IA	1 : 1	✗	✓
[C$_2$Bet]Br	LA	1 : 2	✗	✓
[C$_2$Bet]Br	LaA	1 : 2	✓	✓
[C$_2$Bet]Br	MA	1 : 1	✗	✓
[C$_2$Bet]Br	MaleA	1 : 2	✗	✗
[C$_2$Bet]Br	ManA	1 : 2	✗	✓
[C$_2$Bet]Br	OA	1 : 2	✗	✗
[C$_2$Bet]Br	SA	1 : 2	✗	✗
[C$_2$Bet]Br	SoA	1 : 2	✗	✗
[C$_2$Car]Br	EG	1 : 2	✗	✓
[C$_2$Car]Br	GlA	1 : 2	✓	✓
[C$_2$Car]Br	Gly	1 : 2	✓	✓
[C$_2$Car]Br	LA	1 : 2	✗	✓
[C$_2$Car]Br	LaA	1 : 2	✓	✓
[C$_2$Car]Br	MaleA	1 : 2	✗	✗
[C$_2$Car]Br	ManA	1 : 2	✗	✓
[C$_2$Car]Br	OA	1 : 2	✗	✗
[C$_2$Car]Br	SA	1 : 2	✗	✗
[C$_2$Car]Br	SoA	1 : 2	✗	✗
[C$_4$Bet]Br	CiA	1 : 2	✓	✓
[C$_4$Bet]Br	D-Fru	1 : 2	✓	✓
[C$_4$Bet]Br	EG	1 : 1 1 : 2	✓ ✓	✓ ✓
[C$_4$Bet]Br	GlA	1 : 2	✓	✓
[C$_4$Bet]Br	Gly	1 : 2	✓	✓
[C$_4$Bet]Br	IA	1 : 1	✗	✓
[C$_4$Bet]Br	LA	1 : 2	✓	✓
[C$_4$Bet]Br	LaA	1 : 2	✓	✓
[C$_4$Bet]Br	MA	1 : 1	✓	✓
[C$_4$Bet]Br	MalA	1 : 1	✓	✓
[C$_4$Bet]Br	MaleA	1 : 1	✗	✗
[C$_4$Bet]Br	ManA	1 : 2	✗	✓
[C$_4$Bet]Br	OA	1 : 1	✓	✓
[C$_4$Bet]Br	SoA	1 : 2	✗	✗
[C$_4$Bet]Br	Urea	2 : 1	✗	✓

6.2.4 Binary Mixtures Containing Biologically Relevant Hydrogen Bond Donors

Tab. 6.2.4-1: Binary mixtures containing biologically relevant HBDs with carboxylic acid function considered for the formation of DESs.

HBA	**HBD**	**Molar ratio HBA : HBD**	**Liquid at rt**	**Liquid at 90 °C**
ChCl	CA	2 : 1	✓	✓
		3 : 2	✓	✓
		6 : 5	✓	✓
ChCl	*p*-CouA	2 : 1	✗	✓
ChCl	FeA	1 : 2	✗	✗
		1 : 1	✗	✗
		2 : 1	✗	✓
		3 : 1	✗	✓
ChCl	GA	2 : 1	✗	✓
ChCl	QA	1 : 2	✓	✓
ChCl	SalA	1 : 2	✗	✗
		1 : 1	✗	✓
		2 : 1	✗	✗
ChCl	ShiA	1 : 2	✗	✗
		1 : 1	✗	✗
		3 : 2	✓	✓
		2 : 1	✓	✓
		3 : 1	✓	✓
AChCl	CA	2 : 1	✓	✓
AChCl	*p*-CouA	2 : 1	✗	✓
AChCl	FeA	2 : 1	✗	✓
AChCl	QA	2 : 1	✗	✓
AChCl	SalA	2 : 1	✗	✓
AChCl	ShiA	2 : 1	✗	✗

6.2.5 Ternary Mixtures Containing Gallic Acid

Tab. 6.2.5-1: Ternary mixtures containing gallic acid considered for the formation of DESs.

HBA	**HBD1**	**HBD2**	**Molar ratio HBA : HBD1 : HBD2**	**Liquid at rt**	**Liquid at 90 °C**
ChCl	Urea	GA	2 : 0.75 : 0.25	✗	✓
ChCl	Urea	GA	2 : 0.50 : 0.50	✗	✓
ChCl	Urea	GA	2 : 0.25 : 0.75	✗	✓
ChCl	Urea	GA	1 : 0.75 : 0.25	✓	✓
ChCl	Urea	GA	1 : 0.50 : 0.50	✓	✓
ChCl	Urea	GA	1 : 0.25 : 0.75	✗	✗
ChCl	Urea	GA	1 : 1.50 : 0.50	✓	✓
ChCl	Urea	GA	1 : 1 : 1	✗	✗
ChCl	Urea	GA	1 : 0.50 : 1.50	✗	✗
ChCl	D-Fru	GA	2 : 0.75 : 0.25	✓	✓
ChCl	D-Fru	GA	2 : 0.50 : 0.50	✓	✓

HBA	**HBD1**	**HBD2**	**Molar ratio HBA : HBD1 : HBD2**	**Liquid at rt**	**Liquid at 90 °C**
ChCl	D-Fru	GA	2 : 0.25 : 0.75	✓	✓
ChCl	D-Fru	GA	1 : 0.75 : 0.25	✓	✓
ChCl	D-Fru	GA	1 : 0.50 : 0.50	✗	✗
ChCl	D-Fru	GA	1 : 0.25 : 0.75	✗	✗
ChCl	D-Fru	GA	1 : 1.50 : 0.50	✗	✗
ChCl	D-Fru	GA	1 : 1 : 1	✗	✗
ChCl	D-Fru	GA	1 : 0.50 : 1.50	✗	✗
Car	LA	GA	2 : 0.75 : 0.25	✗	✗
Car	LA	GA	2 : 0.50 : 0.50	✗	✗
Car	LA	GA	2 : 0.25 : 0.75	✗	✗
Car	LA	GA	1 : 0.75 : 0.25	✓	✓
Car	LA	GA	1 : 0.50 : 0.50	✗	✗
Car	LA	GA	1 : 0.25 : 0.75	✗	✗
Car	LA	GA	1 : 1.50 : 0.50	✓	✓
Car	LA	GA	1 : 1 : 1	✗	✗
Car	LA	GA	1 : 0.50 : 1.50	✗	✗

6.3 Nuclear Magnetic Resonance Spectra of Reference Substances According to Section 3.2.2

Carnitine and carnitine hydrochloride were not soluble in deuterated acetonitrile, which was used as NMR solvent for the analysis of the studied Car-CarHCl-MaleA mixtures.

6.3.1 Nuclear Magnetic Resonance Spectrum of Maleic Acid

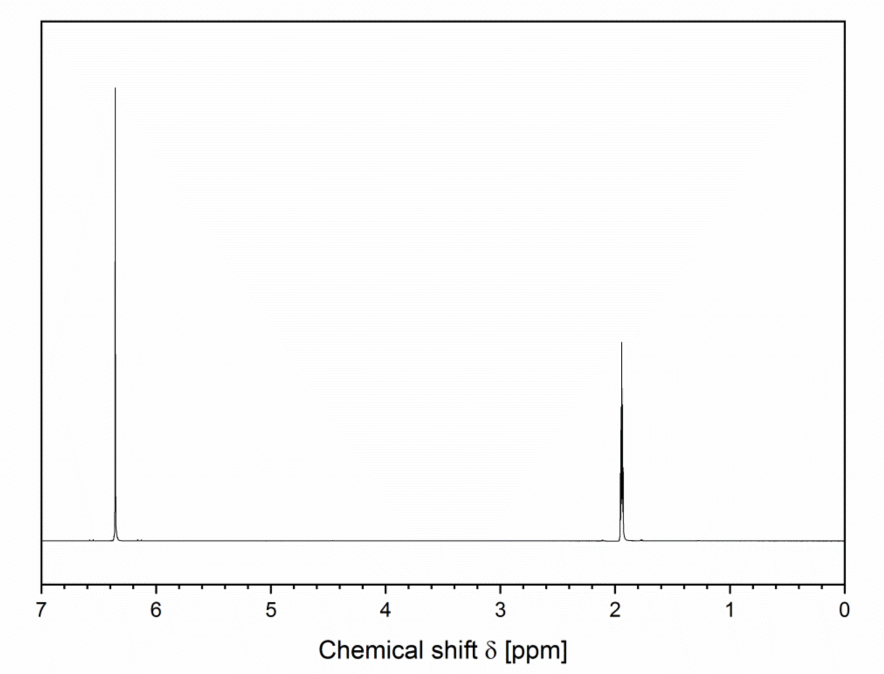

Fig. 6.3.1-1: NMR spectrum of maleic acid in deuterated acetonitrile.

6.4 Complementary Force Curves Recorded by Atomic Force Microscopy

6.4.1 Force Curves of the Pure (ChCl-EG)-Deep Eutectic Solvent

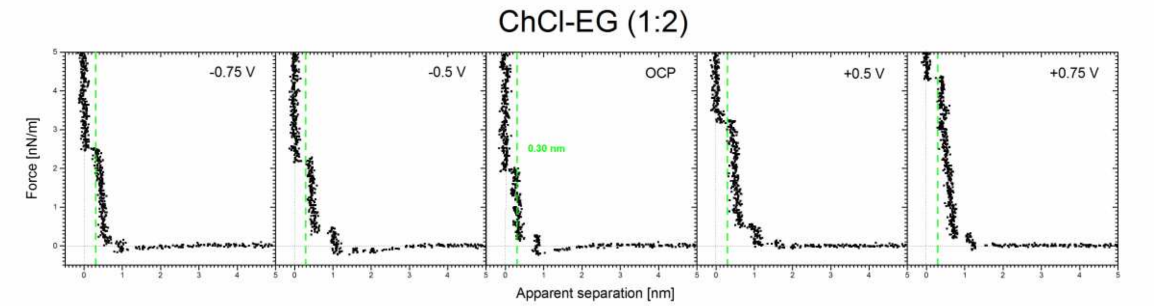

Fig. 6.4.1-1: Force-distance curves (normal force as a function of apparent separation) upon the AFM tip approaching the HOPG surface in pure ChCl-EG at a molar ratio of 1 : 2. The apparent nearest surface layer has a thickness of 0.3 nm at OCP. It is marked with a green, dashed line.

6.4.2 Force Curves of SDS-Deep Eutectic Solvent Solutions

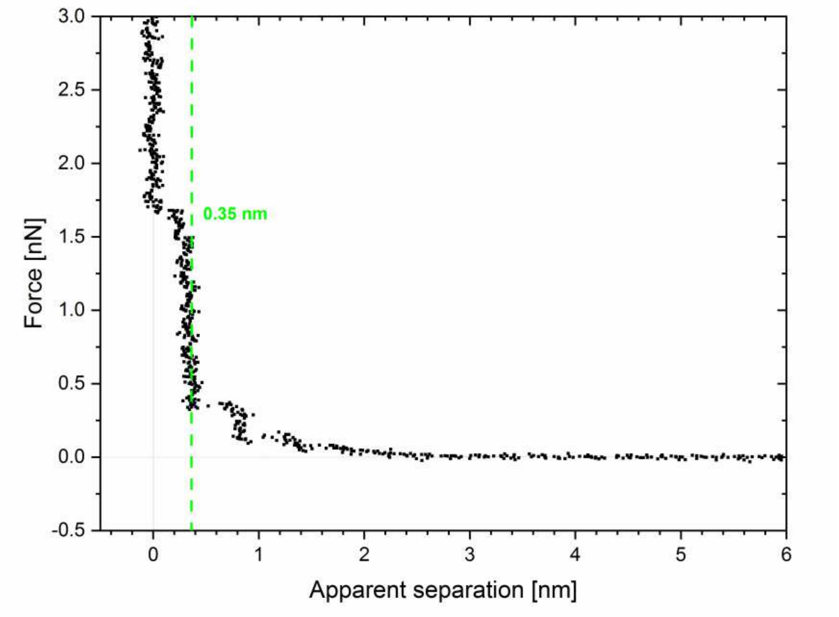

Fig. 6.4.2-1: Force-distance curve (normal force as a function of apparent separation) upon the AFM tip approaching the electrically neutral HOPG surface in a solution of SDS (25 mM) in ChCl-EG. The apparent nearest surface layer has a thickness of 0.35 nm. It is marked with a green, dashed line.

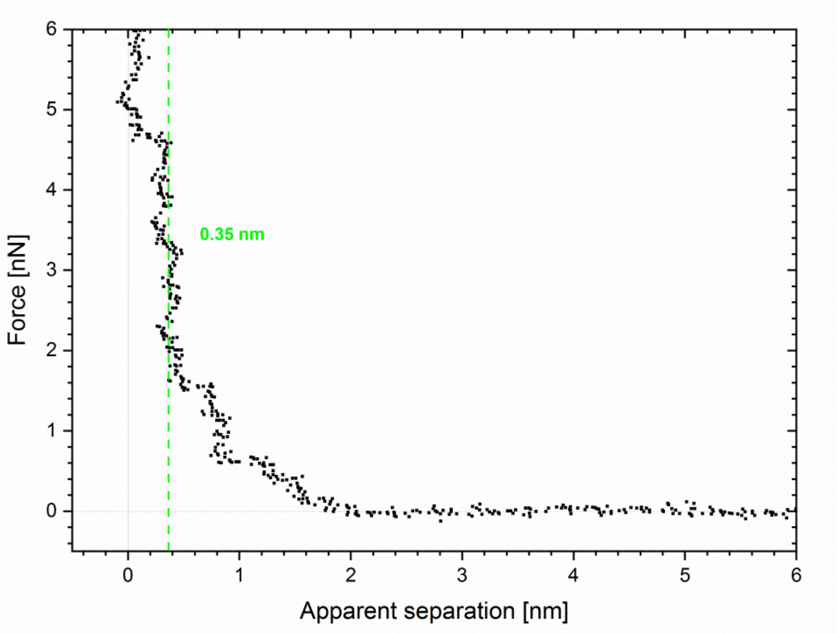

Fig. 6.4.2-2: Force-distance curve (normal force as a function of apparent separation) upon the AFM tip approaching the electrically neutral HOPG surface in a solution of SDS (25 mM) in ChCl-Gly. The apparent nearest surface layer has a thickness of 0.35 nm. It is marked with a green, dashed line.

6.4.3 Force Curves of SDS-Deep Eutectic Solvent Solutions with Applied Electric Surface Potential

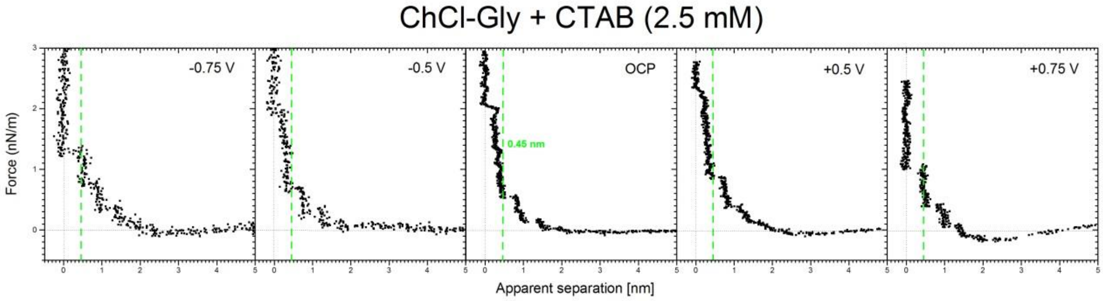

Fig. 6.4.3-1: Force-distance curves (normal force as a function of apparent separation) upon the AFM tip approaching the HOPG surface in (ChCl-Gly) + CTAB (2.5 mM). The apparent nearest surface layer has a thickness of 0.45 nm at OCP. It is marked with a green, dashed line.

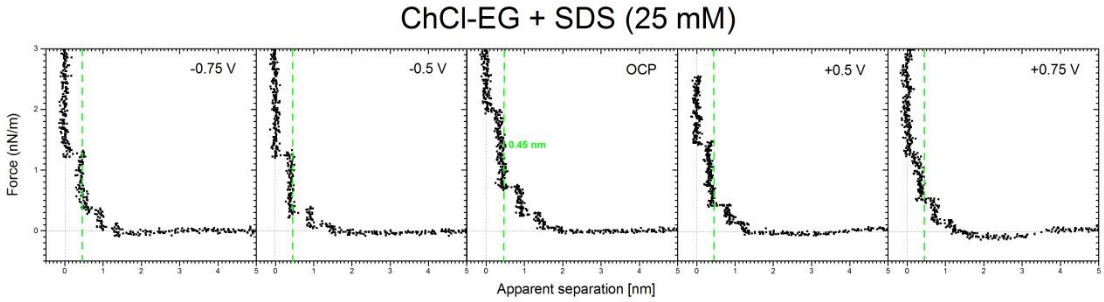

Fig. 6.4.3-2: Force-distance curves (normal force as a function of apparent separation) upon the AFM tip approaching the HOPG surface in (ChCl-EG) + SDS (25 mM). The apparent nearest surface layer has a thickness of 0.45 nm at OCP. It is marked with a green, dashed line.

List of Figures

Fig. 1.1.1-1: Concept of sustainability taking into account social, economic and environmental aspects. 3
Fig. 1.1.1-2: Solvent consumption by industry sectors. 4
Fig. 1.1.2-1: Time scale of the development of green chemistry. 10
Fig. 1.1.2-2: Number of articles containing the concept 'Green Chemistry' published between 1990 and 2018. 13
Fig. 1.1.3-1: Metrics for Life Cycle Analysis.[12] 15
Fig. 1.2.1-1: Variety of valuable products obtained from nature in terms of biorefinery. 16
Fig. 1.2.1-2: Scheme of the biorefinery of biomass. 17
Fig. 1.3.3-1: Chemical structures of some classical green solvents: (1) ethanol, (2) glycerol, (3) solketal, (4) triacetin, (5) 2-methyltetrahydrofuran, (6) γ-valerolactone and (7) ethyl lactate. 22
Fig. 1.3.5-1: Molecular structures of cations and anions typically used as IL constituents: (1) 1-alkyl-3-methylimidazolium, (2) 1,1-dialkylpyrrolidinium, (3) 1-alkylpyridinium, (4) tetraalkylammonium, (5) tetraalkylphosphonium, (6) bis-(trifluoromethanesulfonyl) amide, (7) trifluoromethanesulfonate, (8) tosylate, (9) alkylsulphate, (10) tetrafluoroborate, (11) hexafluorophosphate, (12) acetate and (13) halide. 26
Fig. 1.3.5-2: Reaction scheme of the BASIL process. 27
Fig. 1.3.5-3: Reaction scheme of the Degussa hydrosilylation reaction. 27
Fig. 1.3.5-4: Reaction scheme of the chlorination of 1,4-butanediol with potential side products indicated in grey. 28
Fig. 1.3.6-1: Binary phase diagram illustrating the formation of a eutectic mixture by combining components A and B. 31
Fig. 1.3.6-2: Molecular structure of choline chloride (1) and urea (2). When combined in a ratio of 2 : 1, they form the most investigated DES. 31
Fig. 1.3.6-3: Acid-catalyzed esterification of caffeic acid with phenethyl alcohol and subsequent collection of CAPE by the addition of water.[27, 91] 33
Fig. 1.4.1-1: Molecular structures of typical representatives of commonly used surfactant classes. 38
Fig. 1.4.2-1: Molecular structure of sodium xylene sulphonate (SXS). 39
Fig. 1.4.3-1: Setup of a conventional Langmuir trough for investigating monolayers at the water/air interface. 42
Fig. 1.4.3-2: Typical surface pressure-area isotherm featuring different phases of a Langmuir monolayer and the arrangement of surfactant molecules in the respective phase. This figure is based on Ref. [120]. 42
Fig. 1.4.3-3: Evolution of solution properties with increasing amphiphile concentration.[121] 44
Fig. 1.4.3-4: Binary phase diagram of an aqueous surfactant solution showing different aggregation phases above the CMC: micellar solution (L_1), hexagonal phase (H_1), cubic bicontinuous phase (V_1), lamellar phase (L_α) and inverse micelles (L_2).[125] 45
Fig. 1.4.3-5: Different types of surfactant self-assembly in aqueous solution.[123] 46
Fig. 1.4.3-6: Molecular structure of the hydrophobic dye DR13. 47
Fig. 2.1.1-1: Molecular structure of L-carnitine. 59
Fig. 2.1.1-2: Tested synthesis methods for carnitine-based ILs. 61

Fig. 2.2.1-1: One-step synthesis of carnitine ethyl ester bromide [C_2Car]Br. The same reaction was applicable for the synthesis of carnitine alkyl ester bromides [C_nCar]Br, when R = C_nH_{2n+1} and n = 2, 4, 6, 8, 10, 12, 14. 63

Fig. 2.2.1-2: One-step synthesis of carnitine ethyl ester mesylate [C_2Car]$MeSO_3$. 64

Fig. 2.2.1-3: Conversion of L-carnitine to [C_2Car]$MeSO_3$ as a function of reaction time recorded at a reaction temperature of 80 °C. 65

Fig. 2.2.1-4: Reaction time required to reach the 90 % equilibrium conversion as a function of reaction temperature. 66

Fig. 2.2.1-5: ‚Old' metathesis reaction for the change of the anion of [C_nCar]Br compounds.[11,28] 66

Fig. 2.2.1-6: Reaction scheme for the anion metathesis of [C_nCar]$MeSO_3$. 67

Fig. 2.2.2-1: Degradation temperature T_{deg} (■) and melting temperature T_m (▲) as a function of the molar fraction of [C_2Car]$MeSO_3$ in relation to unesterified L-carnitine. 70

Fig. 2.2.3-1: Classification of the presented reactions 1a, 1b, 2a and 2b according to cost, energy consumption, solvent, waste generation and hazards of the reaction (see. Tab. 2.2.3-1). 71

Fig. 2.3.2-1: Concentration dependent surface tension curves of [C_nCar]Br compounds with n = 2 (■), 4 (●), 6 (▲), 8 (⬢), 10 (◆), 12 (⬟), and 14 (✱) (data partly collected by Mühlbauer A.).[11] 75

Fig. 2.3.2-2: Log (CAC) as a function of alkyl chain length n of [C_nCar]Br (■) and alkyltrimethylammonium compounds C_nTAB (literature values from [29,45]) (▲) with a curve break at n = 8 (marked in green). 76

Fig. 2.3.2-3: Time-dependent self-correlation functions as obtained by DLS for the [C_nCar]Br/water binary system and several reference substances at 25 °C: 1.946 M [C_2Car]Br (–),1.099 M [C_4Car]Br (–),0.313 M [C_6Car]Br (–), 0.190 M [C_8Car]Br (–), 0.114 M [C_{10}Car]Br (–), 0.103 M [C_{12}Car]Br (–), 0.101 M [C_{14}Car]Br (–), 3.5 M [C_1C_4Im]Br (--), 0.5 M SXS (••), 0.111 M C_{12}TAB (-•-), 0.015 M C_{16}TAB (–). 79

Fig. 2.3.2-4: Hydrotropic solubilization of DR13 in [C_nCar]Br compounds with n = 0 (■), 2 (■), 4 (●), 6 (▲), 8 (⬢) and reference substances [C_1C_4Im]Br (●) and SXS (▲) (data partly collected by Mühlbauer A.).[11] 80

Fig. 2.3.2-5: EC_{50} values (logarithmic scale) for [C_nCar]Br compounds with n = 6 – 14 and [C_1C_4Im]Br including literature values for two alkyltrimethylammonium bromides C_{12}TAB and C_{16}TAB.[54] 81

Fig. 2.3.3-1: Molecular structure of vanillin. 82

Fig. 2.3.3-2: Solubility of vanillin in aqueous solutions of [C_nCar]Br with n = 0 (■), 2 (■), 4 (●), 6 (▲), 8 (⬢), 10 (◆), 12 (⬟), and 14 (★) and reference substances [C_1C_4Im]Br (●), SXS (▲), C_{12}TAB (◆), and C_{16}TAB (★) at room temperature. The dotted horizontal line indicates the solubility of vanillin in pure water. 83

Fig. 2.4.1-1: One-step synthesis of carnitine alkyl ester mesylates; R = C_nH_{2n+1} with n = 8, 10, 12, 14. 84

Fig. 2.4.2-1: Concentration dependent surface tension curves of [C_nCar]$MeSO_3$ compounds with n = 8 (⬢), 10 (◆), 12 (⬟), and 14 (✱). 85

Fig. 2.4.2-2: Time-dependent self-correlation functions as obtained by DLS for the [C_nCar]Br/water binary system and several reference substances at 25 °C: 0.06 M [C_8Car]$MeSO_3$ (–), 0.05 M [C_{10}Car]$MeSO_3$ (–), 0.01 M [C_{12}Car]$MeSO_3$ (–), 0.01 M [C_{14}Car]$MeSO_3$ (–), 0.03 M [C_{14}Car]$MeSO_3$ (---) and 0.015 M C_{16}TAB (–). 87

Fig. 2.4.2-3: Gel-like liquid crystal phases of aqueous solutions of $[C_nCar]MeSO_3$ with n = 8 (41 wt% ≙ 1.14 M), n = 10 (32 wt% ≙ 1.06 M) and n = 12 (34 wt% ≙ 0.99 M). 88
Fig. 2.4.2-4: Images recorded by a polarization microscope in tenfold magnification (left) and 20-fold magnification (right). 89
Fig. 2.4.2-5: EC_{50} values for $[C_nCar]MeSO_3$ (grey), $[C_nCar]Br$ (blue) and C_nTAB[54] (green) compounds with n = 8 - 14. 90
Fig. 2.6.8-1: Calibration curve recorded for vanillin solubilized in ethanol including a linear fit. 99
Fig. 3.2.1-1: Various carnitine-based HBA species studied in this chapter: (1) zwitterionic carnitine, (2) carnitine hydrochloride and (3) carnitine alkyl ester bromide. 110
Fig. 3.2.2-1: Formation of 'in situ ILs' by proton exchange when combining carnitine with a carboxylic acid. 112
Fig. 3.2.2-2: Qualitative DSC curves of a series of Car-CarHCl-LaA mixtures in HBA : HBD ratio of 1 : 1 including the initial Car-LaA DES (black curve). The plots are offset on the y-scale for clarity in representation. 113
Fig. 3.2.2-3: Qualitative DSC curves of a series of Car-CarHCl-MaleA mixtures in HBA : HBD ratio of 2 : 1 including the initial Car-MaleA DES (black curve). The plots are offset on the y-scale for clarity in representation. 114
Fig. 3.2.2-4: Selected NMR spectral ranges of a series of Car-CarHCl-MaleA mixtures in HBA : HBD ratio of 2 : 1 including the initial Car : MaleA DES (black curve). The plots are offset on the y-scale for clarity in representation. 115
Fig. 3.2.4-1: Molecular structures of (1) pheomelanin and (2) eumelanin. The arrows indicate further connection points for the expansion of the polymer network. 119
Fig. 3.2.4-2: Absorbance at a wavelength of 500 nm as a function of the initial melanin concentration. The tested solutions contain 25 wt% of water. 120
Fig. 3.2.4-3: Solubility fraction and pH values of the tested solvents having a water content of 25 wt% as inferred from the linear regression lines of Fig. 3.2.4-2. 120
Fig. 3.2.4-4: Absorbance at a wavelength of 500 nm as a function of the initial melanin concentration for Bet-ManA (1 : 1) (25 wt% water) mixtures at pH 3.0, 7.5 and 9.5. The inlay illustrates the respective solubility fractions. 121
Fig. 3.3.2-1: Thermal transitions of the ternary mixture ChCl-urea-GA measured by means of DSC presented in two characteristic temperature ranges. The plots are offset on the y-scale for clarity in representation. 126
Fig. 3.3.3-1: Esterification of gallic acid to form a gallic acid alkyl ester in a DES reaction medium. 127
Fig. 3.3.3-2: Solubility of butanol and octanol in ChCl-GA (indicated in blue), ChCl-urea-GA (indicated in green) and ChCl-D-Fru-GA (indicated in orange) DESs of various molar ratios. 128
Fig. 3.3.3-3: HPLC chromatograms of the esterification of gallic acid with (A) butanol in ChCl-GA, (B) octanol in ChCl-GA and (C) octanol without solvent. Each chromatogram has the following colour code: black curve – without catalyst, blue curve – with Amberlyst 15, green curve – with H_2SO_4. The plots are offset on the y-scale for clarity in representation. 129
Fig. 3.3.3-4: Molecular structure of chlorogenic acid. 130
Fig. 3.3.3-5: Molecular structures of (1) shikimic acid, (2) shikimic acid ethyl ester and (3) oseltamivir phosphate (Tamiflu). 131

Fig. 3.4.2-1: Force-distance curves showing the normal force as a function of the apparent separation between tip and surface upon the AFM tip approaching the HOPG surface in pure ChCl-Gly (A) and pure ChCl-EG (B). The apparent nearest surface layers have thicknesses of 0.45 nm and 0.35 nm, respectively. The corresponding values are marked with green, dashed lines. 134
Fig. 3.4.2-2: Suggested interface model of the interface between graphite and a deep eutectic solvent with a barrier for the AFM tip between the ion rich Stern layer (yellow) and a layer rich in molecular component (green). 134
Fig. 3.4.2-3: Force-distance curves (normal force as a function of apparent separation) upon the AFM tip approaching the HOPG surface in pure ChCl-Gly at a molar ratio of 1 : 2. The apparent nearest surface layer has a thickness of 0.45 nm at OCP. It is marked with a green, dashed line. 135
Fig. 3.4.3-1: Scheme of the proposed mechanism for the formation of surfactant surface aggregates on graphite consisting of the adsorption of a flat surfactant monolayer (A), the formation of hemimicellar aggregates (B), which infinitely spread along the graphite surface in form of hemicylindrical aggregates (C). 136
Fig. 3.4.3-2: Force-distance curve (normal force as a function of apparent separation) upon the AFM tip approaching the electrically neutral HOPG surface in a solution of CTAB (2.5 mM) in ChCl-Gly. The apparent nearest surface layer has a thickness of 0.45 nm. It is marked with a green, dashed line. 137
Fig. 3.4.3-3: Force-distance curve (normal force as a function of apparent separation) upon the AFM tip approaching the HOPG surface in a solution of CTAB (2.5 mM) in ChCl-Gly at a potential of -0.75 V. The shape of the curve is typical for the presence of surface aggregates. The first liquid layer of DES has a thickness of 0.35 nm and is marked with a green, dashed line. 138
Fig. 3.4.3-4: AFM deflection images showing adsorbed surfactant aggregates at the (ChCl-Gly)-graphite interface with indicated shape of surfactant. Image A was recorded for a 21 mM SDS solution, its height scale is 0.5 nm. Image B was recorded for a 2.5 mM CTAB solution, its height scale is 1.0 nm. Image C was recorded for a 21 mM CTAB solution, its height scale is 0.85 nm. 139
Fig. 3.4.3-5: AFM deflection images showing adsorbed SDS aggregates at the (ChCl-EG)-graphite interface with indicated shape of surfactant. Image A was recorded for a 25 mM SDS solution, its height scale is 0.3 nm. Image B was recorded for a 132 mM SDS solution, its height scale is 1.0 nm. 139
Fig. 3.4.4-1: AFM deflection images of adsorbed CTAB aggregates at the (ChCl-Gly)-graphite interface as a function of electric surface potential. 141
Fig. 3.4.4-2: AFM deflection images of an adsorbed SDS monolayer at the (ChCl-EG)-graphite interface as a function of electric surface potential. 141
Fig. 3.6.2-1: One-step synthesis of betaine alkyl ester bromide [C_nBet]Br. 146
Fig. 4.1.1-1: Molecular structure of the sodium salt of dehydroepiandrosterone sulphate (DHEAS) (1), indole-3-acetic acid (2) and indole-3-butyric acid (3). 155
Fig. 4.2.2-1: Enzymatically controlled equilibrium between DHEA and its sulphated form DHEAS. 158

Fig. 4.3.1-1: Surface tension curves of NaDHEAS (▲) (measured at 37 °C), NaIAA (■), NaIBA (●), NaSal (▲) and SDS (●) (measured at 25 °C). Data for the surface tension of SDS is adopted from Lunkenheimer et al.[31] 161

Fig. 4.3.2-1: Specific conductivity κ as a function of the NaDHEAS concentration in aqueous solution with indication of a breakpoint of the curve slope. 163

Fig. 4.3.3-1: Time-dependent self-correlation functions as obtained by DLS for aqueous solutions of NaDHEAS (left, green, measured 2 h after preparation, 37 °C), NaIAA (middle, violet, 25 °C) and NaIBA (right, blue, 25 °C). 164

Fig. 4.3.3-2: Time-dependent self-correlation functions as obtained by DLS for a 0.026 M aqueous NaDHEAS solution 2 h (–), 8 h (–), 16 h (–) and 24 h (–) after preparation of the solution at 37 °C. 164

Fig. 4.4.1-1: Hydrotropic solubilization of DR13 in aqueous solutions of NaDHEAS (▲) (measured at 37 °C), NaIAA (■), NaIBA (●), SDS (●) and NaSal (▲) (measured at 25 °C) as evidenced from the absorbance of DR13 at a wavelength of 503 nm. 166

Fig. 4.4.2-1: Molecular structures of PnP (1) and DPnP (2). 168

Fig. 4.4.2-2: Shifts of the LST of water/PnP upon the addition of NaDHEAS (▲), NaSal (▼) and SDS (●) and the LST of water/DPnP upon the addition of NaIAA (■), NaIBA (●) and NaSal (▲) with linear fits indicating the salting-in activity of the tested substance. 168

Fig. 4.4.2-3: Shifts of the LST of water/PnP upon the addition of NaDHEAS (▲) and SDS (●) and the change of the curve linearity. 169

Fig. 4.4.3-1: Cloud temperature of egg white solutions containing NaDHEAS at different concentrations. 172

Fig. 4.5.1-1: Molecular structure of DPPC. 174

Fig. 4.5.2-1: Surface pressure-area isotherms of DPPC with different concentrations of NaDHEAS (left, green, 37 °C), NaIAA (middle, violet, 25 °C) and NaIBA (right, blue, 25 °C) as additive in the aqueous subphase. 174

Fig. 4.5.2-2: DPPC monolayer surface pressure as a function of the square root of hormone concentration of NaDHEAS (▲),NaIAA (■) and NaIBA (●) in the subphase. The area per molecule A_m is 0.75 nm^2 and the temperature is 37 °C for NaDHEAS and 25 °C for NaIAA and NaIBA. 177

Fig. 6.1.1-1: Molecular structures of the quaternary ammonium compounds and the respective abbreviations used in the course of chapter 3: (1) choline chloride, (2) acetylcholine chloride, (3) betaine, (4) betaine hydrochloride, (5) carnitine, (6) carnitine hydrochloride, (7) betaine ethyl ester bromide, (8) betaine butyl ester bromide and (9) carnitine ethyl ester bromide. 195

Fig. 6.1.2-1: Molecular structures of the hydrogen bond donors and the respective abbreviations used in the course of chapter 3: (1) urea, (2) ethylene glycol, (3) glycerol, (4) D-fructose, (5) caffeic acid, (6) citric acid, (7) p-coumaric acid, (8) formic acid, (9) ferulic acid, (10) gallic acid, (11) glycolic acid, (12) itaconic acid, (13) lactic acid, (14) levulinic acid, (15) maleic acid, (16) malic acid, (17) malonic acid, (18) mandelic acidm (19) oxalic acid, (20) quinic acid, (21) succinic acid, (22) salicylic acid, (23) shikimic acid, (24) sorbic acid and (25) tartaric acid. 196

Fig. 6.3.1-1: NMR spectrum of maleic acid in deuterated acetonitrile. 201

Fig. 6.4.1-1: Force-distance curves (normal force as a function of apparent separation) upon the AFM tip approaching the HOPG surface in pure ChCl-EG at a molar ratio of 1 : 2. The

apparent nearest surface layer has a thickness of 0.3 nm at OCP. It is marked with a green, dashed line. 202
Fig. 6.4.2-1: Force-distance curve (normal force as a function of apparent separation) upon the AFM tip approaching the electrically neutral HOPG surface in a solution of SDS (25 mM) in ChCl-EG. The apparent nearest surface layer has a thickness of 0.35 nm. It is marked with a green, dashed line. 202
Fig. 6.4.2-2: Force-distance curve (normal force as a function of apparent separation) upon the AFM tip approaching the electrically neutral HOPG surface in a solution of SDS (25 mM) in ChCl-Gly. The apparent nearest surface layer has a thickness of 0.35 nm. It is marked with a green, dashed line. 203
Fig. 6.4.3-1: Force-distance curves (normal force as a function of apparent separation) upon the AFM tip approaching the HOPG surface in (ChCl-Gly) + CTAB (2.5 mM). The apparent nearest surface layer has a thickness of 0.45 nm at OCP. It is marked with a green, dashed line. 203
Fig. 6.4.3-2: Force-distance curves (normal force as a function of apparent separation) upon the AFM tip approaching the HOPG surface in (ChCl-EG) + SDS (25 mM). The apparent nearest surface layer has a thickness of 0.45 nm at OCP. It is marked with a green, dashed line. 204

List of Tables

Tab. 1.1.2-1: The 12 Principles of Green Chemistry.[2] 11
Tab. 1.3.6-1: Categories of DESs.[85] 31
Tab. 1.4.3-1: Overview of characteristic Langmuir phase behaviours of a surfactant monolayer at the water/air interface. 43
Tab. 1.4.3-2: Aggregate shapes predicted by the packing parameter N_S. 45
Tab. 1.4.3-3: Collection of properties and effects of chaotropes and kosmotropes. 48
Tab. 2.2.1-1: Overview of the reaction pathways developed for the synthesis of carnitine-based ILs. 63
Tab. 2.2.2-1: Water contents as determined by Karl Fischer Coulometry for ILs obtained from the 'old' synthesis in almost 100 % purity and from the 'new' synthesis in approximately 90 % purity. 68
Tab. 2.2.2-2: Degradation temperature T_{deg}, melting temperature T_m and glass transition temperature T_g of $[C_nCar]X$ ILs obtained from the 'old' synthesis in almost 100 % purity and from the 'new' synthesis in approximately 90 % purity. 69
Tab. 2.2.3-1: Description of the classification categories for the assessed reactions. 72
Tab. 2.3.2-1: Degradation temperature T_{deg}, melting temperature T_m and glass transition temperature T_g of the synthesized $[C_nCar]Br$ compounds for different chain lengths (data partly collected by Mühlbauer A.).[11] 74
Tab. 2.3.2-2: Water-solubility, critical aggregation concentration (CAC) and minimum surface tension σ_{CAC} of $[C_nCar]Br$ compounds with reference data of alkyltrimethylammonium bromides (data partly collected by Mühlbauer A.).[11] 77
Tab. 2.4.2-1: Critical micellar concentration (CMC) and minimum surface tension σ_{CAC} of $[C_nCar]MeSO_3$ compounds. 86
Tab. 2.6.1-1: Register of the chemicals used in this chapter, their purity, their supplier and the sections they are relevant for. 93
Tab. 3.1.1-1: Various terms related to the DES topic and their definitions 109
Tab. 3.2.1-1: Summary of betaine- and carnitine-based DESs with indicated visual appearances, thermal transition temperatures and water contents. 110
Tab. 3.2.2-1: Car-CarHCl-LaA series prepared in HBA : HBD ratio of 1 : 1 with the respective appearances at room temperature, thermal transition temperatures and water contents. 113
Tab. 3.2.2-2: Car-CarHCl-MaleA series prepared in HBA : HBD ration of 2 : 1 with the respective appearances at room temperature, thermal transition temperatures and water contents. 114
Tab. 3.2.2-3: Vicinal coupling constant ^3J of the protons H_1 and H_2 bound to the carbon atom next to the carboxylic group of carnitine/carnitine hydrochloride (see highlighting in Fig. 3.2.2-4) and $\Delta\delta$ between signals 1 and 2. 116
Tab. 3.2.3-1: Bulky betaine and carnitine ester HBAs and their melting points. 117
Tab. 3.2.3-2: DESs formed from $[C_2Bet]Br$, $[C_2Car]Br$ and $[C_4Bet]Br$ with indicated visual appearances, thermal transition temperatures and water contents. 117
Tab. 3.3.1-1: Overview of DESs formed with choline chloride and biologically active HBDs with indicated visual appearances, thermal transition temperatures and water contents. 123

Tab. 3.3.2-1: Gallic acid-based, ternary DESs with indicated visual appearances, thermal transition temperatures and water contents. 124
Tab. 3.3.3-1: Assessed reaction parameters of the gallic acid esterification. 127
Tab. 3.3.3-2: Screened reaction systems for the esterification of gallic acid with n-alcohols and the resulting conversion either without catalyst, in presence of Amberlyst 15 or in presence of H_2SO_4. 128
Tab. 3.4.3-1: Height scale of the presented AFM deflection images and aggregation period determined from power spectral density (PSD) analysis of the AFM deflection images for the studied surfactant solutions at a graphite interface. 140
Tab. 3.4.4-1: Aggregation period determined from PSD analysis of the AFM deflection images in the presence of an applied electric surface potential. 142
Tab. 3.6.1-1: Chemicals used in this chapter, their purity, their supplier and the sections they are relevant for. 145
Tab. 4.3.1-1: Surface excess concentration $\boldsymbol{\Gamma_i}$ and mean surface area per molecule $\boldsymbol{A_i}$ obtained from the Gibbs isotherm with indication of the measuring temperature T. 162
Tab. 4.4.2-1: List of concepts and properties characterizing LST increasing and decreasing compounds. 167
Tab. 4.4.2-2: Coefficient a in units of [°C per mmol of additive in 1 mol of water/PGE mixture] for systems with a PnP mass fraction of 0.45 and a DPnP mass fraction of 0.55. 170
Tab. 4.7.1-1: Chemicals used in this chapter, their purity and their supplier. 180
Tab. 6.2.1-1: Binary mixtures containing betaine or carnitine considered for the formation of DESs. 197
Tab. 6.2.2-1: Binary mixtures containing betaine or carnitine hydrochloride considered for the formation of DESs. 198
Tab. 6.2.3-1: Binary mixtures containing betaine or carnitine alkyl ester salts considered for the formation of DESs. 199
Tab. 6.2.4-1: Binary mixtures containing biologically relevant HBDs with carboxylic acid function considered for the formation of DESs. 200
Tab. 6.2.5-1: Ternary mixtures containing gallic acid considered for the formation of DESs. 200

Scientific Contributions

Poster Presentations

K. Häckl and W. Kunz: *Green Ionic Liquids from Carnitine Derivatives*, **BASF International Summer Course** Ludwigshafen 2016.

K. Häckl, A. Mühlbauer, V. Nardello-Rataj, W. Kunz: *Green Surfactants Based on Carnitine*, **ISGC** La Rochelle 2017.

K. Häckl, A. Mühlbauer, V. Nardello-Rataj, W. Kunz: *Green Surfactants Based on Carnitine*, **Kolloid-Tagung** Munich 2017.

Publications

W. Kunz and K. Häckl
The Hype with Ionic Liquids as Solvents
Chem. Phys. Lett. 661 (2016), 6-12.

K. Häckl, A. Mühlbauer, J. F. Ontiveros, S. Marinkovic, B. Estrine, W. Kunz, V. Nardello-Rataj
Carnitine Alkyl Ester Bromides as Novel Biosourced Ionic Liquids, Cationic Hydrotropes and Surfactants
J. Colloid Interface Sci. 511 (2018), 165-173.

K. Häckl and W. Kunz
Some Aspects of Green Solvents
C. R. Chimie 21 (2018), 572-580.

Declaration

I herewith declare in lieu of oath that I have composed this thesis without any inadmissible help of a third party and without the use of aids other than those listed. The data and concepts that have been taken directly or indirectly from other sources have been acknowledged and referenced.

Other persons have not helped to produce this work as regards to its content or making. In particular, I have not used the services of any professional agencies in return for payment or those of other persons. Nobody has received payment in kind – neither directly nor indirectly – from me for any work that is connected with the content of this doctoral dissertation.

The thesis has not been submitted, wholly or substantially, neither in this country nor abroad for another degree or diploma at any university or institute.

Regensburg, 23rd May 2019

Katharina Häckl